Russian Original Vol. 31, No. 5, November, 1971

Translation published June, 1972

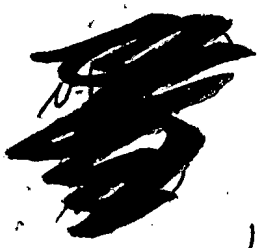

NE - Lost in file in NTIS

SOVIET ATOMIC ENERGY

АТОМНАЯ ЭНЕРГИЯ
(ATOMNAYA ÉNERGIYA)

TRANSLATED FROM RUSSIAN

CONSULTANTS BUREAU, NEW YORK

SOVIET ATOMIC ENERGY

Soviet Atomic Energy is a cover-to-cover translation of *Atomnaya Énergiya*, a publication of the Academy of Sciences of the USSR.

An arrangement with Mezhdunarodnaya Kniga, the Soviet book export agency, makes available both advance copies of the Russian journal and original glossy photographs and artwork. This serves to decrease the necessary time lag between publication of the original and publication of the translation and helps to improve the quality of the latter. The translation began with the first issue of the Russian journal.

Consultants Bureau journals appear about six months after the publication of the original Russian issue. For bibliographic accuracy, the English issue published by Consultants Bureau carries the same number and date as the original Russian from which it was translated. For example, a Russian issue published in December will appear in a Consultants Bureau English translation about the following June, but the translation issue will carry the December date. When ordering any volume or particular issue of a Consultants Bureau journal, please specify the date and, where applicable, the volume and issue numbers of the original Russian. The material you will receive will be a translation of that Russian volume or issue.

Subscription
$67.50 per volume (6 Issues)
2 volumes per year
(Add $5 for orders outside the United States and Canada.)

Single Issue: $30
Single Article: $15

CONSULTANTS BUREAU, NEW YORK AND LONDON

227 West 17th Street
New York, New York 10011

Davis House
8 Scrubs Lane
Harlesden, NW10 6SE
England

Published monthly. Second-class postage paid at Jamaica, New York 11431.

SOVIET ATOMIC ENERGY

A translation of *Atomnaya Énergiya*
Translation published June, 1972

Volume 31, Number 5 November, 1971

CONTENTS

CONTENTS

(continued)

CONTENTS

(continued)

The Russian press date (podpisano k pechati) of this issue was 11/2/1971. Publication therefore did not occur prior to this date, but must be assumed to have taken place reasonably soon thereafter.

ON THE DESIGN OF BLOCKS OF ATOMIC POWER PLANTS

E. P. Anan'ev and G. N. Kruzhilin

UDC 621.311.2:620.9

Power engineers of the old generation remember what an immense achievement was the starting of the first, and at that time unique, vapor turbine with a capacity of 25 MW with a pressure of 30 atm in 1930.

Still more surprising was the subsequent development of steam turbines with capacities of 50 and 100 MW. At the end of the nineteen forties the use of steam at high pressures of 100 to 140 atm began with the installation of steam turbines with capacities of 150 and 200 MW at the electric power plants.

In the development of the first industrial atomic power plants in the early fifties unit capacities up to 200 MW were being considered. In 1960-1961 the first block with a capacity of 100 MW with a canal-type reactor at the Beloyarsk atomic power plant and the first block with a capacity of 210 MW with water–water frame reactor at Novo-Boronezhsk atomic power plants were constructed. The prospects of an extensive construction of new atomic power plants were open.

However, by this period the power engineering based on organic fuel had already reached a new technical level with the use of steam at supercritical pressure. Development of steam turbines at 300-500 MW and even higher capacities became possible. The possibility of constructing steam boiler–turbine–generator blocks manifested itself. The transition to blocks of such large unit capacity ensured a sharp increase in the output of power plants with the same plant areas and a correspondingly more rapid development of power engineering.

As is well known, at the very beginning of this stage there was a widespread feeling that together with the increase in the unit capacity of the blocks there will be a significant decrease in the cost of construction of thermal power plants (for example, by a factor of two in the design of 1 kW of installed power). In fact this expectation was fulfilled only partially.

The above-cited level of the capacity of power blocks operating on organic fuel established new problems in the development of competitive atomic power plants. Due to this nuclear reactors of electric capacity up to 440 MW were sequentially developed in our country and designs for reactors of electric capacity of 1000 MW, capable of being realized, have been worked out. The development of reactors of significantly higher power is being considered.

As regards the specific cost of construction of atomic power plants with the contemporary powerful reactors, according to the experience in the design and construction the cost decreases with the increase in the unit capacity of the reactor, but not drastically. In this respect the experience in the construction of power blocks based on organic fuel, which was already mentioned, repeats itself in general.

A similar pattern is observed also in the USA. For an illustration the graph for the dependence of the cost of 1 kW of installed power on the electric capacity of reactors of type PWR and BWR [1] is given in Fig. 1. It is evident from the figure that on changing the capacity of the block from 800 to 1200 MW the specific cost of construction of atomic power plants in the USA decreases by about 15%. Considering these data it is hardly possible to expect a significant reduction in the expenditure per installed 1 kW even in our conditions at capacities of more than 1000 MW.

Therefore, the point in favor of a further increase in the unit capacity of a block will be its positive effect on the tempo of the growth of the new power capacity.

Besides, it must be taken into consideration that the problem of its reliability under operational conditions gets appreciably complicated with the increase in the capacity of the block. Up till now the increase

Translated from Atomnaya Énergiya, Vol. 31, No. 5, pp. 443-447, November, 1971. Original article submitted March 1, 1971.

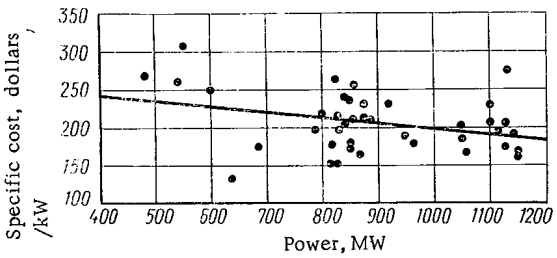

Fig. 1. Specific cost of atomic power plant as a function of the electric capacity.

in the capacity of the blocks of atomic power plants has come about in the course of forced competition with electric power plants operating on organic fuel. It was always kept in mind that the degree of reliability of operation of atomic power plants will remain at an appropriate level. But the practical experience in this respect does not exist. As before the tendency for a further increase in the capacity of blocks of atomic power plants follows from the condition of competition with the ordinary electric power plants and not from the logic of intrinsic development. This tendency appears somewhat premature, at least until such time that the necessary operational reliability of blocks with a capacity up to 1000 MW is actually realized. At the same time it cannot be admitted that such gigantic capacity of a block will be no less remarkable and surprising than the capacity of 100 MW in the late thirties and that this scale is compatible with the possible assumptions in regard to the tempo of development of our power engineering.

The direct connection of the problem of reliability with the block capacity is especially clear in relation to the blocks operating on organic fuel. It is sufficient to say that the heated surface of the steam boiler increases proportionally with the increase in the block capacity and the probability of accidental shutdown of the block correspondingly increases due to leakage in the welded seams of the tubes, damage to the tubes themselves, and so forth. On the other hand each accidental shutdown of a powerful block leads to very signficant "loss" due to the stoppage of delivery of electric power to the power system.

This loss according to minimal estimates is determined in this way: according to the existing rules [2] for the nondelivery of power to the industrial needs of the consumer the electric supply company pays a fine equal to eight times the tariff cost, which is 0.5 kopeck per 1 kWh, i.e., at the level of production cost of electric power in the best contemporary power plants the loss is 4 kopecks per nondelivered 1 kWh. Special estimates show that the loss to the national economy may reach 10-60 kopecks per nondelivered 1 kWh [3]. If it is assumed that the loss is 4 kopecks per 1 kWh, the losses from the shutdown of a block with 300 MW capacity comprises about 300 thousand rubles per day. Therefore, it is correct to assume that with regard to powerful blocks the technology of production of the equipment must be considerably improved to the point that in increasing the unit capacity of the block the probability of accidents does not increase, rather it decreases.

The operation of atomic power plants is connected with radioactivity. The consequences of accidents in the reactor and the primary circuit cannot be eliminated in a period, in which accidents in steam boilers are liquidated. As a rule, even mild accidents in this part of the reactor require shutdown for many days. The repair of the damages in the active zone of frame reactors requires several months. An accident in a reactor of 1000 MW electrical capacity (in the shutdown of which the loss due to nondelivery of electric power will be one million rubles per day in analogy with ordinary power plants) would cause a loss to the national economy, equal to the cost of the construction of the block as a whole.

For the characteristics of the conditions of repair of the reactor part of the atomic power plants we recall that according to the published data an accidental shutdown of the water–water reactor of the firm Westinghouse in the atomic power plant at Ardens (France) lasted 778 days [4]. As a result of strong action of the stream of cooled water on the construction inside the reactor frame a significant part of the pins engaging the end faces of the two cylindrical parts of the shaft in the active zone were torn off in this reactor. For carrying out the necessary repair work it was necessary to dismantle completely the equipment inside the frame and also to carry out some technological operations under high radioactive conditions with prior construction of protecting devices and special instruments.

Accidents with constructions inside the frame also occurred in other reactors of this type. There were serious accidents in the sodium cooled American reactor "Enrico Fermi" operating on fast neutrons. In particular, in 1966 there was a melting of the fuel elements in this reactor due to blocking of the entrance section of two operating channels by a piece of metal. The repair work lasted four years. In 1967 an accident occurred in magnox reactor No. 2 at Chapel Cross (England). In one of 1700 channels, due to the falling of a fragment of a graphite sleeve in its entrance section six fuel elements melted. The reactor was in repair for two years. Taking into consideration the experience of operation and repair of

atomic power plants, that is already available, it can be assumed that any expense will be justified for ensuring reliability of operation of powerful blocks of atomic power plants. In any case it must be recognized that for atomic power plants the problem of reliability is extremely acute due to its being new and specific.

Besides problems of construction of the equipment for atomic power plants, the technology of its setting up and control, certain general principles are also of significance. It is assumed that the auxiliary equipment must be installed with necessary reserve, wherein preference is given to samples which are simpler in scheme and have been checked for reliability. It is interesting to note that based on the experience in the operation of the canal-type boiling heavy water reactor SGHWR with electrical capacity of 100 MW, the English decided to replace the fuel in the whole equipment (twice per year) of this reactor as well as more powerful reactors of this type in the future, since in this case all the operations are simpler and more reliable than reloading in operation proposed earlier [5]. On the other hand reloading of gas cooled reactors in operation was found advisable according to the experience of operation in England and France.

We should also touch upon the problem of automatic control systems and the protection of a nuclear reactor. This, for example, it is noted in [6] that in France there were relatively many accidental shutdowns of reactors due to malfunctioning of the automatic systems themselves; therefore specialists decided on the need for maximum simplification of this system and also to discard automatization of those processes whose operation can be handled by men. The specific nature of the nuclear reactor makes it suitable for complete automation. Due to this the opinion expressed above may be considered paradoxical. Nevertheless, it was well defined long ago and in fact reflects the essence of the matter. At the same time in the systems of automation a reserve equipment is widely used and there is a provision for parallel electrical circuits with the purpose of eliminating reactor shutdowns due to "false" operations of the accident protection. The protection scheme "two of three" is also used; its operation principle amounts to the fact that the protection operates only on receiving two identical signals of the total of three.

In respect of automation one also encounters a reverse tendency, in particular, in the form of assumptions about installing automatic control systems using a computer. This would lead to a corresponding complication of the electrical circuit and to an increase of their number in the overall automation system and as a result, to a decrease in its reliability. Therefore, for the time being the use of these control systems in the blocks of atomic power plants must be considered cautiously.

In connection with the reliability the problems of strength merit special attention. Most of all they refer to the frame of a water–water reactor. According to the design, for an electric capacity of the reactor at 1000 MW the pressure in the frame is 170 atm, the diameter of the frame 4290 mm, the thickness of the wall up to 210-255 mm, the diameter of inlet connecting pipes 850 mm, the thickness of the collar of the frame 385 mm, and the diameter of the pins in the collar 150 mm. For such large dimensions, including the large thickness of the frame wall, with the change of temperature during starting and stopping of the reactor the mechanical stresses in certain regions, especially near the connecting pipes, will inevitably exceed the elastic limit appreciably and after repeated plastic deformations they would cause a lowering of the plasticity, i.e., an increase in the tendency to brittleness, which can later lead to brittle fissure formation. Therefore, the rate of change of temperature in this type of construction is rigidly limited by the conditions of strength. Furthermore, the total number of complete stoppages of a water –water reactor (stoppage to its cold state) must be limited. Unfortunately, as yet there are no methods for a reliable computation of these processes. But in view of quite numerous cases of appearance of fissures in the drums of steam boilers it is known that the admissible number of stoppages to cold state is small for this type of container. According to English specialists [7] the number of such stoppages in the course of the entire life of a reactor should not exceed about 100. Taking the computed total period of operation of a reactor as 30 years it should be assumed that on the average the cold stoppages of the reactor must not be more than three per year. Obviously, these figures are very stringent, but they must be taken into consideration, since they are related to the safety of the reactor.

From this point of view the presence of several circulation loops is favorable in a block with water –water reactor. In the case of accidental stoppage of one of these the operation of the block will continue. Without special difficulties it is possible to make emergency arrangements in the system of automation and protection of the reactor. At the same time it is necessary to make emergency arrangements for turbines. In practice it means that two turbogenerators should be installed in a block with reactor, so that in the case of an accidental disconnection of one of these there will not be a complete shutdown of the reactor to the cold state. This fact has not as yet been considered obligatory.

We should also take into consideration the fact that in accidental shutdowns of the reactor the rate of change of temperature in its walls can be appreciably larger than that stipulated in the design and the instructions. Therefore, the admissible number of such shutdowns can be smaller than it is assumed. The scale factor of the reactor units plays a particularly large role.

We should also touch upon the other aspects of this problem. For a reactor at 1000 MW the installation of two turbogenerators at 500 MW instead of one at 1000 MW will be somewhat costlier. But there are some operational advantages with two turbogenerators. If it is assumed that a turbogenerator in a monoblock is shut off accidently once a year, then with two turbogenerators in the block the same reliability should be expected with one accidental shutdown of each of these, i.e., two disconnections of the turbogenerators per year. In this case the number of disconnections in accidents increases. However, if we assume that the shutdown period of the turbogenerators is the same, then in both cases mentioned above nondelivery of electric power will also be the same. Actually, it can be assumed that a turbine of smaller capacity has a somewhat larger reliability especially due to correspondingly less developed blading, smaller length, and smaller dimensions of the condenser. Besides, it requires correspondingly less expenditure in revision and repair. Therefore, it can be assumed that in general the coefficient of utilization (or, at least, readiness) of two generators in the block is higher than of a single more powerful one. It is also significant that simultaneous accidents in the two turbogenerators are improbable. As a result in the case of accidental disconnection of one of these the block will continue to produce electrical power and the necessary pace of work of the operational personnel of the atomic power plant is also maintained. The conditions of operation of the power system as a whole will also be more favorable and less strained, since the stoppage of, for example, one turbogenerator with 500 MW capacity in the block with a capacity of 1000 MW is incomparably less unpleasant than the whole aggregate with 1000 MW capacity going out of service.

The argument of the larger reliability of a reactor compared to a turbogenerator was presented earlier in favor of installation of a block with two turbogenerators [8]. This argument is correct especially in regard to water–water reactors. As already mentioned, in this reactor the reliability of circulation loops operating in parallel, while the reliability of the automatic control and protection system is ensured by reserves in the equipment. A relatively weak point are the fuel elements, since their total number in the active zone is several tens of thousand and due to this the breakdown of the hermetic sealing of isolated fuel elements is in practice unavoidable. However, experience has shown that the operation of the block can continue quite successfully and, therefore, the shutdown of the reactor is not at all required. Unlike the reactor a turbogenerator is a far more complicated dynamic system. In reliability a turbogenerator is appreciably inferior to a reactor. From this point of view, for equalizing the reliability of the two main aggregates of the block it is apparently advisable to have two turbogenerators in the block.

Thus, in the blocks of atomic power plants, especially with water–water reactors, two turbogenerators should be installed in each block. In particular, in a block at 1000 MW it is necessary to install two turbogenerators of 500 MW each. This variant is interesting also in this respect that saturated steam turbines with 500 MW capacity can be made at 3000 rpm. Turbines at 1000 MW, necessary for monoblocks, must necessarily be slow-speed (at 1500 rpm) with correspondingly larger size and overall weight. Thus, according to [9] the saturated steam turbine of the firm General Electric with 1000 MW capacity at 1800 rpm, consisting of a high-pressure cylinder and three double-flow low-pressure cylinders, has an overall length of the shaft equal to 61 m. In this respect these slow-speed machines cannot be considered progressive. Therefore the problem of departure from these back to turbogenerators at 3000 rpm is apparently of interest. We note that a Soviet turbine with 500 MW capacity and rate of rotation of the rotor equal to 3000 rpm has its shaft over 41 m long.

We would like to stress again that the problem of preventing shutdowns of the reactor to the cold state is the main one due to the danger to the strength of the frame. The authors give preference to the variant of a block with two turbogenerators as the most rational and feasible from these points of view.

LITERATURE CITED

1. P. Zmola, Size, Effect, and Cost of Incremental Capacity for Light-Water Reactors, IAEA Symposium, Vienna, October, 1970.
2. Rules for Use of Electrical and Thermal Energy, Section 72, Energiya, Moscow (1970).
3. Yu. V. Guk, N. A. Kazak, and A. V. Myasnikov, Theory and Computation of Reliability of Electric Supply Systems, Energiya, Moscow (1970), p. 172.

4. L. Abourdarham et al., Energie Nucl., 12, No. 3, 211 (1970).
5. E. Gabriel and D. Smith, The Steam Generating Heavy-Water Reactor (SGHWR) – Technical Status and Operating Experience, IAEA Symposium, Vienna, October, 1970.
6. A. Metteil, Problemes Poses par l'Exploitation des Centrales Nucleaires, IAEA Symposium, Vienna, October, 1970.
7. P. Ashmole and Gregory, Operating Requirements for Nuclear Plant in the UK and Their Effects on Station Design, IAEA Symposium, Vienna, October, 1970.
8. Yu. D. Arsen'ev and G. N. Kruzhilin, At. Energ., 28, 291 (1970); Yu. D. Arsen'ev, On the Justification of Choice of Turbines for Reactors in Atomic Power Plants, IAEA Symposium, Vienna, October, 1970.
9. K. Richard and C. Schabtach, The Future of Nuclear Steam Power Generation, World Power Conference, Tokyo, October, 1966.

EFFECT OF STRESS ON THE HARDENING ORIENTATION IN URANIUM

V. F. Zelenskii and V. S. Krasnorutskii

UDC 669.017.3

In studying the effect of stresses on the orientation in uranium during the $\beta \rightarrow \alpha$ transformation at high cooling rates, it has been found [1] that, in the case of the slip mechanism of $\beta \rightarrow \alpha$ transformation, the resulting hardening orientation in the bulk of the metal is determined primarily by the magnitude and direction of the forces applied. A mechanism of this phenomenon has also been proposed in [1].

We shall consider the effect of stresses on the hardening orientation at different cooling rates in uranium, including rates that are sufficiently low for the slip nucleation and the diffusion growth of α-uranium crystals to play an important role in the $\beta \rightarrow \alpha$ transformation [2].

We used 99.80%-pure uranium in the shape of wire (diameter, 4 mm) or tubes (outside diameter, 4.3 mm; wall thickness, 0.4 mm). The specimens, which had a length of 100 mm and were protected from oxidation by a thin copper layer, were heated in air in a resistance furnace to 750°C (the duration of the β phase was 4 min). They were then stressed by means of a special adapter and cooled under load at the assigned rate to room temperature.

Maintaining stability constitutes the main difficulty in producing uniaxial compressive stresses in long, small-diameter rods. This problem was solved by using tubular specimens. The lower, thicker end of the tube, which had a diameter of 6.5 mm, was rigidly fastened to a base. A long molybdenum rod with a diameter of 3.3 mm and a cap at its upper end was passed through the channel in the specimen and an opening in the base. The required load was suspended from the lower end of the rod, while the cap rested on the top end of the tube and transmitted the load to the specimen.

The experiments were performed at the following cooling rates: ~700, ~20, and ~1 deg C/sec. These rates were maintained while the specimens were cooled in water, in air, and simultaneously with the furnace.

The type of orientation was estimated with respect to the linear expansion coefficient α and the electric resistivity ρ, measured along the specimen's axis, and also with respect to the growth index $G_{\alpha\rho}$, calculated according to the method of Stobo and Pawelski [3].

It is obvious from Fig. 1 that the application of tensile stresses tends to increase the share of the [010] orientation in the direction of the wire axis in hardening at a rate of ~700 deg C/sec; it produces virtually no effect at a cooling rate of ~20 deg C/sec; and it tends to increase the share of the [100] orientation at ~1 deg C/sec. The maximum stresses indicated in Fig. 1 are determined by the strength of uranium under the experimental conditions. The increase in the strength of uranium at higher cooling rates is apparently connected with the sharp reduction in the transformation temperature observed in this case [2, 4].

Figure 2 shows the distribution of the values of α, ρ, and $G_{\alpha\rho}$ in the layers of specimens cooled at different rates. A similar orientation distribution over the cross section is observed at any cooling rate, regardless of changes in the external stresses.

Figure 3 shows the dependence of $G_{\alpha\rho}$ on the cooling rate of specimens from the β phase. It is seen that the [100] orientation becomes more strongly pronounced with a reduction in the cooling rate.

Figure 4 shows the behavior of α and $G_{\alpha\rho}$ as functions of the tensile and compressive stresses applied to the tubular specimens during their cooling in water from the β phase.

Translated from Atomnaya Énergiya, Vol. 31, No. 5, pp. 449-452, November, 1971. Original article submitted September 28, 1970; revision submitted April 20, 1971.

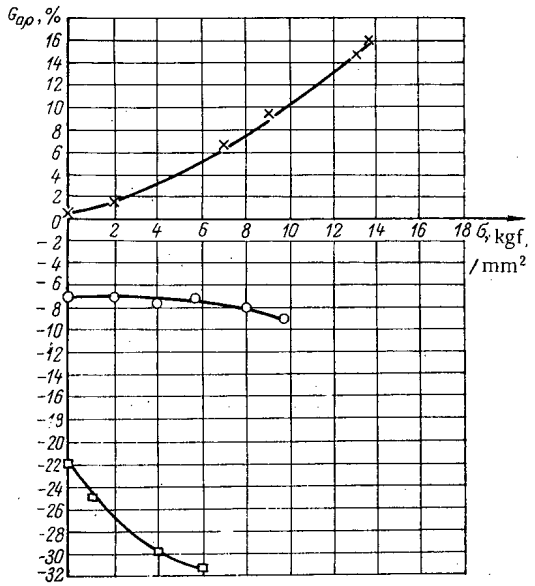

Fig. 1. Dependence of $G_{\alpha\rho}$ on the tensile axial stress at different rates of uranium cooling from the β phase. □) ~1 deg C/sec; ○) ~20 deg C/sec; ×) ~700 deg C/sec.

According to [1], in uranium hardening from the β phase, the degree of orientation is determined by the internal stresses in the specimen and by the system of orientation relationships between the β matrix and the α phase nucleus that plays the basic role in transformation. On the basis of analysis of experimental data on the effect of tensile stresses, it has been suggested that compressive stresses should suppress the growth of α crystals with the [010] orientation in the direction of the forces applied at a cooling rate of ~700 deg C/sec, when the $\beta \rightarrow \alpha$ transformation occurs according to the martensite mechanism.

This conclusion is confirmed by our results, which are given in Fig. 4. Application of external compressive stresses promotes the development of the [100] orientation in the direction of the forces applied. This manifestation of stress action corresponds to the conditions for the third orientation relationship, which was found experimentally in [5] and confirmed theoretically by Lomer [6].

All the above holds under the assumption that the nucleation and growth of crystals in the $\beta \rightarrow \alpha$ transformation in uranium occurs according to the martensite mechanism.

The orientations developing in uranium specimens as they pass through a temperature gradient of 62 deg C/sec at a rate of 0.25 cm/h from an initial temperature of 760°C have been investigated in [7]. It has been shown that an orientation close to [010] in the direction perpendicular to the plane of the phase front develops in commercially pure uranium. On the basis of the assumption of the "diffusion" nature of the $\beta \rightarrow \alpha$ transformation at this cooling rate, the conclusion has been reached that any process leading to a reduction in the

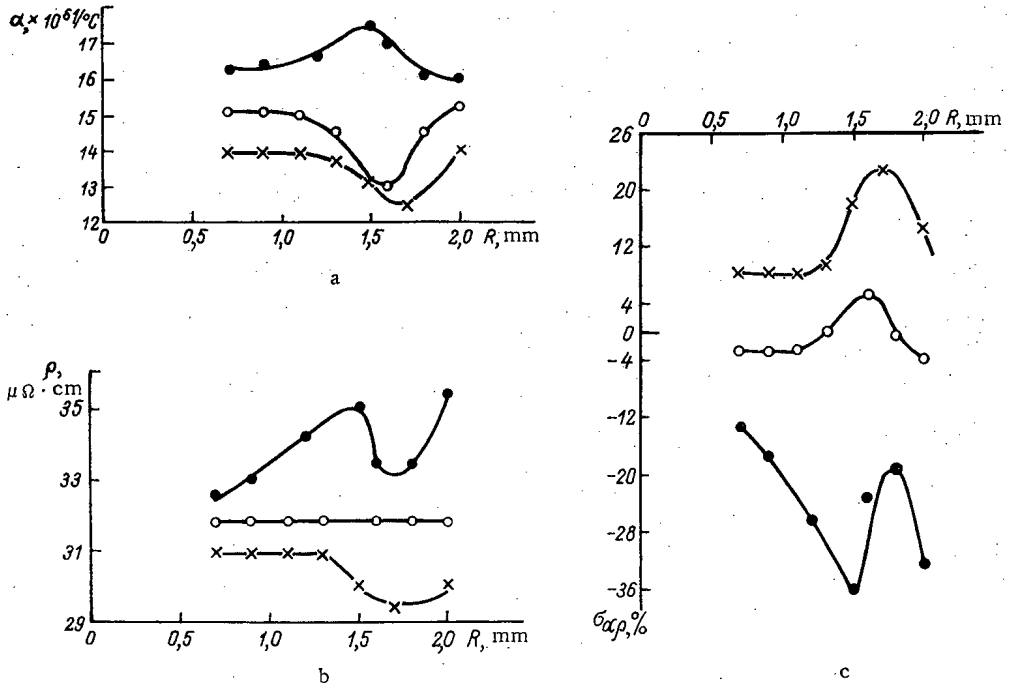

Fig. 2. Distribution of the values of α, ρ, and $G_{\alpha\rho}$ over the cross section of the specimens cooled from the β phase at different rates (a, b, and c, respectively). ●) ~ 1 deg C/sec; ○) ~ 20 deg C/sec; ×) ~700 deg C/sec.

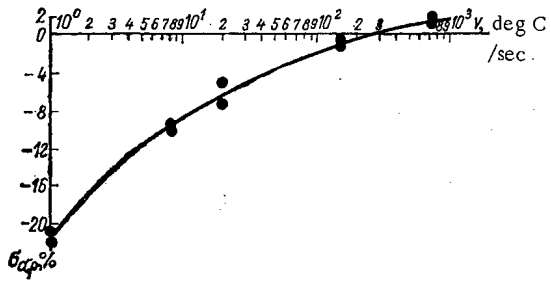

Fig. 3. Effect of the cooling rate on the hardening orientation in uranium.

compressive stresses at the boundary of a growing α-crystal will promote the growth of crystals with the orientation [010] perpendicular to the plane of the phase front.

In our experiments, the cooling has been such that the phase front must have the shape of a cylinder coaxial with the specimen, while the forces producing tensile stresses must be applied along the specimen's axis.

The experimental results given in Fig. 1 indicate that, at the cooling rate ~1 deg C/sec, tensile stresses produce the [100] orientation in the direction of force application, i.e., orientations [010] and [001] are formed predominantly in the direction perpendicular to the phase front. This fact contradicts the concepts developed in [7]. It could be explained on the basis of the earlier propositions [1], assuming, as was done in [2], that the nucleation of α-uranium crystals occurs according to the slip mechanism also at low cooling rates, although the subsequent crystal growth occurs mainly as a result of diffusion.

In this case, the $\beta \rightarrow \alpha$ transformation can take place if one of the three orientation relationships mentioned in [2, 5] is satisfied. Comparison of the deformations experienced by a β crystal during the $\beta \rightarrow \alpha$ transformation (they are given for three orientation relationships in [2]) with the effect of stresses on the hardening orientation in uranium at the cooling rate ~1 deg C/sec indicates that the second orientation relationship must be satisfied in this case.

In particular, the fact that the hardening orientation is independent of the stress in uranium at a cooling of ~20 deg C/sec (see Fig. 1) may be due to the fact that the nucleation of α-uranium crystals in this case can occur with equal probability when either the second or the third orientation relationship is satisfied.

The data on the distribution of the hardening orientation over the cross section given in Fig. 2 become clear if we consider the nature of the stress distribution in cylindrical uranium specimens in cooling from the β phase.

By analogy with [8], it can be stated that large tensile stresses σ_z and small compressive stresses σ_r arise in the external layers of cylindrical specimens in the region of the phase front during uranium cooling from the β phase. As the phase front progresses into the inner part of the specimen, σ_z approaches zero and assumes the opposite sign. The compressive stresses σ_r first increase, and then, after the outside layers have cooled to such an extent that they form a strong shell, they diminish, approaching zero and sometimes assuming even negative values. In specimens cooled at different rates, the stress levels are different, but the stress distribution over the cross section must be constant.

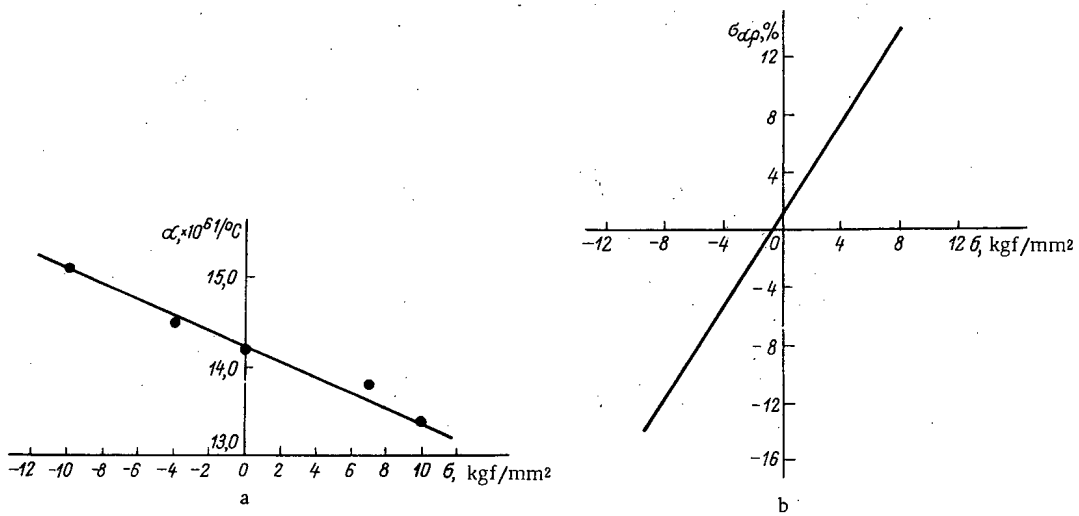

Fig. 4. Dependences of α and $G_{\alpha\rho}$ on the stress applied to tubular specimens cooled in water from the β-phase.

As was shown above, stresses in uranium during the $\beta \rightarrow \alpha$ transformation cause the development of an orientation whose type depends on the cooling rate. While the internal stresses acting on a certain layer promote the development of the [010] orientation, in specimens cooled at ~700 deg C/sec, they promote the development of the [100] orientation in similar uranium specimens cooled from the β phase at the rate of ~1 deg C/sec. This is illustrated by the experimental data given in Fig. 2.

It follows from the above data that uranium cooling from the β phase at different rates produces conditions for the occurrence of various orientation relationships between the β matrix and a growing α crystal. This effect and the different stress levels in specimens determined the various orientation levels in uranium cooled from the α phase at different rates (see Fig. 3).

LITERATURE CITED

1. V. F. Zelenskii, V. S. Krasnorutskii, and V. V. Kunchenko, At. Energ., 27, 411 (1969).
2. A. N. Holden, Physical Metallography of Uranium [Russian translation], Metallurgizdat, Moscow (1962).
3. J. Stobo and Pawelskii, J. Nucl. Materials, 4, No. 1, 109 (1961).
4. P. Duwez, J. Appl. Phys., 24, 152 (1953).
5. B. Buteher and A. Rowe, Inst. Metals. Symposium on the Mechanism of Phase Transformations in Metals (1955), pp. 229.
6. W. Lomer, The Beta–Alpha Transformation in Uranium–1.4 At.% Chromium Alloy. Inst. Metals, London Monograph and Rep. Ser. (1955)., p. 243.
7. J. Stobo et al., "Preferred orientation in alpha uranium," Acta Metallurg., 13, 624 (1965).
8. J. E. Russell, "The stresses in large masses of steel cooling from the austenitic region," Symposium on Internal Stresses in Metals, London (1948), p. 95.

THE ROLE OF STRUCTURAL – MORPHOLOGICAL FACTORS IN FORMATION OF FISSURE-TYPE SUPERGENE ZONES IN URANIUM – MOLYBDENUM DEPOSITS

K. V. Skvortsova and I. S. Modnikov

UDC 550.8:553.495

Investigations of supergene zones of uranium–molybdenum deposits localized in volcanic systems have established that the structures and forms of the ore bodies have a marked effect on the depth of occurrence, the forms of segregation, and sometimes even the associations of supergene minerals.

Smirnov [1] was the first to indicate the importance of structural– morphological factors in the formation of oxidation zones of sulfide deposits. Subsequently, many investigators of the oxidation zones of uranium and molybdenum deposits noted the importance of the structure and morphology of ore bodies during oxidation (see, for example, [2, 3]). However, the principal attention was devoted to mineralogical –geochemical factors, of which the most important was deemed to be the composition of hypogene ores. The uranium–molybdenum deposits studied by the present authors differ from one another not only in the composition of the hypogene ores, but also in the structural–morphological characteristics of the ore bodies, due mainly to the position of the volcanic systems adjoining the ores in the geological structures of the region.

The deposits are located within an intrageoanticlinical uplift, complicated by large troughs near faults and by troughs with a three-stage structure.

The lower structural stage is complicated by Ordovician and Lower Silurian sand–shale deposits, the middle stage by Lower and Middle Devonian volcanic–sedimentary formations of an andesite–molasse association, and the upper stage by Upper Devonian rocks of the rhyolite–granite association.

The ore fields are located in the near-fault troughs and coincide spatially with large paleovolcanic centers, fromed during repeated activation of abyssal faults with various orientations. The principal ore-adjoining structures are volcanic systems, located in the marginal sectors of the paleovolcanic centers.

The ore-adjoining volcanic systems complicated by rhyolite–porphyries and their explosive breccia originated during formation of the lower and upper structural stages. At the time of ore formation, the volcanic systems occupied different positions in the cross section of the adjoining rocks. Modnikov distinguished three types of ore-adjoining bodies: closed, screened, and open. The volcanic systems of the middle structural stage, overlain at the time of ore formation by gently pitching volcanic–sedimentary strata, were assigned to the closed type. The screened and open bodies are characteristic of the upper stage. In the screened bodies the apical parts are intersected by thick gently-pitching dykes of microgranite. During the period of ore formation, bodies of the open type were exposed at the surface.

In the closed and screened volcanic bodies, the economically workable mineralization, which has a considerable vertical range, is represented by stockworks, localized in the nodes of steep faults of different orders (Fig. 1). Preore quartz–sericite (with pyrite) hydrothermal alterations of the country rocks are much in evidence. The chief association of the ore minerals, forming predominantly microimpregnated ores, is an arsenopyrite–pitchblende association, replaced at depths below 300 m by an essentially pitchblende mineralization with coffinite.

Close-lying, extended, gently-pitching fissures and fissured zones predominate in the open volcanic systems, partially in their upper parts. In the marginal parts of the vents, the gently-pitching faults

Translated from Atomnaya Énergiya, Vol. 31, No. 5, pp. 453-458, November, 1971. Original article submitted September 22, 1970.

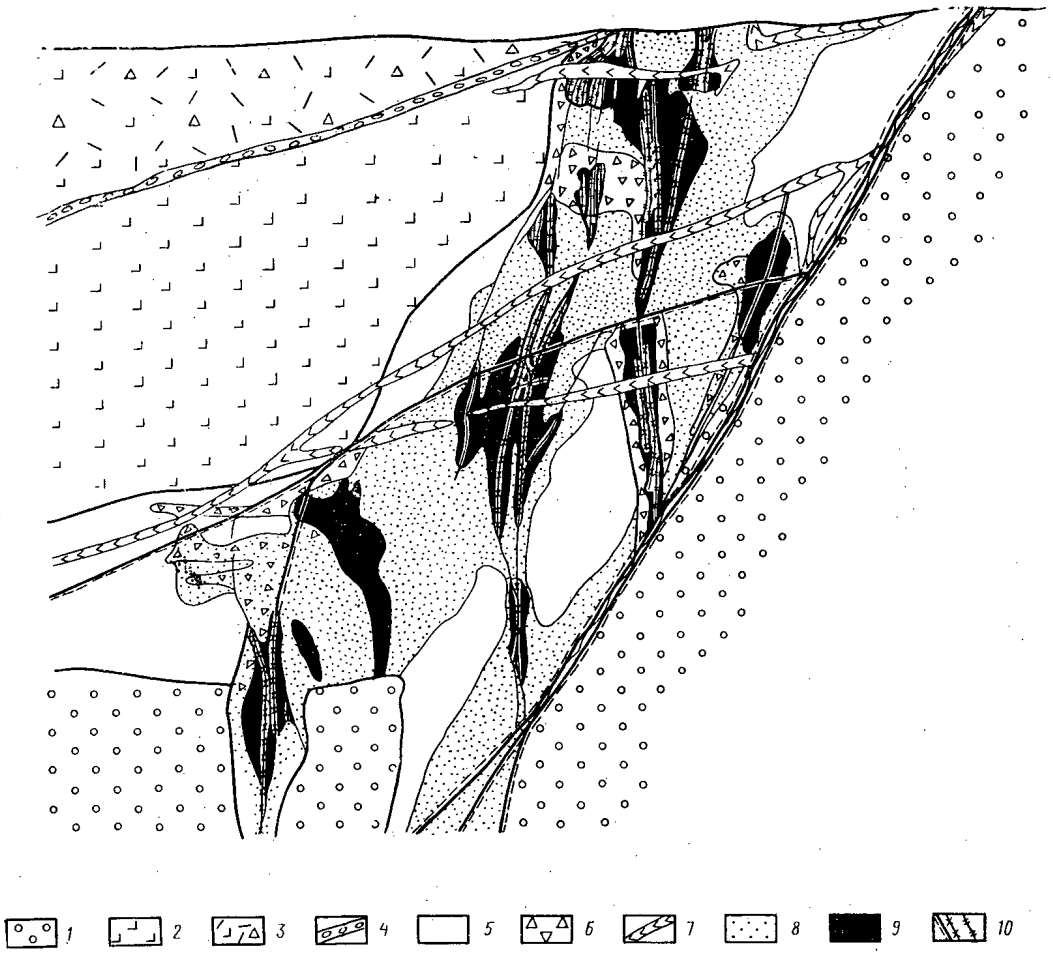

Fig. 1. Distribution of supergene minerals in the ore bodies of a deposit localized in a closed-type volcanic body: 1) red-bed sandstones; 2) superincumbent andesite porphyrites and their tuff breccia; 3) upper tuffaceous–sedimentary strata; 4) basal conglomerates; 5) subvolcanic rhyolite–porphyries; 6) tuff breccia of rhyolite–porphyries; 7) quartz microdiorite dykes; 8) quartzified and sericitized rhyolite–porphyries; 9) hypogene ore; 10) second-order faults and supergene minerals in third-order faults.

gradually become steeper as we approach the main ore-controlling steep fractures (Fig. 2). Preore hydrothermal quartz–sericite alterations occur locally along the principal disjunctive dislocations and steep faults in the peripheral parts of the ore bodies. The latter are found as stockworks and lenses in the upper parts of the bodies, in the regions of intense development of gently-pitching fissured structures. Hypogene ore minerals, forming predominantly streaky and breccia-type ores, are represented principally by an association of pitchblende with femolite (Mo_5FeS_{11}), arsenic-bearing pyrite (with up to 4% As), and smaller amounts of sphalerite, galene, and chalcopyrite. Sulfides (pyrite and femolite) are clearly predominant in the upper horizons of the deposits: they sometimes form independent ore bodies.

All these types of deposits display supergene alternations of the ores. Common factors of primary importance for supergene processes are as follows: the absence of an areal weathering crust, an arid climate, a shallow level of the present-day subsurface waters (seldom more than 20 m below the surface), and the composition of the waters (essentially sodium–sulfate–chloride).

The available hydrogeological data indicate very retarded circulation of subsurface waters in the slightly faulted rocks and more intense circulation in the fault zones. The movement of the subsurface waters in the gently-pitching faults is more retarded than in the steep faults.

In all these deposits most of the ore bodies exposed from the surface have been oxidized and leached at shallow depths. At depths greater than 5-10 m, oxidized minerals occur in the fissure zones adjoining

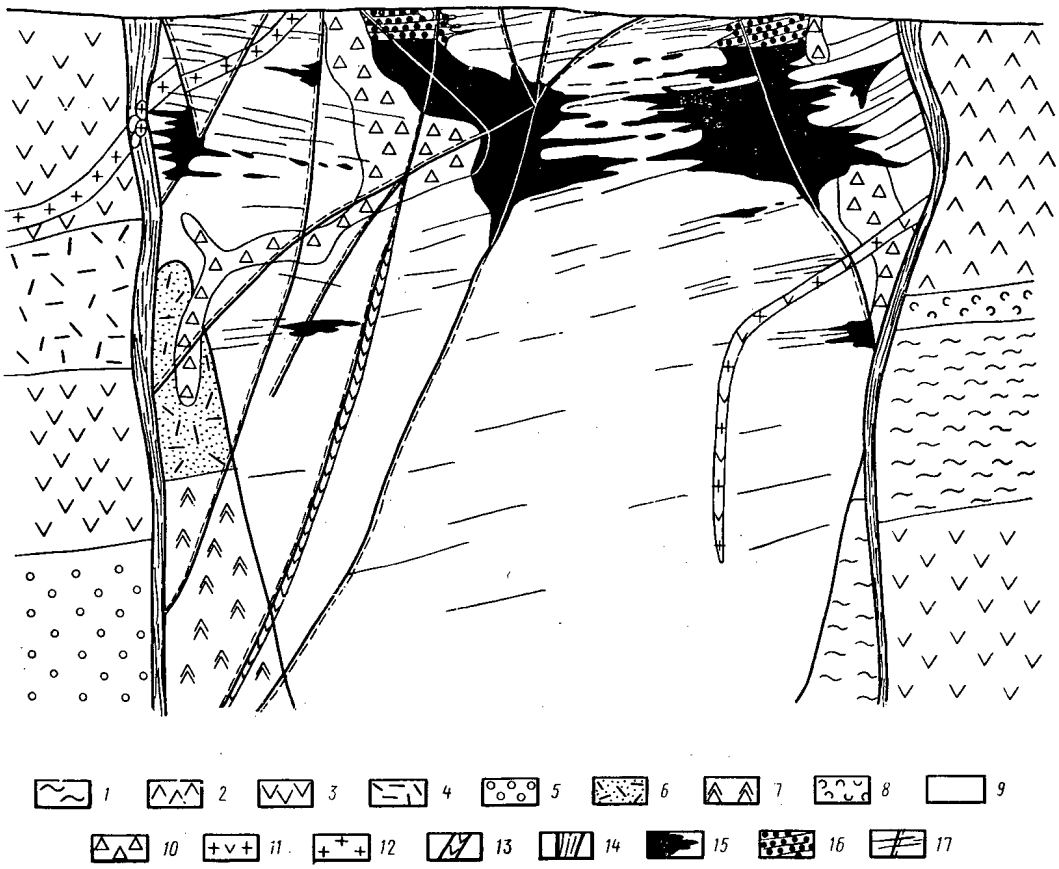

Fig. 2. Distribution of supergene minerals in the ore bodies of a deposit correlated with an open-type volcanic body: 1-8) superincumbent rhyolite–porphyries and their tuffs; 9) subvolcanic rhyolite–porphyries; 10) tuff breccia of rhyolite–porphyries; 11) dykes of extrusive felsite–porphyries; 12) dykes of quartz porphyries; 13) dykes of quartz microdiorites; 14) second-order faults; 15) hypogene mineralization; 16) supergene mineralization; 17) third-order faults and fine fracting.

the faults of different orders, but hypogene or completely unoxidized ores are retained in the monolithic slightly faulted blocks.

In the closed volcanic systems, the apical parts of which have been exposed by erosion, the unoxidized ore front extends to a lesser depth (less than 10-15 m). Below 15 m, among the hypogene ores we observed only linear fissure zones of occurrence of supergene minerals, which are traced to a depth of more than 600 m in the ore-controlling faults (Fig. 1). The zones of large faults exhibit particularly marked oxidation and leaching of the hypogene minerals (up to formation of kaolinites). The largest accumulations of supergene minerals are associated with acute angles of articulation of steep reversed faults or with the points at which the latter intersect the microfissure zones developed along the flow banding of the country rocks (Fig. 3).

In the more fissured zones near the faults, pseudomorphs of supergene minerals (predominantly uranium hydroxides and silicates) after pitchblende predominate among the microimpregnated ores near the faults. Figure 4 shows a photograph of a thin section (Fig. 4a) and a radiograph (Fig. 4b) of mixed ore in brecciated rhyolite–porphyry. Despite the nonuniformly patchy oxidation (see Fig. 4a), the initial brecciated texture of the hypogene ore is retained, as clearly recorded by the radiograph.

The vertical variation of the composition of the supergene minerals agrees closely with the composition of the hypogene ores. In the upper horizons of the deposits, in the zones of maximal occurrence of molybdenum and arsenic sulfides, considerable amounts of Ca–Na uranospinite, powellite, and wulfenite are found in the composition of the supergene ores. Below 300 m, in the zone of occurrence of pitchblende ores with coffinite, we observe a predominance of minerals of an essentially hydroxide–silicate association: hydronasturan, urhite, fourmarierite, β uranotile, and uranophane, with small amounts of wulfenite and powellite.

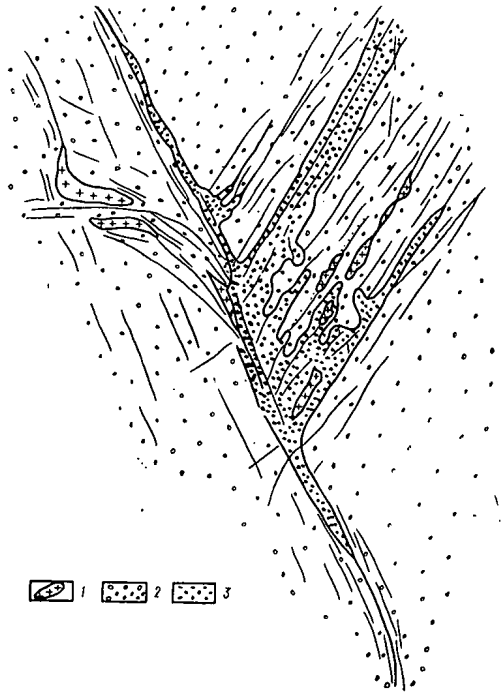

Fig. 3

Fig. 4

Fig. 3. Development of supergene minerals at the junction of a third-order fault and fine fissures along the flow banding of rhyolite–porphyries: 1) calcite; 2) coffinite –pitchblende hypogene ore; 3) supergene ore consisting of powellite, uranophane, and β uranotile.

Fig. 4. Oxidation of coffinite–pitchblende ore with retention of initial texture: a) transparent thin section (×5); b) radiograph (mirror image).

In the screened volcanic bodies, the oxidation zone is developed above a screening granite–porphyry dyke and consists of fine dotted outcrops of supergene ores. Oxidized minerals are found near the surface of pockets, disseminations, or films of uranium hydroxides, β uranotile, uranophane, and to a lesser extent uranospinite, etc. They were apparently all formed from pockets of hypogene minerals. Below the screening dyke the hypogene minerals have not been oxidized.

In the open volcanic bodies, supergene ores are found at depths of up to 20-30 m from the surface (see Fig. 2). A depth of ~5 m is reached by the zone of completely oxidized and partly leached ores, represented by uranium-containing iron and manganese hydroxides, hyalites, uranium vanadates, powellite, and partly by jarosite. At a greater depth, there is a predominance of mixed hypogene and supergene ores; among the hypogene or incompletely oxidized minerals, pockets, films, and veinlets of minerals, characteristic of the zone of complete oxidation, occur in the fissures. While the hypogene ores exhibit much the same composition, different associations of supergene minerals are found in the different structural– morphological zones.

Mourite, wulfenite, iriginite, ferrimolybdite, Ca–Na uranospinite, and sabugalite (Fig. 5) are present in the gently-pitching ore bodies, represented by massive brecciated and streaky pitchblende–femolite ores with high concentrations of ore components. Here all these minerals are enveloped by a considerable amount of gypsum. In the steep zones of pocket and impregnated ores, sericitized and carbonatized rhyolite–porphyries we observe a predominance of associations of supergene minerals containing calcium and sodium: umohoite, powellite, Ca–Na uranomolybdates, β uranotile, uranophane, natrojarosite, geothite, and hydrogeothite (see Fig. 5). Gypsum is absent. The conditions under which these minerals (with particular reference to certain rare and new uranium–molybdenum minerals) are formed during supergene alteration of pitchblende–femolite–pyrite ores were examined in previous communications [4, 5].

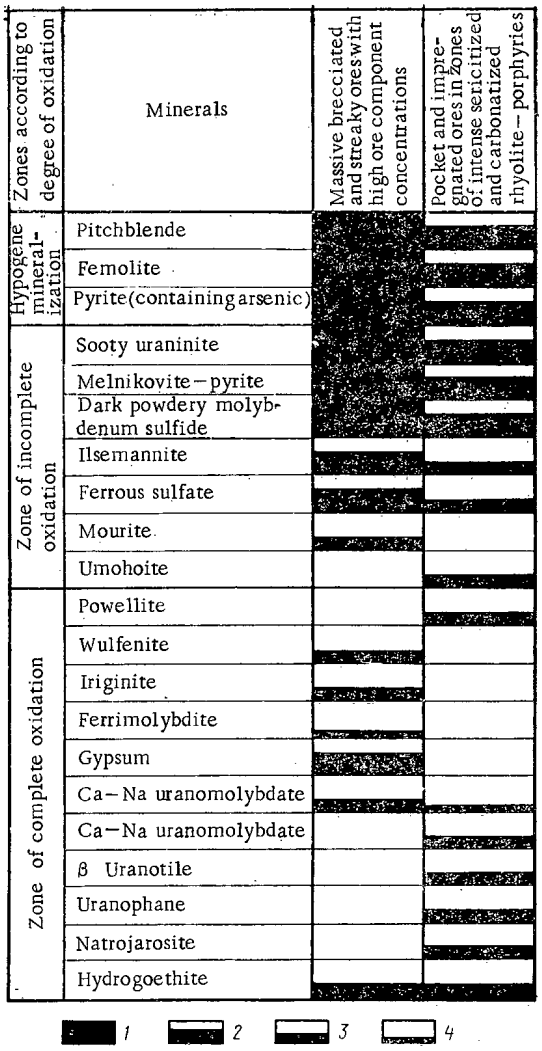

Fig. 5. Associations of supergene minerals in different morphological types of ores: 1) extensive occurrence; 2) average occurance; 3) limited occurrence; 4) found in isolated accumulations.

In those sectors where the ore bodies exposed by erosion shearing are of essentially femolite–pyrite composition, the oxidation zone includes mainly sodium-containing betpakdalite, natrojarosite, geothite, hydrogeothite, and less frequently ferrimolybdite and pharmacosiderite, etc. Near the surface, these minerals are segregated in both massive and impregnated ores.

Comparison of the data on the different types of deposits enables us to draw the following conclusions:

1. In all the deposits the supergene zones have a fissure character. The intensity of development of supergene minerals and the depth of their occurrence are related to the structural and morphological characteristics of the ore bodies, which determine the conditions of circulation of the surface water.

2. For hypogene ores of the same composition, different associations of supergene minerals may be formed in different structural–morphological zones.

3. The marked predominance of molybdenum minerals over uranium, or the presence of uranium –molybdenum, molybdenum, and arsenic minerals at the outcrops of the ore bodies, indicate a shallow erosion profile of the ore bodies.

4. The fact that the fault zones or their immediate vicinities contain pocket, impregnated, or microscopically streaky ores, represented by Ca–Na uranomolybdates, powellite, β uranotile, and uranophane, indicates exposure of the peripheral part of the rich uranium–molybdenum zone.

5. Rich pitchblende–femolite–pyrite ores may be revealed below the outcrops of essentially betpakdalite–jarosite ores with imbalance uranium contents.

6. Outcrops of ores of an essentially hydroxide–silicate association with a relatively low molybdate content may indicate the deep erosion profile of the deposit, composed of pitchblende or pitchblende–coffinite ores.

LITERATURE CITED

1. S. S. Smirnov, The Oxidation Zone of Sulfide Deposits [in Russian], Izd-vo AN SSSR, Moscow (1936).
2. L. P. Belova, Feasibility of Qualitative Interpretation of Oxidation Zones of Hydrothermal Uranium Deposits [in Russian], Nauka, Moscow (1968).
3. A. S. Mikhailov, Geokhimiya, No. 11, 1171 (1964).
4. K. V. Skvortsova et al., Zap. Vsesoyuzn. Mineralog. Ob-va, 98, 1, 29 (1969).
5. K. V. Skvortsova et al., ibid, 98, 679 (1969).

ANALYSIS OF EXPERIMENTS RELATING TO THE THERMALIZATION OF NEUTRONS IN THE GRAPHITE – WATER SYSTEM

V. I. Mostovoi, G. Ya. Trukhanov, Yu. A. Safin, and V. N. Moskovkin

UDC 539.125.5.162.2:621.039.512.45

Investigations into the thermalization of neutrons in the graphite–water system in the presence of a temperature jump and with a graphite temperature of 133-823°K have been carried out over a period of several years in the I. V. Kurchatov Institute of Atomic Energy. Communications regarding these investigations and a preliminary analysis of the experimental data were presented at conferences of the International Agency for Atomic Energy [1, 2]. Recently [3-5] a detailed analysis of experimental data has been given for the case of low graphite temperatures (133-443°K), using methods specially developed for the purpose [3]. In this paper we shall analyze the results of experiments relating to graphite temperatures of 443-823°K.

Experimental Arrangements. The experimental apparatus used for the measurements was detailed earlier [1]. The test system comprised a graphite prism 100 × 100 × 59.5 cm in size and an aluminum water tank of dimensions 170 × 170 × 50 cm, separated by screens, systems for heating the graphite and cooling the water, and an apparatus for measuring the neutrons spectra by the time-of-flight method. The neutron spectra, constituting vector fluxes $\varphi(z, v, 1)$ in a direction perpendicular to the interface, were measured at points z situated at the following distances from the temperature jump: a) in the graphite: 0, 0.5, 1.0, 2.0, 4.5, 9.5, 19.5, 29.5, 29.5, 39.5, 49.5, 59.5 cm; b) in the water: 0, 0.1, 0.2, 0.3, 0.5, 0.7, 1, 1.5, 2.0, 3.0, 5.0, 7.5 cm. The measurements were carried out for the following graphite and water temperatures, respectively: first series 443 and 298°K, second 594 and 302°K, third 725 and 305°, and fourth 823 and 305°K.

Space-Energy Distribution of the Neutrons. The results of the measurements were compared with a numerical solution of the kinetic equation for the neutron flux

$$\mu \frac{\partial \varphi(z, v, \mu)}{\partial z} + \Sigma_t(z, v)\,\varphi(z, v, \mu) = \int_{-1}^{+1} d\mu' \int_{0}^{v_{\lim}} \Sigma_{s0}(z, \mu \leftarrow \mu', v \leftarrow v')\,\varphi(z, v', \mu')\,dv' + S(z, v, \mu). \quad (1)$$

Equation (1) was solved for an isotropic scattering cross section by the quasidiffusion method [6] using the "DEMETRA" program [7]. The differential scattering cross sections were calculated for water by the Nelkin model using the "PRADIS" program prepared by G. F. Liman, and for graphite by the "PRASSIV" program [8], allowing for the $P(\beta)$ spectra obtained by Igelstaff. The limiting energy of the thermal-neutron spectrum E_{lim} was 0.9 eV for a graphite temperature of 443 and 594°K and 1.2 eV for a graphite temperature of 725 and 823°K. The neutron sources were placed in the graphite at a distance of 17.5 cm from the temperature jump and in the water at a distance of 4 cm; the neutron source in the graphite $S_C(v)$ had the form of a spectrum in an infinite medium filled with graphite of the type under consideration (with the T_C specified); the neutron source in the water $S_{H_2O}(v)$ had the form of a neutron spectrum in an infinite medium filled with water.

We see from Fig. 1 that the neutron spectra calculated with due allowance for chemical bonds agree closely with the experimental spectra for all graphite temperatures. The same figure gives the neutron spectrum calculated by the gas scattering model with $T_C \doteq 594$°K. We see that the influence of the chemical

Translated from Atomnaya Énergiya, Vol. 31, No. 5, pp. 459-464, November, 1971. Original article submitted November 16, 1970; revision submitted June 8, 1971.

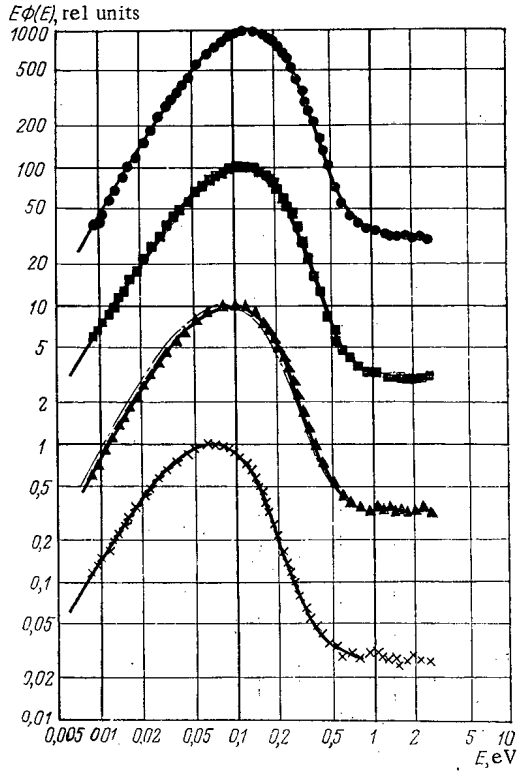

Fig. 1

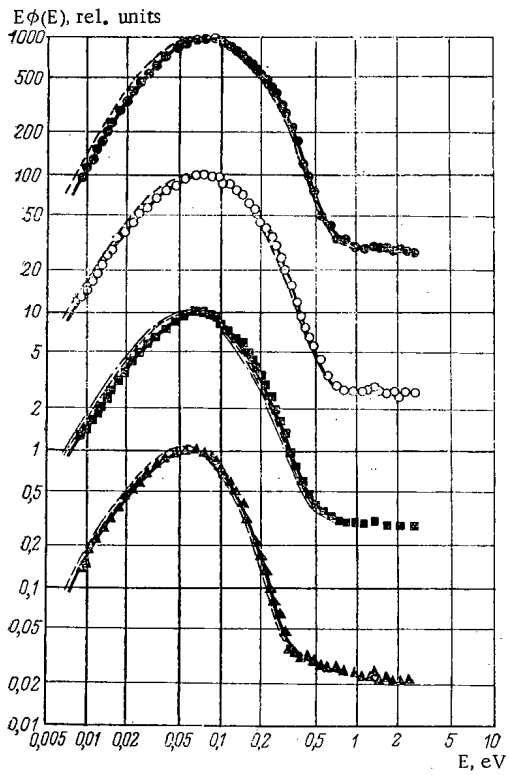

Fig. 2

Fig. 1. Neutron spectra in graphite at a distance of 2 cm from the temperature jump for various graphite temperatures. Experiment: ×) series I; ▲) series II; ■) series III; ●) series IV. Calculation: ———) quasidiffusion solution of the kinetic equation with differential scattering cross section allowing for the chemical bonds; –·–·–·–) quasidiffusion solution of the kinetic equation with the gas scattering model.

Fig. 2. Neutron spectra in water at a distance of 0.5 cm from the temperature jump for various graphite temperatures. Experiment: ▲) series I; ■) series II; ○) series III; ●) series IV. Calculation: ———) solution of the kinetic equation with due allowance for chemical bonds and a correction for scattering anisotropy; – – – –) quasidiffusion solution of the kinetic equation with due allowance for chemical bonds but without a correction for scattering anisotropy; –·–·–·–) quasidiffusion solution of the kinetic equation with the gas scattering model.

bonds is very considerable near the temperature jump. Figure 2 shows the neutron spectra in water. The neutron flux calculated with due allowance for scattering anisotropy was taken from another paper [1] for comparison. We see that the effect of neutron scattering anisotropy in water is quite considerable and requires to be taken into consideration, particularly in the presence of large flux gradients due to temperature and absorption gradients, etc. The difference between the spectra calculated with and without allowing for anisotropy increased with rising temperature gradient. For the second series of experiments, the results of a calculation based on the gas scattering model are presented. The effect of the chemical bond is also appreciable. In the earlier investigation [2], measurements in an apparatus only differing from ours in respect of the geometry and dimensions of the water tank (a cylinder 38 cm in diameter) were analyzed. Abdullaev et al. [2] found a considerable difference between theory and experiment in the transitional energy range at points lying close to the temperature jump; this was explained as being due to the effect of the two-dimensional conditions. In our own experiments, the dimensions of the water tank were greater than those of the graphite prism, which enabled us to check the earlier results [2] for the same graphite temperature of 443°K. Figures 3 and 4 illustrate our measurements of the neutron spectra in graphite at a distance of 19.5 cm and in water at a distance of 0.5 cm from the temperature jump. The same figures give the earlier calculated and experimental spectra [2]. We see that the calculation based on the one-dimensional kinetic equation agrees closely with our own measurements. Thus the reason for the disagreement

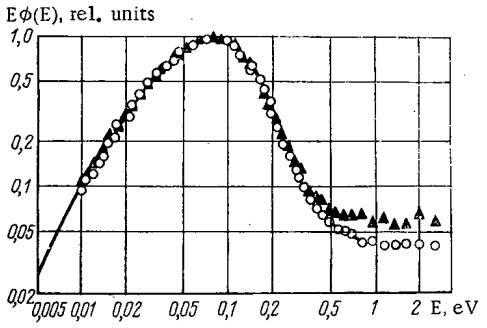

Fig. 3

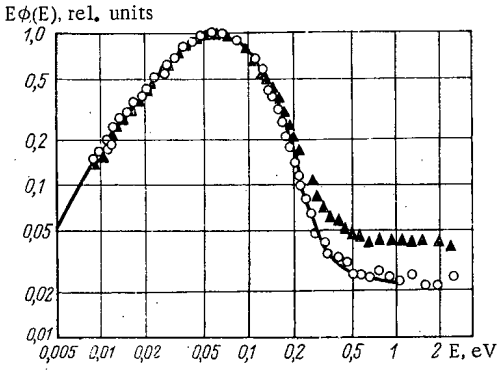

Fig. 4

Fig. 3. Neutron spectra in graphite at a distance of 19.5 cm from the temperature jump for T_C = 443 and T_{H_2O} = 298°K (series I). ○) Experimental (present investigation); ——) calculation in one-dimensional geometry [2]; △) experiment [2].

Fig. 4. Neutron spectra in water at a distance of 0.5 cm from the temperature jump for T_C = 443 and T_{H_2O} = 298°K (series I). Notation as in Fig. 3.

between theory and experimental for the earlier neutrons spectra [2] in fact lies in the two-dimensional effect. Analysis shows that modern computing methods enable us to make correct allowance for the thermalization effect in one-dimensional scattering systems with a severe temperature gradient, at any rate to within the limits of experimental error.

Method of Obtaining the Relaxation Lengths of the Neutron Flux. The relaxation lengths of the neutron flux constitute the reciprocals of the discrete eigenvalues of the problems arising on separating the variables in the kinetic equation; they are determined solely by the properties of the medium and are independent of the form of the sources, i.e., they contain information regarding the scattering law of the medium, and may therefore be used for verifying the models of the scattering center. On the other hand, a knowledge of several of the first relaxation lengths of the neutron flux and the corresponding eigenfunctions sometimes enables us to construct a fairly accurate approximate solution of the kinetic equation. The diffusion length L_0, equal to the reciprocal of the zeroth discrete eigenvalue $\varkappa_0$, and the first relaxation length $L_1 = 1/\varkappa_1$ (and in some cases $L_2 = 1/\varkappa_2$ as well) may be obtained by analyzing the asymptotic behavior of the neutron density or certain other integrated quantities. We may demonstrate this for the plane case if there are only two discrete relaxation lengths L_0 and L_2 in the system. Then the vector neutron flux on the asymptotic for $z > 1/\varkappa^*$ [where $\varkappa^* = \min \Sigma_i(E)$ is the boundary between the continuous and discrete parts of the spectrum of eigenvalues of the kinetic equation, $\Sigma_t(E)$ is the total interaction cross section] may be expressed in the form

$$\varphi(z, E, \mu) = \sum_{n=0;\ 1} C_n f_n(E, \mu) \exp\left(-\frac{z}{L_n}\right). \tag{2}$$

Here $f_n(E, \mu)$ are the eigenfunctions corresponding to the discrete eigenvalues $\varkappa_0$ and $\varkappa_1$; C_n (n = 0; 1) are the coefficients of the expansion. For the integrated neutron density we obtain

$$n(z) \approx \sum_{n=0;\ 1} P_n \exp\left(-\frac{z}{L_n}\right), \tag{3}$$

where P_n are the corresponding integrals with respect to angles and energy in Eq. (2). We see from this that, on describing the experimental neutron density $n_{exp}(z)$ in the asymptotic region ($z > 1/\varkappa^*$) by an expression of type (3), we may derive the fundamental relaxation length L_0 and the first relaxation length L_1, provided that the experimental conditions satisfy those on which Eq. (3) was based.

Let us now find the asymptotic expression for the temperature of the neutron gas. On the assumptions made for obtaining Eq. (3) we obtain† ($z > 1/\varkappa^*$)

† The eigenfunctions $f_0(\mu, E)$ and $f_1(\mu, E)$ are solutions of the kinetic equation in the absence of sources, including sources at infinity, with respect to energy. This means that $f_0(\mu, E)$ and $f_1(\mu, E)$ do not contain a spectrum of 1/E, and hence the upper limit in the integrals of these functions with respect to energy may be taken as infinite.

$$T(z,\mu)=\frac{\int E^{1/2}\varphi(z,E,\mu)\,dE}{\int E^{-1/2}\varphi(z,E,\mu)\,dE}=\frac{\bar{E}_0(\mu)+C(\mu)\,\bar{E}_1(\mu)\exp(-z/L_r)}{1+C(\mu)\exp(-z/L_r)};$$

$$C(\mu)=\frac{C_1\int f_1(\mu,E)E^{-1/2}\,dE}{C_0\int f_0(\mu,E)E^{-1/2}\,dE};\qquad E_n=\frac{\int f_n(\mu,E)E^{1/2}\,dE}{\int f_n(\mu,E)E^{-1/2}\,dE},\quad (n=0,1), \tag{4}$$

where

$$L_r^{-1}=L_1^{-1}-L_0^{-1}. \tag{5}$$

Equation (4) may be transformed into

$$T(z,\mu)\approx T_2+(T_1-T_2)\frac{g}{b+\exp(z/L_r)}, \tag{6}$$

where

$$T_2=\bar{E}_0(\mu);\quad b=C(\mu);$$
$$(T_1-T_2)\,g=[\bar{E}_1(\mu)-\bar{E}_0(\mu)]\,C(\mu).$$

For $z > L_r$ we obtain the relation

$$T(z,\mu)\approx T_2+(T_1-T_2)\,g\exp\left(-\frac{z}{L_r}\right), \tag{7}$$

coinciding with the well-known asymptotic expression for the temperature of the neutron gas: $T(z) \approx T_\infty + (T_0 - T_\infty)\exp(-z/L_r)$; here L_r denotes the so-called relaxation temperature of the neutron-gas temperature. On the approximation of the asymptotic behavior of the experimental neutron-gas temperature, we may use Eqs. (6) and (7) to obtain the relaxation length L_r, which is related to the relaxation lengths of the neutron flux by Eq. (5), provided that the experiment conforms to the conditions assumed in deriving Eqs. (6) and (7).

Method of Restoring the Neutron Rethermalization Lengths. The rethermalization length is the name given to one of the two relaxation lengths characterizing the method of overlapping groups in the P_1 approximation. The second of these is called the overlapping-group diffusion length. The difference between the relaxation lengths of the method of overlapping groups and the true neutron-flux relaxation lengths just considered lies in the fact that the former may be used to describe the neutron flux over the whole range of variation of the space variable with a uniform accuracy, whereas the true relaxation lengths give the correct asymptotic behavior of the neutron flux. We may illustrate this for the case of the overlapping-group equations considered in the P_1 approximation for a two-zone plane system. In accordance with the fundamental principle of the method of overlapping groups, the neutron flux at any point z in either of the zones of the plane two-zone system may be expressed in the form

$$\Psi(z,v)=\sum_{l=1;\,2}\Psi_l(z)\chi_l(v), \tag{8}$$

where $\chi_1(x)$ and $\chi_2(v)$ are trial functions. The weighting functions Ψ_1 and Ψ_2 in the P_1 approximation satisfy the well-known system of equations [1]:

$$D_1\Delta\Psi_1(z)-(\Sigma_{a1}+\Sigma_R^{1\to2})\Psi_1(z)+\Sigma_R^{2\to1}\Psi_2(z)=-S_1(z);$$
$$D_2\Delta\Psi_2(z)-(\Sigma_{a2}+\Sigma_R^{2\to1})\Psi_2(z)+\Sigma_R^{1\to2}\Psi_1(z)=-S_2(z), \tag{9}$$

where the physical quantities have been given their usual notation.

The radical distinction between (8) and (2) lies in the fact, that instead of the eigenfunctions and "eigen" lengths relating to the medium in question, Eq. (8) uses different functions and lengths. Clearly, when the trial functions χ_e give a poor reproduction of the eigenfunctions of the problem, Eq. (8) will give an incorrect asymptotic for the neutron flux. However, there is no real need to secure an accurate asymptotic from Eq. (8), which is used simply in order to reproduce the neutron spectrum to a uniform accuracy

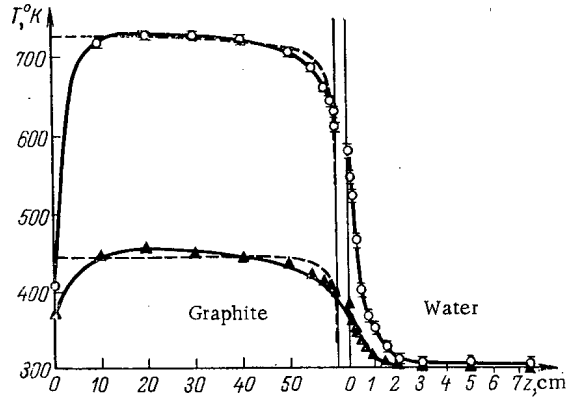

Fig. 5

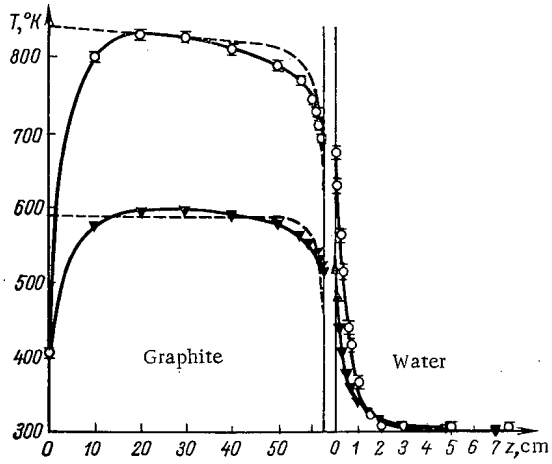

Fig. 6

Fig. 5. Neutron temperature distribution in graphite and water obtained from the measurements of series I [Δ) neutron temperature; ----) temperature of medium] and series III [○) neutron temperature; ----) temperature of medium].

Fig. 6. Distribution of neutron temperatures in graphite and water obtained from measurements of series II [▽) neutron temperature; ----) temperature of the medium] and series IV [○) neutron temperature; ----) temperature of the medium].

TABLE 1. Neutron-Gas Temperature Relaxation Lengths and First Relaxation Lengths of the Neutron Flux in Water

Equation	Relaxation length, cm	Series of measurements			
		first	second	third	fourth
(6)	L_r	0,37±0,04	0,43±0,04	0,36±0,04	0,40±0,04
	L_1	0,33±0,03	0,37±0,04	0,32±0,03	0,35±0,03
(7)	L_r	0,50±0,05	0,47±0,05	0,50±0,05	0,48±0,05
	L_1	0,42±0,04	0,40±0,04	0,42±0,04	0,41±0,04

over the whole range of z. This means that the relaxation lengths of the method of overlapping groups are not universal. The degree of universality of these lengths is directly related to their closeness to the true relaxation lengths. Hence the overlapping-group relaxation lengths are of interest from the following considerations: firstly, they constitute an approximation to the corresponding true relaxation lengths; second, they may be used within the framework of the method of overlapping groups in order to solve reactor problems; thirdly, they constitute a certain intergrated characteristic of the experiment. The overlapping-group relaxation lengths (the overlapping-group diffusion length and the rethermalization length) are characteristic numbers of systems of homogeneous differential equations corresponding to system (9). These numbers may be found if we know the parameters D_l, $\Sigma_{al\,(l=1,2)}$ $\Sigma_R^{1\to 2}$ and $\Sigma_R^{2\to 1}$. The rethermalization length may also be found from the neutron-gas temperature distribution by using Eqs. (6) and (7), subject to the following conditions. Equation (6) is obtained within the framework of the method of overlapping groups provided that, in the system of equations (9), the sources S_1 and S_2 and the rethermalization cross section corresponding to the transition of neutrons from the equilibrium to the nonequilibrium group may be taken as zero for one of the zones. Then the relaxation length of the neutron-gas temperature (within the framework of the method of overlapping groups) L_r is related to the diffusion length L_D and the rethermalization length L_{rt} by an expression analogous to (5):

$$L_r^{-1} = L_{rt}^{-1} - L_D^{-1}. \qquad (5a)$$

Equation (7) for the neutron-gas temperature is obtained within the framework of the method of overlapping groups if, in addition to the conditions just formulated, the equations $D_1 = D_2$ and $\Sigma_{a1} = \Sigma_{a2}$ are satisfied. In both cases the range of minimization of the parameters should coincide with the whole range of variation of the space variable.

Relaxation Lengths in Water. Equations (6) and (7) were used in order to analyze the asymptotic behavior of the temperature of the neutron gas in water, as obtained from experimental spectra. The spatial distribution of the temperature $T = m(\overline{1/v})_m/4k$, where $(1/v)_m$ is the reciprocal velocity corresponding to the most probable velocity in the distribution $v\varphi(z, v, 1)$ in graphite and water is shown in Figs. 5 and 6. The parameters g, b, and $1/L_r$ were determined by minimization of the corresponding functions, using the programs developed earlier [9], in the range z = 0.7-3 cm (here z is the distance from the temperature jump). The relaxation lengths of the neutron-gas temperature L_r are given in Table 1.

TABLE 2. Relaxation Lengths of the Method of Overlapping Groups in Graphite

Rethermalization length in graphite, cm	Series of measurements			
	first	second	third	fourth
	T_1=454° K	T_1=596° K	T_1 = 726° K	T_1 = 830° K
L_r	7,4±0,7	6,3±0,6	5,1±0,5	4,9±0,5
L_{rt}	5,6±0,6	4,9±0,5	4,1±0,4	4,0±0,4
L_{rt} [11]	—	4,2±0,2*	3,5±0,2 †	3,5±0,2 ‡

* T_C = 523°K, T_{H_2O} = 299° K.
† T_C = 690° K, T_{H_2O} = 308° K.
‡ T_C = 828° K, T_{H_2O} = 315° K.

TABLE 3. Relaxation Lengths of the Method of Overlapping Groups in Water

Rethermalization length in water, cm	Series of measurements			
	first	second	third	fourth
	T_2=303° K	T_2=310° K	T_2=311° K	T_2=315° K
L_r	0,52±0,05	0,44±0,04	0,45±0,04	0,48±0,05
L_{rt}	0,44±0,04	0,38±0,04	0,39±0,04	0,41±0,04
L_{rt} [11]	0,35±0,04	0,36±0,04†	0,55±0,05 ‡	—

* T_C = 410° K, T_{H_2O} = 292° K.
† T_C = 558° K, T_{H_2O} = 243° K.
‡ T_C = 720° K, T_{H_2O} = 295° K.

The first relaxation length of the neutron flux L_1 was obtained from Eq. (5); we obtained the diffusion length L_0, equal to 2.83 cm (at T = 300°K), in separate measurements. The average values of the first relaxation length in water L_1 found from Eqs. (6) and (7) equalled 0.34 and 0.41 cm, respectively. We note that, in order to analyze the experiments in the asymptotic region, it was desirable to use Eq. (6) rather than (7), since the former started describing the asymptotic part of the experimental curve for smaller values of z than the latter. The resultant values obtained for L_1 [4] were much smaller than the limiting possible value for water $1/\varkappa^* = 0.74$ cm. On the one hand, this may mean that in water there is only one fundamental relaxation length, and the values actually obtained constitute the result of an attempt to describe the continuous spectrum of eigenvalues by means of a single discrete eigenvalue. On the other hand, the fact that all the values lie in a specific range 0.27-0.42 cm (within the limits of experimental error), may indicate the existence of a quasidiscrete relaxation length for water within the range of the continuous spectrum, just as, in the case of the nonstationary thermalization problem, quasidiscrete attenuation constants may occur [10].

Rethermalization Lengths in Graphite and Water. As a result of analyzing the spatial dependence of the neutron-gas temperature by means of Eq. (6), we obtained the rethermalization lengths is graphite and water. The parameters g, b, and $1/L_r$ were determined by minimizing the corresponding functional, using the program mentioned earlier [9]. The minimization was carried out in the range z = 0-3 cm for water and z = 0-29.5 cm for graphite. The resultant relaxation lengths of the neutron-gas temperature L_r and the rethermalization lengths L_{rt} are presented in Tables 2 and 3.

We see from the tables that the rethermalization length of the neutrons in graphite depends greatly on the graphite temperature. This refelcts the effects of the chemical bonds of graphite. The results obtained agree closely with earlier data [2, 5] and also the results of Bennett [11], thus showing that the rethermalization length in graphite closely approaches the true first relaxation length. The rethermalization lengths of the neutrons in water obtained in the present investigation and by earlier authors [2, 5, 12] differ from one another, and lie in the range 0.35-0.57 cm. There is no obvious dependence on the temperature of the neighboring zone. In our own opinion, the disagreement may be explained by the fact that, in determining the rethermalization lengths, we used constants D(E), Σ_a(E), Σ_s(E), and μ(E) obtained in independent experiments, these being averaged over the trial functions of both zones. This leads to a direct dependence of the rethermalization lengths on the choice of the original constants and on the form of the trial functions. The discrepancy in the rethermalization lengths of water indicates the nonuniversality of neutron-physical characteristics such as rethermalization length in water. Together with the fact that all the rethermalization lengths are much lower than the limiting value for the true discrete relaxation lengths in water (0.74 cm), this difference may serve as an additional indication of the absence of a first relaxation length where water is concerned.

In conclusion, the authors wish to thank L. V. Maoirov for useful discussions.

LITERATURE CITED

1. L. V. Maoirov et al., Pulsed Neutron Research, Vol. 1, IAEA, Vienna (1965), p. 657.
2. Kh. Sh. Abdullaev et al., Neutron Thermalization and Reactor Spectra, Vol. 2, IAEA, Vienna (1968), p. 233.
3. Kh. Sh. Abdullaev, V. D. Nikitin, and G. Ya. Trukhanov, Preprint IAE-1612 (1968).
4. Kh. Sh. Abdullaev et al., At. Energ., 26, 537 (1969).

5. Kh. Sh. Abdullaev et al., At. Energ., 26, 538 (1969).
6. G. Ya. Trukhanov, Preprint IAE-1875 (1969).
7. G. Ya. Trukhanov, Preprint IAE-2010 (1970).
8. L. V. Maiorov et al. (USSR), Third Geneva Conference, Paper No. 360 (1964).
9. G. Ya. Trukhanov, Preprint IAE-1973 (1970).
10. M. V. Kazarnovskii et al., Neutron Thermalization and Reactor Spectra, Vol. 2, IAEA, Vienna (1968), p. 331.
11. R. Bennett, Nucl. Sci. and Engng., 17, 191 (1963).
12. A. Rastas and J. Saastamoinen, Nucl. Sci. and Engng., 36, 351 (1969).

DIRECT-CHARGING DEVICE SENSES NEUTRON FLUX IN POWER REACTORS

E. N. Babulevich, M. Yu. Belavin,
E. I. Grishanin, B. G. Dubovskii,
V. A. Zagadkin, V. S. Kirsanov,
I. M. Kisil', A. A. Kononovich,
V. F. Lyubchenko, M. G. Mitel'man,
K. N. Mokhnatkin, G. P. Pochivalin,
and N. D. Rozenblyum

UDC 539.1.074.88

Efficient operation of nuclear electric power generating stations requires correct mapping and maintenance (or correct controlled variation) of the in-core neutron distribution during the reactor campaign.

The in-pile flux sensors utilized for this purpose are distinguished by their ability to function throughout the reactor campaign at temperatures at 750°C or higher. They are built to respond only slightly to pile γ emission. The sensor shows a linear response to neutron flux over a wide range of neutron flux variation. Burnup of neutron-sensitive material is modest, and can be taken duly into account by computational corrections, precalibration is not required thanks to the technological interchangeability of the flux sensors, reliance on an external power supply is not encouraged, strength and resistance requirements imposed on the insulation material are minimal, and the dimensions of the sensors are not such as to cause difficulties because of their positioning within the reactor core, nor such as to impede the technological process.

In the case of high-temperature reactors, all of these requirements are met by direct-charging detectors* [1-6]. Neutron flux measurements are handled by these sensors in a manner equivalent to the method of foils, but differing from the latter in the way induced activity is determined from the current, thereby rendering measurements easier and keeping a closer check on changes as they occur. The metrological features of the method of foils are also characteristic of direct-charging detectors: linear response to neutron flux, readings independent of the temperature, weak sensitivity to γ-ray background, etc. Direct-charging detectors are simple in design and easy to fabricate, do not require an external power source, and are capable of functioning at high temperatures; their transverse dimensions are small: some direct-charging detectors are less than 1.5 mm in outer diameter. The lower sensitivity limit of direct-charging detectors is determined by the characteristics of the measuring circuitry, while the upper limit is determined by the allowable rate of burnup of the emitter material and by the loss of resistance on the part of insulation material as the temperature increases. Sluggish response due to the finite decay constant of the induced activity, can be compensated by the use of correcting circuits [7, 8].

Figure 1 shows the calculated dependence of the cadmium ratio R_{Cd}^{Rh} on the diameter d of the radium emitter when the neutron spectrum remains unchanged. The ratio $R_{Cd}^{Rh} \gg R_{Cd}^{Au}$, particularly so as the emitter diameter is increased, i.e., the overwhelming bulk of the induced activity is due to thermal neutrons. Hence the effect of variations in the spectrum on the current in direct-charging detectors must be moderate, and must decrease with increasing emitter diameter. The experimental value of the ratio R_{Cd}^{Rh} in the MR reactor, where $R_{Cd}^{Au} = 5.2$, is 25 for an emitter diameter of 0.48 mm, which is in excellent agreement with the calculations.

* Foreign names for these detectors include: beta-emission detectors, PENA (Primary Electrons of Neutron Activations), SPD (Self-Powered Detectors), etc.

Translated from Atomnaya Énergiya, Vol. 37, No. 5, pp. 465-466, November, 1971. Original article submitted May 11, 1970; revision submitted December 7, 1970.

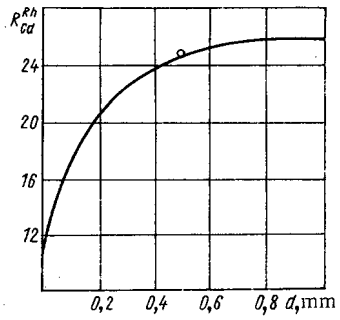

Fig. 1

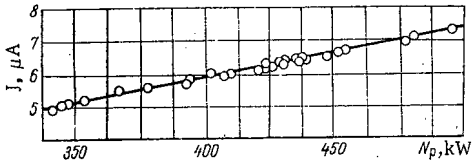

Fig. 2

Fig. 1. Dependence of ratio R_{Cd}^{Rh} (predicted) on emitter diameter; ○) experimentally determined ratio R_{Cd}^{Rh} in reactor, with $R_{Cd}^{Au} = 5.2$.

Fig. 2. Dependence of direct-charging detector current on output power level of MR reactor.

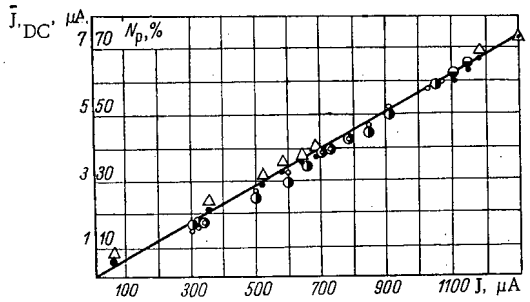

Fig. 3

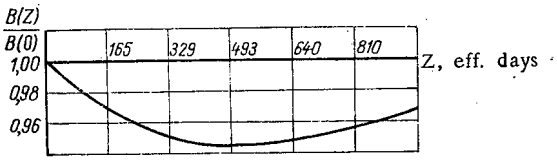

Fig. 4

Fig. 3. Correlation between direct-charging ($\bar{J}_{DC}$) and ionization chamber current ($\bar{J}_{IC}$), as well as reactor power (N_p, %) and J (data points normalized with respect to maximum ordinate). Output power level: ○) J_{DC} on Oct. 17, 1968; ●) $\bar{J}_{DC}$ on Dec. 6, 1968; ○) N_p on Oct. 17, 1968; △) N_p on Dec. 6, 1968.

Fig. 4. Variation of the ratio $B(Z) = J_{N_{fa}}^{DC}$ as a function of the burnup of the fissionable isotope $Z = \Phi\sigma_f t$, where σ_f is the fission cross section; Φ is the neutron flux; t is the exposure time.

The identity of direct-charging detector specimens is determined by the resistance of the insulation and by the dimensional tolerances of their design components. The resistance of the insulation was $\sim 10^5\ \Omega$ at temperatures above 650°C, at the site where direct-charging detectors were installed in the reactor of the Belyi Yar nuclear power station (BAES). This resistance remained practically unchanged throughout the operating history of the reactor and, when the input resistance of the measuring instrument was chosen correctly, exerted almost no effect on the indentity and interchangeability of the direct-charging detectors, which stayed within ±2% [9], and could be brought as close as ±1%.

The linearity in the readings of direct-charging detectors in response to changes in reactor output power has been verified experimentally for some reactors. Figure 2 shows the results plotted for direct-charging detectors in a fuel assembly in the MR reactor. The maximum error in the determination of the fuel assembly heat output was ±2%. The linear dependence of the direct-charging detector current on the fuel assembly output is quite in evidence; the spread in experimental data points falls well within the limits of error of the measurements. The linearity of the direct-charging detector readings in response to a 10^3-fold variation in flux in that reactor was also traced out.

Figure 3 shows the correlation between the average current flowing in twelve direct-charging detectors placed in the steam superheat channels of the reactor in the second power unit of the Belyi Yar nuclear power

station, and the current flowing in the standard ionization chambers, as well as the correlation between the chamber current and the reactor heat power output. The linear relationship between the direct-charging detector current and the neutron flux is evident. The spread in the experimental data points is not greater than ±4%. Similar data were obtained for the other reactors.

Service lifetime tests were carried out at the SM-2 reactor, the MR reactor, and the reactors at the Obninsk power station and Belyi Yar power station. The direct-charging detectors at the SM-2 reactor were kept in the dry capsule channel at temperatures of 650°C, while one of the detectors was exposed to a temperature of 900°C. The detectors kept functioning properly when exposed to integrated flux of $3 \cdot 10^{21}$ neutrons/cm^2 (this flux is greater than the flux integrated over the reactor campaign in the case of the BAES reactor). The detectors in the Obninsk power station and in the reactor of the Belyi Yar power station first power unit were tested over the course of 1.5 to 2.5 years at 600°C. Direct-charging detectors with rhodium and silver emitters were tested in the reactor of the second power unit of the Belyi Yar nuclear power station. The rhodium-emitter direct-charging detectors had been in operation for 22 months by the beginning of January 1970, while the silver-emitter direct-charging detectors had seen 17 months of service by that time. All of the direct-charging detectors tested remained serviceable, with virtually no change in the resistance of the insulation.

The time variation of the ratio of the direct-charging detector current to the power output of the fuel assembly N_{fa} into which the detector had been inserted is an important characteristic. This variation is related to the differential rate of burnup of the emitter material and of the fissionable material. In the case of reactors burning highly enriched uranium (as the Belyi Yar power station reactors), however, calculations show this change to be slight. We can see in Fig. 4 that three effective years of operation of direct-charging detectors in the reactor of the second power unit of the Belyi Yar power station produced a maximum change not greater than 5% in that ratio. A computational correction can be introduced into the direct-charging detector current when the power release distributions with respect to discrete points is recovered. The maximum error in the determination of the relative power output level of fuel channels provided with direct-charging detectors is ±8%.

LITERATURE CITED

1. M. G. Mitel'man, N. D. Rozenblyum, and R. S. Erofeev, At. Energ., 10, 72 (1961).
2. N. D. Rozenblyum et al., in: Large-Dose Dosimetry [in Russian], Fanlar, Tashkent (1966), p. 135.
3. J. Hilborn, Nucleonics, 22, 69 (1964).
4. G. Casarelly, Energia Nucleare, 10, 431 (1963).
5. P. Mass and P. Seiers, Rapp. CEA-R-2560 (1964).
6. W. Loosemore et al., "Radiation measurements," Nucl. Power Proc. Internat'l. Conf. (1966).
7. N. D. Rozenblyum et al., in: Dosimetry of High-Intensity Flux of Ionizing Radiations [in Russian], Fanlar, Tashkent (1969), p. 130.
8. G. Korn and T. Korn, Mathematical Handbook for Scientists and Engineers [in Russian], Vol. 1, Mir, Moscow (1967).
9. Type DPZ Direct-Charging Neutron Detectors [in Russian], V/O Izotop Catalogue, Moscow (1970).

EFFECT OF NONUNIFORMITY OF HEAT RELEASE IN A REACTOR ON THE ELECTRICAL CHARACTERISTICS OF THERMIONIC EMISSION CONVERTER

B. A. Yshakov, V. D. Nikitin, and V. Yu. Korbut

UDC 621.362

A nuclear reactor with built-in thermionic emission converters in the active zone (for example, in type ITR reactor [1]), designed for a sufficiently large electrical power, must have an appreciable number of single thermionic emission converters (TEC), since the usable voltage of each TEC is small. The possible nonuniformities of heat release over the active zones of the reactor may strongly affect the electrical characteristics of a single converter as well as of the reactor as a whole, especially for a series electrical connection of several TEC. Besides, the operating temperatures of the cathodes of the converters with a density of the usable electrical power, that is of practical interest, are close to the limiting admissible operating temperatures of the materials considered for use as cathode material. Therefore, an appreciable nonuniformity in the heat release over the volume of the active zone may cause the admissible operating temperatures of the cathodes to be exceeded locally and, hence, a disruption in the normal functioning of the TEC. A physical profiling of the heat release in the active zone of the reactor with the use of continuous change in the concentration of the fission material enables one to achieve a uniform distribution of the heat release over the active zone of the reactor [2]. However, this problem is technically very complex and is not always possible for technological or constructional reasons. The zonal profiling of heat release, when the concentration of the fission material remains constant in each zone, permits one to obtain integral heat release in each zone that is almost identical over the entire volume of the reactor. But within each zone the heat release is significantly nonuniform [3].

The distribution of heat release over the half-height of the active zone of a reactor with thermionic emission converters is presented in Fig. 1; the assumed electrical power of the reactor is 1 MW [4]. The distribution was obtained in profiling of heat release by changing the concentration of the fission material in three zones (zones I, II, III + IV). If the height of each zone I-IV conforms to the length of the TEC, then it is obvious that the integral heat release in each zone is different and the heat release over the cathode of each TEC is distributed nonuniformly.

Thus, in a reactor with built-in thermionic emission converters in the active zone even in the presence of a physical zone-wise profiling of heat release over the reactor the computation of the electrical characteristics and the temperature regime of each TEC must be done taking account of, firstly, the possible difference of the integral heat release in each zone, and secondly, the nonuniformity of the distribution of heat release in each zone.

In the present article the influence of the above-mentioned factors on the electrical characteristics and the temperature regime of TEC is investigated for the arc regime of operation of TEC, which is of greatest practical interest. The construction of the TEC is similar to the construction (Fig. 2) presented in [1, 4].

Procedure of Computations. The solution of the problem of the effect of nonuniformity of heat release on the temperature regime of the cathodes of the TEC and its electrical characteristics amounts to a self-consistent solution of the equation of heat conduction of the cathode and the equation determining the distribution of potential over the cathode, using the dependence of the emission current density on the temperature and the potential difference between the cathode and anode.

Translated from Atomnaya Énergiya, Vol. 31, No. 5, pp. 467-472, November, 1971. Original article submitted October 15, 1970; revision submitted March 12, 1971.

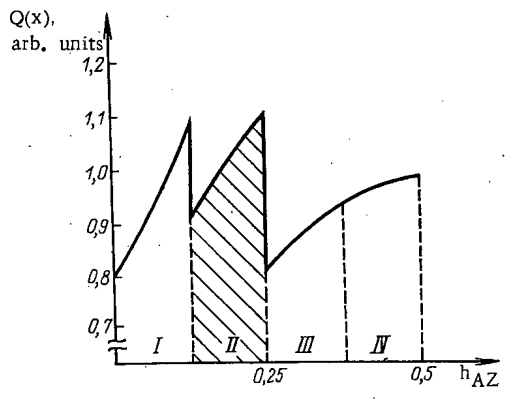

Fig. 1

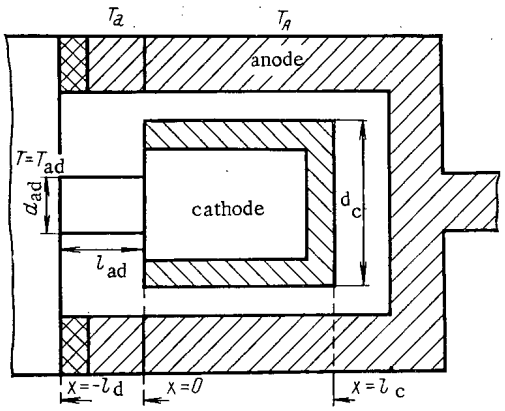

Fig. 2

Fig. 1. Distribution of heat release over half-height of the active zone of the reactor. The shaded area corresponds to the integral heat release in the second zone.

Fig. 2. Schematic diagram of thermal emission converter.

TABLE 1. Values of Parameters Used in the Computations

Parameter	Cathode		Cathode conductor
	casing	fuel	
Radius r, cm	0,5	0,4	0,4
Length l, cm	4,0; 5,0	4,0; 5,0	2,0
Mean coefficient of:			
electrical conductivity ρ, $\Omega \cdot$ cm	$0{,}56 \cdot 10^{-4}$	$4{,}5 \cdot 10^{-4}$	$0{,}5 \cdot 10^{-4}$
thermal conductivity λ, W/cm·°K	1,2	0,18	0,46
effective radiating capacity ε	0,25	—	0,25

In the solution of this problem the following main factors affecting the temperature regime of the cathode of TEC and its electrical characteristics were taken into consideration: the nonuniformity of heat release over the cathode; heat losses by the cathode (thermal conductivity across conductor adapter, connecting the cathode with the anode of the adjacent TEC or with the current injector), electron cooling, thermal conductivity across cesium pair, radiation from free face; Joule heating of the cathode and the adapter; voltage drop along the cathode; voltage drop in adapter and in anode.

The following assumptions were made:

a) Local effects related to the absence of direct contact of the casing and the fuel were disregarded.

b) The temperature dependence of the thermal and electrical conductivity coefficients of the materials of the cathode and the adapter was not taken into consideration, i.e., the values of these coefficients at the corresponding mean operating temperatures were used.

c) The one-dimensional problem was investigated.

The one-dimensional heat conduction equation for the cathode with the above-enumerated effects is similar to the corresponding equation of [5, 6]:

$$\lambda_c \pi r_c^2 \frac{d^2T}{dx^2} = 2\pi r_c \varepsilon_c \sigma [T^4(x) - T_A^4] + 2\pi r_c [\varphi_c(T, T_{Cs}) + 2kT] j(T, V_x) - 2\pi r_c \lambda_{Cs} [T(x) - T_A] - \pi r_c^2 Q_J(x) - \pi r_c^2 Q(x), \quad (1)$$

where T is the cathode temperature, T_{Cs} is the temperature of liquid cesium, σ is the Stefan–Boltzman constant, $Q_J(x)$ is the heat release at the cathode due to Joule heating, W/cm^3, Q(x) is the heat release at the cathode, W/cm^3, T_A is the mean temperature of the part of the anode facing the cathode, j is the emission current density, φ_c is the work function of the cathode, V_x is the voltage drop in the part of the cathode from the point x = 0 to the point x = x; the index "c" refers to the cathode and the remaining symbols are given in Table 1.

The one-dimensional heat conduction equation for the adapter had the form

$$\lambda_{ad} \pi r_{ad}^2 \frac{d^2T_{ad}}{dx^2} = 2\pi r_c \varepsilon_c \sigma [T_c^4(x) - T_a^4] - \frac{I^2 \rho_{ad}}{\pi r_{ad}^2}, \quad (2)$$

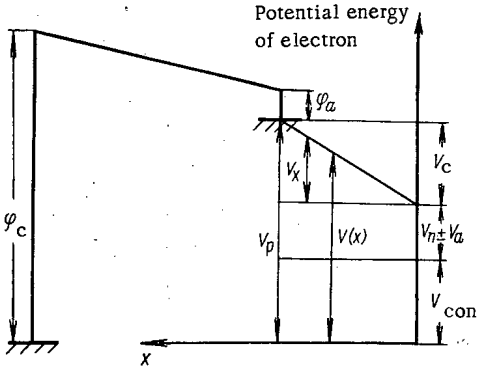

Fig. 3. Diagram of potential energy of electron (φ_a – work function of the anode; V_p – experimental value of usable voltage of the converter with isothermic cathode).

where I is the total current of the converter; the index "ad" refers to the adapter.

The boundary conditions are of the form (see Fig. 2):

$$\begin{aligned} &T|_{x=-l_{ad}} = T_{ad}; \quad T|_{x=+0} = T|_{x=-0}; \\ &\frac{dT}{dx}\Big|_{x=l_c} = \pi r_c^2 \varepsilon_c \sigma [T^4(x=l_c) - T_{at}^4]; \\ &\pi r_c^2 \lambda_c \frac{dT}{dx}\Big|_{x=+0} = \pi r_{ad}^2 \lambda_c \frac{dT}{dx}\Big|_{x=-0}, \end{aligned} \tag{3}$$

where T_a is the temperature of the part of the anode facing the adapter, T_{at} is the temperature of the construction element lying opposite the free face of the cathode, and d is the interelectrode distance. In the general case

$$T_A \neq T_a \neq T_{at} \neq T_{ad}.$$

The dependence of the work function of the cathode $\varphi_c(T, T_{Cs})$, entering into Eq. (1), on T and T_{Cs} was determined with the use of an empirical formula obtained by the authors:

$$\varphi(T, T_{Cs}) = \varphi_0 + \varphi_1 \left\{1 + \exp\left[\alpha\left(\frac{T_{Cs}}{T} - \beta\right)\right]\right\}^{-1}. \tag{4}$$

For tungsten the coefficients occurring in formula (4) have the following values: φ_0 = 2.08 eV, φ_1 = 2.48 V, α = 40.77, β = 0.288.

The coefficients of thermal conductivity λ_c and electrical conductivity ρ_c for a cathode consisting of the fuel and the casing of a high-melting metal were determined from the formula

$$\begin{aligned} \lambda_c &= \lambda_{cas} - \frac{\delta}{r_c}\left(2 - \frac{\delta}{r_c}\right) + \lambda_f \left(1 - \frac{\delta}{r_c}\right)^2; \\ \rho_c &= \rho_{cas}\left[\frac{\delta}{r_c}\left(2 - \frac{\delta}{r_c}\right) + \frac{\rho_{cas}}{\rho_f}\left(1 - \frac{\delta}{r_c}\right)^2\right]^{-1}, \end{aligned} \tag{5}$$

where λ_{cas}, λ_f are coefficients of thermal conductivity of the casing and the fuel, respectively, ρ_{cas}, ρ_f are the corresponding electrical conductivity coefficients, and δ is the thickness of the casing of the cathode.

The potential distribution over the cathode (Fig. 3) is determined by the equation

$$\frac{dV(x)}{dx} = \rho_c \frac{I(x)}{\pi r_c^2}, \tag{6}$$

where V(x) is the potential at a point on the cathode with the coordinate x relative to the anode, and I(x) is the total current flowing in the cathode across a section with coordinate x. This current is determined by the expression

$$\frac{dI(x)}{dx} = -2\pi r_c j(T, V_x). \tag{7}$$

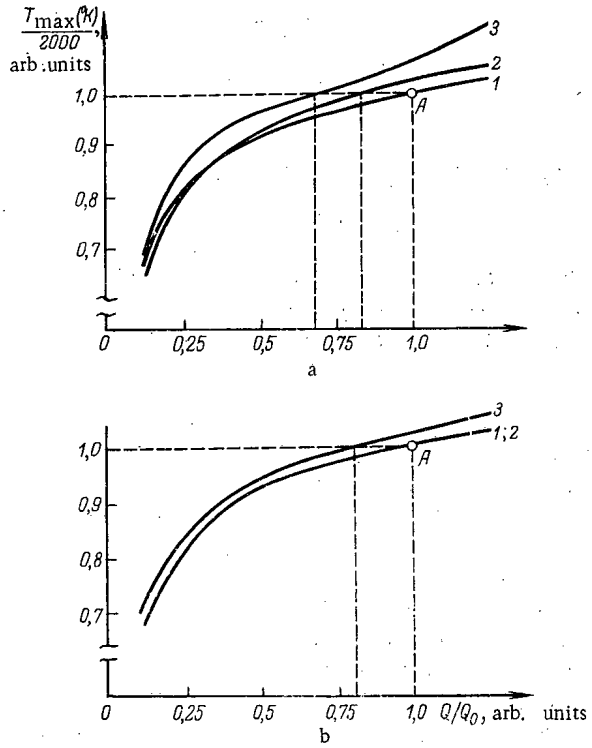

Fig. 4

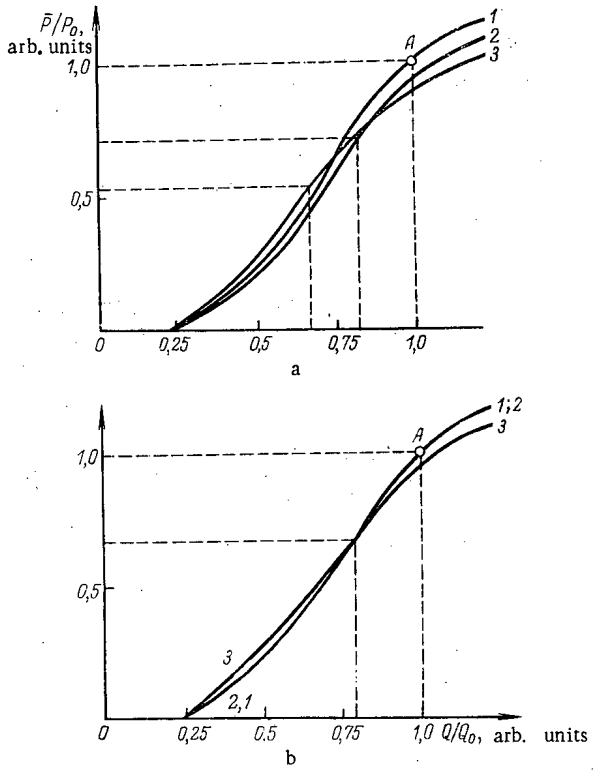

Fig. 5

Fig. 4. Dependence of maximum temperature of cathode on the integral heat release in the converter (Q = 1215 W). For a: 1) $\varkappa_Z = 1.0$; 2) $\varkappa_Z^+ = 1.6$; 3) $\varkappa_Z^- = 1.6$. b: 1) $\varkappa_Z = 1.0$; 2) $\varkappa_Z^+ = 1.3$; 3) $\varkappa_Z^- = 1.3$.

Fig. 5. Dependence of average density of usable electric power of the converter on the integral heat release in the converter (Q = 1215 W, $p_0 = 9.7$ W/cm^2). For a: 1) $\varkappa_Z = 1.0$; 2) $\varkappa_Z^+ = 1.6$; 3) $\varkappa_Z^- = 1.6$; b: 1) $\varkappa_Z = 1.0$; 2) $\varkappa_Z^+ = 1.3$; 3) $\varkappa^- = 1.3$.

It is obvious that I(0) = 1.

Equations (6) and (7) are reduced to the following equation:

$$\frac{d^2V(x)}{dx^2} = -\frac{2\pi\rho_c}{r_c} j(T, V_x). \tag{8}$$

The boundary conditions are of the form

$$\left.\frac{dV(x)}{dx}\right|_{x=l_c} = 0; \quad V(0) = V_{con} + V_{ad} + V_a, \tag{9}$$

where $V_{x|x=l_c} = V_c$ is the voltage drop at the cathode, V_{con} is the usable voltage of the converter, V_{ad} is the voltage drop at the adapter, and V_a is the voltage drop at the anode.

The system of equations (1), (2), and (8) with the boundary conditions (3) and (9) were written in the final form and solved on a computer. The values of $j(T, V_x)$ were specified in the form of a table.

For arbitrary values of the cathode temperature T and the potential V_x the emission current density j was found by interpolation from the values at the neighboring points.

RESULTS

The dependence of the electrical characteristics and the temperature distribution over the cathode on the integral heat release in TEC and the nonuniformity of heat release over the cathode is governed by many

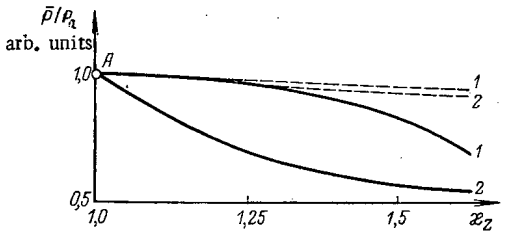

Fig. 6

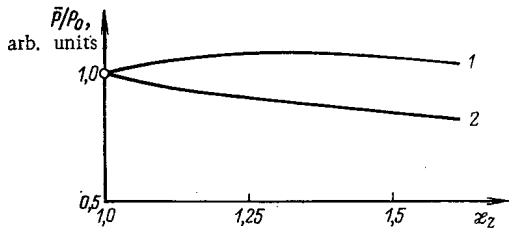

Fig. 7

Fig. 6. Dependence of average density of usable electrical power of the converter on the coefficient of nonuniformity of heat release over the cathode $\varkappa_z$ for the arc regime with $j \approx 40$ A/cm^2: 1) minimum of heat release at the free end of the cathode; 2) maximum of heat release at the free end of the cathode.

Fig. 7. Dependence of the average density of usable electrical power of the converter on the coefficient of nonuniformity of heat release over the cathode $\varkappa_z$ for the arc regime with $j \approx 40$ A/cm^2 and the condition $T_{max} = 2000$°K, $p_0 = 13.25$ W/cm^2: 1) minimum of heat release at the free end of the cathode; 2) maximum of heat release at the free end of the cathode.

parameters of operation of TEC, including the geometrical dimensions, the regime of operation of TEC, and the properties of the materials used. Below we present the results of computation for the arc regime of operation of TEC, which is of greatest practical interest, for a tungsten cathode and for typical values of the remaining parameters presented in Table 1 [4-6]. In determining $j(T, V_x)$ a family of experimental volt–ampere characteristics of a converter with isothermal cathode of tungsten with interelectrode distance $d = 0.05$ mm and $T_{Cs} = 593$°K [7] was used.

The lengths of the cathode l_c and the adapter l_{ad} were taken equal to 5 and 2 cm, which are optimum values from the point of view of useful electrical power of TEC for $\delta = 0.1$ cm, $T_A = T_a = T_{ad} = 1000$°K, $T_{at} = 1300$°K and for the values of the remaining parameters from Table 1. The electrical resistance of the anode R_a was taken equal to 1/4 R_c (where R_c is the total resistance of the cathode), $\varepsilon_c = 0.25$, $\lambda_{Cs} = 0.65 \cdot 10^{-4}$ W/cm·degK.

Different values of the integral heat relelease Q(x) over the cathode (i.e., two types of slope of the distribution of heat release over the cathode relative to the point $x = l_c/2$) were considered.

1) Maximum heat release at the boundary of the cathode with transitional (x = 0) and minimum at the end of the cathode ($x = l_c$).

2) Minimum heat release at the boundary of the cathode with transitional (x = 0) and maximum at the free end of the cathode ($x = l_c$).

The nonuniformity of heat release over the cathode is characterized by the nonuniformity factor x_z, which is defined as the ratio of the maximum heat release at the cathode to the mean heat release at the cathode, i.e.,

$$\varkappa_z = \frac{Q_{max}}{\frac{1}{l_c}\int Q(x)\,dx}.$$

We shall denote the coefficient of nonuniformity corresponding to the first type of nonuniformity of heat release (with minimum at the free end) by $\varkappa_z^+$ and that corresponding to the second type (with maximum at the free end) by $\varkappa_z^-$.

The computations were done for different values of the nonuniformity coefficients $\varkappa_z^{\pm}$ in the range $1 \leq \varkappa_z^{\pm} \leq 1.6$ and for different values of integral heat release over the cathode Q corresponding to the range of variation of the operating temperature of the cathode 1700-2100°K, where $Q = \pi r_k^2 \int_0^{l_c} Q(x)dx$.

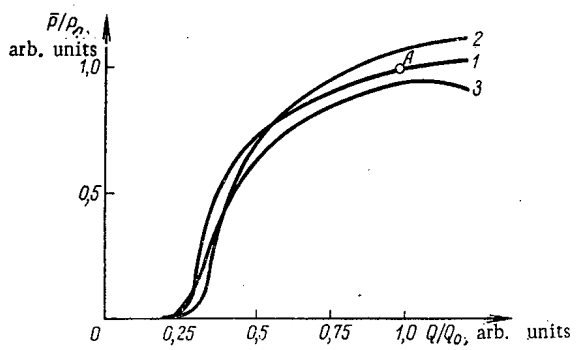

Fig. 8. Dependence of the average density of usable electrical power of the converter on the integral heat release for the arc regime with j $\approx$ 40 A/cm^2, Q = 1790 W, p_0 = 13.25 W/cm^2; 1) $\varkappa_Z$ = 1.0; 2) $\varkappa^+$ = 1.6; 3) $\varkappa^-$ = 1.6.

TABLE 2. Energy Balance of TEC

	Parameter	First regime	Second regime
Thermal balance	Total thermal powder delivered to the cathode, W	1215	1790
	Joule heating of the cathode, W	8	43
	Heat loss, W, by:		
	radiation	309	250
	emission current	554	1370
	heat conductivity across adapter	107	95
	heat conductivity across cesium	197	61
	radiation from the end face	56	57
Electrical balance	Total usable electrical power, W	152	166
	Losses W		
	at the cathode	8	43
	at the anode	2	10
	at the adapter	12,6	50
	Total current, A	180	505
	Average density:		
	of power, W/cm^2	9,7	13,25
	of current, A/cm^2	11,5	40,2
	Usable voltage, V	0,84	0,33
	Efficiency, %	12,5	9,3

The dependence of the maximum temperature of the cathode on the integral heat release over the cathode is presented in Fig. 4a and b for different slopes of the heat release over the cathode; $\varkappa_Z$ = 1; $\varkappa_Z^{\pm}$ = 1.3; $\varkappa_Z^{\pm}$ = 1.6. The data presented in this figure show that for identical integral heat releases, when the minimum of heat release occurs in the region of the cathode adjoining the adapter, the slopes of the second kind have an appreciably stronger effect on the maximum operating temperature of the cathode, than the slopes of the first kind, when the maximum of heat release occurs in the region of the cathode with enhanced cooling (across the adapter).

The dependence of the density of usable electric power, averaged over the cathode, on the integral heat release over the cathode is presented in Fig. 5 for the values of the coefficient of nonuniformity of heat release over the cathode $\varkappa_Z^{\pm}$ equal to 1.3 and 1.6.

The maximum admissible operating temperature of the cathode is one of the most important quantities determining a reliable continuous operation of TEC. For a large number of thermionic emission converters in the reactors with nonuniform distribution of heat release over the active zone it is necessary to maintain such conditions of their operation, at which the operating temperature of each TEC will not exceed the maximum admissible temperature of the cathode. The dependence presented in Fig. 4 permits determination of, for the investigated type of converter and for the indicated parameters, the integral distribution of heat release over the cathode for different slopes of heat release in it, from given values of maximum admissible temperature of the cathode. Then the dependence presented in Fig. 5 enables one to determine the electrical power of the converter for different values of $\varkappa_Z^{\pm}$ from these values of the integral heat release.

Thus, the data presented in Figs. 4 and 5 for different values of $\varkappa_Z^{\pm}$ permit determination of the dependence of the usable electrical power of TEC on the coefficient of nonuniformity of heat release over the cathode $\varkappa_Z^{\pm}$ under the condition that the operating temperature of the cathode does not exceed the given value of the maximum admissible temperature.

This dependence is presented in Fig. 6 for the case, when the maximum admissible temperature of the cathode is taken equal to 2000°K (continuous line). The decrease of the average density of usable electrical power with the increase in $\varkappa_Z^{\pm}$ is due to the fact that for satisfying the condition $T_{max} \leq 2000$°K it is necessary to decrease the integral heat release Q over the cathode. The dashed curves in this figure show the dependence of the density of usable electrical power, averaged over the cathode, on the coefficient of nonuniformity under the condition Q = const = 1215 W.

The dependence of the average density of the usable electrical power of TEC, operating in the arc regime with the density of the extracted current equal to j $\approx$ 40 A/cm^2, on the coefficient $\varkappa_Z^{\pm}$ is given in Fig. 7. These curves were obtained for the condition that the maximum temperature of the cathode does not exceed 2000°K using a family of volt–ampere characteristics of TEC with isothermal cathode with d = 0.127 mm, T_{Cs} = 653°K [8]. In this case the optimum length of the cathode is 4.0 cm.

For the same case of arc regime the dependence of the average density of electrical power of the converter on the integral heat release is given in Fig. 8 for $\varkappa_z = 1.0$ and $\varkappa_z^{\pm} = 1.6$. The energy balance of the TEC for two cases of the arc regime is described in Table 2: in the first regime the current density $j = 10$ A/cm^2, the usable voltage of the coverter $V_{con} \approx 0.86$ V (corresponds to point A in Figs. 4, 5, and 6), in the second regime the current density $j \approx 40$ A/cm^2, the usable voltage $V_{con} \approx 0.3$ V (corresponds to point A in Figs. 7 and 8). A comparison of Figs. 6 and 7 shows that in the operation of TEC in the regime with large current densities its electrical characteristics have a weaker dependence on the nonuniformity of heat release over the cathode than in the case of its operation with moderate values of the current density.

A comparison of the dependence of the usable electrical power of TEC on the integral heat release at the cathode, presented in Fig. 5a, with the analogous dependence for TEC with current density $j \approx 40$ A/cm^2 (see Fig. 8) shows that even in this case in the regime with current density $j \approx 40$ A/cm^2 the electrical characteristics of TEC have a weaker dependence on the change in the integral heat release than in the case of TEC with $j \approx 10$ A/cm^2.

The arc regime can be realized for different values of j and V_{con}, but most of the possible cases of realization of the arc regime lie between the two cases considered above (first and second regime).

The results of the computation, presented here, point out the need for profiling of heat release over the volume of the reactor and for taking account of both the nonuniformity of heat release over the cathode and the nonuniformity in the integral heat release in TEC in determining their electrical characteristics or of the reactor as a whole.

The authors express gratitude to V. P. Grishukin for taking part in the work.

LITERATURE CITED

1. F. Gross et al., Kerntechnik, No. 7, 381 (1969); Atomic Techniques Abroad, No. 2, 3 (1970).
2. N. N. Ponomarev-Stepnoi, At. Energ., 12, 415 (1962).
3. G. A. Bat', V. N. Gulimov, and V. K. Obukhov, At. Energ., 26, 7 (1966).
4. P. Bolan et al., Space Power Systems Engineering, Academic Press (1966), p. 605.
5. A. Shock, Paper F-12 at Second International Conference on Thermionic Emission Converters, Italy (1968).
6. Yu. A. Broval'skii et al., Paper G-3 at Second International Conference on Thermionic Emission Converters, Italy (1968).
7. V. Zilson et al., Effort to Increase Thermionic Output and Efficiency, Preprint International Conference on Thermionic Electrical Power Generation, London (1965).
8. V. Wilson and I. Lawrence, J. Adv. Energy Conf., No. 4, 4 (1964).

DOSE CHARACTERISTICS OF 200-MeV PROTONS

M. Zel'chinskii,* S. Pshona,*
M. M. Komochkov, B. S. Sychev,
and A. P. Cherevatenko

UDC 539.12.08:539.195.4

It is necessary to know the depth-dose distribution and the quality factor for particles producing ionization in tissue in order to predict the radiation danger from ionizing radiation and to determine the permissible particle flux densities for chronic irradiation. Preliminary calculations to determine these characteristics for nucleons with energies of the order of hundreds of MeV were undertaken by Neary and Mulvey in 1957 [1]. On the basis of these calculations, the International Commission on Radiation Protection (ICRP) developed recommendations for permissible values of high-energy neutrons and proton fluxes [2]. Subsequently, a number of theoretical [3-9] and experimental papers [10-14] were devoted to the determination of tissue dose and quality factor for protons. The theoretical calculations mainly used the Monte Carlo method for a geometry involving the irradiation of an infinite plane phantom by a broad beam of protons. The majority of experiments were carried out with small phantoms and finite beam dimensions, and used the recombination method.

The theoretical data is sufficiently complete and detailed so that it is convenient to use for practical purposes. However, the approximations used in the calculations, particularly in the choice of nuclear parameters and probable types of nuclear interactions, lead to considerable uncertainty, as a result of which the dose characteristics arrived at by the various authors differ among themselves and particularly strongly with the recommendations of the ICRP. It is impossible to make a proper comparison of the experimental results [10-14] with the calculations because of the differences in the conditions under which the experiments and calculations were performed.

The purpose of the present work is an experimental determination of the basic dose parameters for high-energy protons under irradiation conditions for which there are detailed theoretical calculations: normal incidence of a broad beam of monoenergetic protons on an infinite tissue-equivalent slab 30 cm thick. The phantom used was 100 × 100 × 30 cm in size; it was filled with a liquid with the atomic composition $C_5H_{40}O_{18}N$. The beam transport system is shown in Fig. 1. Protons with an energy of 660 ± 6 MeV were extracted from the JINR synchrocyclotron, slowed down in a polyethylene absorber, and after deflection in a magnetic field, were directed through a collimator 5 cm in diameter and 200 cm long onto a phantom perpendicular to its front surface. The energy of the decelerated protons, which was determined from their momentum in the magnetic field of the deflecting magnet was 209 ± 9 MeV.

The proton yield was measured with relativistic nuclear emulsions located at the collimator exit and the phantom surface, and was $\Phi = (2.6 \pm 0.2) \cdot 10^6$ proton/sec. The radial and depth distribution of dose rate and quality factor were determined with a parallel-plate ionization chamber, which was moved by remote control along the principal axes of the phantom. The walls and electrodes of the chamber were made of a tissue-equivalent material with the atomic composition $C_{29}H_{40}N$. The chamber-filling gas was a 1:1 mixture of propane and nitrogen. The pressure of the mixture was $3.4 \cdot 10^5$ N/m^2. The sensitive volume of the chamber was 23 cm^3, the diameter of the electrodes 8.5 cm, and the gap between the electrodes 2 mm. The ionization current of the chamber in the saturation mode was measured at a voltage $U = U_S = 800$ V between electrodes and in the linear column recombination mode at $U = U_r = 52$ V.

Electrometer readings were displayed on a recorder together with the readings from the monitors.

* Institute of Nuclear Research, Switzerland, Poland.

Translated from Atomnaya Énergiya, Vol.31, No.5, pp.473-476, November, 1971. Original article submitted October 12, 1970.

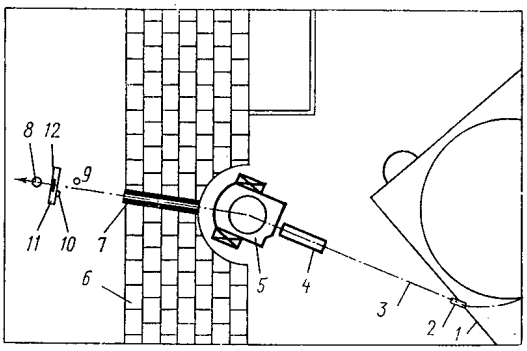

Fig. 1

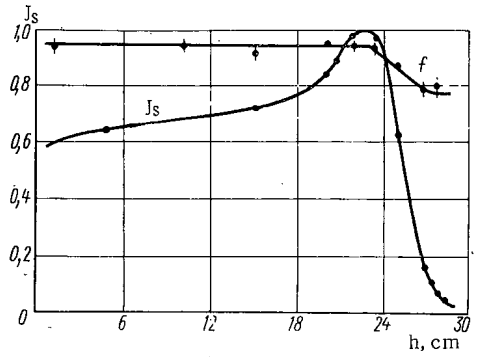

Fig. 2

Fig. 1. Experimental geometry: 1) accelerator chamber; 2) magnetic channel; 3) proton beam; 4) polyethylene moderator; 5) deflection magnet; 6) shield wall; 7) collimator; 8-10) monitors; 11) phantom; 12) ionization chamber.

Fig. 2. Depth distribution of chamber ion collection efficiency f and saturation current J_S along the beam axis.

The tissue dose rate P and the quality factor QF of the radiation were determined from the relations

$$P = KJ_S, \tag{1}$$

$$QF = A - Bf, \tag{2}$$

where J_S is the saturation current and $f = J_r/J_S$ is the ion collection efficiency in the recombination mode; the numerical values of the coefficients, obtained from calibration data, are K = (87.5 ± 5) Mrad/h-nA, A = 31.4 and B = 32.

The lack of dose-rate dependence for the ion collection efficiency, i.e., the negligible contribution from volume recombination of ions in the chamber, was verified by us in a previous paper [14] for a broad range of proton flux densities and was completely ensured.

Figure 2 shows the depth distribution on ion collection efficiency and saturation current along the axis of the beam in the phantom. The radial distribution of the dose rate at the phantom surface and at a depth h = 5 cm is shown in Fig. 3. The distributions were obtained by measurement of chamber currents at various distances from the beam axis. In this case, the transverse dimensions of the chamber were taken into account by means of Eq. (3) which is solved by the method of successive approximations. The geometric parameters appearing in Eq. (3) are illustrated in Fig. 4:

$$\bar{P}(y, h) = \frac{2}{\pi R_0^2} \int_{r=y-R_0}^{r=y+R_0} p(r, h)\, r\alpha\, dr = \frac{2}{\pi R_0^2} \int_{y-R_0}^{y+R_0} rp(r, h) \arccos \frac{y^2 - R_0^2 + r^2}{2yr}\, dr. \tag{3}$$

Here, $\bar{P}(y, h)$ is the average absorbed dose rate recorded by a parallel-plate chamber of radius R_0 at a distance y from the beam axis at the depth h; p(r, h) is the dose rate at a distance r from the beam axis at the depth h in the phantom. The distribution p(r, h) is the dose rate at any point of an infinite, plane, tissue-equivalent phantom irradiated by a narrow beam of protons. By means of this distribution, one can find the dose rate in an infinite plane phantom irradiated by a beam of arbitrary profile; it is sufficient to perform an integration over a plane bounded by the profile of the beam cross section. In particular, the dose rate for an infinitely broad parallel proton beam of unit flux density is calculated from the equation

$$P(h) = \frac{1}{\Phi} \int_0^{\infty} p(r, h) \cdot 2\pi r\, dr. \tag{4}$$

Using the principle of superposition for the saturation current and individual treatment for the current in the recombination mode, we define the quality factor QF at a depth h for an infinitely broad beam to be

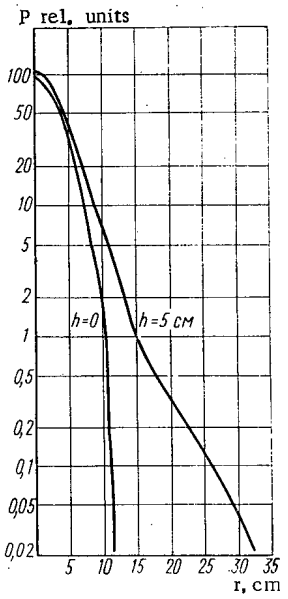

Fig. 3. Radial distribution of dose rate P at the phantom surface and at the depth h = 5 cm of tissue.

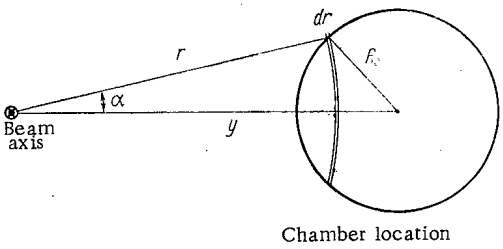

Fig. 4

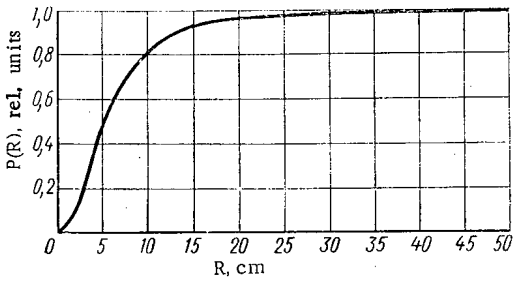

Fig. 5

Fig. 4. Calculation of dose rate at a point a distance r from the beam axis.

Fig. 5. Dose rate $P(R) = \int_0^R p(r)\, 2\pi r\, dr$ as a function of the radius of integration R.

$$QF(h) = \frac{\int_0^\infty p(r, h)\,[A - Bf(r, h)]\, r\, dr}{\int_0^\infty p(r, h)\, r\, dr}, \qquad (5)$$

where f(r, h) is the collection efficiency for ions produced by radiation at the point (r, h) when the phantom is irradiated by a narrow beam.

Some reduction in ion collection efficiency was observed experimentally as the chamber was removed from the beam axis. Because of the steep radial drop in dose, however, the quality factor calculated by Eq. (5) is practically the same as the quality factor determined from the ion collection efficiency in a chamber which is on the beam axis. The quality factor is 1.4 ± 0.3 rem/rad and increases in the region of the Bragg peak. The error of ±0.3 rem/rad includes both the measurement error and some variation in quality factor with depth. Beyond the Bragg peak at a depth h = 28 cm, the quality factor was 5.5 ± 2.5 rem/rad.

In Table 1, these measurements, adjusted for a broad beam, are compared with other results for the following parameters: dose rate absorbed at a depth h = 5 cm in a plane phantom for irradiation by unit flux of protons and quality factor also at a depth of 5 cm. Our experimental results are in agreement with the calculations by Zerby and Kinney [3], Turner et al. [4], and Neufeld et al. [5, 6] except for the QF value beyond the Bragg peak, but disagree with the ICRP recommendations. This disagreement, which is greater

TABLE 1. Quality Factor QF and Dose Rate P in a Phantom Irradiated by a Broad Beam of Protons Having Unit Flux Density (Normal incidence)

E_p, MeV	h, cm	QF, rem/rad	P, nrad/proton-cm^2	Phantom	Phantom material	Method	Year	Reference
209	0—26	1,7	145	Infinite slab 30 cm thick	Soft tissue	Theoretical estimate	1957	[1,2] *
209	5	1,5	80	The same	The same	Monte Carlo	1964	[4]
209	5	1,32	84	" "	" "	The same	1965	[3]
209	5	1,36	86	" "	" "	" "	1966	[5]
200	5	—	86	" "	" "	" "	1964	[8]
209	0—30	~ 1,26	120	" "	" "	Calculation	1969	[9]
250	10	1,33	88	Elliptic cylinder, 20×40×70 cm	" "	Calculation	1966	[6]
260	0—30	—	84	Slabs	Polyethlene	Experiment	1965	[12]
260	5	1,2±0,2		Cylinder 35x90 cm	Water	Recombination chamber	1967	[14]
196±10	5	1,55±0,25		Slab, 100x100x30 cm	Tissue-equivalent liquid	Scintillator	1968	[5]
209±9	5±0,3	1,4±0,25	81±8	The same	The same	Recombination chamber	1968	†

*ICRP recommendation

†This work

than experimental error, is obviously the result of the too pessimistic assumptions which were the basis for the calculations of [1] and calls for a review of the recommendations with respect to the maximum permissible levels for high-energy proton flux densities.

The conditions in our investigation are insignificantly different from those assumed in calculations [3-8] and have no important effect on the correctness of the comparisons we have made. The differences in phantom dimensions can lead to a deviation of no more than 1% in the estimate of dose rate; as is clear from Fig. 5, the contribution from distant regions of a phantom to the integral dose rate is negligibly small – a phantom 1 m by 1 m in size is a good approximation to an infinite slab. The measurements also indicate the insignificant effect of phantom dimensions on the resultant value of the quality factor. The presence of a gas-filled cavity introduces no significant distortions in the dose rate distribution and in the effective linear energy transfer (LET) of the particles, particularly where these parameters are constant with depth. The error because of the presence of a gas-filled cavity did not exceed 1% at measurement points located between the phantom surface and the location of the Bragg peak. The replacement of oxygen by carbon has practically no effect on dose rate and on the LET of the ionizing particles in the gas volume of the chamber because of the similarity of proton interactions in carbon and oxygen at the energies under consideration. The small mass of the electrodes in comparison with the total mass of the tissue-equivalent liquid in the phantom makes this error negligible. A difference in the shape of the QF dependence of LET, which determines the quality factor of radiation [16], can introduce an error of as much as 4% in the determination of QF for 200-MeV protons. A difference in the maximum energy of delta rays for local averaging of LET only changes the dose distribution insignificantly with respect to the LET of high-energy protons in the LET region which is important for the determination of quality factor. The proton energy spread under experimental conditions has little effect on the determination of dose rate and quality factor at the depth h = 5 cm because of the slight energy dependence of the measured quantities; it has a noticeable effect only at a depth corresponding to the Bragg peak, washing it out and thereby lowering the value of the dose rate at the peak.

What has been said indicates that the conditions under which the experiment was performed were practically analogous to those assumed in the theoretical calculations. Therefore the agreement of calculations with the experimental results is evidence of the correctness of the computational models.

The data obtained in calculations [3-8] can be recommended for the development of permissible levels for particle flux densities in the 200-MeV region.

LITERATURE CITED

1. J. Neary and J. Mulvey, Report of Medical Research Council, Radiological Research Unit, AERE, Harwell (1957).
2. Recommendation Intern. Commission on Radiological Protection (ICRP Publication 4), Pergamon Press (1964).
3. C. Zerby and W. Kinney, Nucl. Instr. and Methods, 36, 125 (1965).
4. J. Turner et al., Health Phys., 10, 783 (1964).
5. J. Neufeld et al., Health Phys., 12, 227 (1966).
6. J. Neufeld et al., Proc. of the First Intern. Congress of Radiation Protection, Vol.2, Pergamon Press (1968), p.1469.
7. H. Wright et al., Health Phys., 12, 13 (1960).
8. P. Steward, UCRL 10980 (1964); CONF 670305, 211 (1967).
9. V. E. Dudkin et al., JINR Preprint 16-4888 (1970), p.179.
10. R. Tanner et al., Radiation Res., 36, 861 (1967).
11. J. Baarli and A. Sullivan, HealthPhys., 11, 353 (1965).
12. V. P. Afanas'ev et al., in: Dosimetry and Radiation Protection Problems [in Russian], No.4, Atomizdat, Moscow (1965), p.102.
13. M. Zel'chinskii, Radiobiologiya, 5, 161 (1965).
14. M. Zel'chinskii et al., JINR Preprint P9-3363 (1967); Nukleonika, 13, 165 (1968).
15. S. Pshona et al., JINR Preprint E16-5384 (1970).
16. M. Zel'chinskii, Nukleonika, 15, 823 (1970).

SCATTERING OF SLOW PROTONS

E. P. Arkhipov and Yu. V. Gott

UDC 621.039.539.7

A study of the penetration of slow particles through matter takes on great importance in connection with the use of thin foils for the energy analysis of slow atom fluxes in laboratory and space research [1, 2].

This paper is concerned with an investigation of proton scattering in matter for E < 30 keV.

It has been shown [3, 4] that the angular distribution of particles passing through a thickness d of material can be expressed in the form

$$f(\theta, d) = \frac{1}{2\pi} \sum_{0}^{\infty} \left(l + \frac{1}{2}\right) e^{-N\sigma_l d} P_l(\cos\theta), \tag{1}$$

where

$$\sigma_l = 2\pi \int_0^{\pi} [1 - P_l(\cos\alpha)]\, \sigma(\alpha) \sin\alpha\, d\alpha; \tag{2}$$

$P_l(\cos\alpha)$ is a Legendre polynomial, $\sigma(\alpha) = d\sigma(\alpha)/d\Omega$ is the differential cross section for particle scattering by an angle α, Ω is the solid angle, and N is the number of particles per unit volume of the target. In the derivation of Eq. (1), it was assumed the variation in particle energy during penetration of the material layer could be neglected.

The determination of σ_l presents the greatest difficulty in the calculation of the angular distribution.

We select a potential for the interaction between particles and target atoms in the form

$$v(r) \sim \frac{1}{r^s}, \quad s > 1. \tag{3}$$

The interaction cross section will then be

$$\sigma(\alpha) = \frac{A_s}{\sin^{2(1+1/s)} \frac{\alpha}{2}} = \frac{2^{1+\beta} A_s}{(1-x)^{1+\beta}}, \tag{4}$$

where $\beta = 1/s$; A_S is a factor for which an explicit form will be determined below, and $x = \cos\alpha$.

We shall find a recurrence relation between σ_l with different values of l. Using the recurrence relation between $P_{l+1}(x)$ and $P_{l-1}(x)$, and the relation

$$\int_{-1}^{1} f(x) P_l(x)\, dx = \frac{1}{2^l l!} \int_{-1}^{1} f^{(l)}(x) (1-x^2)^l\, dx, \tag{5}$$

we obtain

$$\sigma_{l+1} = 8\pi A_s \left\{ 2\omega_{l-1} + (2l+1) \frac{s^2 (1+s)(1+2s)\ldots[1+s(l-1)]}{(s-1)(2s-1)\ldots[(l+1)s-1]} \right\}, \tag{6}$$

where $\omega_l = \sigma/16\pi A_S$.

Translated from Atomnaya Énergiya, Vol. 31, No. 5, pp. 477-480, November, 1971. Original article submitted October 12, 1970.

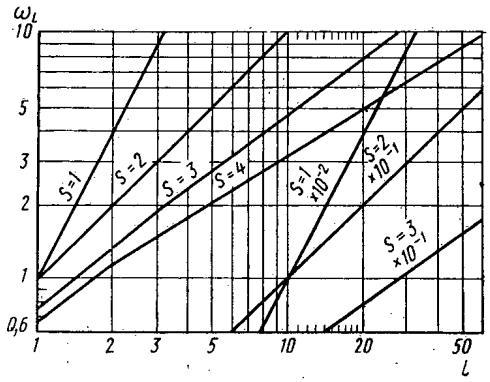

Fig. 1. Dependence of ω_l on l.

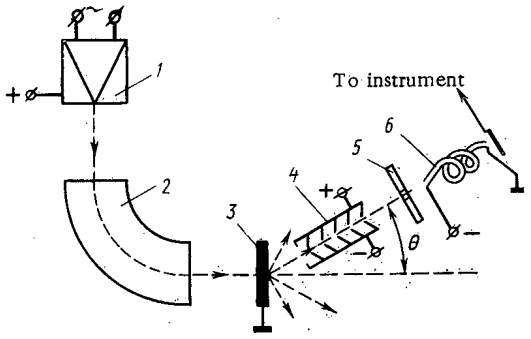

Fig. 2. Experimental arrangement.

The first few values σ_l can be calculated directly from Eq. (2). Indeed, since

$$P_l(\cos\alpha) = \sum_0^l (-1)^k \frac{(l+k)!}{(l-k)!\,(k!)^2} \left(\sin\frac{\alpha}{2}\right)^{2k}, \tag{7}$$

by substituting (7) and (4) into (2), we then have

$$\sigma_l = 4\pi A_s \sum_1^l (-1)^{k+1} \frac{(l+k)!}{(l-k)!\,(k!)^2} \cdot \frac{s}{ks-1}. \tag{8}$$

For s = 2, we find from (6) and (7) that

$$\sigma_{l+1} = 8\pi A_2 (2\omega_{l-1} + 4); \quad \sigma_1 = 16\pi A_2; \quad \sigma_2 = 32\pi A_2; \quad \sigma_3 = 48\pi A_2. \tag{9}$$

Using mathematical induction, it is easy to show that

$$\sigma_l = 16\pi A_2 l. \tag{10}$$

For $s > 2$ σ_l is determined by Eqs. (6) and (7) using a numerical method. Values of ω_l are shown in Fig. 1 for s = 1, 2, 3, 4 (for s = 1, $\omega_l = l(l+1)$ [5]).

Knowing σ_l, therefore, the angular distribution of particles passing through a layer d of matter can be determined numerically from Eq. (1).

For s = 2, the quantity A_2 in (4) is [6]

$$A_2 = \frac{4.1e^2 a Z_1 Z_2 (M_1+M_2)}{M_2 E}, \tag{11}$$

where Z_1e, Z_2e, M_1, and M_2 are the charges and masses of the incident particles and the target atoms; E is the energy of the incident particles, and

$$a = \left(\frac{\hbar^2}{me^2}\right) 0.8853 \left(Z_1^{2/3} + Z_2^{2/3}\right)^{-1/2}.$$

For s = 3, the quantity A_S can be determined in the following manner. The scattering cross section in a Thomas–Fermi potential has been calculated [7]. For our purposes, a good approximation to this cross section is

$$\sigma(\alpha) = \frac{0.179a^2}{\varepsilon^{2/3}\left[1 + 2.83\varepsilon^{1/3}\sin^{1/3}\frac{\alpha}{2} + 1.37\varepsilon^{1/2}\sin^{1/2}\frac{\alpha}{2}\right]\sin^{8/3}\frac{\alpha}{2}} \tag{12}$$

where

$$\varepsilon = E\frac{aM_2}{Z_1 Z_2 e^2 (M_1+M_2)}$$

for very low energies, i.e., in cases where $\varepsilon \ll 1$, we have

$$\sigma(\alpha) = \frac{0.179a^2}{\varepsilon^{2/3}\sin^{8/3}\alpha/2}. \tag{13}$$

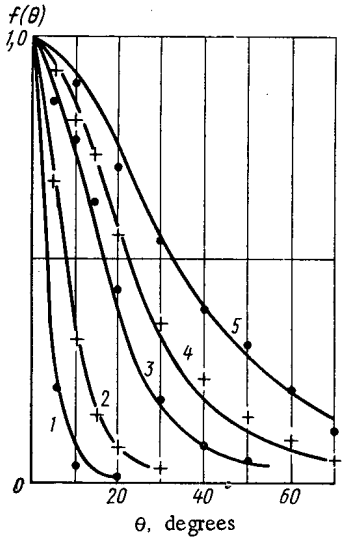

Fig. 3

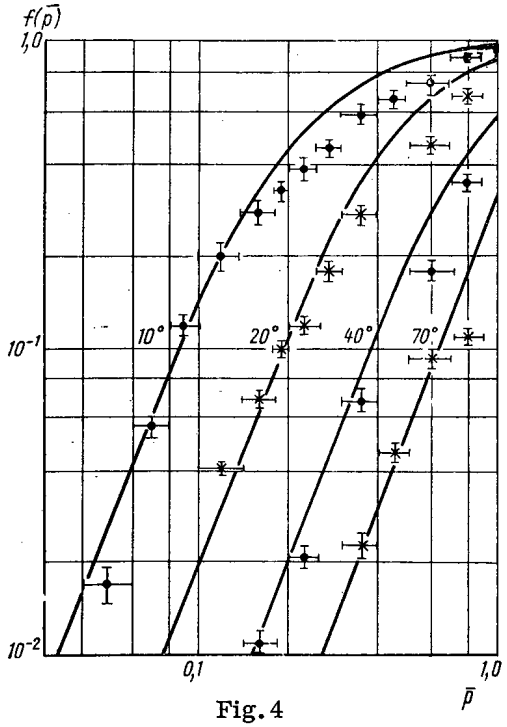

Fig. 4

Fig. 3. Proton scattering in nickel. 1) 26 keV, 140 Å; 2) 19 keV, 280 Å; 3) 26 keV, 590 Å; 4) 19 keV, 580 Å; 5) 2.5 keV, 140 Å; ——) calculation.

Fig. 4. Comparison of experimental and theoretical values for proton scattering in matter: ——) theory.

Comparing Eqs. (13) and (4), we find that s = 3 and

$$A_3 = 0.179\left[\frac{a^2 Z_1 Z_2 e^2 (M_1+M_2)}{M_2 E}\right]^{2/3}. \tag{14}$$

Equation (12) also indicates that approximation of the interaction potential between incident particles and target atoms by a potential of the form r^{-3} is valid only at energies less than a few hundred electron volts.

If scattering only at small angles is considered, Eq. (1) can be simplified considerably for s = 1 and s = 2.

Actually, for small angles $P_l(\cos\theta) \approx J_0(l\theta)$, where $J_0(l\theta)$ is a Bessel function of zero order. Substituting this Bessel function in Eq. (1) and replacing summation by integration over l, we obtain:

for s = 1

$$f(\theta, d) \simeq \frac{1}{2\pi}\int_0^\infty l\, e^{-p_k l^2} J_0(l\theta)\, dl = \frac{1}{4\pi P_k} e^{-\theta^2/4p_k}; \tag{15}$$

for s = 2

$$f(\theta, d) \simeq \frac{1}{2\pi}\int_0^\infty l\, e^{-pl} J_0(l\theta)\, dl = \frac{1}{2\pi}\cdot\frac{p}{(p^2+\theta^2)^{3/2}}. \tag{16}$$

Here

$$p_k = \frac{\pi Z_1^2 Z_2^2 e^4 L_K}{2E^2}; \tag{17}$$

L_K is the Coulomb logarithm, and

$$p = \frac{2.05\, e^2 a Z_1 Z_2 (M_1+M_2)}{M_2 E} Nd. \tag{18}$$

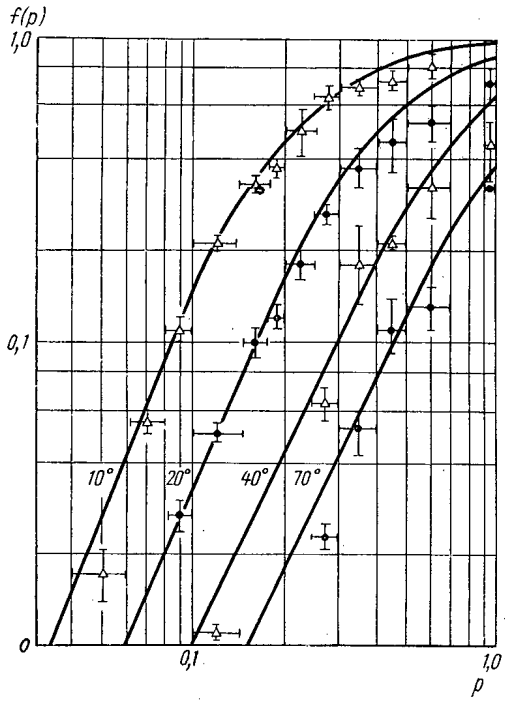

Fig. 5. Experimental data averaged over p compared with calculations based on Eq. (23).

In Eqs. (15) and (16), 1 was neglected in comparison with l in the integration. The result obtained for s = 1 agrees in accuracy with the data of Williams [8] with a mean square deflection $\langle\theta^2\rangle = 4p_k$.

It is thus clear from Eqs. (1), (15), and (16) that the angular distribution of particles after penetrating a layer of matter depends on a single parameter which is a combination of the quantities characterizing the incident particle and the target.

For s = 2, the series (1) can be summed.* Actually, we set $e^{-p} = t$. Then

$$f(\theta,\ d) = \frac{1}{2\pi}\sum^{\infty}(l+1/2)\,t^l P_l(\cos\theta)$$

$$= \frac{1}{4\pi}\cdot\frac{1-e^{-2p}}{[1+e^{-2p}-2e^{-p}\cos\theta]^{3/2}}. \qquad (19)$$

For $p \ll 1$ and $\theta \ll 1$, it is easy to obtain (16) from (19).

As already noted above, all the equations were obtained on the assumption that energy losses by the particles in the layer of matter could be neglected.

In order to account for the change in particles energy, it is necessary to replace the quantity p in Eqs. (16) and (19) by $\bar{p}$,

$$\bar{p} = N\int_0^d \sigma_1\,dy = N\int_{E_{ex}}^{E_0}\sigma_1\left(\frac{dE}{dy}\right)^{-1}dE, \qquad (20)$$

where σ_1 is the transport cross section ($l = 1$); E_0 is the initial energy ofthe particles, and E_{ex} is the particle energy upon leaving the foil.

For protons with energies less than 30 keV, the energy loss is approximately proportional to the velocity, i.e.,

$$-\frac{dE}{dy} = B\sqrt{E}. \qquad (21)$$

Then, substituting (21) in (20), it is easy to obtain

$$\bar{p} = \frac{2p}{Bd}\left[\frac{E_0}{\sqrt{E_0}-\frac{Bd}{2}}-\sqrt{E_0}\right]. \qquad (22)$$

EXPERIMENT

We studied the scattering ofprotons having energies of 2.5-30 keV in Ni, Si, Fe, and Bi foils 100-1600 Å thick over the angular range 0-70°. The experimental arrangement is shown in Fig. 2. Ions emerging from the duoplasmatron source 1 are mass separated in the magnetic field of the separator 2. After separation, the protons are incident on the foil 3 being investigated. Particles escaping from the foil are detected by the channel multiplier 6. In order to eliminate the effect of ions which pass directly through an opening in the foil, charged particles are removed from the flux by means of condenser 4 and diaphragm 5, and all measurements are made on neutral particles emerging from the foil. The condenser 4, diaphragm 5, and multiplier 6 are shifted over the angle θ with respect to the foil in the range 0-70°. The resolution of the measurement system is ±1°.

The method for preparing foils of the materials studied has been described in detail [9].

The angular distribution of protons scattered in nickel is shown in Fig. 3. The solid curves were calculated from Eq. (19) using (22).

*This possibility was pointed out to the authors by O. B. Firsov.

A comparison of the experimental values for proton scattering probability at various angles with those calculated from Eq. (19) is shown in Fig. 4. All the experimental values were averaged over the parameter $\bar{p}$. In the averaging, we used our data for the scattering of protons having energies of 2.5-30 keV in Ni, Si, Fe, and Bi foils as well as data on the scattering in nickel of 15- to 90-MeV protons [10], data for copper scattering of approximately 160-MeV protons [11], and data for scattering in gold of d^+ ions having an energy of approximately 13 keV [12]. The solid curves in the figure were calculated from Eq. (19). It is clear that the theoretical and experimental values agree within experimental error in the $\bar{p}$ range from 0.05 to 0.2. For $\bar{p} > 0.3$, the experimental scattering probabilities are less than the theoretical values. This may be associated with the fact that large values of $\bar{p}$ correspond to low energies and greater thicknesses of materia. In this situation, the ranges for some particles may be less than the foil thickness, and such particles will not be recorded.

It is interesting to note that if we do not neglect 1/2 in comparison with l in Eq. (16), we obtain

$$f(\theta, d) = \frac{1}{4\pi} \cdot \frac{p^2+2p+\theta^2}{[p^2+\theta^2]^{3/2}} . \quad (23)$$

It turns out that Eq. (23) also gives a good description of the experimental data for scattering angles less than 50° (Fig. 5) if the change in particle energy is not taken into account. Consequently, Eq. (23) can be used in a number of cases as a semiempirical formula for describing proton scattering in matter at angles less than 50-60°.

In conclusion, the authors wish to express their gratitude to O. B. Firsov for valuable discussions and advice.

LITERATURE CITED

1. Yu. V. Gott and V. G. Tel'kovskii, Zh. Tekh. Fiz., 34, 2114 (1964).
2. W. Bernstein et al., J. Geophys. Res. Space Phys., 74, 3601 (1969).
3. S. Goudsmit and J. Saunders, Phys. Rev., 57, 24 (1939).
4. H. Lewis, Phys. Rev., 78, 526 (1950).
5. B. A. Trubnikov, in: Problems in Plasma Theory [in Russian], No. 1, Gosatomizdat, Moscow (1963), p. 98.
6. J. Lindhard and M. Scharff, Phys. Rev., 124, 128 (1961).
7. J. Lindhard, M. Scharff, and V. Nielsen, Kgl. Danske Vid. Selskab. Mat.-Fiz. Medd., 36, No. 10 (1968).
8. E. Williams, Proc. Roy. Soc., A169, 531 (1939).
9. E. P. Arkhipov and Yu. V. Gott, Zh. Eksp. Teor. Fiz., 56, 1146 (1969).
10. G. F. Bogdanov and F. V. Lebedev, At. Energ., 23, 347 (1967).
11. A. A. Bednyakov et al., Zh. Eksp. Teor. Fiz., 42, 740 (1964).
12. C. Andreen, Ark. Fyz., 35, 583 (1968).

PHYSICAL MEANING AND STRUCTURE OF ASYMPTOTIC AND TRANSIENT PARTS OF γ-RAY BUILDUP FACTOR FOR A MULTILAYER SHIELD

V. A. Zharkov

UDC 621.039.538.7

In analyzing data on the transmission of γ radiation through multilayer shields, several authors [1-4] have regarded the buildup factor as a superposition of asymptotic and transient parts. It is assumed that the transient part falls off rapidly enough with the distance from the last interface so that in a few mean free paths at the source energy into the material of the last layer the buildup factor becomes approximately equal to its asymptotic value. The asymptotic solution is expressed in terms of the buildup factor for the material of the last layer.

We give a physical treatment of this representation of the buildup factor, first for two-layer shield configurations.

We introduce the following notation. Let E_0 be the energy of the source radiation; λ_i the thickness of of the i-th layer of the shield in mean free paths; N the number of shield layers; $I^s_{N-1}(E, \Omega, \sum_{i=1}^{N-1} \lambda_i, \lambda_N)$ the the spectral-angular intensity distribution (dose, number of photons, etc.) of scattered radiation at an arbitrary point on the boundar between the (N – 1)-th and N-th layers (taking account of reflection from the N-th layer) for a direction Ω from the (N – 1)-th layer into the N-th. $I^s_N(E, \Omega, \lambda'_{N-1}, \lambda_N)$ is the analog of I^s_{N-1} when the first N – 1 layers are replaced by material of the last layer of thickness λ'_{N-1}, where λ'_{N-1} is an arbitrary parameter; $J^s_{N-1}(E, \sum_{i=1}^{N-1} \lambda_i)$ and $J^s_N(E, \lambda'_{N-1})$ are the results of integrating the distributions I^s_{N-1} and I^s_N over Ω for $\lambda_N = 0$; μ_i and μ_{si} are respectively the attenuation coefficient and the Compton scattering coefficient for the material of the i-th shielding layer at energy E_0, and n is a unit vector characterizing the direction of propagation of the primary radiation. We take the source strength as unity. We assume that the buildup factor for a multilayer shield is determined in slab geometry with the detector placed on the shield surface.

Two-Layer Shields

Plane Monodirectional Source behind a Plane-Parallel Shield. In order to obtain an expression for the buildup factor as a sum of asymptotic and transient parts satisfying the conditions formulated at the beginning of the article, at each point on the interface and for each Ω directed from the first layer into the second we separate out, in the algebraic sense, the part of the spectrum of the scattered radiation $\varkappa I^s_2(E, \Omega, \lambda'_1, \lambda_2)$, where $\varkappa$ is a constant equal to the ratio of the intensities of the most penetrating photons of the scattered radiation after passing through a shield of the material of the first layer of thickness λ_1 and a shield of the material of the second layer of thickness λ'_1. For source energies lower than the value corresponding to the minimum of the attenuation coefficient μ the hardest photons will be those singly scattered directly forward, and

$$\varkappa = \frac{e^{-\lambda_1 \lambda_1 (\mu_{s1}/\mu_1)}}{e^{-\lambda'_1 \lambda'_1 (\mu_{s2}/\mu_2)}} \equiv \frac{e^{-\lambda_1 \lambda_1}}{e^{-\lambda'_1 \lambda'_1}} k .$$

Translated from Atomnaya Énergiya, Vol.31, No.5, pp.481-486, November, 1971. Original article submitted October 19, 1970.

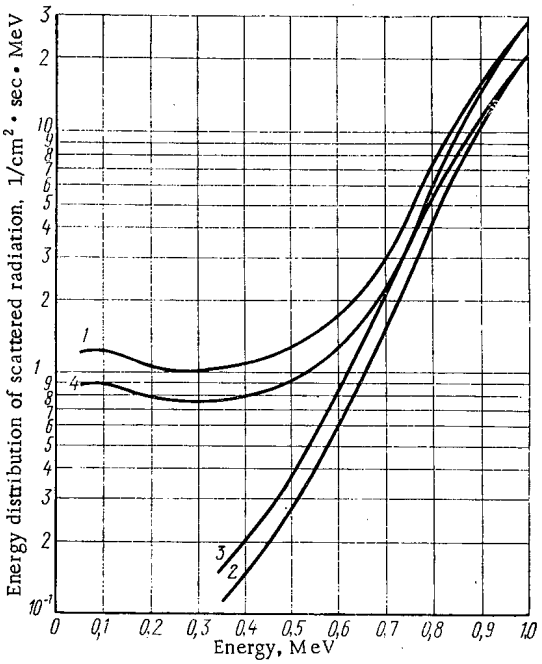

Fig. 1. Scheme of separating out spectral-angular distribution giving transient part of buildup factor. Systems H_2O + Pb and Pb + H_2O, E_0 = 1 MeV, $\lambda_1 = 2$, $\Omega \cdot n = 0.9745$. 1) $I_{H_2O}(E)$ – energy distribution of scattered radiation after penetrating a layer of water with $\lambda_1 = 2$; 2) $I_{Pb}(E)$ – energy distribution of scattered radiation after penetrating a layer of lead with $\lambda_1 = 2$. In both cases reflection from the second layer is neglected; 3) $\varkappa I_{Pb}(E)$ for $\lambda_1' = \lambda_1 = 2$; 4) $\varkappa I_{H_2O}(E)$ for $\lambda_1' = \lambda_1 = 2$. The difference in distributions 1 and 3 is in the spectrum of the transient solution for the system H_2O + Pb. The difference in the distributions 2 and 4 is in the spectrum of the transient solution for the system Pb + H_2O.

It is easy to show that the probability that a primary photon undergoes only the scattering directly forward in a layer of thickness λ is $w = e^{-\lambda}\lambda(\mu_s/\mu)df/dE(E_0)$, where $df/dE(E_0)$ is the probability density for the scattering of a photon by an electron with change in energy.

We now represent the spectral-angular distribution of scattered radiation on the interface in the form

$$I_1^s(E, \Omega, \lambda_1, \lambda_2) = \varkappa I_2^s(E, \Omega, \lambda_1', \lambda_2) + [I_1^s(E, \Omega, \lambda_1, \lambda_2) - \varkappa I_2^s(E, \Omega, \lambda_1', \lambda_2)]. \quad (1)$$

Clearly for any direction Ω' including the direction of n, the part of the spectral-angular distribution represented in Eq. (1) by the expression in brackets does not contain photons with energies E_0, and contains few photons with energies close to E_0. This part of the spectrum characterizes the scattered radiation which falls of rather rapidly with the distance from the interface whatever the sign of the expression in brackets. The first term in Eq. (1) represents the spectral-angular distribution which would be produced at the interface by a source of strength $\varkappa$ after penetration of a layer of the second material of thickness λ_1', taking account of reflection from a layer of the second material of thickness λ_2.

The following sources contribute to the intensity (dose, number of photons) of scattered radiation at the point where the buildup factor is calculated:

1) a distributed source on the interface with the spectral-angular distribution $I_1^S(E, \Omega, \lambda_1, \lambda_2) - \varkappa I_2^S(E, \Omega, \lambda_1', \lambda_2)$;

2) a distribution source on the interface of the form $\varkappa I_2^S(E, \Omega, \lambda_1', \lambda_2)$;

3) radiation arising from the scattering of primary radiation in the second layer, taking account of reflection from the first layer.

These are the three really important sources of scattered radiation. We now formally add and subtract the scattered radiation produced at the point under consideration by a system consisting of a source of primary radiation of strength $\varkappa e^{-\lambda_1'}$ at the interface and a reflector of the material of the second layer of thickness λ_1'. All sources except 1) emit photons of energy E_0, and therefore the first source produces the transient part of the buildup factor, and the other sources give the asymptotic part. The scheme of separating out the spectral-angular distribution giving the transient part of the buildup factor is shown in Fig. 1. The data on the spectral-angular distributions are taken from [4].

By combining the radiation sources the buildup factor for a two-layer shield $B(\lambda_1, \lambda_2)$ can be written in the form

$$B(\lambda_1, \lambda_2) = B_{as}(\lambda_1, \lambda_2) + \Delta B_{tr}(\lambda_1, \lambda_2), \quad (2)$$

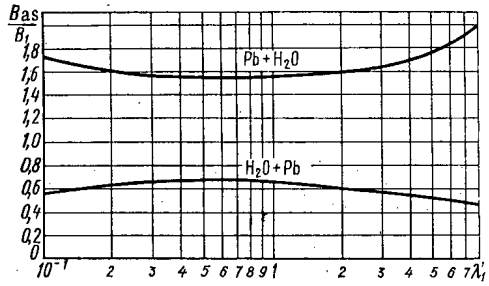

Fig. 2. $B_{as}(\lambda_2 = 0, \lambda_1 = \text{const}, \lambda_1')/B_i(\lambda_1)$ for the determination of the optimum value of λ_1'. Systems H_2O + Pb and Pb + H_2O, E_0 = 1 MeV, $\lambda_1 = 4$.

where

$$B_{as}(\lambda_1, \lambda_2) = 1 + e^{(\lambda_1+\lambda_2)}\{[B_2(\lambda_1'+\lambda_2)-1]\varkappa^{-(\lambda_1'+\lambda_2)}$$

$$-[B_2^*(\lambda_2)-1]\varkappa e^{-(\lambda_1'+\lambda_2)}+[B_2^{**}(\lambda_2)-1]e^{-(\lambda_1+\lambda_2)}\} = \frac{\lambda_1}{\lambda_1'}kB_2(\lambda_1'+\lambda_2)+B_2^{**}(\lambda_2)-\frac{\lambda_1}{\lambda_1'}kB_2^*(\lambda_2); \quad (3)$$

$$\Delta B_{tr} = e^{\lambda_1+\lambda_2}\int\int dE\,d\Omega\,[I_1^s(E, \Omega, \lambda_1, \lambda_2)-\varkappa I_2^s(E, \Omega, \lambda_1', \lambda_2)]\frac{1}{k(E, \Omega, \lambda_2)}.$$

In these formulas $B_2(\lambda_1' + \lambda_2)$ is the buildup factor for a plane monodirectional source and a homogeneous plane-parallel shield of the material of the second layer of thickness $\lambda_1' + \lambda_2$ in slab geometry; $B_2^*(\lambda_2)$ is the buildup factor for a plane monodirectional source and a plane-parallel shield of the material of the second layer of thickness λ_2 in slab geometry, taking account of reflection from a layer of the second material of thickness λ_1' placed on the source side; $B_2^{**}(\lambda_2)$ is the buildup factor for a plane monodirectional source and a plane-parallel shield of material of the second layer of thickness λ_2 in slab geometry, taking account of reflection from a layer of the first material of thickness λ_1 placed on the source side; $k(E, \Omega, \lambda_2)$ is the attenuation of γ radiation of energy E by a shield of thickness λ_2 in slab geometry for a distributed source.

Equation (2) can also be written in the form

$$B(\lambda_1, \lambda_2) = \alpha B_2(\lambda_1'+\lambda_2)+[B_1(\lambda_1)+\alpha_0 B_2(\lambda_1')]e^{\lambda_2}f(\lambda_2), \quad (4)$$

where $B_1(\lambda_1)$ is the buildup factor for a plane monodirectional source and a plane-parallel shield of the material of the first layer of thickness λ_1 in slab geometry, and $B_2(\lambda_1') = B_2(\lambda_1' + \lambda_2)$ for $\lambda_2 = 0$; α is the asymptic coefficient equal to

$$\alpha = \frac{\lambda_1}{\lambda_1'}k + \frac{B_2^{**}(\lambda_2)-\frac{\lambda_1}{\lambda_1'}kB_2^*(\lambda_2)}{B_2(\lambda_1'+\lambda_2)}; \quad (5)$$

$$\alpha_0 = \alpha(\lambda_2 = 0) = \frac{\lambda_1}{\lambda_1'}k + \frac{1-\frac{\lambda_1}{\lambda_1'}k}{B_2(\lambda_1')}; \quad (6)$$

$$f(\lambda_2) = \frac{\int\int dE\,d\Omega\,[I_1^s(E, \Omega, \lambda_1\lambda_2)-\varkappa I_2^s(E, \Omega, \lambda_1', \lambda_2)]\frac{1}{k(E, \Omega, \lambda_2)}}{\int J_1^s(E, \lambda_1)\,dE-\varkappa\int J_2^s(E, \lambda_1')\,dE} \quad (7)$$

is a monotic rapidly decreasing function, falling of more rapidly than $e^{-\lambda_2}$, equal to unity for $\lambda_2 = 0$, and approaching zero as $\lambda_2 \to \infty$.

If it is assumed that $\lambda_1' = \lambda_1$ and reflection is neglected for the buildup factors $B_2^*(\lambda_2)$, $B_2^{**}(\lambda_2)$, and the function I_1^S and I_2^S, which in most cases leads to a small error, Eq. (4) agrees with Shimizu's formula obtained under these conditions within the framework of the method of invariant imbedding [4]. Setting $\lambda_1' = \lambda$, $\alpha = \alpha_0$ and independent of λ_2, and writing $f(\lambda_2) = \text{const}, e^{\text{const}_2\lambda_2}$, although the latter two assumptions are generally not physically justified, we obtain empirical formulas similar to those of Kitazume [1], Miyasaka and Tsurvo [2], Schubart [3], and finally for $\alpha = \alpha_0 = 1$ and $f(\lambda_2) = e^{-\lambda_2}$ Broder's formula [5].

Let us now consider the choice of the parameter λ_1'. Changing λ_1', and therefore $\varkappa$, changes the ratio of the scattered radiations determining the asymptotic and transient parts of the buildup factor [cf. (1)]. Physically this means that for a given Ω one can try to choose λ_1' so as to achieve the maximum similarity of

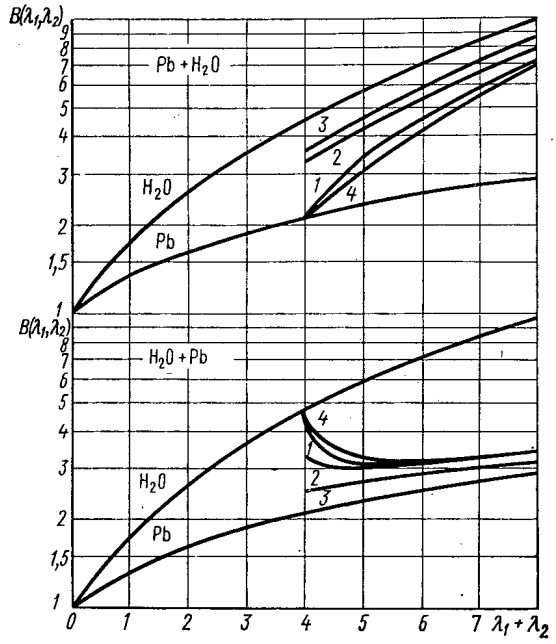

Fig. 3. Dose buildup factors in a slab geometry for a plane monodirectional source. Systems are H_2O + Pb and Pb + H_2O, E_0 = 1 MeV, $\lambda_1 = 4$. 1) Solution by the method of invariant imbedding [4]; 2) asymptotic value of buildup factor with optimum value of $\lambda_1' = 0.6$; 3) asymptotic value of buildup factor for $\lambda_1' = \lambda_1 = 4$; 4) asymptotic solution for $\lambda_1' = 1$ plus transient solution in which $f(\lambda_2)$ is calculated by assuming normal emission of scattered radiation from interface.

the energy distributions $I_1^s(E, \Omega, \lambda_1', \text{and } \lambda_2)$ and $I_2^s(E, \Omega, \lambda_1', \lambda_2)$. We note that the largest contributions to the scattered radiation determining the buildup factor in a heterogeneous shield obviously come from directions Ω close to n. For example, for the combination Pb + H_2O it is desirable to choose a value of λ_1' such that for $\Omega \cdot n \approx 1$ the spectrum in water contains a minimum number of low energy photons, i.e., energies which made a small contribution to the spectrum in lead. As λ_1' varies from 0 to 1 the spectrum of the scattered radiation in water changes sharply. When $\lambda_1' = 0$ the spectrum contains only monoenergetic photons with $E = E_0$ while for $\lambda_1' = 1$ the spectrum contains many soft photons. For this reason the optimum value of λ_1', giving the maximum similarity between the spectrum in water and the rather hard spectrum in lead, must be between 0 to 1.

The optimum value of λ_1' can be determined from the condition for the minimum of the function

$$\left| \frac{B_{as}(\lambda_2=0,\ \lambda_1=\text{const},\ \lambda_1')}{B_1(\lambda_1)} - 1 \right|.$$

Figure 2 shows $B_{as}(\lambda_2 = 0, \lambda_1 = 4, \lambda_1')/B_1(\lambda_1 = 4)$ as a function of λ_1' for Pb + H_2O and H_2O + Pb in slab geometry. The values of the buildup factors of the individual materials are taken from [4]. It is clear from that the optimum value of $\lambda_1' \approx 0.6$ for either order of the materials.

Figure 3 shows the buildup factors for homogeneous layers in slab geometry, the buildup factor for a two-layer shield with E_0 = 1 MeV and $\lambda_1 = 4$ (data from Shimizu [4]), and the asymptotic value of the buildup factor for $\lambda_1' = 4$ and $\lambda_1' = 0.6$. Figure 3 shows that the asymptotic expressions for the buildup factors of a heterogeneous shield, particularly with optimum asymptote, are of practical value when it is required to determine an approximate value of the buildup factor for a heterogeneous shield having a second layer more than or of the order of one mean free path in thickness.

The relatively small value of the transient solution for the optimum asymptote and also the fact that the relative error in the buildup factor for a heterogeneous shield is less than the error in the transient solution permits the use of rather crude approximations in the calculation of $f(\lambda_2)$, e.g., the assumption that the scattered radiation is emitted in a direction normal to the interface, thus eliminating the integration over the angles. Although the latter assumption leads to an overestimate of $f(\lambda_2)$, it has a certain physical justification since it is well known that the intensity of the scattered radiation falls off rapidly as $\Omega \cdot n$ decreases. The values of the buildup factor for two-layer shields obtained in this approximation are shown in Fig. 3. The calculations were performed for $\lambda_1' = 1$ since data on the spectra $J_2^s(E, \lambda_1')$ for $\lambda_1' = 0.6$ are not available in the literature. We note that the asymptotic solution for $\lambda_1' = 1$ is only slightly different from the optimum for $\lambda_1' = 0.6$ (Fig. 2). In calculating $f(\lambda_2)$ the values of J_1^s and J_2^s and the attenuation of radiation from a plane monodirectional source in infinite geometry [6, 7] were used in the integrand. This leads to a further overstimate of $f(\lambda_2)$. Nevertheless, the buildup factor for a two-layer shield is in good agreement with the value obtained by a more accurate method.

Point Isotropic Source at the Center of a Spherical Shield. We assume that $I_2^S(E, \Omega, \lambda_1', \lambda_2)$ is the spectral-angular distribution of the intensity (dose) of scattered radiation at the interface when a spherical shell of material of the first layer is replaced by a spherical shell of material of the second layer of thickness λ_1' adjoining the interface; $\varkappa$ is given by the same formula as for a plane-parallel shield [$w = e^{-\lambda\lambda}(\mu_s/\mu)\partial f/\partial E(E_0)/4\pi r_1^2$, where r_1 is the distance from the source to the inteface]. In spherical geometry the possible values of λ_1' have an upper bound given by $0 < \lambda_1' \leq \mu_2 r_1$. The choice of the optimum values of λ_1' must be made by taking account of this restriction. As $r_1 \to \infty$ this case approaches a plane monodirectional source behind a plane-parallel shield.

By an argument similar to that presented above we obtain for $B_{as}(\lambda_1, \lambda_2)$ a relation which agrees in form with Eq. (3). However, the buildup factors appearing in it have a somewhat different physical meaning. $B_2(\lambda_1' + \lambda_2)$ is the buildup factor for a point isotropic source at the center of homogeneous spherical arrangement of the material of the second layer of inner radius $r_1 - \lambda_1'/\mu_2$ and thickness $\lambda_1' + \lambda_2$; $B_2^*(\lambda)$ is the buildup factor for a uniform spherical surface source of radius r_1 radiating radially and a spherical arrangement of material of the second layer of inner radius r_1 and thickness λ_2, taking account of reflection from a layer of the second material of thickness λ_1' located on the source side and directly adjacent to it; $B_2^{**}(\lambda_2)$ is the buildup factor for a uniform spherical surface source of radius r_1 radiating radially and a spherical arrangement of material of the second layer of inner radius r_1 and thickness λ_2, taking account of reflection from a spherical layer of the first material of thickness λ_1 located on the source side and directly adjacent to it. The buildup factors B_2, B_2^*, and B_2^{**} are evaluated at points on the outer surface of the shield.

The formula for the buildup factor of a two-layer spherical shield, taking account of the transient solution, can be written in the form

$$B(\lambda_1, \lambda_2) = \alpha B_2(\lambda_1' + \lambda_2) + [B_1(\lambda_1) - \alpha_0 B_2(\lambda_1')]\, e^{\lambda_2} f(\lambda_2)\, S_{geom}$$

where α and α_0 are given by (5) and (6), and $f(\lambda_2)$ by Eq. (7); S_{geom} is the geometric factor equal to $(r_1 + \lambda_2/\mu_2)^2/r_1^2$; for a plane monodirectional source $S_{geom} = 1$. We note that the geometric factor does not appear in any of the previously mentioned empirical formulas for a point isotropic source.

Other Types of Sources and Shielding Geometries. For other types of sources and shield configurations the buildup factor cannot be written as the sum of asymptotic and transient parts satisfying the conditions formulated at the beginning of the article since $\varkappa$ cannot be considered constant in such cases.

For example let us consider a plane isotropic source behind a plane-parallel shield. For a plane monodirectional source the scattered photons of energy E_0 at a point on the interface travel in one direction only, but for a plane isotropic source such photons travel in all directions from the first slab into the second. In order that the transient solution not contain photons of energy E_0, i.e., that there be a relatively rapid decrease, it is necessary to separate out the part of the spectrum $\varkappa(\Omega) I_2^S(E, \Omega, \lambda_1', \lambda_2)$ for a given Ω. Since $\varkappa$ depends on Ω for an isotropic source, the asymptotic solution cannot be expressed in terms of the buildup factor for the material of the second layer, i.e., the separated spectrum differs from $I_2^S(E, \Omega, \lambda_1', \lambda_2)$ spectrum. It is also impossible to use the same constant value of $\varkappa$, e.g., $\varkappa$ for the direction of the normal to the interface, since the transient solution would contain photons of energy E_0 and would not diminish rapidly. For a point isotropic source behind a plane-parallel shield $\varkappa$ depends on both Ω and the angle between the propagation vector for the primary radiation and the normal to the shield surface.

Since the buildup factor is determined mainly by the radiation scattered in directions close to the normal, the approximation using the constant value of $\varkappa$ for this direction may turn out to be adequate for practical purposes.

Shields with an Arbitrary Number of Layers

In order to generalize the equations obtained for two-layer shields to shields of N layers we regard the first N – 1 layers as a single layer. Then all the above discussion still applies. Just as in the case of a two-layer shield buildup factors can be obtained as a sum of an asymptotic and transient parts only for a plane monodirectional source behind a plane shield, and a point isotropic source at the center of a spherical shield.

We shall understand by $\varkappa_N$ the ratio of intensities of photons singly scattered directly forward after penetrating the heterogeneous shield of N – 1 layers and a shield of the material of the last layer of

thickness λ'_{N-1}. In a special case λ'_{N-1} can be equal to $\sum_{i=1}^{N-1} \lambda_i$. For a spherical shield λ'_{N-1} is the thickness of the layer of material of the N-th layer adjacent to the inner side of the boundary between the (N – 1)-th and N-th layers.

Clearly $\varkappa_N = \frac{\sum_{i=1}^{N-1} w_i}{w_N}$, where w_i is the probability that a primary photon is scattered directly forward in the i-th layer and then travels to the boundary between the (N – 1)-th and the N-th layers without interaction; w_n is the probability that a photon at the source energy is scattered directly forward in a homogeneous shield of material of the last layer of thickness λ'_{N-1} and then travels through the remaining thickness without interaction.

It is easy to show that

$$w_i = e^{-\sum_{i=1}^{N-1} \lambda_i} \lambda_i \, (\mu_{si}/\mu_i) \frac{\partial f}{\partial E}(E_0) \begin{cases} 1 & \text{— for a plane monodirectional source} \\ \frac{1}{4\pi r_{N-1}^2} & \text{— for a point isotropic source, where } r_{N-1} \text{ is the distance from the source to the boundary between the Nth and (N – 1)-th layer.} \end{cases}$$

Thus for both cases

$$\varkappa_N = \frac{e^{-\sum_{i=1}^{N-1} \lambda_i}}{e^{-\lambda'_{N-1}}} \sum_{i=1}^{N-1} \frac{\lambda_i}{\lambda'_{N-1}} \cdot \frac{(\mu_{si}/\mu_i)}{(\mu_{sN}/\mu_N)}.$$

By an argument similar to that used for two-layer shields it is easy to show that the formula for the buildup factor of a shield of N layers can be written in the form of the following recurrence relation:

$$B(\lambda_1, \lambda_2, \ldots, \lambda_N) = \alpha_N B_N(\lambda'_{N-1} + \lambda_N) + [B_{N-1}(\lambda_1, \lambda_2, \ldots, \lambda_{N-1}) - \alpha^0_N B_N(\lambda'_{N-1})] \, e^{\lambda_N} f(\lambda_N) S_{\text{geom}},$$

where α_N is the asymptotic coefficient equal to

$$\alpha_N = \sum_{i=1}^{N-1} \frac{\lambda_i \, (\mu_{si}/\mu_i)}{\lambda'_{N-1} \cdot (\mu_{sN}/\mu_N)} + \frac{B^{**}_N(\lambda_N) - B^{*}_N(\lambda_N) \sum_{i=1}^{N-1} \frac{\lambda_i}{\lambda'_{N-1}} \left(\frac{\mu_{si}/\mu_i}{\mu_{sN}/\mu_N} \right)}{B_N(\lambda'_{N-1} + \lambda_N)};$$

$$\alpha^0_N = \alpha_N(\lambda_N = 0);$$

$$S_{\text{geom}} = \begin{cases} 1 & \text{— for a plane monodirectional source behind a plane-parallel shield;} \\ \left(\frac{r_{N-1} + \frac{\lambda_N}{\mu_N}}{r_{N-1}} \right)^2 & \text{— for a point isotropic source at the center of a spherical shield;} \end{cases}$$

$$f(\lambda_N) = \frac{\int\int dE \, d\Omega \left[I^s_{N-1}(E, \Omega, \sum_{i=1}^{N-1} \lambda_i, \lambda_N) - \varkappa_N I^s_N(E, \Omega, \lambda'_{N-1}, \lambda_N) \right] \frac{1}{k_N(E, \Omega, \lambda_N)}}{\int J^s_{N-1}\left(E, \sum_{i=1}^{N-1} \lambda_i\right) dE - \varkappa_N \int J^s_N(E, \lambda'_{N-1}) \, dE}.$$

The factors $B_N^*(\lambda_N)$ and $B_N^{**}(\lambda_N)$ are analogous to $B_2^*(\lambda_2)$ and $B_2^{**}(\lambda_2)$, but $B_N^{**}(\lambda_N)$ represents the build-up factor taking account of reflection from the first N – 1 layers.

For a plane source there are no restrictions imposed on λ_{N-1}; for a point isotropic source the possible values of λ'_{N-1} must satisfy the relation $0 < \lambda'_{N-1} \leq \mu_N r_{N-1}$.

The optimum values of λ'_{N-1} is found from the condition for the minimum of the function

$$\left| \frac{B_{as}(\lambda_N = 0, \sum_{i=1}^{N-1} \lambda_i, \lambda'_{N-1}}{B(\lambda_1, \lambda_2, \ldots, \lambda_{N-1}} - 1 \right|,$$

which physically leads to the maximum similarity of the distributions

$$I^s_{N-1}(E, \Omega, \sum_{i=1}^{N-1} \lambda_i, \lambda_N) \text{ and } I^s_N(E, \Omega, \lambda'_{N-1}, \lambda_N).$$

For a thick penultimate layer the exact value of $B(\lambda_1, \lambda_2, \ldots, \lambda_{N-1})$ can be replaced by its asymptotic value, also optimized in advance.

To determine $f(\lambda_N)$ when the transient solution can be neglected, it is sufficient to know the spectra in the (N – 1)-th and N-th homogeneous layers. The spectrum in the (N – 1)-th layer is complex, being a superposition of the spectra of three sources; cf. section on "Plane monodirectional source behind a plane-parallel shield" and (3).

LITERATURE CITED

1. M. Kitazume, Nippon Genshiryoku Gakkaishi, 7, No.9, 496 (1965).
2. S. Miyasaka and A. Tsuruo, J. Nucl. Sci. and Technol., 3, 393 (1966).
3. H. Schubart, ABC-THH-1025 (1965).
4. A. Shimizu, Nucl. Sci. Engng., 32, 385 (1968).
5. D. L. Broder et al., At. Energ., 12, 30 (1962).
6. H. Goldstein and J. Wilkins, The Shielding of Mobile Reactors [Russian translation], IL, Moscow (1961), p.212.
7. V. Ch. Pal'vanov and A. S. Sterlkov, in: Problems in Dosimetry and Radiation Shielding [in Russian], Vol.7, Atomizdat, Moscow (1967), p.138.

NUCLEAR POWER IN THE SEVENTIES

S. Eckland*

UDC 621.039

The seventies, having seen the start of the first important steps toward control of atomic weapons, i.e., the conclusion of the treaty concerning nonproliferation of nuclear weapons and talks on the limitation of strategic weapons will witness the emergence of new possibilities for the peaceful use of atomic energy. It should be stressed that international collaboration is needed for a complete realization of these possibilities.

More than ten years ago F. Sporn said that "the utilization of atomic energy is aimed at a moving target, i.e., at the cost of electrical energy produced in usual electric power stations."

The latest example of a strong fluctuation in the cost of ordinary fuel is the appreciable and unexpected increase in the price of oil in large commercial centers such as Rotterdam from the "normal" level of $10 to more than $25 per ton of crude oil in the summer and fall of 1970. The main reasons for this increase are the following:

1) a large underestimation of power requirements, especially in Western Europe;

2) continued stoppage of the trans-Arabian pipeline and the Suez canal;

3) a cut in the yield of crude oil in Libya;

4) an acute shortage of oil tankers.

Some of these reasons are undoubtedly interrelated. Due to the closure of the trans-Arabian pipeline and the Suez canal a large quantity of oil from the Middle East must be transported via the Cape of Good Hope, which lengthens the route by 20,000 km; the carrying capacity of the tankers therefore decreases by a factor of five to six (compared to the route through the Mediterranean Sea). At the same time the Libyan Government imposed a decrease in supply of oil so as to make the oil companies agree to a 15% increase in the prices established earlier.

However, it is probable that the prices will return to the $10 per ton level by the summer of 1972, when the effect of an appreciable number of tankers going into service will be felt.

Another source of energy which merits mention is natural gas. Whereas in the USA the stocks of gas are becoming depleted, a large amount of natural gas has been discovered in Western Europe and the eastern part of the USSR. Dutch gas still supplies the industrial area of the Ruhr in the FGR at competetive prices and Soviet gas is used in Austria.

All this has been mentioned to stress the need for careful analysis, which must be done by the power companies in changing over to the use of new sources of energy.

It is calculated that the total capacity of the atomic power stations will increase from 24,000 MW at the end of 1970 to ~330,000 MW at the end of 1980. The fraction of atomic power contributing to the world's electric power will increase from 2 to 15%. This increase of nuclear power to a level at which it occupies an appreciable fraction in the world market will have important reprecussions from a national as well as international point of view.

* General Director, IAEA.

Translated from Atomnaya Energiya, Vol. 31, No. 5, pp. 487-495, November, 1971.

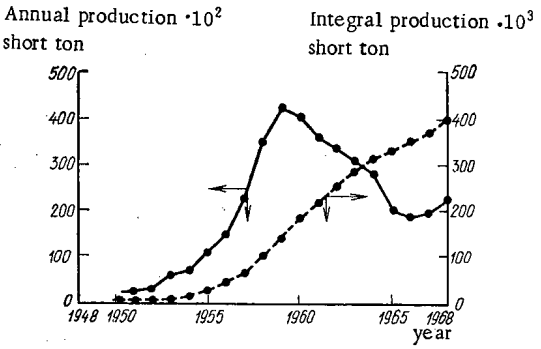

Fig. 1

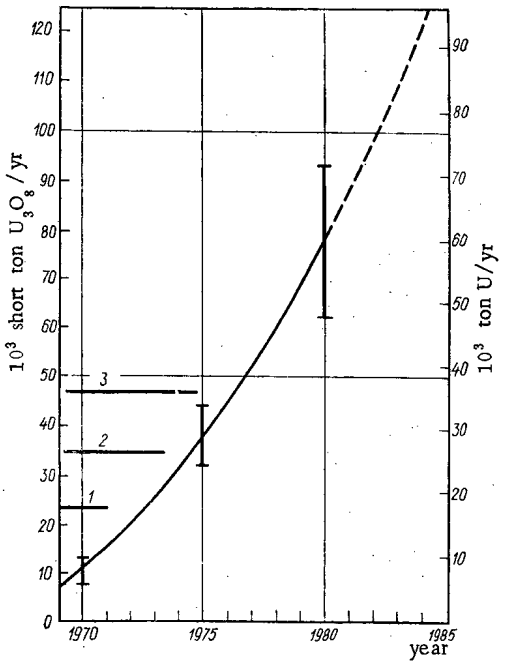

Fig. 2

Fig. 1. Yield of U_3O_8 in 1948-1968 in Australia, Canada, USA, Congo, and in South African countries (1 short ton = 907 kg).

Fig. 2. Estimate of the worldwide annual requirement of uranium: 1) annual production of uranium in 1970; 2) expected production of uranium in 1973; 3) estimated annual production of uranium in 1975.

Uranium Production and Demand

Due to the prospective increase in the use of atomic energy for peaceful purposes the interest in the production of uranium has increased considerably in the past few years. The yield of uranium for the period 1948-1968 is shown in Fig. 1.

Before 1959 it seemed that the forcasted demand for uranium would be achieved within at least 15 years. However, since the growth in the demand at atomic power stations could not be computed accurately, a noticeable drop in the prospecting, extraction, and production of uranium occurred in the early sixties.

The demand for uranium started to change in the mid-sixties, when the estimate of the growth of production of atomic power was constantly increased. The last authoritative estimate of the demand for uranium up to 1985 is contained in the report of the European Atomic Energy Agency and the IAEA. This report presents data on the assumed increase in the capacity of atomic power stations in the countries having actual or planned programs for the period up to 1985 (see Table 1).

The reliability of the information undoubtedly decreases when the period under consideration increases; the indeterminacy increases from ±4% in 1972 to ±30% in 1985. This range of uncertainty is illustrated in Fig. 2. It follows from this figure that the integral requirement for the period 1970-1985 is ~1 million ton of U_3O_8. The figures presented here do not include data from the USSR, Eastern Europe, and Chinese Peoples Republic (this refers also to all other data related to the demand and stocks of uranium, presented in the present lecture). On the basis of the computed total output of atomic power stations up to the year 2000 (at the level of 2 million MW) and some assumptions regarding the use of appropriate types of reactors, and also taking account of the possible repeated use of plutonium in thermal reactors (or storage of plutonium for use in fast reactors) the possible requirement of uranium up to the year 2000 has been computed. The uncertainty in these computations is large, since it depends on the time of introduction of fast reactors and the fraction of electrical power that will be required by the atomic industry. The requirement for the period of 1970-2000 varies in the range 2-4.5 million ton of U_3O_8. However, a majority of the specialists are of the opinion that 3 million ton of U_3O_8 is the "best" estimate. Let us examine how this requirement of uranium compares with the computed worldwide stocks.

TABLE 1. Worldwide Demand for Uranium (According to conditions in May, 1970)

Year	Yearly requirement		Integral requirement from 1970	
	U_3O_8 thousand short ton†	Uranium, ton	U_3O_8 thousand short ton†	Uranium, ton
1970	10	8	10	8
1971	15	12	25	19
1972	20	15	45	35
1973	26	20	71	55
1974	32	25	103	80
1975	38	29	141	110
1976	45	35	186	140
1977	53	41	239	185
1978	61	47	300	230
1979	69	53	369	285
1980	78	60	447	345
1985 *	135	104	1000	770

*The accuracy of the computations for 1985 is appreciable lower than for the preceding years

†1 short ton = 907 kg

Stocks of Uranium

In the above-mentioned report of the European Atomic Energy Agency and the IAEA data from two categories (classes) of uranium stocks are presented depending on the production cost (1970 prices): up to \$22 per kg for U_3O_8 and from \$22-33 per kg for U_3O_8.

Each of these categories is subdivided into "explored stocks" and "probable additional stocks" depending on the degree of certainty of their presence.

On January 1, 1970, the explored stocks of uranium were estimated at 840,000 short ton of U_3O_8, which is larger than the number given in the previous report (after 1967) by 140,000 tons.

The United States, Canada, South Africa, and France possess 85-90% of the known stocks of cheap uranium; the remaining stocks occur in 12 other countries. About 1/3 of all uranium is secondary uranium, whose production depends on the extraction of gold in South Africa and the production of copper and phosphates in the USA.

Although it is possible that this is a crude method of representing the distribution of uranium stocks in the world, it shows that many countries do not have uranium stocks and that the stocks of cheap uranium are very limited.

On the other hand, during the period 1967-1970 a large increase in explored stocks of uranium occurred as a result of intensive searches in Nigeria (12,000-26,000 ton), Gabon (400-135,000 ton), and Central African Republic (0-10,400 ton). The explored stocks of uranium also increased in Canada and USA.

Taking account of the various factors it can be assumed that the above figure for the explored stocks of uranium (~840,000 short ton of U_3O_8) is reliable.

The annual world production is at present about 23,500 ton U_3O_8, which is somewhat larger than a half of the level of world production achieved in 1959. If no drop occurs, then by 1985 the annual production should reach 135,000 ton U_3O_8, i.e., it would exceed the present production by five times. By the year 2000 165,000 ton U_3O_8 will be required per year, i.e., almost seven times the existing level.

It follows from Fig. 2 that at present there is a temporary overproduction of uranium and the demand is below the capacity of the existing plants for the production of uranium. However, in the period 1976-1978 the annual demand may surpass the production capacity, if we consider the uncertainty in the computation of the demand. Thus, in the mid-seventies additional production capacity will be required and we should be ready to prospect for and find new uranium deposits so as to avoid the need for exploiting those uranium deposits from which extraction is expensive.

Price of Uranium Concentrates

The opinions of the consumers and producers of uranium with respect to the future prices in the early sixties are coincident. According to the firms producing uranium the average computed prices of uranium are \$16.1 per kg in 1971, \$16.7 per kg in 1972, \$17.2 per kg in 1973, and \$17.6 per kg in 1974.

In the middle and at the end of the seventies the price will apparently be \$17.7 per kg; this price is considered entirely reasonable.

If we take into consideration the last successful results of the prospecting operations, at present it is improbable that the price of uranium will exceed \$22 per kg before 1980 (and perhaps up to the end of the eighties). Therefore, at any period there will not be any strong stimulus for prospecting and working supplementary stocks of uranium, whose extraction would cost \$22-23 per kg.

Thus, if the annual demand for uranium will grow in accordance with the data of Fig. 2, during the seventies it would become necessary to have a constant supplementation of the stocks of uranium by

discovering new deposits. Furthermore, if the annual demand after 1985 remains at the level 125,000 short ton of U_3O_8 (or more), then by 1985 it would be required to discover and prepare to exploit additional uranium deposits with stocks of at least 1 million short ton of U_3O_8.

Such requirements indicate the need for continuing the prospecting work at the present pace.

The periods of high demand of uranium are short. As was shown, during the period 1985-1990 large amounts of uranium will be required annually, but by 2005 or 2010 the demand of uranium may decrease appreciably due to breeders. The period of maximum demand for uranium is perhaps 25-30 years hence.

Enriching of Uranium

For most power reactors an enriching of the uranium is required, which is at present done only in France, Great Britain, USA, USSR, and China. Only USA and USSR have at their disposal sufficient production capabilities to enable them to supply enriched uranium to the world market. The USA has almost had a monopoly in this sphere but the position may change in the seventies.

In the General Assembly of the IAEA the representative of the USSR reported that the Soviet Union has worked out conditions for enriching natural uranium on the commission of any government that signed the treaty for nonproliferation of nuclear weapons. According to the information appearing in the press the Soviet Union has contacted some countries including FRG, Switzerland, and Sweden regarding possible conclusion of contracts for enriching uranium.

Approximately a year ago the governments of FRG, the Netherlands, and Great Britain reached an agreement envisaging joint development and operation of plants for enriching uranium with the use of gas centrifuges. These governments consider this method most suitable for European conditions from the economic point of view. In the first stage the joint program provides for the construction and operation of plants with an output of 350 kg s. w./yr in the Netherlands and Great Britian. According to the computations, the output of each installation during 1972 would reach 50 ton s. w./yr.

The formation of a company composed of firms of the three countries has been delayed due to legal problems (Britain must introduce an amendment to its law concerning atomic installations in order to ratify the agreement). However, the construction of experimental plants for enriching uranium has already been started as planned; they should be in operation at the end of 1971 or in 1972. The British firm "British Nuclear Fuels" is apparently having financial difficulties in connection with the need for covering 66% of the expenses for the construction of the plant in Capenhurst. The role of Belgium and Italy as possible partners is not clear. For the sake of completeness of information we must also mention the method of enriching with the use of nozzles developed in FRG.

Although it is early to talk about the economic advantages of a given method, the initiative of three participating governments led to an interesting discussion on the possibility of constructing diffusion-type enriching equipment in Europe. The atomic energy commissariat of France announced that porous membranes have been developed, which, in respect of their effectiveness, are "a little inferior" to the porous membranes constructed in USA. A new prototype high-output compressor has been developed, which is capable of distilling 40 kg of UF_6 in a second. The commissariat has ordered prototype compressors whose output is three times larger or corresponds to the output required for the full-scale diffusion enriching equipment.

France holds the view that the diffusion process is the principal base in designing high-output equipment that would meet the requirements of the European countries in 1978. The USA is studying the ways of selling plans of gas-diffusion equipment to the European countries, which will be resolved by a system of guarantees. Besides political and commercial advantages the gaurantee of the USA for the European diffusion equipment offers the possibility of realizing the production capacity in the USA.

In 1969 Japan initiated investigations on uranium enrichment and the study of the gas-diffusion as well as the centrifuge process.

When uranium enriching is done on a commercial scale, there arises a problem: whether the scale of the equipment be limited in such a way as to ensure the fulfillment of the needs of its own country or to satisfy all its needs and have the possibility of supplying enriched uranium to other countries.

As is well known, South Africa has announced that it has developed a new process of enriching uranium.

During the conference of the governments which do not have nuclear weapons, held in September 1968, many countries expressed a desire to obtain fission materials from the IAEA fund. There exists such a fund, but the materials of the fund are used exclusively for carrying out investigations. However, in 1969 the countries that supply this material expressed their readiness to grant these fission materials in quantities necessary for the operation of the existing power reactors through IAEA channels.

Reactors

The increase of the installation power of the atomic power plants during the period 1970-1980 from 24,000 to 330,000 MW (±20%) signifies an increase in the number of power reactors to 500 in 1980 (100 at present). The number of research reactors, which number 367 in 47 member-countries of the IAEA, will not increase appreciably in this decade, since the introduction of new research reactors will be compensated for by the closing of the old ones.

In the seventies light-water reactors will predominate. Toward the end of the decade industrial fast reactors may be constructed.

It should be mentioned that at present there exist many concepts of reactors, but it can be seriously questioned if there exist electric power production firms which envisage using any types of reactors other than those mentioned (water reactors with light and heavy water, improved reactors with gas cooling, and later breeder reactors) for full-scale operation.

The same picture is seen in respect of plants for the regeneration of used fuel. The firm "Nuclear Fuel Services" in the United States of America, which is the first private enterprise in this field started in 1966, has announced its intention of increasing the output of their regeneration installations from 1 to 3 ton/day. Other American firms are at present planning the construction of such installations which should reach an output of 11 ton/day in mid-seventies.

The Environment

Another important factor affecting the future of nuclear power is the environment. Ironically, this energy source, "pure" in the sense that it practically does not pollute the air, is accused of having poisonous effects on the environment. Different statements and publications have shown that the problem confronting the authorities in the field of nuclear power is an educational problem. The community appears worried about the so-called thermal effects of nuclear power reactors in the environment or the possible ejection of radioactivity into it.

In selecting the area for the construction of an electric power station the heat deposited in the surrounding medium is undoubtedly taken into consideration. The medium, into which the wasted heat is dumped, must have a sufficiently low temperature or an appreciable volume for absorption of the excess heat. The assumed heating of the water of river Rhine to 28°C after the start of operation of the atomic power stations which are being planned at present, confirms this problem.

At present atomic power stations dump 50% or more heat into cooled water than the power stations operating with organic fuel. This difference will decrease after the efficiency of the atomic power stations increases.

Further development of nuclear power may incur the necessity for using other means of dumping heat (for example, the use of water-cooling towers in regions with limited water resources).

In Sweden it is proposed to investigate the various methods of utilization of this dumped heat; the results are awaited with great interest not only in Sweden but in other countries.

The community is worried also with the problem of radioactivity in the environment. This accusation is brought against those branches of industry which have the strictest rules of safety. One of the factors which is not taken into consideration by the community, is that the problem of waste disposal appears in the plants for regeneration of fuel, and not in the power stations.

A larger part of the radioactive wastes (about 99% of the total amount) is dumped by the regeneration plants. This does not mean that the cost of treating and disposing the wastes is proportional to the processed

amount, or that the remaining 1% is of no significance. According to the computations, as a result of the completion of the programs of development of nuclear power of all countries in the whole world, in ten years 1200 tons of fission products will be accumulated in the form of 32,000 m^3 of liquid.

As already mentioned, the larger part of the radioactive wastes are formed as a result of fission in the process of treating the fuel. The main sources of activity are the fission products of Cs^{137}, Sr^{90}, Tc^{99}, Ru^{103}, Ce^{144}, I^{131}, and Kr^{85}. In the wastes of regenerated fuel there also exist other transuranium elements such as neptunium and plutonium, which are hazardous long-life components.

Only a very small part of the wastes (including long-life elements) are dispersed in the surrounding medium; these wastes do not affect the level of radioactivity already existing in the medium and are appreciably lower than the levels which could be considered harmful to man. The larger part of the wastes is concentrated and placed in hermetically sealed containers and remain in storage.

The policy of concentration and hermetic sealing of liquid wastes containing long-life elements poses the problem of surveillance.

The existing practice of using containers is called temporary storage in the sense that the wastes are stored until such time when methods for final burial or disposal will be worked out and put into use. The policy of temporary storage avoids the problem of disposal into the surrounding medium. However, it is necessary to carry out observations. The wastes must be in such a state that they can be removed and be subjected to final processing. Some specialists think that the surveillance of the stored wastes should be carried out for five hundred to a thousand years. Therefore, the methods of final disposal of wastes which eliminate the need of surveillance, are attractive.

The absence of the possibility for carrying out final disposal is made up by the temporary storage. In this case the wastes remain on the earth and are subjected to slow decay, wherein the form and the method of storage must be safe.

In the seventies much action will be undertaken toward storing solid highly active wastes in such geological formations as salt mines.

The waters of the oceans serve as the place of storage of low-activity wastes under careful control. The sea and the atmosphere of the earth are both national and international property.

Humanity must reach a proper equilibrium between the use of the sea for transportation needs, the use of all forms of sea resources, conservation of the beauty and the charm of the sea, and also its use for the disposal of wastes.

During the conference on the problem "Procedures for establishing levels of the isotope content in sea water," held in November 1970 in Vienna, principles for reaching international agreements on the storage of radioactive wastes in seas were defined. In establishing the level of dumping of these wastes consideration was given largely to scientific investigations, although economic and social aspects were also taken into account.

Besides determining the principles and procedures of establishing the storage limit of wastes in seas it is desirable to compute also the amount of radioactive wastes dumped into the environment by atomic industrial enterprises all over the world. This computation could be carried out by compiling registration documents prepared in accordance with national programs of processing and disposing of radioactive wastes.

However, to make the community understand that the development of nuclear power will not be accompanined by any significant irradiation of the population, is a very complicated problem. People become indignant when scientists say that there is no basis for worry and that nonspecialists cannot discuss this problem in all its complexity and technological aspects. The fact that the atomic energy commissions carry out further development of nuclear power and take decisions, whether it is safe or not, also annoys the critics. In the near future more intensive attempts should be made toward allaying people's fears and obtaining the support of the community; as was recently observed in USA, that can be very important for the development of nuclear energy in some regions.

In order to perceive the advantages of atomic power stations over those operating with organic fuel, it is necessary to study only the statistical data on the contamination of air. In the United States of America

the stations operating with organic fuel are "responsible" for 3/4 of the 35 million ton of SO_2 dispersed annually; the atomic installations do not disperse SO_2.

We shall hope that the UN conference devoted to the problems of contamination of the environment (the conference will be held in 1972 in Stockholm) will contain an exposition of these problems as applicable to nuclear power.

In August 1970 in the symposium in New York, for which one of the organizers was IAEA, it was concluded that atomic energy stations contaminate the environment appreciably less than other enterprises connected with power production.

Use of Atomic Explosions for Peaceful Purposes

Atomic explosions used for peaceful purposes can be divided into two categories: 1) In carrying out underground explosions the isotopes formed in the process do not emerge at the surface of the earth; the explosions at relatively large depths are carried out for increasing the yield of oil and gas, breaking up mining substances, or creating underground reservoirs for storage of gases and liquids. 2) Explosions with the formation of craters have been carried out in numerous experiments over the last 20 years. Both atomic and chemical explosions have been conducted which have potential use in the construction of harbors, canals, dams, reservoirs, in processing deposits by the open-cast method, and in the obtention of filling materials.

The energy or elementary particles obtained as a result of atomic explosions are used for scientific purposes, for example, in conducting experiments on the interaction of neutrons, in the production of heavy elements, and in the study of seismological phenomena.

The main advantage of using atomic explosions compared to chemical explosions is the significant economy of atomic explosions. The cost of an atomic explosion outfit, equivalent to 10,000 ton TNT is $300 to $400 thousand, whereas the cost of 10,000 ton TNT is about $5 million. Besides, the cost of placing the atomic explosion outfit is appreciably lower than that of chemical due to its compactness.

However, in using atomic explosions the problem of ejection of radioactivity still remains; in view of this it is necessary to find ways to reduce this ejection to a minimum.

Among the countries carrying out investigations for the use of atomic explosions for industrial purposes are France, USSR, and USA. However, only recently the experimental technique has been perfected to a degree that interest in this potential constructional method has developed on an international scale.

In March 1970 IAEA convened a meeting with the idea of encouraging exchange of information in this field. The meeting arrived at the unanimous conclusion that the most realistic possibility of using atomic explosions for peaceful purposes in the near future is their use for the extraction of such useful minerals as gas and oil, and also for the exploitation of metal deposits. In using atomic explosions for these purposes the nuclear charges will remain sufficiently deep below the earth's surface.

According to the treaty of nonproliferation of nuclear weapons, countries not possessing nuclear weapons are prohibited to develop and produce any kind of nuclear explosion devices. However, the treaty provides for a situation, according to which the gains from the use of nuclear explosions for peaceful purposes could be accessible to these countries through the conclusion of agreements with the countries having nuclear weapons within the framework of international supervision. The IAEA is studying procedures which could be useful for exercising "appropriate international supervision."

In view of the fact that considerable hope is placed in the use of atomic explosions, especially in the developing countries, it is pertinent to make a completely justified precautionary remark. This technique is still in the experimental stage; it will be a considerable time before the future gains of the use of atomic explosions can be exactly evaluated.

Guarantees

The use of guarantees is intended to prevent the leakage of nuclear materials into the sphere of their use for military purposes. By 1980 all the atomic power stations with the overall capacity of 330 million kW will be producing 80 ton/yr of plutonium, which can be used for peaceful purposes or for the production

of nuclear weapons. If the plutonium is used for making weapons, then in one week 100 bombs could be produced, 1/3 of these by countries which do not at present possess nuclear weapons.

The idea of a system of guarantees has been used by IAEA for some time, i.e., from the time of conclusion of the bilateral agreements according to which the USA, and later other nuclear powers also, supplied countries with nuclear equipment and materials at the same time requiring the implementation of the guarantees (working out of a regional system of guarantees within the limits of the European Atomic Energy Community and the implementation of IAEA guarantees). This system of guarantees, whose implementation was limited to certain regions and equipment, was found to be effective; however, it was not sufficiently qualitative to ensure people's confidence in nonproliferation of nuclear weapons.

In the seventies the position will change, since guarantees, whose implementation is required in accordance with the treaty on nonproliferation of nuclear weapons, that went into force on March 5, 1970, will be put into action. The treaty obligates the countries not possessing nuclear weapons not to produce or acquire by any other means weapons or any other atomic explosion devices. According to the treaty the countries must accept the IAEA guarantees in all their peaceful nuclear activities with a view to check the fulfillment of the obligations imposed on them by the treaty. All the governments participating in the treaty are obliged not to give nuclear material or equipment to any government not possessing nuclear weapons until such time that the source of the special fission material is not placed under IAEA guarantees.

The effectiveness of the treaty in achieving the restrictive purpose, i.e., the nonproliferation of nuclear weapons, is undoubtedly dependent on its universal character. On November 1, 1971, 98 countries signed the treaty (including majority of the countries having the technical capability of producing weapons) and 68 countries have ratified it. Even if not all the countries ratify the treaty, the guarantees, whose implementation is required in accordance with the treaty, will have effect, since the main suppliers of fission material have ratified the treaty (France did not sign the treaty, but announced that in future she will act exactly as the countries that signed it). They cannot export material or equipment until such time that the guarantees are applicable to it. For this reason all the countries, which rely on the import of special fission materials, will experience the effect of the IAEA guarantees irrespective of whether they signed or ratified the treaty on nonproliferation of nuclear weapons or not.

This new position in regard to international guarantees has been a reason for the uneasiness of certain countries in relation to the fact that the implementation of the guarantees in all their nuclear activities will in some way hinder the progress in the field of investigations, development, and production of atomic energy, and will also impair commerce. The reasons for this anxiety are understandable, but they are unjustified.

The atomic industry needs nuclear materials for its own use. They should be treated in such a way that it is possible to keep a strict account of them, for example, due to their high price, toxic nature, and the danger of reaching critical mass (accidently or calculated), not to talk of the possibility of their use as explosive materials in exceptional cases. These considerations demand a definite form of control, whose basic function is accounting of the fission materials.

The same account of materials will serve as the basis for the system of guarantees. The accounting and guarantees of safety at national or regional level should, to a large extent, harmonize conditions for the fulfillment of the requirements of the system of IAEA guarantees. Then the role of the IAEA will be to check the data supplied by the control system of the country. This principle is at present being incorporated in the proposed statutes of the agreements on the guarantees, which will be concluded in accordance with the treaty on nonproliferation of nuclear weapons. The committee on guarantees, which is composed of the representatives of 50 governments, was engaged in compiling the main documents on the technical procedures of implementation of the guarantees in accordance with the treaty. In accepting the guarantees (especially if the equipment is designed taking account of the implementation of the guarantees of it) the atomic industry must not carry out any appreciable "loading." On the other hand, it can be said that the guarantees used by the international organization to a large extent make the national measures reliable.

Although inspection is only a part of the system of guarantees, this operation is of great significance, since it is related to the problem of national sovereignty. It is not surprising that inspection and the danger of industrial espionage are the main points, over which there are objections to the treaty on nonproliferation of nuclear weapons.

Probably the importance of inspection could be reduced. One of the tasks of the program of investigations in the field of IAEA guarantees is rendering assistance in the development of a control–inspection device, which would permit the IAEA to concentrate its attention on strategic points in the flow of nuclear materials and the procedure of implementation of guarantees to a still larger extent; certain forms of measuring equipment, developed by the member states of IAEA, are being used by the IAEA in an experimental capacity.

However, it is generally accepted that a considerable effort and technological developments are needed before the equipment can be widely used, which means that the inspections for the purpose of effective implementation of the guarantees will continue.

As regards the apprehensions about industrial espionage, the critics usually fail to take into consideration three basic factors. Firstly, in the execution of his ordinary duties the inspector does not demand access to information of industrial value. Secondly, all the agreements on the guarantees include statutes preventing industrial espionage. And, finally, the assignment of an inspector to a given state is done after a thorough consideration and with explicit approval of the representatives of that government.

The government has a right to change at any time its decision regarding the assignment of the inspector.

In view of the growth of the atomic industry and the concomitant guarantees it is necessary to make constant efforts to ensure confidence that the effectiveness of the guarantees is maximum, that the necessity for the presence of inspectors is reduced to a minimum, and that the cost of implementation of the guarantees decreases. In this respect the IAEA has the collaboration of industry and the national atomic energy commissions.

The transition from the system of control, applicable only to individual installations, to a system applicable to national nuclear programs as a whole in accordance with the treaty on nonproliferation of nuclear weapons will require some time.

Although at present the system of guarantees has been applied only to installations, in future the implementation of guarantees will be concentrated on the flow of nuclear program as a whole. This would permit simplification of the system of IAEA guarantees as fast as it would be possible to obtain an accurate "picture" of the movement of materials. The transition to operations in accordance with the treaty on nonproliferation of nuclear weapons will occur in the next two years.

ON THE MECHANISMS OF RADIATION DEFORMATION OF GRAPHITE

Yu. S. Virgil'ev and I. P. Kalyagina

UDC 621.039.532.21

When graphite is used in a neutron field, its linear dimensions change; the magnitude and the sign of the changes are determined by the size and intensity of the damaging field, the irradiation temperature, the anisotropy of the graphite, its degree of perfection, the level of the so-called "frozen-in" stresses appearing in graphite blanks in their thermal treatment, and so forth. Each of the enumerated factors contributes to the observed dimensional changes to different degrees (depending on the conditions of irradiation).

Several theories have been proposed for a qualitative description of the radiational deformation of the structure of graphite. The most common among these are the mathematical models of Simmons [1] and also of Price and Bokros [2].

Simmon's method of computation is based on the assumption that the deformation of graphite $\Delta l/l$ is determined by the change in the dimensions of individual crystals in the directions of the axes c and a: $S_c = \Delta X_c/X_c$; $S_a = \Delta X_a/X_a$. The characteristics of a given form of graphite (porosity, grain orientation, etc.) are taken into consideration through the accomodation coefficients K_1, K_2, K_3, K_4, which are similar to those in the equations determining the coefficients of thermal expansion of a polycrystalline material $\alpha_{\parallel}$ $\alpha_{\perp}$ in terms of the coefficient of thermal expansion of a monocrystal at the investigated temperature α_c and α_a:

$$\left.\begin{aligned}\alpha_{\parallel} &= K_1\alpha_c + K_2\alpha_a;\\ \alpha_{\perp} &= K_3\alpha_c + K_4\alpha_a;\end{aligned}\right\} \quad (1)$$

$$\left.\begin{aligned}(\Delta l/l)_{\parallel} &= K_1 S_c + K_2 S_a;\\ (\Delta l/l)_{\perp} &= K_3 S_c + K_4 S_a.\end{aligned}\right\} \quad (2)$$

In the first approximation $K_1 + K_2 = 1$ and $K_3 + K_4 = 1$; therefore the accomodation coefficients are determined from Eq. (1):

$$\left.\begin{aligned}K_1 &= \frac{\alpha_{\parallel}-\alpha_a}{\alpha_c-\alpha_a}; \quad K_2 = \frac{\alpha_c-\alpha_{\parallel}}{\alpha_c-\alpha_a};\\ K_3 &= \frac{\alpha_{\perp}-\alpha_a}{\alpha_c-\alpha_a}; \quad K_4 = \frac{\alpha_c-\alpha_{\perp}}{\alpha_c-\alpha_a}.\end{aligned}\right\} \quad (2a)$$

The method of Price and Bokros gives more accurate expressions for the radiation deformation taking account of the preferred orientation of the crystals:

$$(\Delta l/l)_x = (1-R_x)\,\Gamma_x S_c + R_x S_a, \quad (2b)$$

where R_X is a parameter describing the preferred orientation of the crystals in the sample, determined from x-ray data; Γ_X is the accomodation coefficient estimating that part of the expansion of the crystals in the direction of axis c, which leads to the change in the overall dimension.

In Eqs. (2) all the quantities except S_c and S_a are measured directly. The change of the dimensions of the crystals can be determined in the irradiation of pyrolytic recrystallized graphite, which can be regarded as a monocrystal within reasonable approximation. The increase of the dimensions of the crystals in the direction of axis c and the compression in the direction parallel to the plane of the base, are caused by two forms of defects that appear on irradiation: imbedded atoms and vacancies. The imbedded atoms are sufficiently mobile (with migration energy of 0.016 eV [3]) and a majority of these recombine with the vacant places of the lattice or with the defects that appeared earlier; the remaining atoms combine in complexes, whose stability is determined by the conditions of irradiation. Some complexes are the centers of the

Translated from Atomnaya Energiya, Vol. 31, No. 5, pp. 497-504, November, 1971. Original article submitted December 7, 1970.

appearance of loops of imbedded atoms, whose nucleation in monocrystals has a homogeneous character for irradiation below 300°C. At the same time for materials with a low degree of crystal formation, a heterogeneous nucleation of the defects occurs.

The growth of the loops of imbedded atoms is restricted by two factors: 1) the distance between the atoms; 2) the number and the nature of the vacancies existing in the irradiated graphite in the three forms. Individual vacancies and their small clusters behave as point defects; they are observed at temperatures up to 500°C. Loops of vacancies appear at higher temperatures, but they can appear also at low temperatures (about 150°C); however, for this high doses of radiation are needed [4]. Under the same conditions a flattening of the lines of vacancies is observed in the lattice; along with all other forms of vacancies they cause a compression in the direction a. The radiation defects produce a deformation field in the material, which causes changes both in the parameters of the lattice and the dimensions of the crystals.

Considering the nature of the defects, the authors of [5] express the relative change in the volume of a crystallite $(\Delta v/v)_x$, equal to $(\Delta v/v)_x = S_c + 2S_a$, in terms of the relative changes of the lattice parameters $\Delta c/c$ and $\Delta a/a$ and the volume changes due to imbedded atoms n_i, the vacancies in the form of point defects n_v, and the vacancies in loops n:

$$(\Delta v/v)_x = -n_i + n_i + n_v + \Delta c/c + 2\Delta a/a. \tag{3}$$

Without introducing a large error they simplify this equation to

$$(\Delta v/v) = n_l - A\Delta a/a, \tag{4}$$

where A is a coefficient equal to 7.5-8.7. At temperatures lower than 500°C n_l tends to zero; therefore, the value of n_l can be found from the equations of growth at higher temperatures. At temperatures of the order of 1000°C, when the motion of the imbedded atoms can be three-dimensional and the vacancies have a large mobility, the presented discussion of the nature of the defects is inapplicable.

The presented models describe the characteristics of the changes in the dimensions of a sample of a polycrystalline graphite under the effect of irradiation as a result of the expansion of the crystals in the direction of the axis c and compression in the direction of the axis a. However, the radiation change of the dimensions of graphite samples with the change in the dose is of a complex nature; at the beginning of irradiation a departure from the assumed linear law has been detected [3].

For explaining the change in the linear dimensions at low doses, when an increase in the sample is observed instead of compression and vice versa, the relaxation of the so-called localized "frozen-in" stresses in the crystals should be taken into consideration. The indicated anamolous behavior can be explained by the presence of stresses compressing the crystals in the direction parallel to the c axis and stretching them in the plane of the base. In the investigation of graphites with a sphaerolitic structure Mrozovskii arrived at this conclusion about the presence of stretching stresses. Therefore, for nonsphaerolitic structures, compression stresses in the direction of the c axis should perhaps be considered the predominant form of stresses.

This is confirmed by experiments on low-temperature irradiation and subsequent thermal annealing of the samples of pyrolytic graphite deposited at 2100°C.* In this case, after irradiation at 140°C by a dose of $2 \cdot 10^{20}$ neutrons/cm^2 the dimension of the sample parallel to the plane of the base (length) decreases, while the dimension perpendicular to the plane of the base (thickness) increases significantly. As a result of subsequent annealing at temperatures above 1000°C there occurs not only a restoration of the parallel dimensions but also an increase compared to the initial value. At the same time the thickness of the sample decreases noticeably compared to its initial value.

The relative deformation of the crystals due to relaxation is given by the expression

$$S'_c = \Delta X_c/X_c = \frac{\sigma^0_{\parallel}}{E_{\parallel}}(1 - e^{-K_{\parallel}E_{\parallel}D}); \quad S'_a = \Delta X_a/X_a = \frac{\sigma^0_{\perp}}{E_{\perp}}(1 - e^{-K_{\perp}E_{\perp}D}), \tag{5}$$

where D is the radiation dose; σ^0 is the magnitude of the "frozen-in" stresses; E is the modulus of elasticity of the first kind; $K_{\parallel, \perp}$ is the coefficient of nonstationary creep in the directions parallel and perpendicular to the axis of formation, respectively.

*Measurements made by R. N. Ivanova and B. G. Makerchenko.

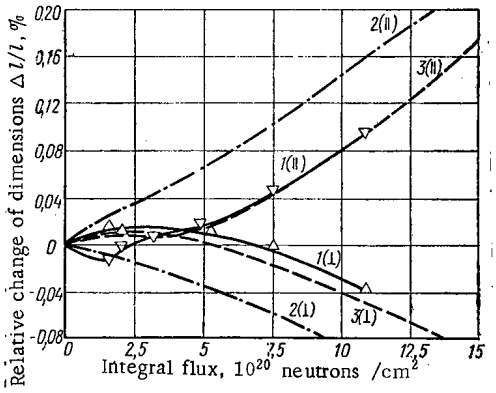

Fig. 1

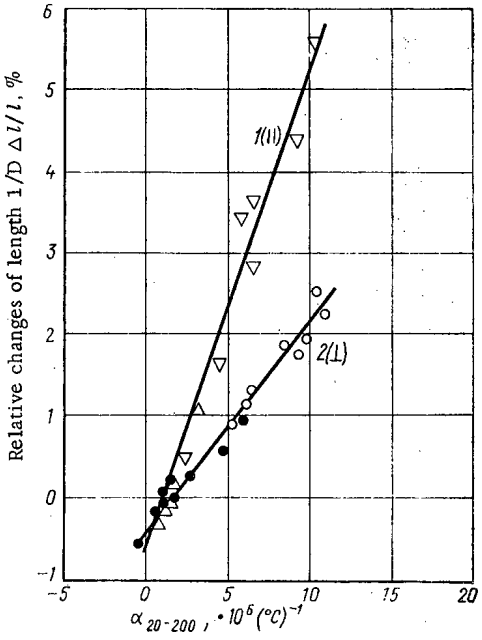

Fig. 2

Fig. 1. Relative change in the linear dimensions of samples of highly anisotropic graphite as a function of the dose of irradiation: 1) experimental data; 2) computation according to the elastic model; 3) computation taking account of the relaxation of stresses; temperature of irradiation 600°C.

Fig. 2. Relation of the relative change of the linear dimensions of the samples of different grades of graphite with their thermal expansion coefficient. Irradiation at a temperature of 140°C with doses of: 1) $6 \cdot 10^{25}$ neutrons/cm^2 ($E \geq 0.18$ MeV); 2) $3.5 \cdot 10^{20}$ neutrons /cm; ▽, ○) parallel direction; △, ●) perpendicular direction.

As seen from Eq. (5), the deformation of the crystals due to the relaxation decreases with the dose and the decrease is more rapid for higher values of the modulus of elasticity and the coefficient of nonstationary creep and, since the latter increases with temperature the decrease starts earlier. Thus, the dimensional changes of crystallites S_c, S_a under irradiation decreases due to the relaxation of the stresses. Taking account of the above statement expression (2) can be written in the form

$$(\Delta l/l)_{\parallel} = K_1(S_c - S_c') + K_2(S_a - S_a'); \quad (\Delta l/l)_{\perp} = K_3(S_c - S_c') + K_4(S_a - S_a'). \tag{6}$$

A comparison of the computed results, obtained with and without taking relaxation into consideration, with the results of experiments for a highly anisotropic graphite irradiated at 600°C is presented in Fig. 1. There is a good agreement between the experiment and the computation. It should also be mentioned that for weakly irradiated samples of this graphite preliminary measurements of the parameter c of the crystal lattice showed some decrease. An increase in the sizes of the regions of coherent scattering is also noticed, which also indicates removal of a part of the internal stresses. It should be mentioned that at high-intensity irradiation of the samples, due to an appreciable rate of deformation of the crystallites and a rapid completion of the relaxation of stresses the deviation of the curves of measurement of dimensions of the samples from the linear behavior will not be so clear; as shown in Fig. 1. Only in this case some slowing down of the rate of deformation at small doses is observed.

Numerous relationships of the relative change in the dimensions of crystallites S_c and S_a, computed from Eq. (2) for small doses which are presented in the literature [3, 6], are also found to be nonlinear. Nevertheless, the indicated models satisfactorily describe the dimensional changes of graphite at temperatures up to 1000°C and for doses of the order of 10^{21} neutrons/cm^2.

The model of Simmons was found to be more convenient; its representations permit a satisfactory estimate of the change in the linear dimensions of different forms of the structure of graphite from their coefficients of thermal expansion. It follows from expression (2) that the radiation change of the linear

TABLE 1. Properties of Materials of Different Grades

Material grade	Temperature of thermal treatment °C	Weight per unit volume, g/cm³	Physico-mechanical characteristics: endurance limit, kg/cm² for compression σ_c	endurance limit, kg/cm² bending σ_{ben}	Modulus of elasticity $E \cdot 10^{-5}$ kg/cm²	thermal expansion coefficient $\cdot 10^{-6}$ 1/deg linear α	thermal expansion coefficient $\cdot 10^{-6}$ 1/deg volume α	Dimension of the crystals Å	Reference
PGA	2800	1,74	327/352	145/100	1,20/0,56	0,8/2,8	10,8	1930	[6, 10]
CSF	2750	1,66	525/455	—	—	1,3/5,0	11,3	1500	[6, 10]
PH	2800	1,80	—	118/105	0,98/0,84	3,5/3,9	11,3	1500	[7, 11]
PI	2800	1,85	—	98/84	1,18/1,05	3,5/3,9	11,3	1500	[7, 11]
TSGBF	2450	1,80	520/600	—	—	3,2/3,7	10,6	—	[6, 10]
Pyrolytic graphite	2800	2,22	—	—	—	—0,8/28,0	24,9	—	[10]

Note: Indicated in the numerator are the properties in the direction parallel to the plane of the base, in the denominator – in the perpendicular direction. The thermal expansion coefficient was determined at 20-120°C. The dimension of the crystal is computed by the method of thermal conductivity.

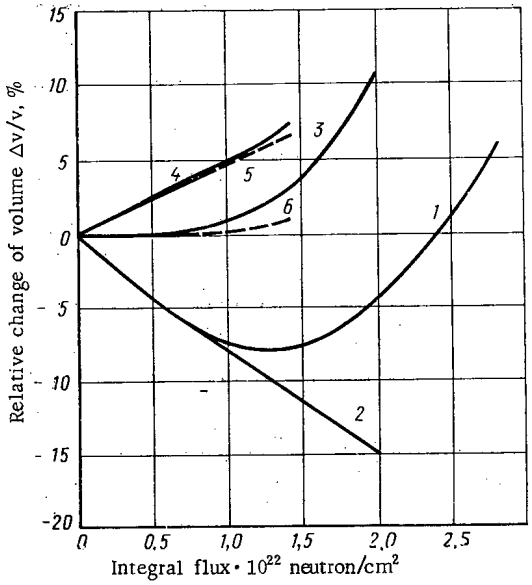

Fig. 3. Dependence of the relative change in the volume of samples on the dose of irradiation for grade PI isotropic graphite and recrystallized graphite respectively: 1, 4) experimental data; 2, 5) computation according to elastic model; 3, 6) change due to the increase in the volume of vacancy pores.

dimensions in a given direction is directly proportional to the thermal expansion coefficient:

$$\left.\begin{aligned}(\Delta l/l)_{\parallel} &= A\alpha_{\parallel} - C;\\ (\Delta l/l)_{\perp} &= A\alpha_{\perp} - C,\end{aligned}\right\} \qquad (7)$$

where

$$A = \frac{S_c - S_a}{\alpha_c - \alpha_a}; \quad C = \frac{\alpha_a S_c - \alpha_c S_a}{\alpha_c - \alpha_a}.$$

This dependence for different marks of the structure of graphite is presented in Fig. 2.

The anisotropy in the change of the linear dimensions, which is estimated as the algebraic difference of the relative changes of the dimensions in parallel and perpendicular directions, is directly proportional to the difference of the thermal expansion coefficients. It should be mentioned that the position of the curves in Fig. 2 is determined by the conditions of irradiation, the dose, and the temperature.

As shown in [1], the slope of the straight lines decrease with increase in temperature. For high doses ($2\text{-}4 \cdot 10^{22}$ neutrons/cm²) and temperatures above 400°C the monotonic compression of the graphite samples changes into growth: their dimensions are first restored to the initial values and later increase rapidly [4, 7]. Therefore, under these conditions the indicated models become unsuitable not only for a quantitative but also for a qualitative description of the deformation of graphite. Consequently, another

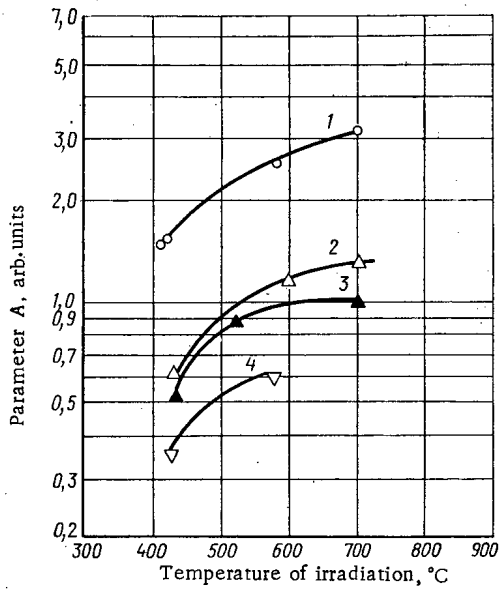

Fig. 4

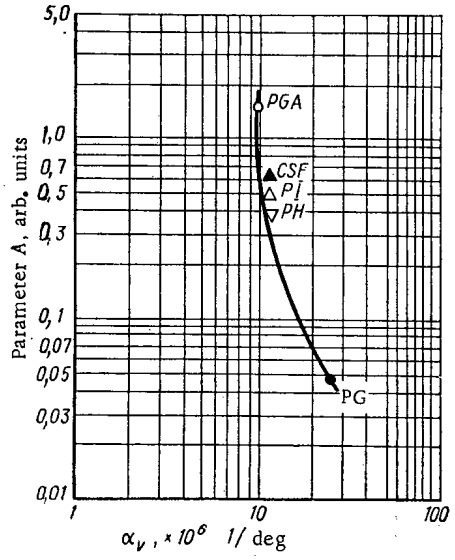

Fig. 5

Fig. 4. Dependence of the parameter A on the temperature of irradiation for different materials: 1) PGA; 2) CSF; 3) PI; 4) PH.

Fig. 5. Relation of the parameter A with the volume thermal expansion coefficient.

process, the formation of vacancy pores, occurs in the irradiated graphite to a smaller extent; the contribution of this process at high doses is decisive. A similar phenomenon was observed for steel. It was found [8] that irradiation of steel in a fast reactor leads to the appearance of uniformly distributed vacancy pores in the microstructure. The process of their formation has a strong temperature dependence: it starts at a temperature lower than 350°C, reaches a maximum at 500°C, and then decreases sharply with further increase in temperature; the relative volume of the vacancies increases exponentially in proportion to the increase in the integral dose. For integral doses below $\sim 10^{22}$ neutrons/cm^2 the pores are not formed, which may indicate the presence of an incubation period. The theory proposed for steel relates the relative increase in the volume of the sample F to the time t, the diffusion coefficient of the vacancies D_V, the number of vacancies N_V, and the rate of formation of the vacancy clusters I by the following equation:

$$F = 1 - \exp\left[-kI\,(D_v N_v)^{3/2} t^{5/2}\right], \tag{8}$$

where k is a constant.

It has been proposed [5, 7] that the intensive growth of the volume of graphite at high doses of irradiation is due to the process of generation of vacancy pores. Since the changes S_c and S_a are quite large, the difference between the rate of deformation in parallel and perpendicular directions relative to the c axis must lead to an accomodation of the dimensional changes due to the plastic deformation of the crystals. However, it was noted that the nature of the occurrence of this process is not at all clear [5]. Using the method proposed in [9] the values of S_c and S_a (for doses of the order of $1.5 \cdot 10^{22}$ neutrons/cm^2 and temperatures in the range 375-750°C) were computed from the results of the experiments for the irradiation of high-perfection pyrolytic graphite and grade PGA graphite. A good agreement is observed between the computed values of S_c and S_a and the changes of the dimensions in the c and *a* direction in the samples of pyrolytic graphite. With the increase in the dose of irradiation the difference $X_m = S_c + S_a$ increases and for a dose of $1.4 \cdot 10^{22}$ neutrons/cm^2 it is $\sim 15\%$. The relationship between the volume change of the graphite sample $\Delta v/v$ and the volume change of the crystallite $(\Delta v/v)_x$ has the form [5]

$$\Delta v/v = F(X_m) + (\Delta v/v)_x, \tag{9}$$

where $F(X_m)$ is a function determining the change due to filling and generation of pores. It was found that $F(X_m)$ depends on the temperature and the rate of change of X_m. An investigation of this problem showed [5] that an analysis of the changes in the dimensions, taking the fraction of the vacancy loops into consideration is not possible.

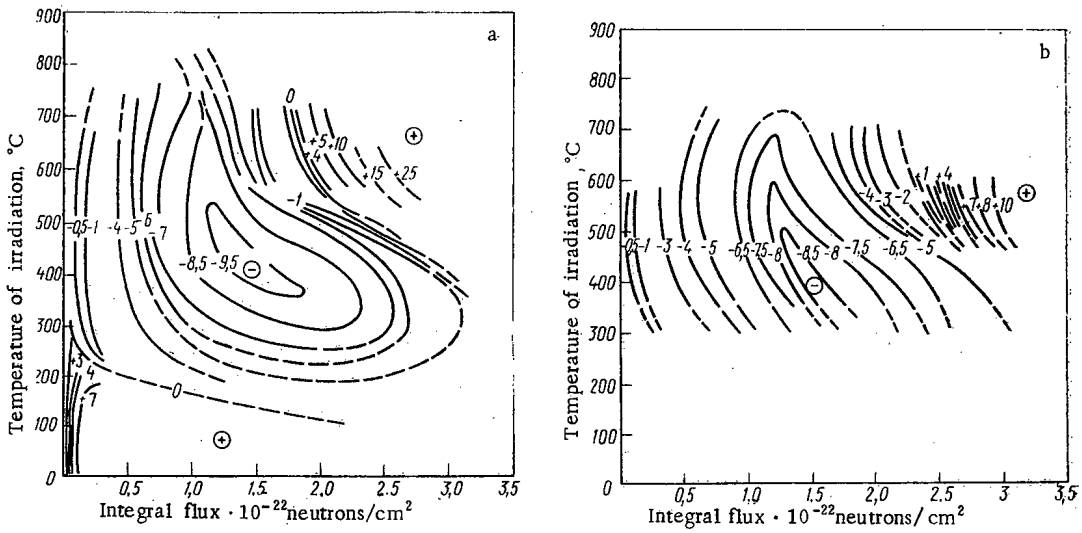

Fig. 6. Diagram of the dependence of the relative change of volume of samples of graphite PGA (a) and PI (b) on the temperature and the dose of irradiation.

Published experimental data on the change of linear dimensions of different grades of graphite (their properties are given in Table 1) irradiated by doses up to $3 \cdot 10^{22}$ neutrons/cm^2 at temperatures of 375-800°C offer the possibility of analyzing factors that affect the intensive increase in the volume of the graphite. Assuming that the volume change of graphite $\Delta v/v$ is caused by two processes: an elastic change of the volume of crystals in accordance with Simmons model $\Delta v/v$ and the change in the volume due to the appearance and generation of vacancy pores $(\Delta v/v)_{pore}$, we write

$$\Delta v/v = (\Delta v/v)_x + (\Delta v/v)_{\text{pore}} \tag{10}$$

Thus, in order to separate from the volume changes that part which is caused by the accumulation of vacancy pores, the volume change of the graphite samples which would occur only in elastic deformation, was computed from Eq. (2a). Then values computed from Eq. (2a) were subtracted from the experimental values of $\Delta v/v$.

This is illustrated by the computations carried out for grade isotropic graphite (Fig. 3) irradiated at 500-550°C [7]. The relative change in the volume of samples of high-perfection recrystallized pyrolitic graphite is also plotted (Fig. 3), which can be taken as linear with a reasonable accuracy up to doses of the order of $1 \cdot 10^{22}$ neutrons/cm^2. Above this dose a departure from the linear behavior is noticed toward higher increases. Separating also in this case the part which describes the linear increase of the volume with the time of irradiation (as done for graphite PI) from the experimental curve, we obtain the difference curve described by Eq. (11). Thus, in the case of pyrolitic graphite the occurrence of vacancy holes occurs at large doses is also noted, but this effect is appreciably weaker than in the investigated grades of artificial graphite. In all cases the process of formation of the pores is satisfactorily approximated by an equation of the form

$$(\Delta v/v) = 1 - \exp(-AD^n), \tag{11}$$

where A is a constant, D is the dose of irradiation, and n is a power exponent characterizing the nature of the process.

The parameters of Eq. (11) can be determined from the graph of the dependence of $\ln\ln[1 - (\Delta v/v)_{pore}]$ on ln D. It is interesting to analyze the values of parameter A thus obtained as a function of the irradiation temperature and also of the properties of the graphite. It is seen from the graph in Fig. 4 that the process of increase of the volume of pores becomes stabilized in the temperature range 600-800°C, which does not occur in the irradiation of steel. The absence of data on deformation at temperatures above 800°C does not permit an estimate of the variation of parameter A under these conditions. However, a computation for grade TSGBF showed that A increases sharply with the increase in temperature from 850 to 975°C, i.e., it can be assumed that a continuous increase in volume of the graphite occurs.

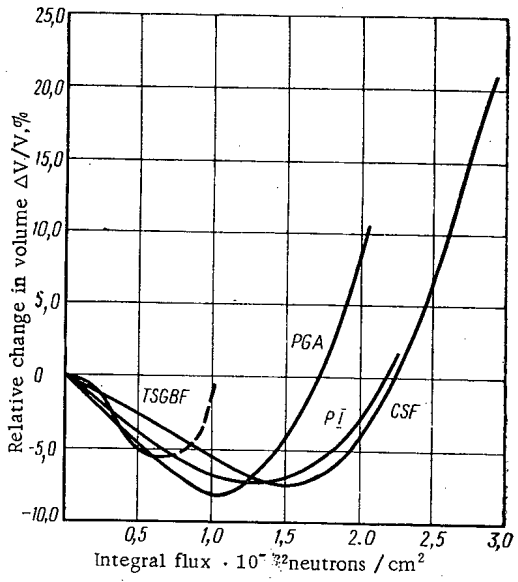

Fig. 7. Dependence of the relative change of volume in samples of graphite of different grades on the dose of irradiation at a temperature of 700°C.

Analyzing the relation of the parameter A with the properties one can note a sharp decrease in its value with the increase in the volume thermal expansion coefficient (Fig. 5). However, the obtained relations cannot be explained by the change in the volume thermal expansion coefficient only. Thus graphite of grades PGA, CSF, PI, and PH have practically identical α_v but different parameters A. Of the other physical properties the degree of perfection plays a large role. For example, the effect of the degree of graphitization can explain the enhanced increase in volume of grade TSGBF graphite which is less perfect than CSF, at equal values of the volume thermal expansion coefficient. However, the analysis of the effect of the physical and structural properties on parameter A is difficult due to insufficient data. In view of the fact that the main factors determining the behavior of graphite under irradiation are the temperature and the dose of irradiation, it is advantageous to present the changes in the volume dimensions of the graphite samples in the form of three-dimensional diagrams,* as is usually carried out in physicochemical analysis in the investigation of the dependence of properties on the form of composition. In the present case the values of the dose and the temperature are plotted along the two axes and the value of the relative change in the volume of graphite is plotted along the vertical axis: the positive values are above the plane of the drawing, the negative values are below.

Such diagrams were constructed from the available data [3, 5, 7] for PGA and PI graphite (Fig. 6). The relief of the surface is depicted in the figure by a system of isolines. The temperature count starts from 0°C. A sharp drop of the surface from the dose axis is characteristic of all the presented diagrams. At temperatures above 200-250°C a given surface, dropping further (below the plane of the diagram), restricts the volume with negative change. The region representing a deep "trough" is separated out extending toward higher temperatures and lower doses. More to the right of the "trough" a sharp ascent is observed with transition through zero values of $\Delta v/v$. Its slope increases with the increase in the irradiation temperature. Individual characteristics of each material show up in the position of the different regions on the diagram. An isothermic section of the diagrams for the investigated materials at 700°C shows (Fig. 7) that low-perfection grade TSGBF graphite increases in volume at smaller values of integral dose, whereas more perfect graphites (PGA, CSF, and isotropic PI) increase at appreciably large dose values. Thus it can be concluded that the maximum radiational stability of dimensions in high-temperature irradiation is possessed by high-perfection isotropic graphite with a high value of the volume thermal expansion coefficient.

In conclusion we investigated the behavior of materials with weak graphitization such as glass and pyrocarbon, compounds containing carbon black, and otherpoorly-graphited carbon compounds. A specific feature of their behavior is that the radiation compression begins at lower temperatures compared to graphite and proceeds at a higher rate. It is advisable to attempt a description of the change of the linear dimensions of imperfect materials with the aid of the elastic model discussed above. For this, one would have to take a large rate of change of dimensions of the crystals S_c and S_a in Eq. (2a).

* The first attempt of this kind of plotting of three-dimensional diagrams was made by V. R. Zolotukhii and V. I. Klimenko.

Computations showed that the change of the dimensions of the crystals is exponentially related to the diameter of the region of coherent scattering.

LITERATURE CITED

1. J. Simmons, Proc. III Conference on Carbon, Pergamon Press, Oxford (1959), p.559.
2. R. Price and J. Bokros, Appl. Phys., 36, 1897 (1965).
3. W. Reynolds, Physical Properties of Graphite, New York (1968).
4. T. Mantell, Carbon and Graphite Handbook, New York, LST (1968), p.420.
5. R. Henson et al., Carbon, 6, 789 (1968).
6. R. Nightingale, Nuclear Graphite, New York–London (1962).
7. P. Nettley et al., Atom, No. 146, 329 (1968).
8. R. Karlender et al., Atom. Tekhn. za Rubezh., No.5, 32 (1970).
9. B. Kelly et al., Philos. Trans. Roy. Soc., London, A, 260, No.1109, 51 (1966).
10. S. E. Vyatkin et al., Nuclear Graphite [in Russian], Atomizdat, Moscow (1967).
11. R. Gaylor et al., Carbon, 6, 537 (1968).

ABSTRACTS

REACTOR DYNAMICS CALCULATIONS FOR REACTOR WITH NATURAL CIRCULATION OF SINGLE PHASE COOLANT*

V. M. Selivanov, A. A. Gorev, I. I. Sidorova, and V. M. Gribunin

UDC 621.039.56

The nonlinear mathematical model of the dynamics of the primary loop of a water-cooled water-moderated reactor with natural circulation of single-phase coolant is discussed. The solution of the nonstationary heat transfer equations is represented by an expansion in orthogonal Legendre polynomials with time-varying coefficients [1]. The introduction of this expansion makes it possible to reduce the entire system of equations describing the dynamics of the reactor to the form

$$\frac{dx}{d\tau} = Ax + f(x),$$

where A is the (n × n) matrix of constant coefficients; x is the column vector of the phase coordinates; f(x) is the column vector of the nonlinear terms.

The model under consideration is utilized in the case $f(x) \equiv 0$ to obtain the frequency response to an experimental arrangement simulating a reactor system [2]. It is pointed out that in accordance with the Gyftopoulos criterion [3], an increase in the negative temperature coefficient of reactivity (in absolute magnitude) will result in impaired system stability. Our calculations show that, in the presence of modest power perturbations, a reactor with natural coolant circulation and temperature feedback features is dynamically equivalent to a reactor with forced coolant circulation.

LITERATURE CITED

1. S. K. Sanathanan et al., Nucl. Sci. Engng., 23, No.2 (1965).
2. V. M. Selivanov et al., At. Energ., 27, 101 (1969).
3. E. Gyftopoulos, Nucl. Sci. Engng., 26, No.1 (1966).

NOTE ON OPTIMIZATION OF A STATIONARY REFLECTOR IN A PULSED FAST REACTOR †

B. I. Kuprin and E. P. Shabalin

UDC 621.039.51

The pulsed neutron source method is highly recommended as a tool for solving many problems in neutron physics and in the physics of condensed media. Promising neutron sources for this line of research

* Translated from Atomnaya Énergiya, Vol.31, No.5, p.505, November, 1971. Original article submitted submitted January 20, 1971; revision submitted April 22, 1971.

† Translated from Atomnaya Énergiya, Vol.31, No.5, pp. 505-506, November, 1971. Original article submitted October 15, 1970.

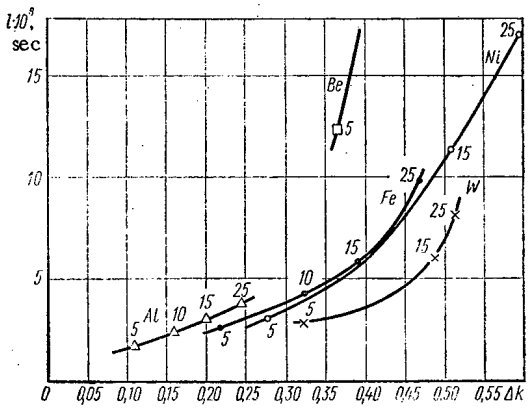

Fig. 1. Dependence of effective mean lifetime of prompt fission neutrons $\bar{l}$ on effectiveness Δk of reflector. Numerals at data points indicate thickness of reflector in centimeters; Δk given in fractions of unity.

are pulsed batch reactors and subcritical assemblies with electron accelerators as boosters. One of the most important characteristics of both of these types of sources, determining the quality of the neutron pulse generated, is the effective neutron lifetime in the reactor [1]. An unreflected core has the shortest neutron lifetime, but engineering requirements dictate the presence of scattering materials around the core: control and protection devices and moderator. Stationary and movable reflectors playing the role of control devices must have sufficient efficiency for the application; at the same time, reflector dimensions increase in proportion to the effective neutron lifetime. The position of the moderators must ensure a sufficiently high intensity of slow neutrons in the beams, and appropriate shielding of the core against those neutrons.

The purpose of this work was to search for some compromise solution which would satisfy the above requirements. The effect of different reflector materials on the effective mean lifetime of prompt fission neutrons was examined; the reflectors ranged from 0 to 25 cm in thickness and the reflector materials were: aluminum, iron, tungsten, nickel, beryllium. Also examined was the effect of various shielding interlayers placed between the core and moderator and serving to diminish the effect of moderator on the effective mean lifetime of the neutrons, on the yield of thermal neutrons. The calculations were carried out in two programs: a many-group program (18 groups) in the P_1-approximation of the method of spherical harmonics, and a three-dimensional many-group program using the Monte Carlo method [2, 3].

The following basic conclusions were drawn: 1) tungsten lends itself most readily to use as a control material and stationary reflector for a pulsed neutron reactor (see Fig. 1); 2) the optimum thickness of tungsten placed between the core and the moderator and serving as a shield against slow neutrons is 6-7 cm.

LITERATURE CITED

1. V. D. Anan'ev et al., JINR Preprint, 2372 (1965).
2. G. I. Marchuk, Methods of Nuclear Reactor Calculations [in Russian], Atomizdat, Moscow (1962).
3. V.I. Kochkin and E. P. Shabalin, JINR Preprint, 11-4098 (1968).

PATTERN OF VARIATION IN WALL TEMPERATURE OF FUEL ELEMENT (LENGTHWISE) IN HEAT TRANSFER WITH SURFACE PSEUDOBOILING

N. L. Kafengauz and M. I. Fedorov

UDC 621.039.546:536.24

In the exchange of heat between a fluid and the heated walls of channels, pseudoboiling characterized by a rapid increase in the heat transfer coefficient occurs in the range of supercritical pressures. Pseudoboiling is accompanied in many instances by high-frequency oscillations of the fluid.

Translated from Atomnaya Énergiya, Vol.31, No.5, p.506, November, 1971. Original article submitted March 23, 1971.

The wall temperature distribution over the length of the channel exhibits a singular pattern when pseudoboiling prevails. Investigations of the problem were carried out on a fuel element 30 mm in length and 1.6 mm in inner diameter. The working fluid in these investigations was a kerosene type hydrocarbon constituting the petroleum fraction with the boiling range 476-540°K. The critical parameters were: pressure 1.96 MN/m^2, temperature 680°K. The experiments were carried out at pressures of 2.94, 4.41, and 5.9 MN/m^2, and at fluid flowspeeds of 5, 10, 15, 25, and 30 m/sec. The inlet temperature of the fluid was 290°K, while the exit temperature did not exceed 330°K.

It was found that the wall temperature fell off at the exit end of the fuel element under pseudoboiling conditions; as the heat load was increased this fall-off extended over the entire length of the element in the direction opposite to the direction of flow of the fluid, while the temperature distribution acquired a wavy character. The temperature variation along the length of the fuel element became more pronounced as the flowspeed slackened.

Reasons for this pattern of variation in the wall temperature may be found in the assumption that pseudoboiling commences in the first instant at sites where the temperature of the fluid at the wall is higher, i.e., at the exit end of the fuel element. The appearance of pseudoboiling intensifies heat transfer markedly, and brings about a drop in the wall temperature. As the heat load is stepped up, the pseudoboiling process extends back toward the inlet end of the fuel element. The undulating temperature distribution pattern may be explained by the formation of standing pressure waves of the oscillating fluid over the length of the fuel element.

RADIATION DAMAGE IN GRAPHITE OVER A WIDE RANGE OF TEMPERATURES AND NEUTRON FLUX LEVELS

V. I. Klimenkov and V. R. Zolotukhin

UDC 621.039.553:539.2

The problem of how to impart dimensional stability to graphite in high-temperature reactors is of great practical interest at the present time. In the light of the demand for radiation-resistant graphites, it is sometimes sufficient to know what changes are likely to take place under certain sets of conditions in the graphite used, so that these changes can be taken into account in the design and development of reactors. Radiation-induced changes in the dimensions of reactor graphite depend in a complex way on the irradiation temperature, considering the broad variety of processes taking place in the graphite and associated with radiation defects whose behavior must be studied over an extended range of temperatures and neutron flux levels.

As a result of the discussion, a concept is formed of the generalized diagram of radiation-thermal changes in graphite volume. A refined variant of the diagram (see Fig. 1) is proposed, using all the available data to plot the diagram, including data obtained by the authors when irradiating specimens of polycrystalline graphite in the SM-2 high-flux reactor. Volume changes indicated in the diagram were calculated in terms of known changes in the linear dimensions in the direction perpendicular to and parallel to the axis of formation $\Delta v/v = 2(\Delta l/l)_{\perp} + (\Delta l/l)_{\parallel}$, which is entirely valid as a procedure applied to such grades of isotropic graphite as Soviet graphite GMZ, ZOPG, PGG, the foreign Gilsocarbon, etc.

On the diagram, the zero isochore $\Delta v/v = 0$ separates the regions in which the graphite experiences either swelling or shrinkage. Possible mechanisms underlying the phenomena occurring in the different regions are discussed. The fact that the diagram is not strictly quantitative in nature, owing to the complexity of the phenomena and the inadequacy with which they have been studied, is duly pointed out.

Translated from Atomnaya Énergiya, Vol.31, No.5, pp.506-507, November, 1971. Original article submitted February 15, 1971. Abstract submitted August 2, 1971.

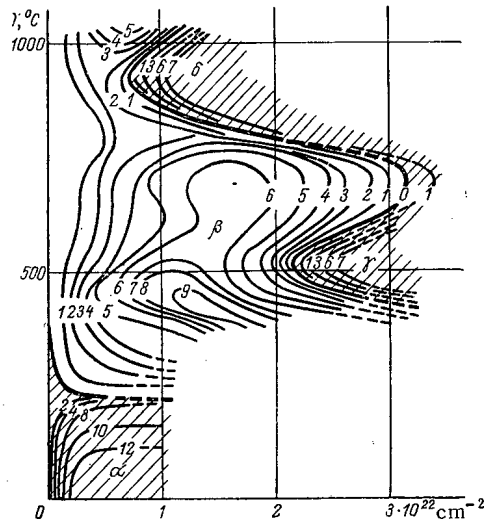

Fig. 1. Generalized diagram of radiation-thermal variation in graphite volume (expansion zone cross hatched). Isochore designation values, $\Delta v/v$ (%).

However, the diagram does provide a general concept of the radiation strength, and can be used to form a tentative estimate, allowing certain assumptions, of the linear dimensions of the graphite in the parallel and perpendicular directions at neutron flux 10^{13} to 10^{14} neutrons/cm^2 · sec ($E_n \geq 0.18$ MeV).

The paper proposes a simple method for computations, based on the use of empirical anisotropy formulas (for the case of swelling and the case of shrinkage) and the formulas $\Delta l/l = n\Delta v/v$.

The following values of the coefficient n, for the parallel and perpendicular directions respectively, were obtained: 1/2 and 1/4 for shrinkage, and 1/5 and 2/5 for swelling. The error was not greater than 15%.

THERMALIZATION OF NEUTRONS IN INFINITE HOMOGENEOUS MEDIA

V. A. Baikulov

UDC 539.125.52

We discuss a method for calculating the spectrum of slow neutrons in an infinite homogeneous medium at uniform temperature T containing a uniform distribution of fast neutron sources. In thermalization problems the energy of the source neutrons can be considered infinite. The energy distribution of neutrons in such a medium is described by the integral equation

$$\sigma_a(z)\,\Phi(z) + \int_0^\infty [\sigma_s(z \to z')\,\Phi(z) - \sigma_s(z' \to z)\,\Phi(z')]\,dz' = 0,$$

where $z = E/kT$ with E the neutron energy and k the Boltzmann constant; $\Phi(z)$ is the flux of neutrons with relative energy z.

No restrictions are imposed on the neutron absorption cross section $\sigma_a(z)$ in the thermalization region. The incoherent approximation is used for the differential scattering cross section $\sigma_s(z - z')$. The energy distribution of neutrons is represented by a linear combination of functions of two different classes, which gives the correct behavior of the neutron flux over the whole energy region:

Translated from Atomnaya Énergiya, Vol. 31, No. 5, pp. 507-508, November, 1971. Original article submitted June 18, 1971.

$$\Phi(z) = ze^{-z}\left[\sum_{i=0}^{K} a_i L_i^{(1)}(z) + \sum_{n=0}^{N} b_n \varphi(\lambda_n, z)\right],$$

where K + 1 is the number of generalized first order Laguerre polynomials $L_i^{(1)}(z)$ and N + 1 is the number of associated functions $\Phi(\lambda_n, z)$ with indices λ_n. The effectiveness of the system of Laguerre polynomials and the associated functions with integral index $\lambda_n = n$ in solving similar problems in media with absorption $\sim 1/\sqrt{z}$ is shown in [1, 2].

The enlargement of the system of associated functions by the introduction of functions with half-integral index makes the method converge much more rapidly [1, 2]. The proposed system of functions is effective also for an absorption cross section of the resonance type. We introduce the scalar product of two functions

$$\{X(\beta_l, z), X(\beta_m, z)\} = \int_0^\infty \frac{1 + z + \frac{z^2}{2}}{z} X(\beta_l, z) X(\beta_m, z)\, dz,$$

where l, m = 0, ...K, K + 1; ...K + N + 1; $X(\beta_l, z) \equiv zl^{-z}L_l^{(1)}(z)$ for $l \leq K$, $X(\beta_l, z) \equiv zl^{-z}\varphi(\lambda_{l-K-1}, z)$ for $l > K$.

Equation (1) is solved in the Hilbert space of the functions $X(\beta_l, z)$ with the scalar product (3). The expansion coefficients (2) a_i and b_n are determined by the Bubnov–Galerkin method. The expansion coefficients found in this way ensure a uniform approximation of representation (2) to the required solution over the whole energy range.

Using the free gas model with mass M equal to 1 and 12, the method converges rapidly for a cadmium absorber and an absorber with the absorption cross section $\sim 1/\sqrt{z}$. For example, for $\sigma_a(1)/\xi\sigma_s(\infty) \approx 1$, where $\xi\sigma_s(\infty)$ is the asymptotic value of the slowing down power, it is sufficient to take K = 5 and N = 4 in Eq. (2).

The method described can be used in solving space-energy problems to reduce the original kinetic equation to a set of group equations. Because of the rapid convergence of the method the number of energy groups cannot be larger, and this makes the solution of the spatial part of the problem much simpler.

LITERATURE CITED

1. N. I. Laletin, At. Energ., 17, 193 (1964).
2. N. I. Laletin and I. G. Pasynkov, Neutron Thermalization and Reactor Spectra, Vol. 1, IAEA, Vienna (1968), p. 58.

ACTIVATED PLASTIC-SCINTILLATOR DETECTORS FOR FAST NEUTRONS

E. E. Baroni, D. V. Viktorov,
A. F. Kulakov, I. M. Rozman,
and V. M. Shoniya

UDC 539.107.48

Plastic scintillators containing salts or oxides of various elements in amounts of up to 15-20% by weight were developed. Samples of these scintillators were exposed in a neutron field to be investigated and afterwards the induced activity was measured by counting the scintillations which occurred in the sample.

Translated from Atomnaya Énergiya, Vol. 31, No. 5, p. 508, November, 1971. Original article submitted December 21, 1970; revision submitted April 2, 1971.

The parameters of the neutron field can be deduced from the counts which were evaluated with the method commonly employed in the case of threshold detectors.

The testing program of the detectors consisted of a) determination of the light output S from the Compton spectrum of scintillations (γ line of Zn^{65} [1]); b) activation of the detectors in a flux of neutrons with the energy 14.1 MeV and comparison of the results of the measurements by extrapolating the activities of various nuclides; c) checks of the applicability of the extrapolation for the purpose of determining the absolute activity of the admixtures in the plastic scintillators.

Suspended admixtures lead to a considerable decrease in the scattering length of the luminescence photons and, hence, to a decrease in S. In order to determine the light flux, a setup was used wherein the photons left the scintillator through its entire surface and were directed onto a photocathode with the aid of a reflective layer situated at a certain distance from the scintillator surface. Consequently, the efficiency of the β particle count was not less than 80% at the minimum discrimination level ε for the isotopes considered. Furthermore, it turned out that at a maximum energy $E_{max} > 300$ keV of the β spectrum, the extrapolation of the integral scintillation spectrum can render the accurate value of absolute activity.

Samples containing 20% Al_2O_3 and 10% Ga_2O_3 had the greatest sensitivity to neutrons with an energy of 14.1 MeV among the detectors examined. When the irradiation lasted for a time equal to the half-life of the isotope to be measured, a counting rate of 10 pulses/min corresponded to a flux density of 107 and 117 neutrons/$cm^2 \cdot$ sec for the first and the second detector, respectively.

LITERATURE CITED

1. D. V. Viktorov, S. F. Kilin, and I. M. Rozman, Pribory i Tekh. Eksperim., No.4, 90 (1964).
2. R. Baker and L. Katz, Nucleonics, 11, 14 (1953).

EXPERIMENTAL TREATMENT OF NEUTRON SELF-SHIELDING IN NEUTRON ACTIVATION SPECIMENS, IN IMPURITY DETERMINATIONS IN SOME BORON-CONTAINING MATERIALS

T. A. Yankovskaya, M. M. Usmanova, and S. A. Sadykov

UDC 543.53

Absorption of neutrons in a matrix is one of the principal sources of error in neutron activation analysis of impurities present in neutron-absorbing materials, boron-containing materials included. With the object of finding a way to minimize the errors due to self-absorption of neutrons, we tried the method of treating neutron absorption by experimentally determining the self-shielding factor in neutron activation of specimens artificially fabricated from boron-containing material.

The specimens prepared had a base of ultrapure boric acid powder with impurities added in the form of salt solutions. The uniformity of the impurity distribution was checked by neutron activation autoradiography techniques. Pellets fabricated from the artificial specimens by sintering under 150 atm pressure showed an identical material density of 1.44 g/cm^3 and weighed from 100 to 350 mg. The pellets and standards were spaced no closer than 1.5 cm apart while being exposed to irradiation, in order to avert any substantial distortion of the neutron flux at the site where the specimens were irradiated.

A quantitative estimate of the impurity content was carried out by using both short-lived and long-lived radioactive isotopes. The irradiation was carried out in the channel of a reactor thermal column,

Translated from Atomnaya Énergiya, Vol.31, No.5, pp.508-509, November, 1971. Original article submitted June 19, 1970; abstract submitted June 14, 1971.

with neutron flux of $1.2 \cdot 10^{12}$ neutrons/cm^2 · sec, and in the channels of the VVR-S reactor with neutron flux $1.8 \cdot 10^{13}$ neutrons/cm^2 · sec. The exposure time was selected individually for each impurity, and ranged from as short as 5 min to as long as 2 h.

The correction factor was found by comparing the quantity of impurity introduced into the specimen to that found by neutron activation analysis. The method described was applied to the study of the effect of neutron self-shielding in boric acid specimens, for the determination of such impurities as Mg, Al, Si, Cl, Ca, Ti, V, Cr, Mn, Fe, Co, Cu, Zn, Mo, Ag, Ta, W, Au.

The optimum weighed portion for boric acid samples was set at 150 mg, with the self-shielding factor not exceeding 2. The following values were obtained for k_{exp} in the case of the impurity elements investigated, at the optimum sample weights: $1.0 \leq k \leq 1.3$ in the case of Mn, Co, Ag^{110m}, Ta, W, Au; $1.3 \leq k \leq 2.0$ in the case of Mg, Al, Si, Cl, Ca, Ti, V, Cr, Fe, Cu, Zn, Mo, Ag^{108}.

The procedure relied upon for determining the self-shielding factor can be applied to neutron activation analysis of many other objects characterized by high thermal neutron absorption cross sections.

A METHOD OF ELECTRON-MICROSCOPIC AUTORADIOGRAPHY

V. N. Chernikov, L. S. Khruleva,
A. P. Zakharov, K. M. Romanovskaya,
and V. M. Luk'yanovich

UDC 620.18

A brief review of the method of electron-microscopic autoradiography is presented and its use in the investigation of metals is elucidated in detail. Special attention is devoted to the problems of preparing M emulsions (with average diameter of nondeveloped grains of AgBr equal to 0.14 μ), and to obtaining an emulsion layer of a given thickness on the investigated surface of the sample and in particular a monolayer of the emulsion. An interferometric method of controlling the thickness of the emulsion layer is proposed and the construction of devices for obtaining thin emulsion films is described. The characteristics of the monolayer of nuclear emulsion on the surface of the investigated sample are analyzed.

In order to illustrate the potentialities of the method, results from the investigation of the structure of two molybdenum alloys, Mo + 0.5% weight C and Mo + 3% weight ZrC, are presented (the isotope carbon C^{14} was used as the radioactive indicator). It is shown that the alloy of molybdenum with carbon is a two-phase alloy and consists of grains of α-solid solution based on molybdenum and eutectics $\alpha + \beta$ precipitated along the boundaries and sub-boundaries, where β is Mo_2C. Autoradiogram-replicas from this alloy clearly show the fine structure of the eutectic (see Fig. 1). The alloy Mo + 3% weight ZrC is a three-phase alloy. Besides the α- and β-phases a γ-phase is formed (solid solution based on zirconium carbide ZrC), entering into the composition of the eutectic $\alpha + \gamma$, and also present in the alloy independently in the form of a large number of finely dispersed carbide precipitates in the lattice of the matrix α-solid solution (Fig. 1).

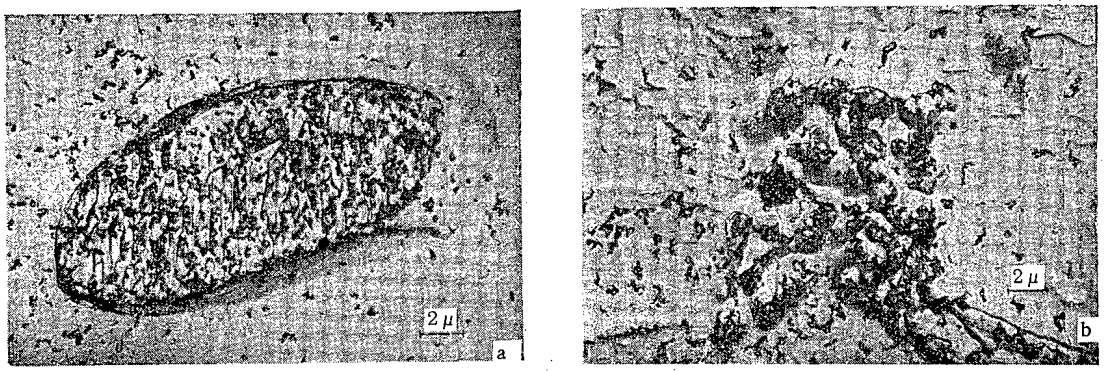

Fig. 1. Autoradiogram-replicas from alloys Mo + 0.5% weight C (a) and Mo + 3% weight ZrC (b): a) carbon enriched region, $\alpha + \beta$ eutectic, having a laminated structure; b) carbon rich region—eutectic precipitate $\alpha + \gamma$; laminas of carbides precipitated from α-solution were observed.

Translated from Zhurnal Atomnaya Énergiya, Vol. 31, No. 5, p. 509, November, 1971. Original article submitted November 18, 1970.

DOSIMETRY OF IONIZING RADIATIONS USING TINTED LAVSAN AND CELLOPHANE

L. M. Kobalenko, L. N. Gaichenko,
Ya. I. Lavrentovich, and A. M. Kabakchi

UDC 541.15:539.12.08

Dosimetric properties of ten industrial films produced from Lavsan and cellophane, tinted in different colors by organic dyes are investigated.

The films were subjected to the action of γ-radiation of Co^{60}, electrons (0.23 MeV), deutrons (13 MeV), and α-particles (23 MeV). The amount of LPE (linear energy loss) was varied from 0.2 to 30 keV /μ, the strength of the dose from 1 to 100 krad/sec, and the temperature from 30 to 100°C. In the case of thin Lavsan films packages consisting of three to four films were irradiated.

As a result of the irradiation a discoloration of the films is observed; the degree of discoloration measured at the maxima of the absorption of the dyes is proportional to the absorbed dose. Some characteristics of the tinted films are presented in Table 1.

From the tinted films of Lavsan only for the dark green, red, and turquoise color the dependence of the degree of discoloration of the dyes on the dose has a linear character. Dark-green films of Lavsan are most sensitive to irradiation in the wavelength range near 450 nm. The dependence of discoloration of cellophane films on the dose is close to linear; the red films are more sensitive to irradiation than yellow films.

A change in the dose strength and the temperature does not have any effect on the nature of discoloration of films on irradiation in the investigated ranges. The optical density of both irradiated and nonirradiated films does not change during the storage of the films for a year under ordinary conditions. Scattered daylight has no effect on the optical properties of the samples.

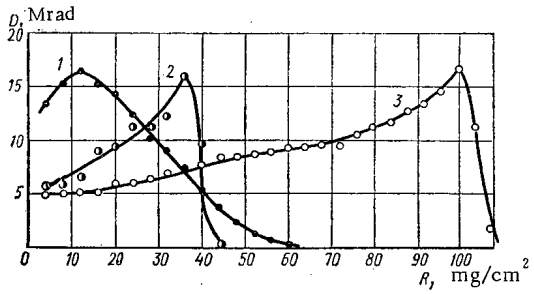

Fig. 1. Distribution of absorbed doses D along the depth R of the package of films of red cellophane under the action of electrons (1), α-particles (2), and deutrons (3).

A significant dependence of the readings of the dosimeter from Lavsan on the value of LPE is noted; this dependence is less pronounced for cellophane dosimeters. Tinted cellophane films can be used for dosimetry of heavy charged particles. They are suitable for determining the spatial distribution of doses, and also of the path of charged particles and their energy. Figure 1 shows the distribution of the doses in cellophane on irradiation by electrons, α-particles, and deutrons.

Tinted films of Lavsan and cellophane can be used for dosimetry in the range of 1-300 Mrad with an accuracy of ±10%.

TABLE 1. Characteristics of Tinted Films

Material	Wavelength at absorption maximum, nm	Initial optical density	Thickness of the film or package	Range of discoloration dose, Mrad
Lavsan (thin films)				
red	500	0,825	35 (3 films)	10—150
green	400	0,590	55 (4 films)	5—20
yellow	410	0,890	45 (3 films)	10—100
blue	470	1,222	55 (4 films)	10—200
dark green	450; 570; 600	1,645; 0,482; 0,518	15	10—300
Lavsan				
red	510	1,150	210	2—10
gree	675	1,780	220	1—15
turqoise	670	1,840	195	5—50
Celluose				
red	400; 520	0,808; 1,710	30	1—30
yellow	410	0,568	30	1—30

Translated from Atomnaya Energiya, Vo. 31, No. 5, p. 510, November, 1971. Original article submitted December 18, 1970; revision submitted May 6, 1971.

NOTE ON DISPOSAL OF RADIOACTIVE WASTES IMMOBILIZED IN CERAMIC SLUGS*

V. G. Shenderova, B. S. Pavlov-Verevkin, A. I. Pavlova-Verevkina, and I. I. Glotov

UDC 621.039.714

Experiments on the fabrication of ceramic slugs from hydroxide pulp produced in the course of sedimentation processes of deactivation of radioactive waste waters, and covering loams, for the purpose of determining their suitability in definitive disposal of radioactive wastes, were staged. Fabrication of ceramics at optimum pulp and loam ratios brought about a contraction of 15% in the pulp volume and contraction of the volume of processed water to 0.3-0.4% the original volume.

The stability of the resulting ceramic slugs increases with increasing calcining temperature from 900° to 1100°C, and increases at a particularly steep rate in the range between 1050° and 1100°C. The weight loss of the ceramic obtained at 1100°C in the course of 397 days was $3.4 \cdot 10^{-6}$ g/cm^2 day in tap water and $1.2 \cdot 10^{-5}$ g/cm^2 day in 0.1 N HCl.

The ceramic slug material contained a mixture of isotopes, with specific α-activity equal to the specific β-activity, viz., $1.3 \cdot 10^{-10}$ Ci/g. There was no attempt made at isolation or isotope analysis in view of the small absolute quantity of radioactive elements recovered.

It was found, as a result of a study of leaching of radioactive isotopes, that ceramics fabricated at 1050-1100°C leached out to a depth of 1.5 to 2.5 mm over the entire duration of the experiments. The relative loss of radioactive isotopes consequently must be greatly affected by the assigned dimensions of the ceramic slugs (by the ratio of the volume of the surface layer of the ceramic to the total volume), and may be made quite small in design.

Comparison of the behavior of the α-emitters and β-emitters revealed that the latter, among which are counted many highly mobile elements, leach out much more readily than the former. This is on account of the chemical properties of the elements represented by the specific isotopes.

The ceramic material obtained from the hydroxide pulp and covering loams at 1050-1100°C is suitable, in its characteristics, for final immobilization and disposal of radioactive wastes, and does not require leak-tight burial grounds for safe storage.

NOTE ON THE STRUCTURE OF THE MAGNETIC FIELD IN A SPLIT-MAGNET SECTOR-FOCUSED CYCLOTRON†

L. N. Katsaurov, E. M. Moroz, and L. P. Nechaeva

UDC 621.384.633.5

Information is presented on the distribution pattern of the magnetic field in the sector-focused cyclotron of FIAN [Lebedev Institute of Physics of the Academy of Sciences of the USSR] [1]. The possibility of replacing the real distribution by a model of a stepwise distribution of the magnetic field, for the purpose of utilizing familiar formulas [2] for computing the principal characteristics of the motion of particles in the

* Translated from Atomnaya Énergiya, Vol.31, No.5, p. 511, November, 1971. Original article submitted October 15, 1970; revision submitted May 27, 1971.

† Translated from Atomnaya Énergiya, Vol.31, No.5, pp. 511-512, November, 1971. Original article submitted December 8, 1970; revision submitted May 27, 1970.

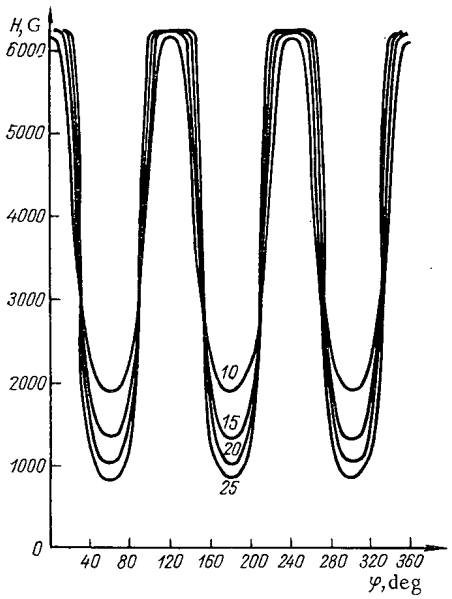

Fig.1. Dependence of magnetic field on azimuth at different distances from center (in centimeters).

cyclotron (geometry and position of equilibrium trajectories, cyclotron frequency and betatron frequency and the radial variation of those frequencies, and so forth), is discussed.

The diagram shows how the magnetic field varies azimuthally at different radii (distances from the symmetry center of the magnetic field). The azimuths of the boundaries of the magnetic sectors must be selected, to begin with, in order to construct a model of a stepwise varying field which will correspond to the magnetic field shown in the diagram. It was found that the position of the sector boundaries within the region of rapid variation of the magnetic field is not very critical. For example, the boundaries of the sectors are assigned the azimuths 30°, 90°, etc., in this paper. If these boundaries are displaced ±6°, i.e., through almost the entire range of rapid variation in the magnetic field (see Fig.1), the basic parameters of the cyclotron as computed from the formulas for the stepwise varying magnetic field will undergo a change of approximately ±1.5%.

The magnetic field is assumed to be independent of azimuth in the sectors and between them, in the model of the stepwise varying magnetic field. For this model to actually correspond to the field shown on the diagram, the magnetic field has to be averaged with respect to azimuth within the ranges assigned to the sectors.

It is clear from the diagram that this azimuth-averaged magnetic field increases within the sector, but decreases in the intervals between the sectors, with increasing radius. Formulas convenient for computing the basic parameters of the cyclotron in the presence of a slight radial gradient of the magnetic field are cited in the paper. The results of computations of the basic parameters of the FIAN sector-focused cyclotron, based on those formulas, are then compared to computer results dealing with the equations of motion. Comparison discloses that the formulas for the stepwise varying field determine the position and shape of the equilibrium orbits to within 2-3% at low energies, and to ~ 2% at high energies, determine the cyclotron frequency to ~ 1.0%, determine the betatron frequency ν_r to within 1.0-2.0%, while the value obtained for ν_z is too low (by as much as 20%) at small radii (to ν_z 16 cm), and within 1-2% at the remaining radii.

The paper thus indicates the feasibility of computing the basic parameters of the cyclotron by relying on a model of a stepwise varying field, with results accurate to with 1-2%.

This procedure enables us to sidestep the problem of excessive reliance on computer data processing in the design of this type of cyclotron, even in some cases of simulation design since, by referring to [3], the magnetic field of such a cyclotron can be computed to within 1-2%, and its parameters can be computed on the basis of formulas cited in the paper. This means that comparatively simple and straightforward calculations can be relied upon to find the arrangement of magnets capable of forming the cyclotron's magnetic field with all the necessary basic parameters meeting specifications.

The authors are indebted to I. Ya. Barit, and also to V. N. Kanunnikov, for their kind interest in the work, and for their much appreciated remarks.

LETTERS TO THE EDITOR

ON THE METHOD OF SOLVING EQUATIONS OF KINETICS OF A REACTOR

A. I. Kuleshov

UDC 621.039.514

We consider the system of equations of kinetics in the usual form [1] with six groups of delayed neutrons

$$\left.\begin{aligned}\frac{dn}{dt}&=\frac{k(t)(1-\beta)-1}{l}n+\sum_{i=1}^{6}\lambda_i c_i,\\ \frac{dc_i}{dt}&=-\lambda_i c_i+\frac{\beta_i k(t)}{l}n\end{aligned}\right\} \tag{1}$$

with the initial conditions

$$\left.\begin{aligned}n|_{t=0}&=n_0,\\ c_i|_{t=0}&=c_{i0}.\end{aligned}\right\} \tag{2}$$

It is required to find n and c_i in the interval

$$0\leqslant t\leqslant T. \tag{3}$$

If the solution of the problem (1)-(3) is sought in each partial interval $\Delta t \leq T$ in the form of expansions

$$\left.\begin{aligned}n(t)&=A_0+A_1t+A_2t^2+\ldots,\\ c_i(t)&=B_{i0}+B_{i1}t+B_it^2+\ldots,\end{aligned}\right\} \tag{4}$$

then the derivation or direct use of expressions (4) for finding the values of n(t) and $c_i(t)$ is difficult because of the small values of the characteristic number l/β the coefficients A_s and B_{is} in the initial segments of expansions (4) sharply increase with the increase of the index s and may go beyond the digital grid of the computer language; furthermore the series in (4) converge slowly.

It is known that for the summation of poorly converging series continued fractions are successfully applied [2]. In the present case we transform the series in (4) into continued fractions of the form

$$n(t)=\cfrac{A_0}{1-\cfrac{a_1t}{1-\cfrac{a_2t}{1-\ldots}}}\qquad c_i(t)=\cfrac{B_{i0}}{1-\cfrac{b_{i1}t}{1-\cfrac{b_{i2}t}{1-\ldots}}} \tag{5}$$

where a_s and b_{is} are defined by the rhomb rules [2]. These rules can be expressed by the following recurrent formula, which is convenient for programming:

$$e_{s+2}^{(\nu)}\psi_{(-1)^s}e_{s+1}^{(\nu)}=e_{s+1}^{(\nu+1)}\psi_{(-1)^s}e_s^{(\nu+1)}\qquad (s,\ \nu=0,\ 1,\ \ldots), \tag{6}$$

here ψ_1, ψ_{-1} are are arithmetic operations of addition and multiplication, respectively.

The initial conditions for formula (6) will be

$$e_0^{(\nu)}=0;\ e_1^{(\nu)}=\mu_{\nu+1}\quad(\nu=0,\ 1,\ \ldots).$$

Then the elements of the continued fraction, corresponding to n(t), are determined from the relations

$$a_s=e_s^{(0)}\quad(s=1,\ 2,\ \ldots).$$

Translated from Atomnaya Énergiya, Vol. 31, No. 5, pp. 513-514, November, 1971. Original article submitted December 7, 1970

Similarly for the determination of the elements b_{is} we apply formula (6) with the initial conditions

$$e_0^{(\nu)}=0;\ e_1^{(\nu)}=\theta_{i\nu+1}\quad(\nu=0,1,\ldots).$$

Then we get

$$b_{is}=e_s^{(0)}\quad(s=1,2,\ldots).$$

The quantities μ_s, θ_{is} are determined with the use of the system of recurrent formulas obtained by elementary analysis of system (1):

$$\mu_{s+1}=\frac{p+p'/\mu_s+\frac{1}{2!}p''/\mu_s/\mu_{s-1}+\ldots\Sigma\lambda_i\vartheta_{is}}{s+1}$$

$$\vartheta_{is+1}=\frac{-\lambda_i\vartheta_{is}+\beta_i\left(q+q'/\mu_s+\frac{1}{2!}q''/\mu_s/\mu_{s-1}+\ldots\right)}{(s+1)\,\mu_{s+1}},\qquad(7)$$

$$\theta_{is+1}=\mu_{s+1}\frac{\vartheta_{is+1}}{\vartheta_{is}}\quad(s=0,1,\ldots)$$

for the initial conditions

$$\mu_{s\leq 0}=\infty,\quad \vartheta_{i0}=B_{i0}/A_0,\qquad(8)$$

where

$$p=\frac{k(t)(1-\beta)-1}{l},\ q=\frac{k(t)}{l}.$$

Thus the solution of problem (1)-(3) can be obtained in the form of a system of fractions (5), whose elements are computed using simple recurrent formulas (6), (7) and the initial conditions (8).

The system of equations of kinetics of a reactor was solved for the case of periodic instantaneous change of the source strength

$$s(t)=s_0\delta(t-j\Delta T)$$

with the breeding coefficient of neutrons given by the polynomial $k(t)=p_m(t)$, when formulas (7) have a particularly simple form. This problem with the source is reduced to problem (1)-(3) in each segment of length ΔT.

The problem was solved on a computer using two programs. One of these is based on a variant of the scheme of integral type [3]; the other is based on the method of continued fractions. A comparison showed that the solution of the problem using the second program proceeds five times faster maintaining a specified accuracy of the computation. A stepwise process of computation with automatic selection of the step Δt is used in both the programs. The presented method permits one to carry out computation with a much larger count rate coefficient than indicated above, if the length of the segment of the continued fraction is sufficiently large and the elements of the fraction are sufficiently accurate.

It is obvious that this method can also be used in those cases where $k(t)$ is specified through a more complex analytic expression compared to that in the discussed example. But it is possible then that an automatization of analytical differentiation of algebraic expressions will have to be introduced in the program [4].

LITERATURE CITED

1. J. Hertzel, Materials (Atomic Energy Commission), USA Nuclear Reactors, T.I.M. [Russian translation], IL (1965).
2. G. Rutiskhauzer, Logarithm of Partials and Differences [Russian translation], IL, Moscow (1960).
3. E. Koen, II Geneva Conference (1958) [in Russian], T. E. M., Atomizdat (1959), p.549.
4. A. I. Kuleshov, Zh. Vychisl. Matem. i Matem. Fiz., No. 6, 1137 (1966).

A FEATURE OF THE SOLUTION OF THE BOLTZMANN FINITE-DIFFERENCE EQUATION

G. Ya. Rumyantsev

UDC 621.039.512

Analytical methods in the theory of neutron transport (e.g., the method of elementary solutions of Case [1]) have been successfully used for investigating the exact transport equation. However, different numerical methods, which follow immediately, to a very great extent, are based on the Boltzmann equation in the approximate, finite-difference form. In our opinion, it is of interest to use the analytical approach also in the solution of the finite-difference analogs of the Boltzmann equation. In particular, the well-known method of discrete ordinates [2, 3] can lead to the example of an analytical solution of the Boltzmann equation in plane geometry, when the dependence of the distribution function on the angular variable μ is discretely approximated for a continuous dependence on the space coordinate x.

Below we consider the case in which the dependence on x is discrete, and the dependence on μ is continuous or arbitrary (the monoenergetic problem for isotropic scattering).

We divide the x axis into equation intervals Δx and we denote $F(x_i, \mu) \equiv F_i(\mu)$; we then assume that between the two points x_{i-1} and x_i, the function $F(x, \mu)$ is linear. Then the Boltzmann equation averaged over each interval takes the form

$$\left(\mu+\frac{\Delta x}{2}\right) F_i - \left(\mu-\frac{\Delta x}{2}\right) F_{i-1}=\frac{c\Delta x}{4}(\Phi_i+\Phi_{i-1}), \tag{1}$$

where

$$\Phi_i=\int_{-1}^{1} F_i(\mu)\, d\mu.$$

We determine Case's elementary solutions of Eq. (1):

$$F_i(\mu, \nu)=\Psi(\mu, \nu)\,\Phi_i(\nu) \tag{2}$$

with the normalization

$$\int_{-1}^{1} \Psi(\mu, \nu)\, d\mu=1.$$

We next seek the function $\Phi_i(\nu)$ in the form

$$\Phi_i(\nu)=\left(\frac{\nu-\Delta x/2}{\nu+\Delta x/2}\right)^i, \tag{3}$$

which is the finite-difference analog of the exponent $e^{-x/\nu}$.

Substituting Eqs. (2) and (3) into Eq. (1), we obtain

$$\Psi(\mu, \nu)=\begin{cases}\dfrac{c\nu}{2(\nu-\mu)}+\left(1-\dfrac{c\nu}{2}\ln\dfrac{1+\nu}{1-\nu}\right)\delta(\nu-\mu), \\ \qquad\qquad \nu\in(-1, 1); \\ \dfrac{c\nu_0}{2(\nu_0-\mu)},\end{cases} \tag{4}$$

Translated from Atomnaya Énergiya, Vol. 31, No. 5, pp. 514-515, November, 1971. Original article submitted November 20, 1970.

where ν_0 is the root of the equation

$$1-\frac{c\nu_0}{2}\ln\frac{\nu_0+1}{\nu_0-1}=0. \tag{5}$$

Thus the function $\Psi(\mu, \nu)$ proved to be exact and independent of Δx.

The general solution of Eq. (1) is the superposition of all its elementary solutions:

$$\Phi_i = A\left(\frac{\nu_0-\Delta x/2}{\nu_0+\Delta x/2}\right)^i + B\left(\frac{\nu_0-\Delta x/2}{\nu_0+\Delta x/2}\right)^{-i} + \int_{-1}^{1} C(\nu)\left(\frac{\nu-\Delta x/2}{\nu+\Delta x/2}\right)^i d\nu, \tag{6}$$

where the second term corresponds to the root minus ν_0. The formula for $F_i(\mu)$ is of the form

$$F_i(\mu) = A\Psi(\mu, \nu_0)\left(\frac{\nu_0-\Delta x/2}{\nu_0+\Delta x/2}\right)^i + B\Psi(\mu, -\nu_0)\left(\frac{\nu_0-\Delta x/2}{\nu_0+\Delta x/2}\right)^{-i} + \int_{-1}^{1} C(\nu)\Psi(\mu, \nu)\left(\frac{\nu-\Delta x/2}{\nu+\Delta x/2}\right)^i d\nu. \tag{7}$$

The coefficients A, B, and $C(\nu)$ are determined from the boundary conditions, which should be satisfied by the function $F_i(\mu)$. As we know, this problem reduces to the expansion of the angular distribution on the boundaries of the medium (on each boundary within the solid angle 2π, corresponding to the inward direction) in a complete system of functions $\Psi(\mu, \nu)$. We shall not describe this interesting fact in detail, since in general it does not change. On the boundary of a semiinfinite medium, if we take it to be the coordinate origin ($i = 0$ and $x_0 = 0$), we have

$$F_0(\mu) = A\Psi(\mu, \nu_0) + \int_0^1 C(\nu)\Psi(\mu, \nu)\,d\nu \tag{8}$$

(the coefficients B and $C(\nu)$ for $\nu < 0$ equal zero according to the condition $F_i(\mu) \to 0$ as $i \to \infty$). Equation (8), which relates the distribution of neutrons incident on the boundary with the distribution of the emerging neutrons, was obtained exactly, as we see. Hence, in the case under consideration, the coefficients A, B, and $C(\nu)$, and also the function $F_0(\mu)$, i.e., the solution of the problem of the albedo, also will be exact, in spite of the error in the distribution function inside the medium, resulting from the discrete representation of its dependence on x.

The result obtained, on first glance, seems odd. Actually, in the exact solution, at a distance from the boundary $x > 1$, the transition part, having the form of an integral of the function $C(\nu)\Psi(\mu, \nu)\exp(-x/\nu)$, is vanishingly small, and for the choice $\Delta x \gg 1$, we may disregard it entirely. In fact, this is not so. Equations (6) and (7) show that in the finite-difference approximation, for large Δx, this part of the solution represents a sawtoothed broken line, which oscillates about zero with a weakly varying amplitude, and is not identically equal to zero. Its contribution to the angular distribution on the boundary proves to be exact, independently of Δx. The same can be said about the asymptotic part also, if $\Delta x > 2\nu_0$.

In practice, the condition $\Delta x \ll 2\nu_0$ is usually satisfied; then

$$\left(\frac{\nu_0-\Delta x/2}{\nu_0+\Delta x/2}\right)^i \approx e^{-\Delta x i/\nu_0} = e^{-x_i/\nu_0}. \tag{9}$$

Hence, in this case the asymptotic solution will be sufficiently exact also for $x > 0$. Of course, isolation of the asymptotic part has sense only in media with relatively small neutron absorption, or in breeder media, when $|\nu_0| \gg 1$.

If we convert to the method of discrete ordinates, retaining the discrete dependence on x, then a large number of admissible values of ν become finite, in exactly the same way as for the case of a continuous dependence on x. Otherwise, Eqs. (6) and (7) and all the remarks concerning them hold unchanged.

LITERATURE CITED

1. K. M. Case, Ann. Phys. (N.Y.), 9, 1 (1960).
2. S. Chandrasekar, Radiative Transfer, Dover, New York (1960).
3. B. Dévison, Theory of Neutron Transport [in Russian], Atomizdat, Moscow (1960).

DEPENDENCE OF FUEL ELEMENT WALL TEMPERATURE ON COOLING CONDITIONS IN REACTOR SHUTDOWN

S. O. Slesarevskii, M. N. Korotenko,
M. M. Nazarchuk, D. T. Pilipets,
and S. S. Stel'makh

UDC 621.039.566

Experiments were carried out at the VVR-M reactor installation at the Institute of Nuclear Physics of the Academy of Sciences of the Ukrainian SSR [IYaI AN USSR]. Two fuel elements, 36% enriched with U^{235}, with Chromel–Copel microthermocouples attached, were loaded into the reactor core. Reactor shutdowns were staged from different power levels (2 to 20 MW) by dropping the scram rods and simultaneously reducing the flowrate of coolant from 1420 to 950 m^3/h (by shutting off one of the circulation pumps), to 470 m^3/h (by shutting off two circulation pumps), or all the way to 0 m^3/h (by shutting off all three working circulation pumps in the primary loop). A reactor shutdown at 10 MW power output level was carried out in the same manner, with the emergency cooldown system activated (coolant flowrate 470 m^3/h).

It is clear from Fig. 1a that the reactor shutdown with one pump shut off results at first in a rapid plunge downward on the part of the wall temperature of the fuel element, with time, followed by a slower and smoother decline of the fuel element wall temperature with time. The reactor shutdown with two pumps shut off (see Fig. 1b) is responsible for the appearance of a surge in the wall temperature immediately following the shutdown, with a subsequent decline of the temperature. Reactor shutdown with the complete

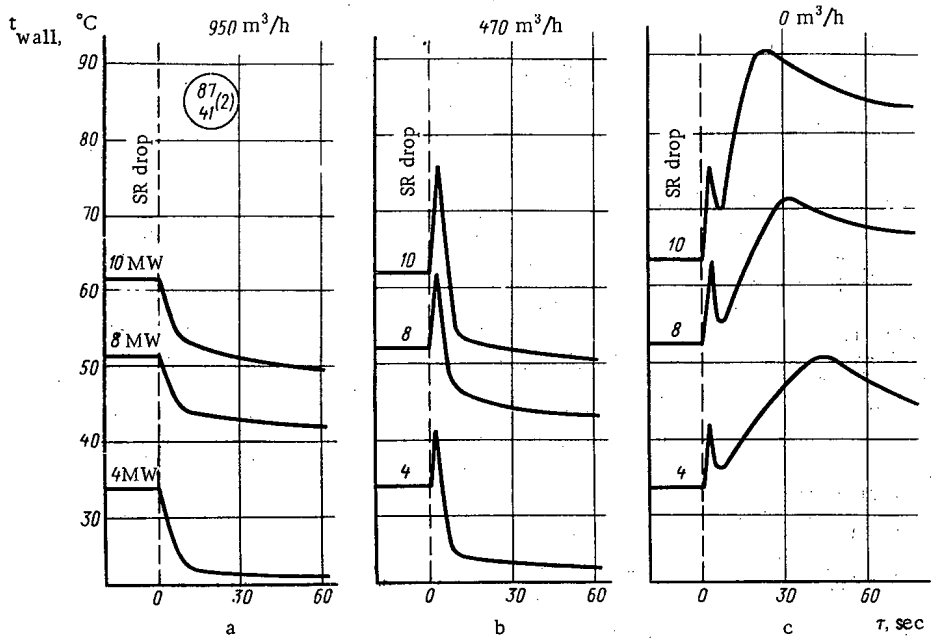

Fig. 1. Variation of wall temperature of fuel element in response to reactor shutdown: a) two circulation pumps in primary loop in operation; b) only one circulation pump in operation; c) cooling by natural convection. [SR = scram rod.]

Translated from Atomnaya Énergiya, Vol. 31, No. 5, pp. 515-516, November, 1971. Original article submitted November 9, 1970; revision submitted January 21, 1971.

cutoff of coolant circulation through the core (see Fig. 1c) results in a temperature curve on which a secondary rise in the wall temperature of the fuel element, much greater in magnitude and stretching out further in time, appears in addition to the first temperature surge. The curve obtained in the shutdown with the activation of the emergency cooldown system differs from the curve in Fig. 1b in the absence of a temperature surge in the initial period. This is accounted for by the different position of the pump gate valves. In contrast to the modes of shutdown where the cutoff of the pump was accompanied by simultaneous closing of the pump gate valves, the shutdown of the reactor accompanied by activation of the emergency cooldown system took place under conditions where all of the pump gate valves remained open. This allowed the possibility of coolant flowing by inertia for some time after the pumps had been shut off.

The abrupt temperature surges occurring in the first 1.5 to 2 sec (see Fig. 1b, c) are due to the fact that a decrease in coolant flowspeed occurs more rapidly under those conditions than the fall-off in reactor power output. The afterheat can attain significant levels [1] during the initial period. Therefore, from the instant the gate valves close, which corresponds to total cutoff of circulation, the second temperature peak begins (see Fig. 1c). After highly developed natural convection has set in the reactor vessel, a smooth decline in the wall temperature of the fuel element is observed. The time it takes to attain natural convection is largely dependent on the power level at which the shutdown was initiated, as is evident in Fig. 1c.

The results of the experiments show that even when the circulation of coolant is shut off completely, with the pump gate valves closed (which entails more "rigid" conditions than a scram shutdown brought about by outage of electric power, when the gate valves remain open), the maximum wall temperature of the fuel element does not reach the boiling point of water. In a planned shutoff of the circulation pumps, attention should be given to possible shutting off of the pumps while simultaneously closing the gate valves, as this will entail additional temperature stresses on the walls of the fuel element.

LITERATURE CITED

1. J. Kleban, Kernenergie, 9, No. 1, 14 (1966).

DIFFUSION OF URANIUM IN REFRACTORY BCC METALS

G. B. Fedorov, E. A. Smirnov,
F. I. Zhomov, V. N. Gusev,
and S. A. Paraev

UDC 539.219.3:669.882

Research on diffusion mobility of atoms in refractory bcc metals [1, 2] is of great practical interest, particularly in view of the known [3] anomalies of the temperature dependence of diffusion coefficients in certain bcc metals. Using the familiar procedure with use of U^{235}, we previously [4] studied diffusion of uranium in zirconium iodide, monocrystalline molybdenum, niobium, tantalum, and tungsten, obtained by electron beam melting.

An analysis of the penetration curves of uranium $\ln C = f(x^2)$ revealed that at all temperatures diffusion took place predominantly in the bulk of the crystal.

Figure 1a and Table 1 give the temperature dependences of the diffusion coefficients of uranium. They show that the Arrhenius equation accurately represents the diffusion mobility of uranium in all bcc metals, with the exception of zirconium. The existence of an anomalous temperature dependence of the diffusion coefficients in β-zirconium [8, 9] is due to various factors [3, 9, 10]. The results of the investigation of the diffusion coefficients of uranium in β-zirconium are represented as the sum of two exponential terms:

$$D = 0.36 \exp(-58\,000/RT) + 5.3 \cdot 10^{-6} \exp(-19\,700/RT), \quad \text{cm}^2/\text{sec}.$$

Resolution of the experimental curve into two exponential terms and calculation of the diffusion parameters were performed by means of the Kidson [10] approximation, using the method of least squares and a Minsk-22 computer.*

* The results of the investigation of diffusion of uranium in β-titanium require additional verification. Despite evidence [3] of abnormal diffusion properties of titanium, the results agree closely with data of Pavlinov et al. [11] and are represented by the equation

$$D = 6.9 \cdot 10^{-5} \exp(-25\,000/RT), \text{cm}^2/\text{sec} (900 - 1500^\circ\text{C}).$$

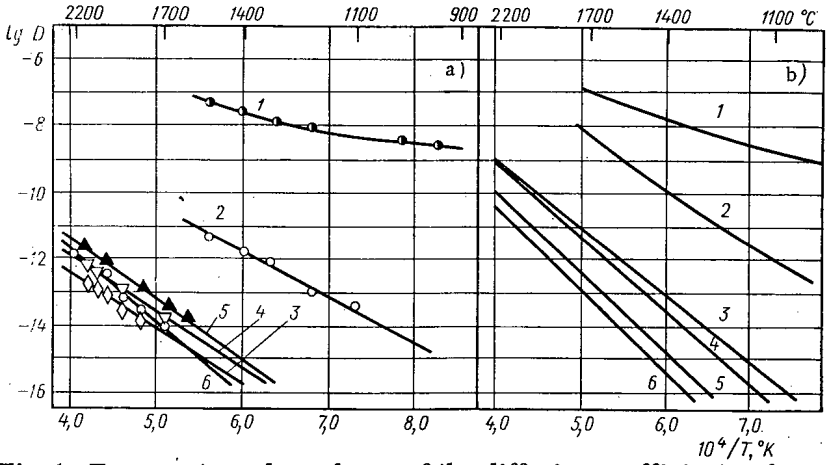

Fig. 1. Temperature dependence of the diffusion coefficients of uranium (a) and of self-diffusion (b) of: 1) zirconium; 2) vanadium; 3) molybdenum; 4) niobium; 5) tantalum; 6) tungsten.

Translated from Atomnaya Énergiya, Vol. 31, No. 5, pp. 516-518, November, 1971. Original article submitted November 23, 1970; revision submitted April 12, 1971.

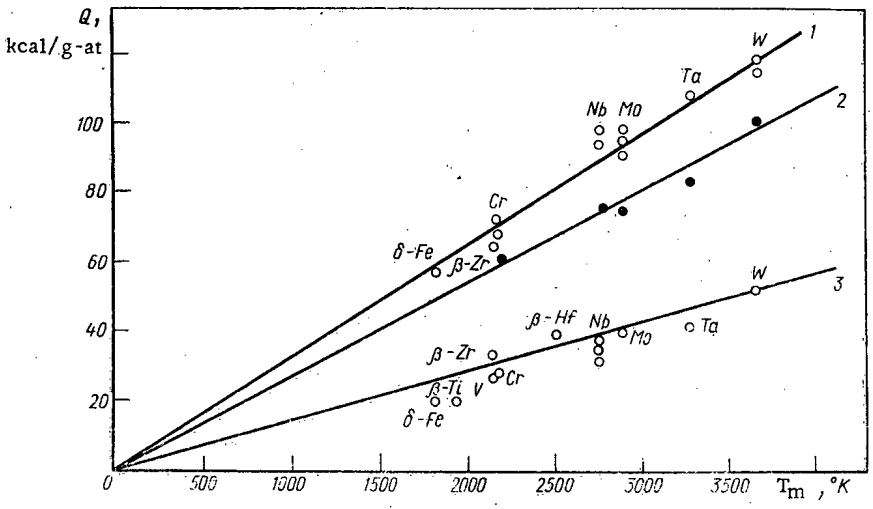

Fig. 2. Activation energies of self-diffusion and diffusion of impurity atoms versus melting point of matrix: 1) self-diffusion; 2) diffusion of uranium; 3) diffusion of carbon.

TABLE 1. Diffusion Parameters of Uranium in Refractory BCC Metals

Material	Q, kcal/g-at	D_0, cm²/sec	Temperature range	Q of self-diffusion, kcal/g-at
Vanadium	61,4	10^{-4}	1100—1500	73,65 [5] (880—1356° C) 94,14 [5] (1356—1883°C)
Niobium	76,7	$5 \cdot 10^{-6}$	1720—2100	100,6 [1]
Tantalum	84,4	$7,6 \cdot 10^{-5}$	1600—2150	110 [6]
Molybdenum	75,6	$1,3 \cdot 10^{-6}$	1800—2100	96,9 [7]
Tungsten	103,5	$2 \cdot 10^{-3}$	1700—2200	116,4 [1]

Figure 1b shows the published temperature dependences of the self-diffusion coefficients of the metals investigated [1, 5-7, 10]. Comparison of Figs. 1a and b reveals that in the investigated temperature range the diffusion coefficients of uranium are usually much less than the corresponding self-diffusion coefficients. (At lower temperatures (below 1000°C), however, the temperature dependences of the diffusion coefficients of uranium and of the self-diffusion coefficients intersect and the relationship between them is reversed.)

Interesting conclusions may be drawn from a comparison of the activation energies of diffusion of uranium and self-diffusion in these metals. It can be seen from Table 1 that the activation energy of uranium diffusion is always less than the corresponding activation energy of self-diffusion, because the impurity atom markedly distorts the crystal lattice of the base metal. Figure 2 plots the activation energies of self-diffusion and diffusion of impurity atoms in refractory bcc metals versus their absolute melting points. Line 1 in Fig. 2 corresponds to the equation $Q = 33.4\ T_m$ [1].

A similar linear dependence is observed between the activation energies of uranium diffusion (line 2, Fig. 2) and the melting points of these metals. Owing to disturbance of the metal lattice by the impurity atoms, the coefficient of proportionality is somewhat less (27 cal/g-at°C). We may therefore assume that in investigations of the diffusion of the same elements in different solvent metals with the same crystal structures, the activation energy of diffusion of the impurity may be characterized by the strength of the interatomic bond in the solvent metals.

Thus an equation of the type $Q = kT_m$ is correct for diffusion of different substitional impurities, but the coefficients of proportionality may have different values, depending on the nature of the diffusing atom. It should also be noted that a similar dependence is displayed in the diffusion of interstitial impurities, the values of the coefficient of proportionality being lower than for self-diffusion and diffusion of substitutional impurities (see Fig. 2).

LITERATURE CITED

1. G. B. Fedorov, F. I. Zhomov, and E. A. Smirnov, in: Metallurgy and Physical Metallurgy of Pure Metals [in Russian], Vol. 8, Atomizdat, Moscow (1969), p. 145.

2. G.B. Fedorov, F. I. Zhomov, and E. A. Smirnov, ibid., Vol.7, Atomizdat, Moscow (1968), p.128.
3. A. D. Le Clair, in: Diffusion in Metals with Body-Centered Lattices [Russian translation], Metallurgiya, Moscow (1969), p.247.
4. G. B. Fedorov, E. A. Smirnov, and V. N. Gusev, At. Énerg., 27, 149 (1969).
5. R. F. Peart, in: Diffusion in Metals with Body-Centered Lattices [Russian translation], Metallurgiya, Moscow (1969), p.247.
6. R. Eager and D. Langmuir, Phys. Rev., 89, 911 (1953).
7. J. Askill and D. Tomlin, Philos. Mag., 8, 997 (1963).
8. G. Kidson and J. McGrun, Canad. J. Phys., 39, 1146 (1961).
9. J. Federer and T. Lundy, Trans. AIME, 227, 592 (1963).
10. G. Kidson, Canad. J. Phys., 41, 1563 (1963).
11. L. V. Pavlinov, A. I. Nakonechnikov, and V. N. Bykov, At. Énerg., 19, 521 (1965).

VARIATION OF THE FILTRATION PROPERTIES OF ROCKS DURING UNDERGROUND LEACHING OF URANIUM BY A SULFURIC ACID SOLUTION

V. I. Beletskii, V. G. Bakhurov, and R. Kh. Sadykov

UDC 622.775:622.349.5

Underground leaching of uranium from sheet deposits of the sedimentary type [1-4] is usually accompanied to a greater or lesser degree by colmatage of the pore space, which may greatly impair the efficiency of the process. Particularly marked variations of the permeability of rocks are observed when they have a high content of carbonate impurities. This paper deals with the effects of calcium carbonate, the initial H_2SO_4 concentration, and the filtration rate of solutions on colmatage of the pore space.

For this purpose we used quartz sand (particle diameter 0.2-0.5 mm), thoroughly mixed with a specific amount of calcium carbonate of the same size. The sand was placed in Plexiglas containers, 50 cm long and 3 cm in diameter. At the beginning of the experiment, the column with the rock was washed with water to stabilize the initial flow values. A sulfuric acid solution was then added. The pressure gradients were kept constant throughout an experiment. With this experimental procedure, the value of the flow characterized the variation in the permeability of the sand.

As an example, Fig. 1 gives a graph of the flow versus time. Three stages are clearly distinguished.

The first stage (in Fig. 1, from the beginning of the experiment to point A) is characterized by marked deterioration of the filtration properties of the sand, due principally to formation of CO_2 and its propagation tion along the column. This period evidently sees the beginning of formation of a saturation solution of gypsum and its deposition in the pore space. In this stage the flow rate of the liquid at the column outlet was greater than at the inlet. The amount of gas increased, the sand became appreciably drier. After the gas reached the opposite end of the column, degassing of the sand began. The gas in the column was displaced mainly as an independent phase, but partly in the dissolved state. At the end of the first stage, the flow rate of the solution entering the column was equal to its discharge rate. This moment (point A) corresponded to the maximal volume of free gas in the column. The solution pH was about 7.

In the second stage (in Fig. 1, between points A and B) the permeability of the sand gradually fell. The flow rate of the solution entering the column was greater than the discharge rate. The pore space was filled with solution. Degassing was predominant over gas formation. In this stage, at the column outlet we observed the appearance of solutions containing a suspended precipitate of gypsum. The medium gradually acquired an acid reaction.

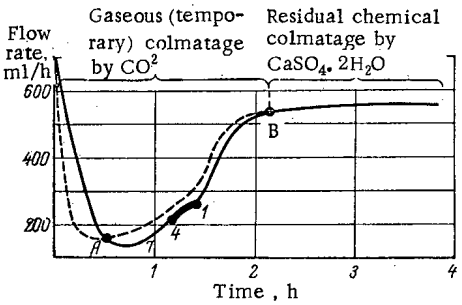

Fig. 1. Effect of chemical reaction of an H_2SO_4 solution (50 g/liter) with the carbonate component of sand on its filtration properties. $CaCO_3$ content 1%: – – – –) flow rate of liquid at entry to column; ——) flow rate at exit of column; ▪) range of discharge of solutions containing suspended gypsum; the figures denote the pH values.

Translated from Atomnaya Énergiya, Vol. 31, No. 5, pp. 518-520, November, 1971. Original article submitted November 16, 1970.

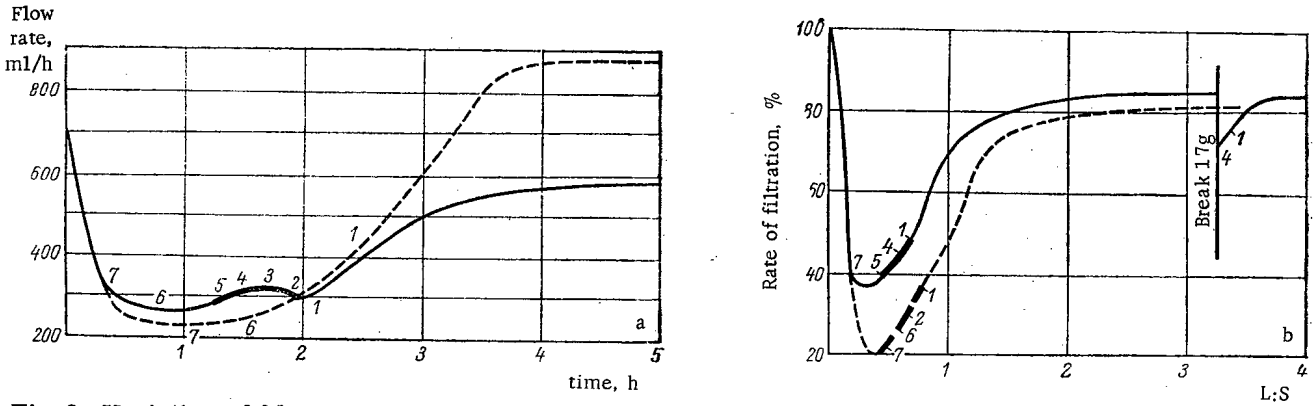

Fig. 2. Variation of filtration properties of sand containing 1% $CaCO_3$ (the flow rates of the solution at the column outlet are shown): a) during filtration of solutions of HCl (– – –) and H_2SO_4 (———) of equivalent concentrations; b) during filtration of an H_2SO_4 solution (10 g/liter) with initial filtration rates at the column inlet equal to 70 cm/h (———) and 36 cm/h (– – –). For notation, see Fig. 1.

TABLE 1. Variation of the Filtration Coefficient, K, of Quartz Sand with an Admixture of $CaCO_3$ during Reaction with a Sulfuric Acid Solution

H_2SO_4, g/liter	$CaCO_3$, %	K, % of initial value	
		minimal	stabilized at end of experiment
5	1	61	85
10	1	37	85
50	1	19	85
100	1	16	85
10	0,25	64	116
10	0,5	45	95
10	5	28	46

The third stage (in Fig. 1, to the right of point B) was characterized by the absence of development of gas and of precipitation. The concentration of the acid reached the initial value, its reaction with the rock ceased, the flow rates of the liquid at the inlet and outlet coincided and became virtually stable. The flow rate at the end of the column was somewhat greater than the initial value, which corresponded to the appearance of irreversible chemical colmatage, due to deposition of a nearly insoluble gypsum precipitate.

For a separate assessment of gaseous and chemical colmatage, we performed experiments with H_2SO_4 and HCl of equivalent concentrations (Fig. 2a). The results enabled us to conclude that the marked deterioration of the filtration properties of sand when acid solutions pass through it is due to gaseous colmatage. At the same time the results showed that the effect of the gypsum precipitate on colmatage of the rocks at the beginning of the experiment was slight. In the first two stages it was manifested mainly in the formation of a thin film on the particle surfaces, which impeded the free course of the reaction and retarded evolution of gas. In the third stage, precipitation of gypsum from the solutions had a marked effect on the reaction velocity. The reaction of hydrochloric acid with the carbonates in the rock, which occurred in absence of chemical colmatage, was completed earlier (3 h 45 min) than in the case of sulfuric acid (4 h 45 min).

The flow rate of sulfuric acid solutions was stabilized at the level of approximately 125% of its initial value, which corresponded to complete solution of the carbonate content of the rock and to formation of wider pore channels. The flow rate of the sulfuric acid solution at the end of the experiment was only 85% of its initial value. The incomplete restoration of the filtration properties was due mainly to formation of a precipitate of $CaSO_4 \cdot 2H_2O$ and to a lesser extent to isolation of a part of the carbonate substance by a gypsum coating.

The results of experiments with sulfuric acid solutions of different concentration (Table 1) show that gaseous colmatage increases with the concentration. The minimal flow rate, which was 69% of the initial value at an H_2SO_4 concentration of 2.5 g/liter, fell to 16% at a concentration of 100 g/liter.

Stabilization of the filtration properties of the sand was observed earlier when stronger acid solutions were used. The flow rates, established at the end of experiments in which the $CaCO_3$ content was 1%, were the same at all acid concentrations and equal to 85% of the initial value. This was due to the fact that in all the experiments of this series we observed formation of the same amount of gypsum, equivalent to the initial calcium carbonate content.

In a number of experiments we used quartz sand with different $CaCO_3$ contents, namely 0.25, 0.5, 1, and 5%. The sulfuric acid concentration was 10 g/liter. The results show that colmatage increases with the $CaCO_3$ content (Table 1). The minimal flow rate decreases from 64% of the initial value at a $CaCO_3$ content of 0.25% to 28% at 5%. The time taken for the acid to react with the rock increased proportionally to the increase in the $CaCO_3$ content of the sand. Gaseous colmatage took correspondingly longer. Stabilization of the flow rates of the solution after completion of the reaction of the substances depended on the amount of gypsum deposited in the pore space, which in turn was determined by the calcium carbonate content. The steady flow rate varied from 116% of the initial value for sand with 0.25% $CaCO_3$ to 46% for sand with 5% $CaCO_3$.

The effect of the rate of filtration of the solution on colmatage of sands was studied at two initial values (70 and 36 cm/h). For greater clarity, the ratio of the volume of liquid which passed through the sand to the weight of the solid (L : S) is plotted on the axis of abscissas of the corresponding graph (see Fig. 2b). The results of the experiments showed that at a lower filtration rate, the reaction of H_2SO_4 with $CaCO_3$ was more complete and took longer than might have been expected from the ratio of the rates. Gaseous colmatage was also more intense. The rates of filtration at the end of the experiments coincided. This indicated that the amount of reacted substances was the same in both cases.

The experimental data enable us to draw the following conclusions:

1. The most marked deterioration of the filtration properties is observed during evolution of gas. However, gaseous colmatage has a temporary (reversible) character because the gas formed is removed from the bend both by filtration as an independent phase and in dissolved form. The decrease in the flow rate of the liquid is determined mainly by the amount of free gas evolved in the pores, which depends on the carbonate content. At a higher acid concentration the same amount of gas is evolved more rapidly, which leads to more pronounced (albeit brief) impairment of the filtration properties of the bed.

2. Chemical colmatage of the pore channels by gypsum is less pronounced than gaseous colmatage, but in contrast with it, has an irreversible character. It is controlled by the initial carbonate content and is independent of the concentration of the sulfuric acid, which is in excess.

3. To improve the water permeability of a bed with high carbonate content, underground leaching with sulfuric acid must be performed as far as possible under conditions in which the minimal amount of gas is formed. This may be facilitated by increasing the hydrostatic pressure of the liquid in the bed and by reducing the initial acid concentration.

4. An increase in the flow rates in boreholes (and therefore of the rate of filtration of solutions) also reduces gaseous colmatage.

LITERATURE CITED

1. A. P. Zefirov, Processing of Low-Grade Uranium Ores, IAEA, Vienna (1967).
2. V. G. Bakhurov, S. G. Vecherkin, and I. K. Lutsenko, Underground Leaching of Uranium Ores [in Russian], Atomizdat, Moscow (1969).
3. B. V. Nevskii and V. G. Bakhurov, At. Énerg., 27, 495 (1969).
4. N. V. Gubkin, A. T. Desyatnikov, and I. K. Rudneva, At. Énerg., 24, 511 (1968).

PRODUCTION OF ELECTRON-HOLE JUNCTIONS BY THE METHOD OF RADIATION ALLOYING IN A NUCLEAR REACTOR

A. K. Podsekin, S. P. Solov'ev and V. A. Kharchenko

UDC 539.1.074.55

The methods of obtaining electron-hole junctions in semiconductors, used at present, require high-temperature heating of the basic crystal, since at moderate temperatures the impurities injected by thermodiffusion have insufficient mobility. The high-temperature heating of the crystals leads to: a decrease in the lifetime of the carriers, to the appearance of structural defects, and to other side effects [1]. These disadvantages make it desirable to develop new methods of obtaining junctions at high temperatures.

A basis for one such method may be the principle of change of conductivity of the crystal as a result of nulcear reactions, ultimately leading to the formation of the required impurity atoms [2]. The initial sample must be sufficiently pure in order to disregard nuclear reactions in the impurities.

In practice this method is most easily applied to silicon, in which donor impurity of phosphorus is formed on irradiation by slow neutrons in accordance with the reaction

$$Si^{30}(n_s, \gamma)\, Si^{31} \xrightarrow[2.6h]{\beta^-} P^{31}.$$

Using this reaction it is possible to obtain an n-type material with specified resistance from hole-type silicon [3-6].

If a part of a p-type sample is shielded from the action of thermal neutrons in the process of irradiation, then the change in the type of conductivity occurs only in the unshielded part of the sample and hence, it is possible to obtain, in principle, a p–n junction of any form determined by the profile of the shielding [7].

From the known parameters of the neutron spectrum and the cross sections of interaction of neutrons with the material of the shield and the semiconductor, the final concentration of the carriers in different parts of the irradiated material is computed.

In an analogous way it is also possible to obtain other electron-hole junctions of more complex structure such as type p–n–p, p–i–n, and so forth.

The present article is devoted to a theoretical analysis of the optimum conditions of production of an electron-hole junction by the method of radiational alloying in a nulcear reactor as applied to silicon.

For estimating the effect of different factors on the process of alloying let us consider one of the possible schemes of the experiment (see Fig. 1), in which a cylindrical sample of silicon of diameter 2r, together with a cylindrical shield, is placed in an isotropic neutron flux. If x is the distance from the surface of the crystal to the point at which the reaction occurs and α is the angle between the x axis and the direction of motion of the neutrons falling in an annular slit of width 2h, then

$$\alpha = \operatorname{arctg} \frac{h}{H + x}, \tag{1}$$

where H is the thickness of the layer of the shield.

Translated from Atomnaya Énergiya, Vol. 31, No. 5, pp. 521-522, November, 1971. Original article submitted October 1, 1970.

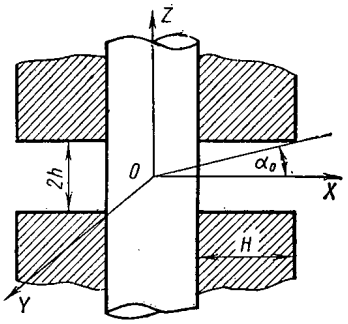

Fig. 1. Scheme for obtaining a p–n junction in a silicon sample placed in an isotropic flux of slow neutrons.

For simplifying the computations we shall determine the attenuation of the neutron flux at the midpoint of the sample (point O in Fig. 1) under the condition that the material of the shield is opaque and the sample is transparent for neutrons. For this case the possible values of the angle α lie in the range from O to $\alpha_0 = \arctan h/H + r$.

If the number of neutrons per unit volume is ρ at the location of the sample in the channel of a nuclear reactor and their velocities v have a Maxwellian distribution, the flux density of neutrons $d\Phi$ having velocities in the range v and v + dv, written in a spherical system of coordinates θ, φ, has the form [8]

$$d\Phi = \rho \left(\frac{m}{2\pi kT}\right)^{3/2} \exp\left(-\frac{mv^2}{2kT}\right) v^3 \sin\theta \, d\theta \, d\varphi \, dv, \tag{2}$$

where m is the neutron mass and T is the temperature in °K.

Denoting the values of the flux density of neutrons falling at the point O of the sample through the slit in the shield and in the absence of the shield by Φ_S and Φ, respectively, we obtain the attenuation coefficient

$$\lambda = \Phi_S/\Phi = \int_{v=0}^{\infty} \int_{\varphi=0}^{2\pi} \int_{\theta=\pi/2-\alpha_0}^{\pi/2+\alpha_0} d\Phi \Big/ \int_{v=0}^{\infty} \int_{\varphi=0}^{2\pi} \int_{\theta=0}^{\pi} d\Phi = \sin\alpha_0. \tag{3}$$

For sufficiently small values of the angle α

$$\lambda \approx \frac{h}{H+r} \approx \frac{h}{H+x}. \tag{4}$$

If N_a is the initial concentration of the acceptor impurity, and A and B are the number of interactions per unit volume of unshielded and shielded parts of the sample, then the final concentrations of the carriers in the n- and p-regions of the junction are equal to

$$\left.\begin{aligned} n &= A - N_a; \\ p &= N_a - B. \end{aligned}\right\} \tag{5}$$

Hence it follows that for the formation of the electron-hole junction it is necessary that

$$\varepsilon = \frac{B}{A} < 1. \tag{6}$$

Further, if it is assumed that the material of the shield reduces the total flux of neutrons N by a factor ω, and is "transparent" for neutrons with energies higher than some threshold value (in the case of shielding made of cadmium and ω-cadmium), then for convenience we shall take that in the unshielded part of the sample

$$A = A_1 + A_2 + A_3, \tag{7}$$

where A_1 and A_2 are the number of interactions of neutrons with energies above and below the threshold, respectively.

It is obvious that

$$A_1 = \frac{N}{\omega}; \tag{8}$$

$$A_2 = \left(N - \frac{N}{\omega}\right)\lambda, \tag{9}$$

where λ takes account of the collimating effect of the slit.

A part of the flux of thermal neutrons (A_3) passes into the sample through the material of the shield of thickness H.

If σ is the cross section of absorption of thermal neutrons by the material of the shield, N_M is the number of nuclei per unit volume of the shield material, $\gamma = e^{-N_M \sigma H}$ is the coefficient of transmission of neutrons through the shield, then

TABLE 1. Values of ω Necessary for Obtaining Nonsymmetric p–n Junctions by Irradiation in a Reactor

n/p	ε	ω	
		λ=10⁻²	λ=10⁻¹
1	$3{,}0\cdot10^{-1}$	$2{,}3\cdot10^{2}$	24
2	$2{,}5\cdot10^{-1}$	$3\cdot10^{2}$	30
5	$1{,}4\cdot10^{-1}$	$6{,}2\cdot10^{2}$	63
10	$8{,}3\cdot10^{-2}$	$1{,}1\cdot10^{3}$	110
10^{2}	10^{-2}	$9{,}9\cdot10^{3}$	990

$$A_3=\left(N-\frac{N}{\omega}\right)(1-\lambda)\,\gamma. \tag{10}$$

In addition we have

$$A=N\{(1-\omega^{-1})[\lambda+(1-\lambda)\,\gamma]+\omega^{-1}\}. \tag{11}$$

Similarly for the shielded part of the sample

$$B=N[(1-\omega^{-1})\,\gamma+\omega^{-1}], \tag{12}$$

and hence,

$$\varepsilon=\frac{(1-\omega^{-1})\,\gamma+\omega^{-1}}{(1-\omega^{-1})[\lambda+(1-\lambda)\,\gamma]+\omega^{-1}}. \tag{13}$$

Thus the coefficient ε is determined by the geometry of the slit (through λ), the effectiveness of shielding (through γ), and the parameters of the neutron spectrum (through ω).

Since it follows from expressions (5) and (6) that

$$p=N_a(1-\varepsilon)-\varepsilon n, \tag{14}$$

by the choice of an appropriate material of the shield, the geometry of the slit, and the neutron spectrum it is possible, in principle, to obtain the desired relation between the concentrations of carriers in n- and p-regions of the junction for known concentrations of acceptor impurities in the basic material and the desired concentration of the carrier in one of the regions.

For simplifying the numerical estimates we take the cross section of absorption of thermal neutrons by the shield material so large that $\gamma = 0$. In this case it follows from formula (13) that

$$\omega=1+\frac{1-\varepsilon}{\varepsilon\lambda}.$$

Let us specify the initial value as $N_a = 2\cdot10^{15}$ cm^{-3} (which corresponds to a specific resistance $\rho = 7\ \Omega\cdot$cm). Assuming further that the carrier concentration in the shielded part of the sample changes by not more than a factor of two (i.e., $p = 10^{15}$ cm^{-3}), and using expression (14), we find those values of ω which must characterize the neutron spectrum for obtaining different ratios n/p in the junction for different values of the parameter λ. The results of the corresponding computations are presented in Table 1.

It follows from Table 1 that with the increase in the ratio n/p the coefficient ε decreases and the value of ω increases significantly. The obtained values of ω, in particular for $\lambda = 10^{-2}$ and for $n/p > 5$, appreciably exceed the cadmium ratio in the channels of standard research reactors, which are, thus, not optimum for obtaining nonsymmetric electron-hole junctions by the method of radiational alloying. Therefore, an adequately efficient realization of the present method of producing junctions requires either the development of special reactors or the use of thermal-column type devices.

LITERATURE CITED

1. H. John, Proceedings of Institute of Electrical and Electronics Engineers [Russian translation], Mir, Moscow (1967).
2. K. Lark-Gorovits, in: Semiconductor Electronic Devices [Russian translation], IL, Moscow (1953).
3. M. Tanenbaum and A. Mills, J. Electrochem. Soc., 108, 2 (1961).
4. USA Patent No. 307632 (1963).
5. FRG Patent No. 1214789 (1967).
6. V. A. Kharchenko and S. P. Solov'ev, Fizika. i Tekhn. Poluprovod., 5, No. 8 (1971).
7. S. Klahr and E. M. Lifshits, Statisticheskaya Fiz., Nauka, Moscow (1964).

COLLIMATOR EFFECT ON FAST NEUTRON SPECTRA FROM RADIOACTIVE SOURCES

S. N. Balakhnichev, A. G. Banin,
V. Ya. Evfanov, A. N. Rudakov,
and A. P. Yanovskii

UDC 539.1.074.88

The UKPN-1 device has been built at the D. I. Mendeleev All-Union Scientific-Research Institute of Metrology for checking and calibrating neutron dosimeters and meters in a collimated beam [1] for which an

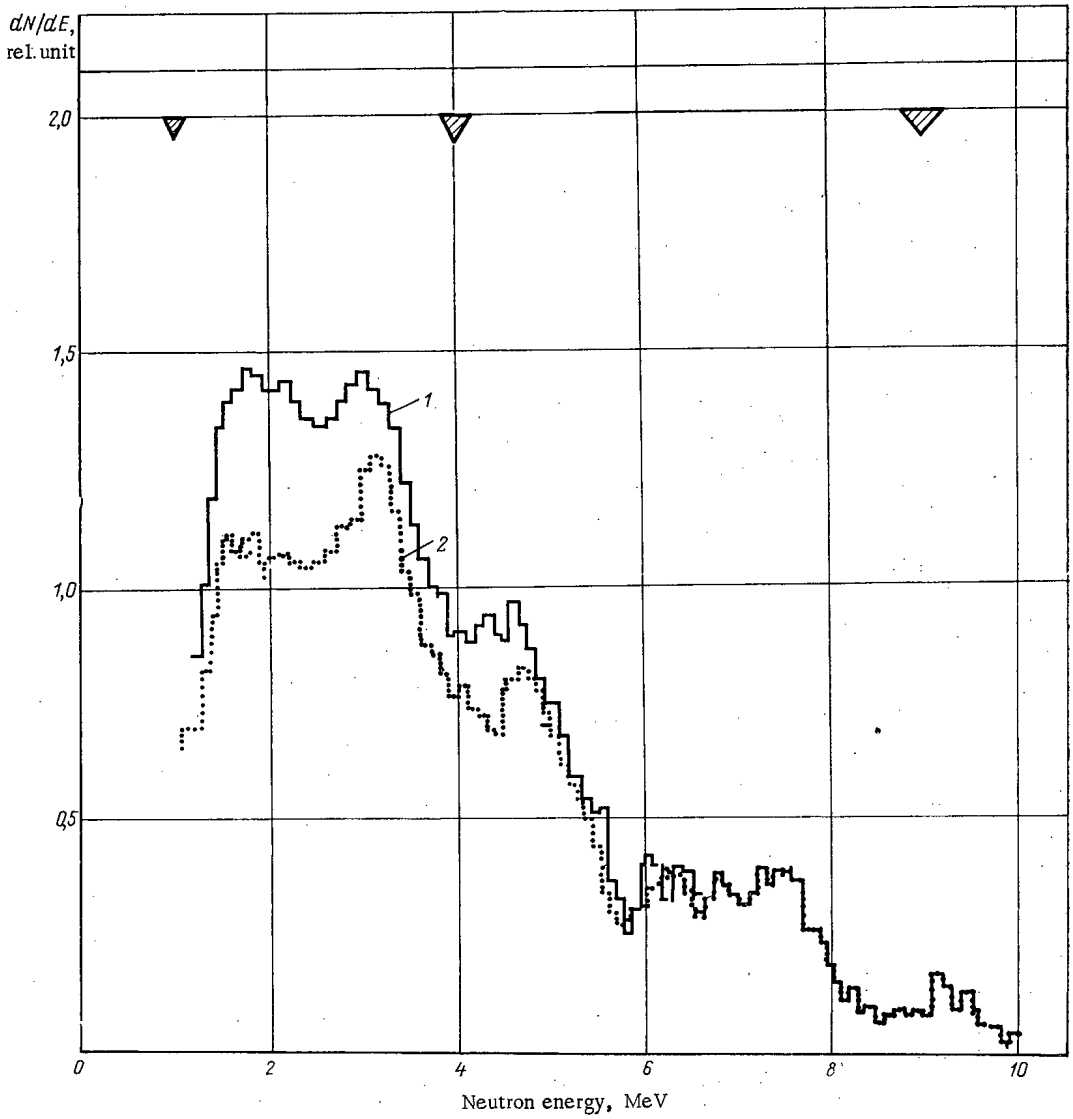

Fig. 1. Neutron spectra from Pu–Be source. 1) Source in collimator; 2) source without collimator.

Translated from Atomnaya Énergiya, Vol. 31, No. 5, pp. 523-525, November, 1971. Original article submitted July 29, 1970; revision submitted June 21, 1971.

TABLE 1. Comparison of Spectra from Pu–Be (α, n) Sources

Author*	Reference	$\frac{E}{A}$ †																						
Stewart (1955)	[5]				0,7‡ 0,59	—	—	2,0 0,56	3,1 0,98	—	—	4,4 1,0	—	—	—	—	—	—	7,2 0,65	—	9,6 0,29	—	10,3 0
Hess (1959)	[6]	0 0	—	—	—	—	1,4 0,82	—	—	—	—	3,7 1,00	—	—	—	—	—	—	7,2 0,34	—	—	—	10,7 0
H. Brock, Anderson (1960)	[7]						1,3 0,56	—	3,2 1,08	—	—	4,6 1,00	—	5,6 0,56	—	—	—	—	—	—	9,6 0,28	—	10,6 0
M. Anderson, Bond (1963)	[8]			0,4 1,29	—	—	—	2,5 0,86	3,3 1,16	—	—	4,7 1,00	—	—	—	6,8 0,60	—	—	7,7 0,60	—	9,8 0,22	—	11,0
Tochilin (1963)	[9]			0,4 0,97	—	—	—	—	3,0 1,40	—	—	4,8 1,00	—	—	—	—	—	—	7,2 0,45	—	9,6 0,15	—	10,4 0
L. A. Trykov, V. I. Kukhtevich, O. A. Trykov (1965)	[10]	0,2 4,16		0,3 5,28	0,75 1,40	—	1,3 0,50	1,9 0,60	3,1 0,99	—	—	4,7 1,00	—	—	—	6,3 0,42	—	—	7,3 0,50	—	9,4 0,23	—	11,2 0
McCarthy (1967)	[11]					1,0 0,96	—	2,5 0,67	3,3 1,02	—	—	5,1 1,00	—	—	—	6,8 0,61	—	—	7,9 0,67	—	9,8 0,22	—	10,8 0
Lehman (1968)	[3]			0,3 0,62	—	—	—	2,1 0,55	3,2 0,97	—	—	4,7 1,00	—	—	—	6,7 0,31	—	—	7,9 0,40	—	9,9 0,14	—	10,3 0
M. Anderson (1968)	[4]	0,2 0,36	—		0,6 0,99	—	—	2,0 0,60	3,0 1,17	—	—	4,8 1,00	—	—	—	6,9 0,63	—	—	7,8 0,66	—	9,7 0,25	—	10,9 0
Yu. V. Ivanov, B. I. Kuzaev, G. S. Orlov (1970)	[12]					1,0 0,06	—	2,2 0,61	3,1 0,94	3,7 0,86	4,0 0,88	4,8 1,00	5,1 0,94	5,5 0,79	—	6,8 0,76	—	—	7,5 0,77	—	9,5 0,26	10,8 0,17	11,5 0
Authors of this paper	this work					1,0 0,80	1,7 1,37	1,9 1,37	3,2 1,57	—	—	4,8 1,00	—	—	6,4 0,48	6,8 0,47	7,3 0,50	7,6 0,48	7,8 0,33	9,2 0,23	9,5 0,18	10,0 0,07	10,5 0
Peak number		—	—	1	2	—	3	4	5	6	7	8	9	10	11	12	13	14	15	16	17	18	K
Number of papers with identical peaks	—	—	—	1	2	—	2	7	9	1	1	10	1	2	—	6	—		9	—	9	1	10
Average value of E for first ten papers	—	—	—	0,3 ±0,0	0,68 ±0,08	—	1,4 ±0,1	2,2 ±0,2	3,1 ±0,1	3,7	4,0	4,6 ±0,2	5,1	5,6	—	6,7 ±0,1	—	—	7,5 ±0,3	—	9,6 ±0,1	10,8	10,8 ±0,3
Average value of A for first ten papers	—	—	—	5,28 ±0,00	1,20 ±0,20	—	0,53 ±0,03	0,64 ±0,08	1,1 ±0,1	0,86 —	0,88 —	1,0 —	0,94 —	0,68 —	—	0,6 ±0,1	—	—	0,6 ±0,1	—	0,24 ±0,04	0,17	0

*The year the experiment was done is given in parentheses.

† The upper value is E, the energy in MeV, the lower value is A, the relative height of a given peak with respect to the height of peak No. 8 ($\overline{E_8}$ = 4.6 MeV).

‡The beginning of a spectrum is not taken into account in averaging the peaks.

Declassified and Approved For Release 2013/02/26 : CIA-RDP10-02196R000300090003-0

TABLE 2. Comparison of Coefficients k and c

Methods of obtaining results	k	δ_k, %	c	δc, %
Long counter and double moderation [1]	1,37	±5	0,89	±12
Monte Carlo calculation [2]	1,31	±5	0,90	±7
Spectrometer (present work)	1,17	±5	0,92	±2

experimental determination was made of the coefficient k, which corrects for the increase in the flux density P (neutrons/cm^2-sec) because of the neutrons scattered in the collimator, and of the coefficient c, which corrects for the reduction in the average energy $\bar{E}_k$ (MeV) of the neutrons in the beam because of scattering in the collimator in comparison with the average energy $\bar{E}_0$ (MeV) of the neutrons emitted by a Pu–Be (α, n) source, in the equations

$$P = k\frac{Q}{4\pi R^2}; \quad (1)$$

$$\bar{E}_k = c\bar{E}_0, \quad (2)$$

where Q is the total flux from the source, neutrons/sec, and R is the distance from the center of the source in the collimator to a given point on the beam axis, cm. These same coefficients were obtained also by means of a Monte Carlo calculation [2].

In the present work, the neutron spectra from a Pu–Be (α, n) source in "open geometry" and in a beam from a standard collimator (with an aperture of 0.26 sr) of the UKPN-1 device were determined. The measurements were made with a single-crystal sincillation spectrometer having γ-ray discrimination by way at the luminescence time of stilbene (crystal dimensions, 40 × 19 mm). The spectrometer detector and the collimator containing the source were placed on light supports for the measurements. The distance to massive scatterers was not less than 1.8 m. The background of scattered neutrons was negligibly small. Analysis of the instrumental recoil-proton spectra was carried out on an M-20 computer by means of a specially developed program using smoothing differentiation.

The resultant spectra from the Pu–Be (α, n) source are shown in Fig. 1. The coefficients k and c obtained from these spectra are compared in Table 2 with data from integral experiments [1] and with the results of Monte Carlo calculations [2].

From the resultant neutron spectral distributions (see Table 2 and Fig. 1), it is clear that the scattering in the collimator increases the intensity in the "soft" region. The spectra are similar in shape. In the present work, the coefficient k is lower than the values obtained by other methods. This can be explained by the smaller dynamic range of the scintillation counter as compared to a "long counter." It does not record neutrons in the region below 1 MeV, and this region, according to recent papers [3, 4], makes a significant contribution to the flux density; this is even more true after scattering in the collimator. The total source flux obtained in this work by integration of the "open geometry" spectrum agrees within 5% with the certificate data.

Because of the widespread use of Pu–Be (α, n) sources, a comparison of the spectral distribution we obtained with the principal published data is of interest. Table 1 presents the results of a comparison of the location of maxima (peaks) in the distributions and of their relative heights (with respect to the most common maximum in the papers at E = 4.6 MeV, for which the amplitude A is taken to be one).

LITERATURE CITED

1. S. N. Balakhnichev, M. F. Yudin, and A. P. Yanovskii, Trudy Metrologicheskikh Institutov SSSR, No. 12 (184), 107 (1970).
2. L. Ya. Ludkova et al., ibid., p. 99.
3. R. Lehman, Nucl. Instrum. and Methods, 61, 252 (1968).
4. M. Anderson and R. Neff, Trans. Amer. Nucl. Soc., No. 2, 454 (1968).
5. L. Stewart, Phys. Rev., 98, 740 (1955).

6. W. Hess, Ann. Phys., 6, 115 (1959).
7. H. Brock and C. Anderson, Rev. Sci. and Instrum., 31, 1063 (1960).
8. M. Anderson and W. Bond, Nucl. Phys., 43, 339 (1963).
9. E. Tochilin, Neutron Dosimetry, Vol.I, IAEA, Vienna (1963), p.553.
10. L. A. Trykov, V. I. Kukhtevich, and O. A. Trykov, Byul. Informatsionnogo Tsentra Po Yadernym Dannym, No.2, Atomizdat, Moscow (1965), p.341.
11. F. Haas and McCarthy, J. Nucl. Instrum. and Methods, 50, 343 (1967).
12. Yu. V. Ivanov, B. I. Kuzaev, and G. S. Orlov, Trudy Metrologicheskikh Instituta SSSR, No.124 (184), 188 (1970).

COMPONENT SELECTION IN ACTIVATION ANALYSIS

N. V. Zinov'ev

UDC 543.53:519.281.2:518.5

Methods for unfolding pulse-height spectra on computers have become a part of activation analysis. Such a situation leads to the necessity for discussion and demonstration of effective algorithms in this field.

In this connection, we consider the following formulation of the problem: a large number of uniform samples are analyzed; the entire set of measured activities from a given group of materials can be built up from a library of standard spectra; the number of library spectra is large and statistics does not permit the inclusion of the entire set as possible components; in each specific sample, the number of significant activities present is not large, but their qualitative composition is unknown; experimental statistics are sufficient for analysis to a given accuracy if the algorithm excludes all, or nearly all, insignificant activities from the least squares formalism.

For simplicity in the discussion of such an algorithm, we introduce the following notation: $\Phi(k)$ is the spectrum being unfolded; $f(i, k)$ is the spectrum of the i-th library standard; $p(k)$ is the statistical weight of the k-th channel; $\alpha(i)$ is the contribution of the i-th standard spectra; k is the analyzer channel number; and i is the index number of a standard, which varies from 1 to m. At a given step in the calculations, let the Pearson criterion be represented by

$$X^2 = \sum_k P(k)\,\Delta^2(k), \tag{1}$$

where

$$\Delta(k) = \Phi(k) - \sum_{r=1}^{s} \alpha(I_r)\, f(I_r, k), \tag{2}$$

in which the quantitites $I_1, I_2, \ldots, I_S$ are numbers from the set $1, 2, \ldots, m$.

Assume that the hypothesis concerning the sufficiency of s components is clearly false. The resulting problem of additional components can be solved in the following manner: we calculate the quantities

$$Q(i) = \left[\sum_k P(k)\,\Delta(k)\,f(i, k)\right]\left[X^2 \sum_g P(g)\,f^2(i, g)\right]^{-1/2} \quad (i \neq I_1, I_2, \ldots I_s), \tag{3}$$

which represent the correlation of $\Delta(k)$ with the $f(i, k)$ which were not taken into consideration in Eq. (2). Analyzing the set $Q(i)$, we determine the numbers I_{S+1} and I_{S+2} which correspond to the maximum positive ($Q(I_{S+1})$) and negative ($Q(I_{S+2})$) correlations. On the basis of the relation between $Q(I_{S+1})$ and $Q(I_{S+2})$, we include either $f(I_{S+1}, k)$ or $f(I_{S+2}, k)$, or both spectra, in the least squares formalism. The procedure described is repeated until a satisfactory X^2 is obtained.

This algorithm is not absolute because the form of the components is not orthogonal; nevertheless, programs based upon it can be used successfully in instrumental activation analysis. In place of the Gauss least squares method, furthermore, it is better to use the gradient method with exclusion of negative activities and to include a procedure for rejection of weak components.

Translated from Atomnaya Énergiya, Vol.31, No.5, pp.525-526, November, 1971. Original article submitted November 12, 1970.

OPTIMIZATION OF ACTIVATION MEASUREMENTS

G. S. Vozzhenikov

UDC 550.835

For a certain period of activation (t_a^{opt}), the total time expended in irradiation of the target and counting the induced activity to a given accuracy is a minimum [1]; this makes it possible to optimize the process of activation measurements.

The solution presented in [1] was obtained for the case where a change in the magnitude of the induced effect could be neglected. This assumption is well satisfied for activation measurements of long-lived products of high activity, but it is not acceptable for measurements of short-lived, low-activity sources. This paper considers the case where the optimal activation time is calculated with allowance for an exponential decrease in activity with time.

Assume that the counting rate resulting from the induced activity of an isotope with a decay constant λ is I_0 (counts/min) at the start of counting, which is the count above natural background, will be [2]

$$\delta=\frac{\sqrt{I_0/\lambda(1-e^{-\lambda t})}}{I_0/\lambda(1-e^{-\lambda t})}, \tag{1}$$

from which it is easy to find the time t in which one should measure the induced effect with an error no greater than that given:

$$t=-\frac{1}{\lambda}\ln\left(1-\frac{\lambda}{I_0\delta^2}\right). \tag{2}$$

It is clear from Eq. (2) that the given accuracy of measurement can be assured only when the inequality $\lambda < I_0\delta^2$ is satisfied. Otherwise, obtaining the required accuracy of measurement is impossible because the required number of counts will not be recorded as the result of the rapid decrease in induced activity with time.

In the particular case where $\lambda \ll I_0\delta^2$, Eq. (2) simplifies to

$$t\approx\frac{1}{I_0\delta^2}. \tag{3}$$

We then turn to the calculation of the optimal activation time t_a^{opt}, for which it is sufficient to solve the equation

$$\frac{d}{dt_a}(t_a+t)=0. \tag{4}$$

We shall assume that the beginning of counting coincides with the end of activation. Keeping in mind the well-known relation between the value of the induced activity at the time of removal from irradiation and the saturation value I_∞, we rewrite Eq. (2):

$$t=-\frac{1}{\lambda}\ln\left[1-\frac{\lambda}{I_\infty(1-e^{-\lambda t_a})\delta^2}\right]. \tag{5}$$

Using Eq. (5), we write Eq. (4) in the following manner:

$$\frac{d}{dt_a}\left\{t_a-\frac{1}{\lambda}\ln\left[1-\frac{\lambda}{I_\infty(1-e^{-\lambda t_a})\delta^2}\right]\right\}=0. \tag{6}$$

Solving Eq. (6) with respect to t_a, we obtain the following expression for the optimal activation time:

Translated from Atomnaya Énergiya, Vol. 31, No. 5, pp. 526-527, November, 1971. Original article submitted October 28, 1970.

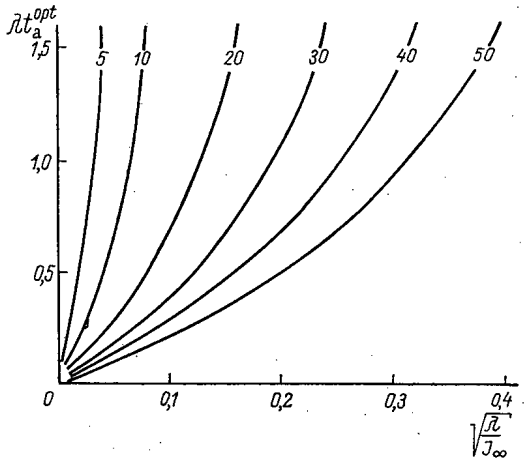

Fig. 1

$$t_a^{opt} = -\frac{1}{\lambda} \ln \left(1 - \frac{1}{\delta} \sqrt{\frac{\lambda}{I_\infty}}\right). \quad (7)$$

Equation (7) indicates that the optimal irradiation time only exists when $\lambda < I_\infty \delta^2$. Otherwise, it is necessary to increase the induced activity (by means of neutron sources) in order to insure the required accuracy of measurement.

When the inequality $(1/\delta)\sqrt{\lambda}/I_\infty \ll 1$ is satisfied, Eq. (7) simplifies to:

$$t_a^{opt} \approx \frac{1}{\delta \sqrt{I_\infty \lambda}}.$$

We return to Eq. (5), in which we set $t_a = t_a^{opt}$. Then

$$t = -\frac{1}{\lambda} \ln \left\{1 - \frac{\lambda}{I_\infty \left[1 - e^{\ln\left(1 - \frac{1}{\delta}\sqrt{\lambda/I_\infty}\right)}\right] \delta^2}\right\}. \quad (8)$$

Since

$$\exp\left[\ln\left(1 - \frac{1}{\delta}\sqrt{\lambda/J_\infty}\right)\right] = 1 - \frac{1}{\delta}\sqrt{\lambda/J_\infty},$$

then

$$t = -\frac{1}{\lambda} \ln \left(1 - \frac{1}{\delta} \sqrt{\frac{\lambda}{J_\infty}}\right).$$

In orther words, the irradiation time and the counting time are the same for $t_a = t_a^{opt}$.

Figure 1 shows the dependence of the product λt_a^{opt} on the parameter $\sqrt{\lambda/I_\infty}$ for various values of δ(%). Considering that Eqs. (5) and (7) agree for $t_a + t = \min$, this figure makes it possible to determine both t_a^{opt} and t.

LITERATURE CITED

1. G. S. Vozzhenikov, Activation Analysis in Mining Geophysics [in Russian], Nedra, Moscow (1965), p. 8.
2. V. I. Gol'danskii, A. V. Kutsenko, and M. I. Podgoretskii, Counting Statistics in Nuclear Particles Detection [in Russian], Fizmatgiz, Moscow (1959), p. 84.

IMPROVING THE VERTICAL RESOLUTION OF A NEUTRON-TYPE FIELD HYGROMETER

L. I. Beskin, I. Ya. Bogdanov,
V. A. Emel'yanov, S. Kiyanya,
and V. I. Sinitsyn

UDC 631.42:697.93

The neutron method is being more and more widely used in practice in field investigations of soil moisture, since it is the only method by which the moisture can be measured without taking a sample. Moisture values determined from the rate of counting of slow neutrons are obtained in the form of averages taken over some spherical volume whose radial dimensions are inversely proportional to the moisture per unit volume [1, 2] (Fig. 1). When the probe of the hygrometer is placed near boundries separating layers with different moisture values, the measurement results are found to be too high or too low, depending on the position of the probe with respect to the boundaries. Consequently, very large errors may arise in the measurements [1, 3].

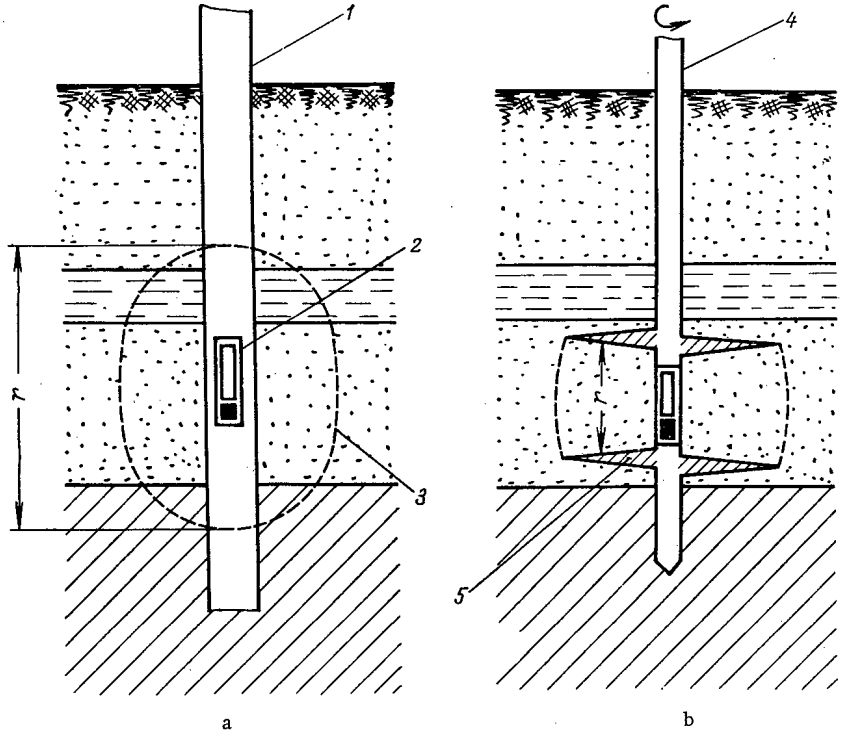

Fig. 1. Methods for inserting probes of neutron hygrometers (a – into a borehole; b – using a drill with helical blades): 1) casing pipe; 2) probe of neutron hygrometer; 3) sphere over which moisture data are averaged; 4) stem of hygrometer drill; 5) helical blade of drill; r) resolution of neutron hygrometer.

Translated from Atomnaya Énergiya, Vol. 31, No. 5, pp. 527-530, November, 1971. Original article submitted July 22, 1970; revision submitted June 4, 1971.

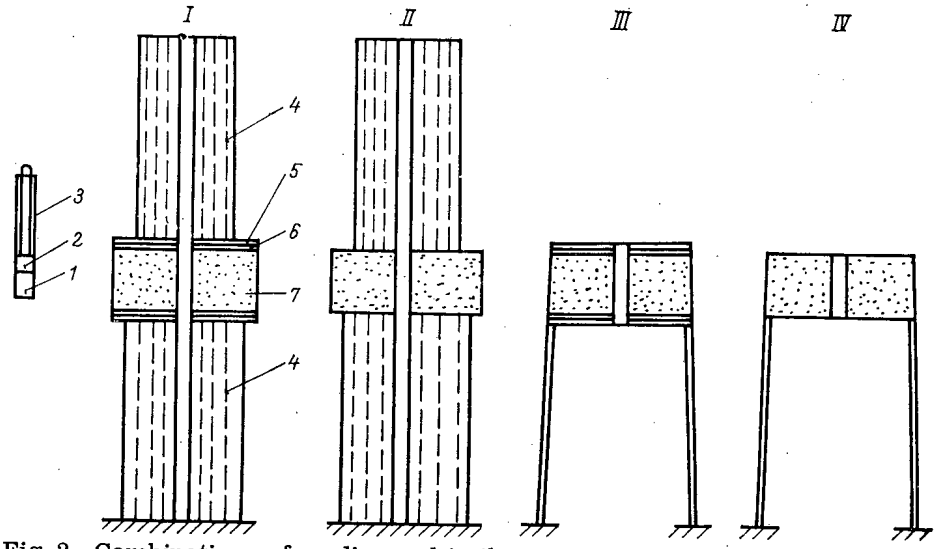

Fig. 2. Combinations of media used in the experiment. Left: hygrometer probe in the zero position: 1) neutron source; 2) operating part of the SNM-11 counter; 3) cadmium cylinder; 4) plastic cylinder; 5) steel plate; 6) boric acid layer; 7) saturated sand.

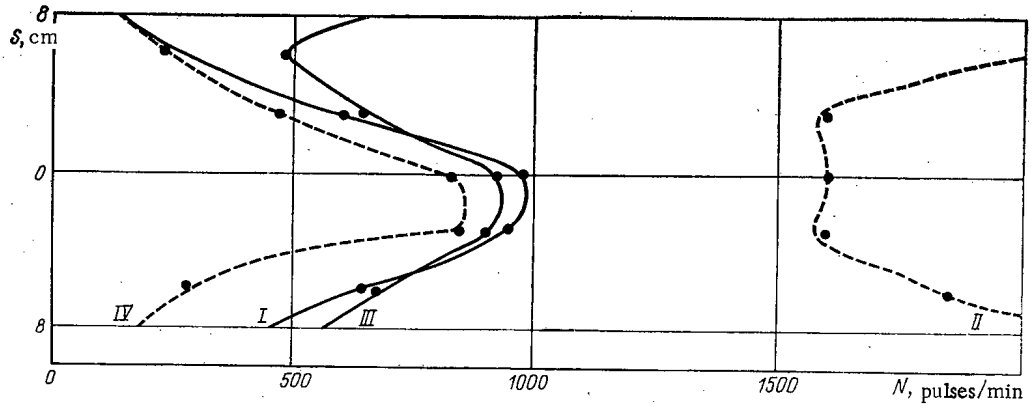

Fig. 3. Rate of counting of slow neutrons as a function of probe placement with respect to the midplane of a layer of sand 16 cm thick saturated with water (Roman numerals next to the curves correspond to the numbers of the experimental variants shown in Fig. 2).

Such methods as using short counters, placing a neutron source in the center of the counter, using different shields on the source and the counter, etc., do not substantially improve the resolution [4] or guarantee that it will be constant. In order to obtain a substantial improvement in the resolution of neutron hygrometers, it is proposed to place a neutron probe in the stem of a helical drill [5], between two blades (20-40 cm in diameter) which contain anomalously strong neutron absorbers (see Fig. 1b). Thus, only a limited number of neutrons slowed down outside the layer being analyzed will reach the counter. This proposal was experimentally verified under laboratory conditions with an NVU-1 hygrometer [2, 6].

In our experiments we investigated the influence of layers with higher moisture content on a less moist layer between them and the influence of dry layers on a moist layer between them. In order to stimulate the layers situated between the helical blade shields, we used fine-grained quartz sand saturated with water (about 40% water by volume). The sand layers were 16 cm or 24 cm thick. The blade shields were simulated by combined reflecting and absorbing layers: each was 1 cm thick and consisted of steel with boric acid.

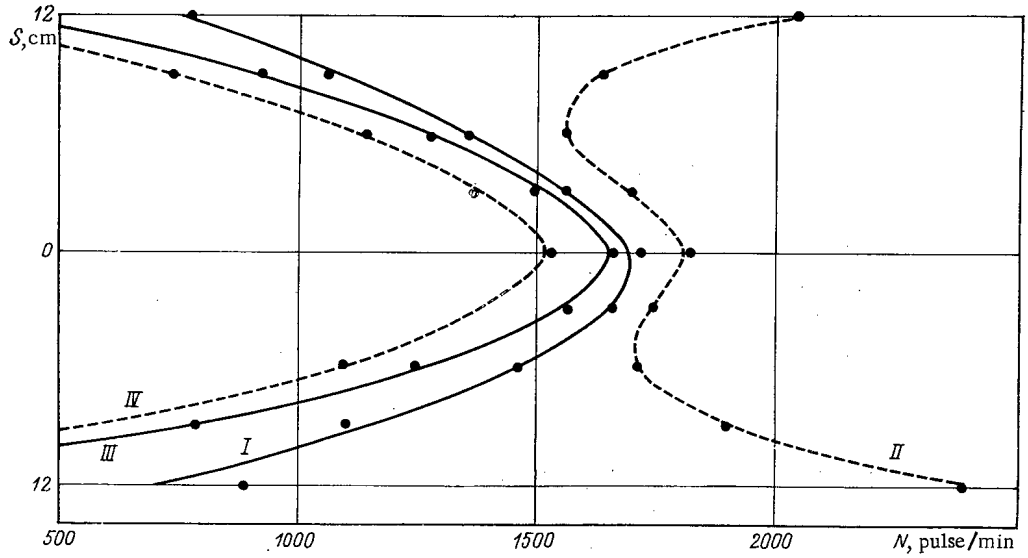

Fig. 4. Rate of counting of slow neutrons as a function of probe position with respect to the midplane of a layer of sand 24 cm thick saturated with moisture (Roman numerals next to the curves correspond to the numbers of the experimental variants in Fig. 2).

Variants of the experiment are shown in Fig. 2. Plastic cylinders were used to simulate layers with 100% moisture content (I, II in Fig. 2), and air above and below the layers of sand simulated zero moisture content (III, IV in Fig. 2).

The hygrometer probe contained an SNM-11 boron counter and a Pu + Be neutron source supplying about 10^5 neutrons/sec. The part of the counter cathode not shielded with cadmium, i.e., the sensitive part, was 4 cm long (total length 28 cm). The distance from the middle of this part of the counter to the center of the neutron source (the length of the probe) was 6 cm. The zero of the probe was the midpoint of this interval (see Fig. 2).

It can be seen from Fig. 3 and Fig. 4 that when we used shields, the counting rates in the midplane of the layer under investigation were found to be almost identical (within the limits of experimental error), irrespective of the moisture content of the boundary layers. The errors in determining the moisture content of the layer under investigation without using shields would have been no less than 100% and 25%. The difference between the curves of Fig. 3 and those of Fig. 4 is due to the differences in the thickness of the sand layer (16 cm and 24 cm, respectively).

The proposed method for improving the vertical resolution of a neutron hygrometer is worth investigating with real helical-blade shields, which may prove to be less effective than parallel plane shields. In addition, research must be done on the development of methods for interpreting the measurements made with the proposed helical-blade shield probe.

LITERATURE CITED

1. G. Lawless et al., Soil Sci. Soc. of America Proc., 27, 5 (1963).
2. V. A. Emel'yanov, Radiometric Field Hygrometers and Densimeters [in Russian], Atomizdat, Moscow (1966).
3. J. McHenry, Soil Sci., 95, 5 (1963).
4. V. A. Emel'yanov, Field Radiometry of Soil Moisture Content and Density [in Russian], Atomizdat, Moscow (1970).
5. Procedural Guidelines for Measuring Soil Moisture Content and Density with Radiometric Hygrometers and Densimeters in Soil Surveys, Engineering Geological Surveys, and Water and Land Improvement Surveys, Issue No. 4, Izd. VNIIGiM, Moscow (1969).
6. L. I. Beskin, Isotopes in the USSR, No. 7 (1967).

ORIGIN OF Ne^{21} ISOTOPES IN RADIOACTIVE MINERALS

Yu. A. Shukolyukov, V. B. Sharif-Zade, G. Sh. Ashkinadze, and E. K. Gerling

UDC 546.292:553.495

Neon emitted from minerals containing uranium and from natural gases containing helium is rich in Ne^{21} and Ne^{22} isotopes [1-4]. Nuclear reactions with α-particles, neutrons [1-7], and cosmic muons [1, 8] were suggested in order to explain this enrichment:

$O^{18}(\alpha, n)Ne^{21}$ $\quad \mu \rightarrow \gamma$ $\quad Na^{23}(\gamma, 2n)Na^{21} \xrightarrow{\beta^+} Ne^{21}$

$O^{18}(\alpha, p)F^{21} \xrightarrow{\beta^-} Ne^{21}$ $\quad Na^{23}(\gamma, np)Ne^{21}$

$Mg^{24}(n, \alpha)Ne^{21}$ $\quad Na^{23}(\gamma, n)Na^{22} \xrightarrow{\beta^+} Ne^{22}$

$F^{19}(\alpha, n)Na^{22} \xrightarrow{\beta_+} Ne^{22}$ $\quad Na^{23}(\gamma, p)Ne^{22}$.

$F^{19}(\alpha, p)Ne^{22}$

Up to now, however, the calculations have been qualitative, since it was not possible to account for the loss of neon in the minerals during a geologic period, and therefore it was impossible to correctly estimate the amount of Ne^{21} generated in minerals.

This work contains data which enable us to eliminate the uncertainties connected with the loss of neon in minerals.

The element He^4 is formed in minerals during the α-decay of the elements of the uranium family. In addition, krypton and xenon isotopes are produced in the spontaneous breakup of U^{238} and in the breakup of U^{235} induced by thermal neutrons. The known isotope composition of xenon and krypton in the spontaneous breakup of U^{238} [9] and in the neutron induced breakup of U^{235} [10] enables us to estimate the fraction of

TABLE 1. Radiogenic Neon Isotopes in Radioactive Minerals

Sample number	Sample	Age in million years	U, %	Th, %	Sample weight, g	Isotope composition of neon, %			C_{He}	C_{Kr}	C_{Xe}	C_{Ne}	Radiogenic neon, $\cdot 10^{-9}$ cm^3/g				
													measured		corrected for loss		
						20	21	22					Ne^{21}	Ne^{22}	Ne^{21}	Ne^{22}	calculated according to Eq. (2) for Ne^{21}
1	Uraninite g-4 (Eastern part USSR)	230	18,8	0,5	0,062	90,3	0,396	9,30	0,011	0,36	0,75	0,030	38±7	30	1270	1000	250±100
2	Uraninite g-3 (Eastern part USSR)	230	69,0	0,5	0,956 0,160	89,40 89,0	0,541 1,27	10,1 9,75	0,019	0,52	0,92	0,050	108±3	235±170	2130	4700	920±350
3	Hatchettotite (Ilmen mountains, Ural)	293	2,39	0,35	0,31	81,2	0,470	18,3	0,078	0,81	1,14	0,16	9,6±2,0	416±130	57	2500	45±15
4	Betafite (Ilmen mountains, Ural)	293	9,39	6,6	0,50 0,50	81,6 82,1	0,772 0,614	17,7 17,4	0,093	0,42	0,60	0,12	15±2	320±100	125	2700	250±100
5	Samarskite (Ilmen mountains, Ural)	330	5,48	1,94	0,25 0,25	90,1 86,7	0,366 0,430	9,64 12,8	0,36	0,88	0,88	0,45	21±5	180±150	47	400	130±50
6	Monazite (Kol'skii P-ov)	1950	0,146	2,5	0,50 2,00	85,2 82,9	4,62 4,74	10,22 12,50	0,48	0,54	0,70	0,50	316±60	220±120	732	440	200±80
7	Atmosphere	—	—	—	90,50	90,50	0,268	9,23									

Translated from Atomnaya Energiya, Vol.31, No.5, pp.530-531, November, 1971. Original article submitted January 2, 1971.

spontaneous breakup products of a given total amount of xenon and krypton (decay products of spontaneous breakup of the U^{238} only) and of radiogenic He^4, and having estimated the age t of the minerals by an independent uranium–thorium–lead method [11, 12] we can calculate preservation coefficients C_{He}, C_{Kr}, and C_{Xe} of these radiogenic gases. Results of a study of several tens of radioactive minerals [9] indicate that the values of preservation coefficients of helium, krypton, and xenon depend on the atomic weight of the gas. Therefore, we can use interpolation to estimate the preservation coefficient for neon in each mineral.

Parallel determinations of neon (see Table 1) were carried out for each mineral sample (except No. 3). This gave a somewhat different isotope composition, not so much because of the measurement error (±0.3%), but because the atmospheric neon with an isotope composition slightly different from that of the samples (see Table 1) unavoidably contaminated the equipment.

Since in an isotope mixture the relative amount of Ne^{20} exceeds that of Ne^{22} (and Ne^{21}) by at least a factor of 5, all of Ne^{20} was assumed to be atmospheric, and the value of excess radiogenic Ne^{21}_r and Ne^{22}_r was computed according to the equation:

$$\left.\begin{aligned} Ne^{21}_p &= Ne^{21}_{meas} - Ne^{20}_{meas}\left(\frac{Ne^{21}}{Ne^{20}}\right)_{atm}, \\ Ne^{22}_p &= N^{22}_{meas} - Ne^{20}_{meas}\left(\frac{Ne^{22}}{Ne^{20}}\right)_{atm}. \end{aligned}\right\} \quad (1)$$

The amounts of radiogenic neon determined this way were corrected for the loss of gases by the minerals. In order to do this the coefficients of loss of neon were determined by interpolation.

The knowledge of α-radiation dose for each mineral (the content of α-sources and the irradiation time were known) enabled us to calculate the probable amount of Ne^{21}, provided that it was formed during the reaction O^{18} (α, n) according to the equation [6]:

$$Ne^{21}_{calc} = \frac{N_\alpha q_0 S_0 N_0}{\sum_i N_i S_i}, \quad (2)$$

where N_α is the integrated amount of α-particles in the unit volume of the mineral; q_0 is the yield of the reaction of oxygen (thick target) under the action of α-particles of uranium–thorium balanced families (this quantity is weighed to account for the ratio Th/U); N_0 is the concentration of oxygen nuclei; S_i is the relative retardation power of chemical elements present in the mineral; S_0 is the same for oxygen. Taking into account the low accuracy of Ne^{21}_{calc} because of the possible influence of the undetermined amount of beryllium which has a large yield in the (α, n) reaction, and because of the lack of validity of the assumption about the homogeneous distribution of emitters and absorbers of α-particles in the minerals, we can regard these data as a preliminary experimental confirmation of the hypothesis on the formation of Ne^{21} in minerals in the reaction O^{18} (α, n) Ne^{21}.

The origin of Ne^{22} is not clear yet, since the amount of Ne^{22} is too large to be explained by the fluorine contained in minerals leading to reactions $Fe^{19}(\alpha, n)$ and $F^{19}(\alpha, p)$.

LITERATURE CITED

1. G. Wetherill, Phys. Rev., 96, 679 (1954).
2. D. Bogard et al., J. Geophys. Res., 70, 703 (1965).
3. D. Emerson et al., Geochim. Acta, 30, 847 (1966).
4. D. Emerson et al., Internat. J. of Mass Spectr. and Ion Phys., 1, No. 1, 150 (1968).
5. L. K. Kishkarov and V. V. Cherdyntsev, Geokhimiya, No. 7, 632 (1968).
6. G. V. Gorshkov et al., Natural Neutron Background of the Atmosphere and of the Earth's Crust [in Russian], Atomizdat, Moscow (1966).
7. J. Takagi et al., J. Geophys. Res., 72, 2267 (1967).
8. J. Takagi, Nature, 227, No. 5256, 362 (1970).
9. Yu. A. Shukolyukov, Breakup of Uranium Nuclei in Nature [in Russian], Atomizdat, Moscow (1970).
10. Yu. A. Zysin, A. A. Lbov, and L. N. Sel'chenkov, Yields of Breakup Products and Their Mass Distribution [in Russian], Atomizdat, Moscow (1957).
11. I. E. Starik, Nuclear Geochronology [in Russian], Izd-vo AN SSSR, Moscow–Leningrad (1961).
12. E. V. Sobotovich, Isotopes of Lead in Geochemistry and Cosmochemistry [in Russian], Atomizdat, Moscow (1970).

VOLUME OF PERSONNEL MONITORING AT REACTORS

Yu. V. Chechetkin, I. G. Kobzar',
P. I. Kotikov, and V. D. Moshkin

UDC 539.12.08

As a rule, people working at nuclear reactors are subject to the effect of a set of hazardous radiation factors: external irradiation by fluxes of γ rays, neutrons, and β particles and internal irradiation by radioactive materials entering the body. The contribution from each type of radiation depends on the type of nuclear installation, the mode of operation, and other conditions. To determine the optimal volume of dosimetric monitoring and to evaluate the nature of the complex radiation effect, it is necessary to know the contribution of the individual radiation components to the total dose. Such an estimate is made in this paper for the people working at the SM-2, MIR, and VK-50 reactors at the V. I. Lenin Atomic Reactor Institute (Melekess).

The water-cooled, water-moderated 75-MW SM-2 research reactor was intended for irradiation of reactor materials, investigations of material properties during irradiation, production of transuranic elements, etc. Tests of fuel elements for power plants are carried out in the 100-MW MIR swimming-pool reactor of the channel type. The VK-50 150-MW boiling-water reactor with a natural water circulation loop inside the vessel was constructed to do research and accumulate experience in the operation of boiling-water reactors.

To determine the contribution of the separate components to the total radiation dose, control individuals were issued IFKU personnel dosimeters. This dosimeter records the dose from γ rays in the energy range 0.1-3 MeV, from β particles with energies above 1 MeV, and from thermal neutrons [1, 2]. PM-1 film, which is capable of recording doses in the range 0.05-2 rem, was used in the IFKU dosimeter.

One of the features of external β radiation of the body is that organs located close to the surface of the body – skin, subcutaneous tissue, and the crystalline lens of the eye – undergo irradiation because of marked absorption of the β particles. The depth of these organs, their radiosensitivity, and the maximum

TABLE 1. Evaluation of Irradiation of Skin, Subcutaneous Tissue, and Eye Lens Corresponding to Contamination Levels and β Spectra in Repair Work Locations at the SM-2, MIR, and VK-50 Reactors

Reactor	Effective β spectrum		Contamination level, particles /150 cm^2 · min	Degree of irradiation in fraction of MPL			Main isotopes
	energy range, MeV	contribution, %		skin	subcutaneous tissue	lens of eye	
SM-2	0—0,1 0,1—1,4 > 1,4	10—15 50—80 15—40	$(2\text{-}3)\cdot10^5$	0,025—0,028 0,058—0,14 0,039—0,046	~ 0 0,066—0,15 0,086—0,11	~ 0 0,018—0,042 0,24—0,29	Cr^{51}, Co^{60}, Zr^{95} + Nb^{95}, Ru^{106} + Rh^{106}, Ce^{144} + Pr^{144}
MIR	0—0,1 0,1—1,4 > 1,4	20—30 65—70 10—15	$(0{,}6\text{-}1{,}0)\cdot10^5$	0,015—0,031 0,032—0,055 0,005—0,008	~ 0 0,036—0,062 0,013—0,018	~ 0 0,01—0,017 0,035—0,048	The same
VK-50	0—0,1 0,1—1,4 > 1,4	25—40 40—50 15—25	$(1{,}5\text{-}2{,}1)\cdot10^4$	0,008—0,009 0,005—0,01 0,003—0,005	~ 0 ~ 0,01—0,01 0,007—0,011	~ 0 0,002—0,003 0,02—0,03	Co^{60}, Zn^{65}, Ru^{106} + Rh^{106}, Ce^{144} + Pr^{144}

Translated from Atomnaya Énergiya, Vol.31, No.5, pp.532-533, November, 1971. Original article submitted October 15, 1970.

TABLE 2. Personnel Radiation Doses at the Reactors, 1967-1969

Reactor	Year	Fraction of people (%) receiving an annual rem dose of			Mean annual individual dose, rem			$\frac{\bar{D}_\beta}{\bar{D}_\gamma}$	Maximum annual individual dose, rem				$\frac{D_{\beta max}}{D_{\gamma max}}$
		<1,0	1–2,5	2,5–5	$\bar{D}_\beta$	$\bar{D}_\gamma$	$\bar{D}_{T.N}$		$D_{\beta max}$	$D_{\gamma max}$	$D_{T.N max}$	Σ^*_{max}	
SM-2	1967	43	50	7	0,15	1,04	—	0,14	0,47	3,88	0,05	4,35	0,12
	1968	48	43	9	0,07	1,29	—	0,05	0,93	3,24	0,05	4,2	0,29
	1969	77	22	1	0,02	0,97	—	0,02	0,45	3,1	—	3,25	0,14
MIR	1967	98	2	—	0,05	0,54	—	0,09	0,06	1,02	—	1,08	0,06
	1968	90	10	—	0,03	0,66	—	0,05	0,1	2,17	—	2,27	0,05
	1969	95	5	—	0,005	0,55	—	0,01	0,1	2,2	—	2,29	0,04
VK-50	1967	78	22	—	0,1	0,68	—	0,15	0,34	2,08	0,05	2,18	0,16
	1968	80,2	19,4	0,4	0,05	0,58	—	0,09	0,37	2,25	—	2,64	0,16
	1969	65	30	5	0,08	0,93	—	0,09	0,61	3,53	0,05	4,03	0,17

* Σ_{max} is the maximum total individual dose.

permissible doses of radiation are different. On the basis of the data in [2], the lens of the eye was selected as the critical organ for external β radiation, and the IFKU dosimeter recording β radiation was shielded by a tissue-equivalent layer 300 mg/cm^2 thick.

Table 1 shows the results of the measurements made by the authors and of an analysis of the contamination of working areas by β emitters of various energies (with respect to the maximum energy of the effective β spectrum). For these conditions, an estimate was made of the degree of irradiation of skin, subcutaneous tissue, and lens of the eye in fractions of the maximum permissible level (MPL). A ratio of isotopes obtained experimentally was used in the evaluation.

Table 2 gives the recorded mean annual and maximum radiation dose to personnel at the reactors mentioned during 1967-1969. These values include irradiation during periods of normal operation, preventive maintenance, and repair.

From an analysis of this data, one can arrive at the following conclusions:

1. Thermal neutron irradiation of personnel can be neglected (at all three reactors); the chance for detection lies outside the limits of sensitivity of the method used.

2. The maximum recorded β dose did not exceed 29% of the γ dose.

The fractional β radiation of individuals falls within 5-14% of the total average annual dose.

3. The radiation dose to 90-100% of the people at the plants is no more than 2.5 rem. Less than 10% of the individuals had a dose greater than 2.5 rem. Among them are mainly people who perform repair work on the basic technical equipment. The irradiation of 50% and more of the individuals falls within the range of 1 rem.

According to the health rules for working with radioactive materials and sources of ionizing radiation, 1960, [3], the lens of the eye and the skin belong to the second and third groups of critical organs, respectively, for which the maximum permissible doses are 600 and 300 mrem/week. Since the β radiation contribution to the total dose of external radiation is less than 14%, there is no need to have continual special individual monitoring of the dose from β radiation at the installations indicated. Such monitoring is only necessary in the few cases of repair work on highly contaminated equipment.

Considering the insignificant mean annual irradiation of reactor personnel and the practical absence of hazardous radiation work in some branches (administrative and housekeeping branch, electrical branch, reactor control group, reactor research laboratory, and dosimetry laboratory), the exchange period for IFKU personnel dosimeters can be increased to two months. When performing preventive-maintenance repairs or emergency operations, the exchange period for personnel dosimeters should be reduced on the basis of specific conditions.

LITERATURE CITED

1. N. G. Gusev et al. (editors), Dosimetric and Radiometric Methods – A Compilation [in Russian], Atomizdat, Moscow (1966).
2. M. S. Egorova et al., in: Collected Papers on Dosimetry Problems and the Radiometry of Ionizing Radiation [in Russian], A. D. Turkin (editor), Atomizdat, Moscow (1966).
3. Health Rules for Working with Radioactive Materials and Sources of Ionizing Radiation [in Russian], No. 330-60, Atomizdat, Moscow (1960).

ON THE ACCURACY OF MEASUREMENT OF SIZE DISTRIBUTION PARAMETERS BY IMPACTOR

V. I. Bad'in, Yu. K. Moiseev, and Z. G. Batova

UDC 541.182

Coarse-grained α-active aerosols take a special place among radioactive aerodispersed systems in regard to being a radiational hazard. A majority of these particles belong to a potentially hazardous class of aerosols creating a source of radiation in the course of a long period. The computation of the doses is based on the biophysical model, where the degree of fineness of the aerosol particles plays the most important role [1]. The degree of fineness can be determined by the different methods, including the use of impactors [2]. The practical interest in the latter arises due to its fast operation and simplicity, since a multicascade impactor (inertial precipitator) enables one to carry out the entire analysis in a few tens of minutes.

Besides, this device which is calibrated with a calibration aerosol with particle density $\rho = 1$ g/cm^3 offers the possibility of obtaining the results of measurement of the size of the grains directly in units of the so-called reduced sedimentation (aerodynamic) radius. For particles whose shape is not too different from spherical, the aerodynamic radius coincides with the reduced radius equal to $r\sqrt{\rho}$. This permits calibration of the impactor for any aerosol with known density. Thus, the degree of fineness of an aerosol measured by an impactor can be expressed in aerodynamic dimensions of the particles; different coefficients of entraping of the dust particles by living organisms are functions of the aerodynamic dimensions [3] and the need for determining the density and the shape of the investigated dust particles is avoided.

The calibration of the impactor for inactive aerosols consists in determining the median radius r_m of the countable size distribution of the calibration aerosol particles sedimented in each cascade [4]. Unfortunately, the countable median of the sizes of the particles, sedimented in a cascade, depends both on the input countable size spectrum f(r) and the efficiency of sedimentation e(r). The same indeterminacy appears in the calibration of active aerosols, in the process of which the active median radius r_{am} is determined.

In sedimentations in cascades the log-normal size distribution of the radioactive particles is observed most often, since the countable and the active distributions usually obey this law [5]. For an n-cascade impactor the equation connecting the mean geometric radius over the activity of the measured dust $\hat{r}_{ag} = r_{am}$ with the mean geometric radii r_{agi} of the corresponding split fractions has the form

$$r_{ag} = \prod_{i=1}^{n} r_{agi}^{g_{ai}}, \tag{1}$$

where g_{ai} is the fraction of the activity of the investigated dust settled in the i-th cascade. Denoting the mean (over activity) geometric radius of the particles of the calibration aerosol entrapped in this cascade by $\bar{r}_{agi}$, and considering that $r_{agi} = P_i \bar{r}_{agi}$, we get

$$r_{ag} = P r_{ago}, \tag{2}$$

where r_{ago} is the mean geometric radius of the measured aerosol, obtained with the use of the impactor calibrated by the standard method, $P = \prod_{i=1}^{n} P_i^{g_{ai}}$ is a correction factor taking account of the inaccuracy

Translated from Atomnaya Énergiya, Vol. 31, No. 5, pp. 534-536, November, 1971. Original article submitted July 24, 1970; revision submitted November 27, 1970.

TABLE 1. Comparative Results of Determination of the Degree of Fineness of Coarse-Grained α-Active Aerosols by Direct Autoradiographic Method and by Impactor

Method of determination	Parameters of active size distribution and corrections	No. of experiment 1	2	3	Mean values	Remarks
Use of impactor	Active mean geometric radius r^0_{ag}, μ	1,8	1,2	1,8	1,6	Without introducing corrections
	Standard geometric deviation β^0_g	3,2	3,1	3,2	3,2	The same
	X_i $\overline{K}_i$ φ_i	2 2,5 10	2 1,9 7,6	4 5,7 23	— — —	Determined from the experiment on solvability of aerosol particles (P = 2)
	Active aerodynamic mean geometric radius r_{ag}, μ	18	9	41	23	After introduction of correction ($r_{ag}=\varphi r^0_{ag}$; $\varphi = P\overline{K}\sqrt{\rho}$)
Direct autoradiographic method	Active aerodynamic mean geometric radius r_{ag}, μ	22	12	50	28	Autoradiography showed that the activity of the particles is proportional to r^3, computation from measured r_g by the formula $r_{ag}=r_g\beta_g^{3\ln\beta_g}$
	Standard geometric deviation β_g	2	2,9	2,8	2,9	Direct measurement

of calibration for the aerosol as a whole, and P_i is a correction factor taking account of the transition from the calibration spectrum to the size spectrum of the investigated particles settled in the i-th cascade. The tentative coefficient P_i has a maximum depature from unity for the final cascades and in the case of the coincidence of the radii of the cascades lying between active modes of the investigated r_e and the calibration $\bar{r}_g$ aerosols. $P_i > 1$, if $\bar{r}_e < r_e$ and $\bar{r}_{ag}\bar{\beta}_{ag}^{-\ln\beta_g} < r < r_{ag}\beta^{-\log\beta_g}$, and $P_i < 1$ if $\bar{r}_e > r_e$ and $r_{ag}\beta^{-\log\beta_g} < r < \bar{r}_{ag}\bar{\beta}_g^{-\ln\beta_g}$. Here β_g and $\bar{\beta}_g$ are the standard geometric deviations of the investigated and the calibration dusts; $\bar{r}_g$ is the active mean geometric radius of the calibration aerosol particles. For extended aerosol generators ($\bar{r}_{ag} = 1\ \mu$) and coarse-grain dust ($r_{ag} \approx 20\mu$) $1 < P \leq 3$ approximately. Hence the impactor is a device possessing "motion with degree of fineness."

In practice an appreciable self-absorption of α-radiation in the aerosol particles is observed; this absorption is proportional to the radius of the dust and reaches 2-4-fold for spectra averaged in a prolonged sampling of the air specimen [6]. If the correction for the self-absorption for the entire size spectrum is denoted by $X = 1/\eta_0$ and the fraction of the radiometrically (without taking self-absorption into consideration) determined activity, settling in the i-th cascade by g^0_{ai}, then the equation connecting the theoretically and experimentally determined characteristics has the form

$$\Phi(\xi) = 2\frac{\sum_{i=1}^{k} g^0_{ai}}{X} - 1,$$

where $\Phi(\xi) = \frac{2}{\sqrt{2\pi}}\int_0^{\xi} e^{-\xi^2/2}\,d\xi$ is the probability integral, $\xi = (\log r - \log r_{ag})/\log\beta_g$; β_g is the standard geometric deviation for the real size distribution; η_0 is the fraction of radiation emitted by all aerosol particles in the ensemble, and $k \leq i_{max} - 1$.

Usually, when the active size distribution is obtained with the use of an impactor, $g^0_a(r)$ is approximately described by the log-normal law. Then Eqs. (2) goes over into $\Phi(\xi) \approx [(1 + \Phi(\xi^0))/X] - 1$ for

$$\Phi(\xi) < \frac{2-X}{X} \text{ and } \Phi(\xi^0) < \frac{2(Y-X)}{Y-1} - 1, \qquad (3)$$

where $\xi^0 = (\log r - \log r^0_{ag})/\log \beta^0_g$; β^0_g is the standard geometric deviation of the distribution $g^0_a(r)$, and Y $= \frac{\sum_{i=1}^{i_{max}-1} g^0_{ai}}{g^0_{ai_{max}}}$ is the correction for the self-absorption for the cascade with the index i_{max} under the assumption that self-absorption is significant only for this cascade.

Solving Eq. (3) for r_{ag} and β_g for several pairs of values of r and real X, r^0_{ag}, and β^0_g, we find the mean (because of the approximate nature of Eq. (3)) value r_{ag} expressed in units of r^0_{ag}, $K = r_{ag}/r^0_{ag} = 2$-6 for X = 2-4.

The active mean geometric aerodynamic radius, determined with the use of the impactor without considering the corrections P and K is found to be underestimated by a factor of 4-12 for coarse-grained dusts. A comparison of the experimental data on the degree of fineness of α-active aerosols, obtained by autoradiography [7] and an impactor, confirmed the large difference in the results (see Table 1). The impactor was calibrated with inactive polydispersive aerosols with $\rho = 4$ g/cm^3. The countable size distribution for each cascade was found with an optical microscope; then the changeover to the weighted distribution $g_p(r)$ was made, from which r_{ag} was determined. The difference between the values of r_{ag} and r^0_{ag} is easily explained by the reasons stated above. After introducing the correction the data obtained by different methods coincided within the limits of accuracy of the computation and the experiment.

It is well known that with the use of an impactor it is not possible to sediment particles of sizes smaller than 0.4-0.8 μ in different cascades. However, even in fine, but polydispersive aerosols coarser dusts may be present which can split into fractions (their relative fraction is determined by η_g and β_g). As is shown by experience, for the log-normal active size distribution of homogeneous aerosol particles the limiting values of r_{ag} measured by inertial sedimentation is $r_{ag} = 0.1$-$0.5\ \mu$. In the majority of cases the standard geometric deviation is confined to the range $2 < \beta_g < 3$. The corresponding limiting values of countable mean geometric radii, computed from the relation $r_g = r_{ag}\beta_g^{-3 \log \beta_g}$, lies in the range $3 \cdot 10^{-3}$ to 0.1 μ. Hence the impactor can be used for the determination of the degree of fineness of fine-grained radioactive aerosols, if the type of asymmetry of the size distribution of the investigated particles is known beforehand.

The error in the computation of radiation charging depends strongly on the form of the curve of entrapment of the activity $K^t_a(r_{ag})$ in organisms besides depending on the accuracy of determination of r_{ag}. In this sense the curve $K^t_a(r_{ag})$ can be divided in three parts. For $r_{ag} < 0.1\ \mu$ impactors available at present are inapplicable. In the range $0.1\ \mu \leq r_{ag} \leq 1.5\ \mu$, $K^t_a(r_{ag}) \approx$ const at 20-30% and for $\bar{K} = 1$ the inaccuracy in the computation of K^t_a in using r^0_{ag} does not exceed 20-30%. If $\varphi = 12$, the error increases and for $r_{ag} > 0.5\ \mu$ it reaches several hundred percent. For $r_{ag} > 1.5\ \mu$ K^t_a changes from 20-30% to 0. Here the errors are of special significance.

In the investigated range of measurements of the corrections P and K, disregarding the errors in the determination of the degree of fineness of active dust involves an increase in the accumulation of α-active substances in living organisms by a factor of 2-10 when the estimation of the radiation hazard of inhaling coarse-grained aerosols is calculated according to the Morrow model.

LITERATURE CITED

1. P. Morrow, Health Phys., 12, 173 (1966).
2. K. Spurnyi et al., Aerosols [in Russian], Atomizdat, Moscow (1964), p. 130.
3. V. I. Bad'in, Gigiena i Sanitariya, No. 10, 52 (1969).
4. N. A. Fuks, Advances in the Mechanics of Aerosols [in Russian], AN SSSR, Moscow (1961), p. 54.
5. G. M. Parkhomenko et al., in: All-Union Scientific Technical Conference on Production and Use of Isotopes and Sources of Nuclear Radiation in the National Economy of the USSR [in Russian], Atomizdat, Moscow (1968), p. 73.
6. V. I. Bad'in, in: Science and Engineering News [in Russian], No. 4, Aerosols, TsNIIAtominform, Moscow (1969), p. 4.
7. V. I. Bad'in and R. Ya. Sit'ko, in: Dosimetric and Radiometric Techniques [in Russian], Atomizdat, Moscow (1966), p. 166.

STRUCTURE OF THE MAGNETIC FIELD IN THE TRIHELIX SATURN-1 STELLARATOR – TORSATRON MACHINE

V. S. Voitsenya, A. V. Georgievskii,
V. E. Ziser, D. P. Pogozhev, S. I. Solodovchenko,
V. A. Suprunenko, and V. G. Tolok

UDC 621.039.623

The trihelix Saturn-1 stellarator– torsatron plasma machine is designed for research on the properties of the magnetic field established with the aid of coils of different types external to the working volume, and for experimental verification of the effect of those properties on plasma containment.

The principal parameters of the machine (Fig. 1) are: intensity of longitudinal magnetic field under quasistationary conditions $H_0 \approx 6$ kOe; under pulsed conditions $H_0 \geq 10$ kOe; semimajor radius of toroidal helical winding R = 35.6 cm; semiminor radius a = 10 cm; number of periods of field m = 8.

The machine features two distinct operating modes: the stellarator mode and the torsatron mode, first suggested by Aleksin and later discussed by several other authors [1]. The system of the helical magnetic field is set up in the form of two autonomous windings connecting poles with the same current directions. In torsatron operation one winding is energized. The longitudinal magnetic field H_φ is established by a special winding (see Fig. 1). Depending on direction, it either adds to the longitudinal field $H_{\varphi hx}$ set up in the torsatron mode of the helical winding, or subtracts from that field. The ratio of these fields is given by the coefficient $K_\varphi = H_{\varphi hx}/H_0$, where $H_0 = H_{\varphi hx} + H_\varphi$. There are also windings employed to establish a magnetic field transverse to the plane of the torus; the compensating field H_{com} for the torsatron mode [1] and the correcting field H_{cor} for establishing the "magnetic well" [2]. The maximum inhomogeneity of the transverse field in the working volume of the machine is 5%.

This article discusses an experimental investigation of the stellarator magnetic surfaces in the torsatron mode. Magnetic measurements were taken at H_0 = 0.5 to 1 kOe over a wide range of k_φ measurements.

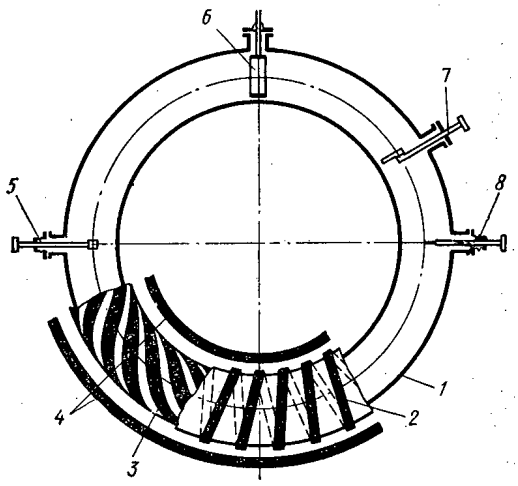

Fig. 1. Layout of Saturn-1 plasma machine in plan view: 1) vacuum chamber; 2) winding for longitudinal magnetic field; 3) helical winding; 4) winding for transverse magnetic field; 5) electron gun; 6) annular probe; 7) rotating probe; 8) local probe.

Translated from Atomnaya Énergiya, Vol. 31, No. 5, pp. 536-538, November, 1971. Original article submitted August 10, 1970.

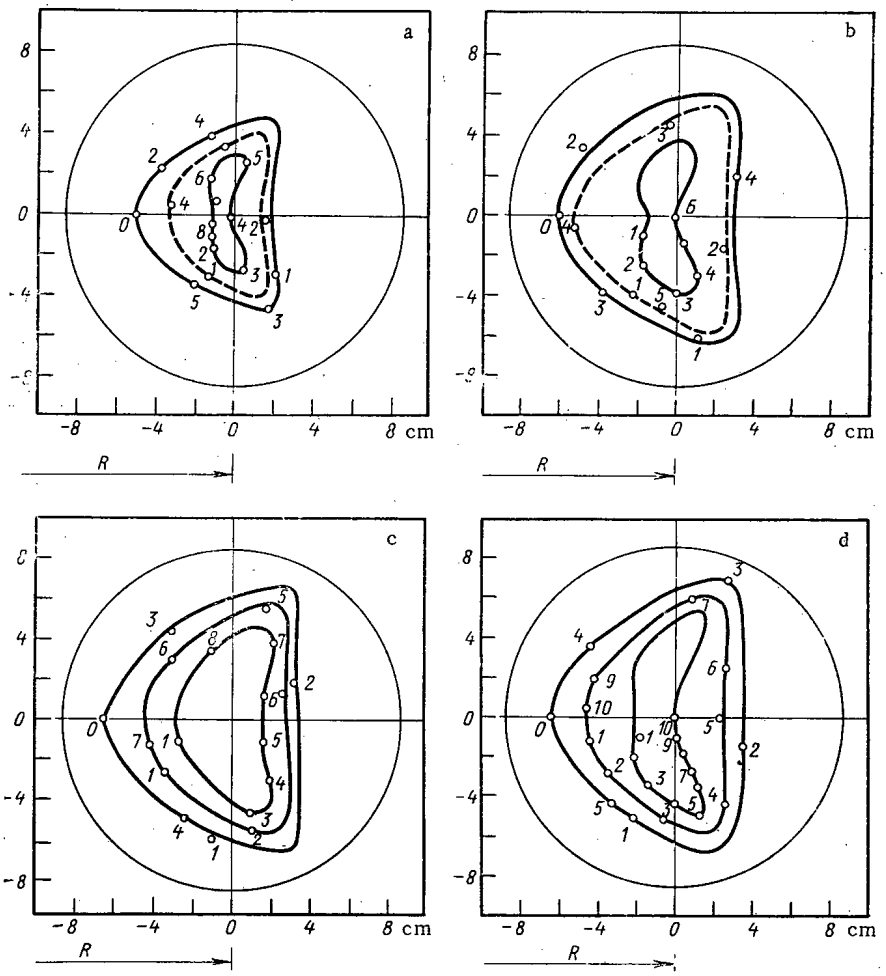

Fig. 2. Shape of magnetic surfaces for different k_φ values: numerals on surface give number (sequential) of revolutions of electron beam: R = 35.6 cm; a) $k_\varphi = 1.0$, $H_0 \sim 2$ kOe; b) $k_\varphi = 0.66$, $H_0 \sim 3$ kOe; c) $k_\varphi = 0.5$, $H_0 \sim 4$ kOe; d) $k_\varphi = 0.4$, $H_0 \sim$ kOe.

Low-energy (20 to 50 eV) electron beams [3] generated by an electron gun which was free to move radially in the horizontal and vertical directions were used in the investigation of the magnetic surfaces (see Fig. 1). The region within which the closed magnetic surfaces exist were determined from the signal picked up from the annular probe as the gun was moved about, and the shape and rotational transform angle i_0 were determined with the aid of the local probe and rotating probe, with the position of the electron gun held fixed.

The parameters of the measured magnetic fields were compared to the predicted parameters. The calculations were performed on a BESM-6 computer, with attention given to the toroidality of the machine and to the real distribution of the transverse magnetic field, with the poles of the helical windings specified in the form of an infinitely tenuous conductor carrying current.

The experimental investigations showed that there exist closed magnetic surfaces (closed over several tens of resolutions) in the stellarator–torastron plasma machine. Typical shapes of the measured magnetic surfaces for different k_φ values in the absence of correcting field are shown in Fig. 2. The theoretically predicted magnetic surfaces are plotted by the broken curves, for comparison. The average reduced radius r_0 of the experimentally derived extreme intact surfaces lie slightly higher, and the rotational transform angle i_0 lies below the corresponding predicted values on these surfaces. This is accounted for to a partial extent by the assumptions entertained in the calculations as to the current distribution at the pole.

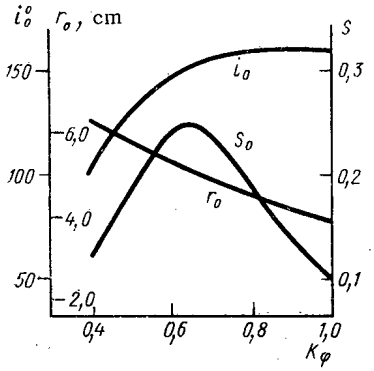

Fig. 3. Dependence parameters of magnetic surface in Saturn-1 plasma machine (r_0, i_0, S_0) on k_φ.

The rotational transform angle i_0 increases with increasing k_φ (Fig. 3) on the extreme surface inscribed in the chamber. When $k_\varphi \geq 0.6$, however, the value of i_0 remains practically unaffected, since the extreme intact magnetic surface is inscribed in the chamber at that point. As k_φ increases, the shear $S_0 = (di_0/dr_0) \cdot (r_0^2/2\pi R)$ at first follows suit and then attains a maximum $S_0 \approx 0.25$ at $k_\varphi = 0.6$, after which it begins to decline in response to the fall-off in r_0.

It was established experimentally that there exist closed magnetic surfaces with fairly high parameters ($i_0 \approx 0.9\pi$, $S_0 \approx 0.1$) in the limiting mode when the longitudinal field is established solely by the helical winding ($k_\varphi = 1$) (see Fig. 2 and Fig. 3).

The effect of the correcting magnetic field on the displacement of the center of the magnetic surfaces exterior to or interior to the torus, as a function of the direction of H_{cor}, was investigated. The displacement of the center, in excellent agreement with the predicted value, allowed us to estimate the size of the magnetic well or magnetic "antiwell" respectively. For instance, when $H_{cor} = 7.5\% H_{com}$ and when the former is directed opposite to H_{com}, a magnetic well $\approx 10\%$ results, and the depth of this well is practically independent of k_φ. Further experiments will enable us to determine the dependence of the size of the magnetic well and the dependence of the pattern of variation in i_0 and r_0 on the magnitude and shape of the correcting field.

LITERATURE CITED

1. C. Gourdon et al., Report CN-24/F-2, delivered to the III Conference on Research in the Field of Plasma Physics and Controlled Thermonuclear Fusion Reactions [in Russian], Novosibirsk (1968).
2. J. Taylor, Phys. Fluids, 8, 1203 (1965).
3. M. S. Berezhetskii et al., Zh. Tekh. Fiz., 35, 2167 (1965).

SUMMARY OF THE SECOND SYMPOSIUM OF COMECON MEMBER-NATIONS ON "RESEARCH IN THE FIELD OF REPROCESSING OF SPENT NUCLEAR FUEL"

A. F. Panasenkov and V. K. Tolpygo

The Seventies are typified by a great bound forward in the development of power on the basis of new principles: widespread utilization of the energy stored within the atomic nucleus.

At the present time all of the member-nations of the Council for Mutual Economic Aid [COMECON] are busy developing their nuclear power developmental programs. Some of these nations are already building or planning construction of nuclear power generating stations based around VVÉR type nuclear reactors. The reprocessing of spent nuclear fuel and the disposal of radioactive wastes, as well as the achievement of close collaboration between COMECON member-nations in this field, thereby acquire great importance. This collaboration is both important and imperative, since a comprehensive solution of the many problems in this area on many levels by any individual country would entail enormous economic and technical difficulties.

Reprocessing of irradiated nuclear reactor fuel is viewed as an economically justified venture at the present level of development of the nuclear power industry, and holds forth promise of great economic returns in the future: reserves of nuclear fuel are actually being increased by this option, volumes of radioactive waste are being contracted and safe storage of radioactive wastes facilitated, while fuel cycle costs become more manageable.

The COMECON permanent commission on the peaceful uses of atomic energy is devoting considerable attention to the reprocessing of spent fuel. It was reported at the VIII session of the permanent commission in 1965 that the outlook for broad development of nuclear power is related to an appreciable extent to how industry handles the task of fabricating and reprocessing nuclear reactor fuel elements. It was pointed out on that occasion that chemical reprocessing of nuclear fuel is mandatory, and is capable of reducing electric power generation costs by 10-15%, but that capital investment and operating costs for spent fuel recovery plants take up quite a large fraction of the cost budget in the construction of the first nuclear power stations.

The cost figures for reprocessing of spent fuel depend on the capacities of the plant and the load carried by the plant. For example, according to data reported at the IV congress of the European Atomic Forum [Euratom], a plant boasting a capacity of one ton uranium per day and operating at 100% load finds the total cost of the processing to be 55 dollars per kilogram of uranium. At the same time, a plant with a capacity of 5 tons uranium per day operating at load factors of 20, 50, 80, and 100% will find the total processing cost to be respectively 93, 40, 26, and 22 dollars per kilogram of uranium, i.e., the process cost dwindles by a factor of 2.5 as the plant capacity increases fivefold. This means that an economically competitive plant handling processing of spent nuclear reactor fuel should be designed for capacities of from 3 to 5 tons of uranium per day (or 900 to 1500 tons of uranium per year). Reprocessing plants in that range of capacities would handle the load coming from nuclear power plants incorporating VVÉR type reactors with output ratings from 27,000 to 45,000 MW(elec.).

In line with the work plan of the permanent commission for 1971-1972, a second symposium of COMECON member-nations was held on the topic "Research in the field of reprocessing of spent nuclear fuel," at Marianske Lazne (Czechoslovakia) in May 1971. The purpose of this symposium was to draw up the balance

Translated from Atomnaya Énergiya, Vol. 31, No. 5, pp. 539-541, November, 1971.

sheet for the work done by the various COMECON nations in 1969-1970 in accordance with the coordination plan of scientific and engineering research on reprocessing of nuclear powr of information on the status of work and achievements in this area.

The work of the symposium was contributed to by over 100 specialists from Bulgaria, Hungary, East Germany, Poland, Rumania, the USSR, Czechoslovakia, the COMECON secretrait, and a representative of IAEA. The symposium participants hear and discussed 55 reports touching upon reprocessing of spent fuel by aqueous and nonaqueous methods, nuclear fuel recovery costs, radioactive wastes disposal, and analytical work. The principal topics relating to the overall problem of nuclear fuel recovery and reprocessing were thus reflected in the symposium agenda.

Solvent-extraction (aqueous) methods and flowsheets for fuel reprocessing are, as demonstrated by the symposium reports, presently the basis of technological processes in almost all the industrial plants now on stream or being designed for service in the immediate future, in reprocessing of spent fuel from thermal reactors. The development of these methods is characterized, on the one hand, by research work aimed at improving the technology and cost picture of reprocessing of fuel with low-level and medium-level burnup, and on the other hand, by the steadily increasing volume of research aimed at uncovering possibilities for the utilization of aqueous process methods in recovering fuel with a high percentage of burnup and short cooling time, i.e., fuel from fast reactors.

In the opinion of the participants of the symposium, reprocessing of high-burnup fuel will most likely be carried out in the immediate future by aqueous methods, after some modifications at the head-end and tail-end stages necessitated by the amount of heat given off and by the large quantity of plutonium and fission products, and also involving the use of centrifugal extractors with short phase contacting times, which will make it possible to shorten the time required to complete the extraction process by 30 to 50 times the duration of the process when relying upon gravity-dependent equipment.

Papers submitted by representatives of the USSR and Czechoslovakia on verification of solvent–extraction technologies in spent fuel recovery evoked considerable interest on the part of the symposium participants. These flowsheets offer some general solutions which include handling of tail ends in the preliminary stages, cutting fuel assemblies into small pieces, dissolving fuel without first dissolving the fuel-element cladding and structural materials of fuel assemblies. Tributylphosphate in diluents is employed as the solvent-extraction agent for purifying the uranium and preliminary purification of the plutonium present.

At the same time, these flowsheets present some special features of their own, the main difference residing in the type of diluent used on the extracting solvent.

In the flowsheet presented by Czechoslovak specialsts, an oxygen blow is used to aid the dissolution of the fuel elements, and fluorine ion is added to the extraction step in the preparation of the solutions, for the purpose of eliminating any formations at interphase contacts, and n-dodecane with a flash point of +74°C is employed as diluent for the tributylphosphate. One extraction agent is employed to purify the uranium and plutonium, but two extraction cycles are provided for in combined purification of uranium and plutonium followed by separation of the two elements in the second cycle. Furthermore, another cycle is added to the process for definitive purification of the uranium and plutonium. The flowsheet also provides for isolation of neptunium, production of oxides of uranium and plutonium, and production of concentrates of the transplutonium elements; but there is no technology for reprocessing waste slurries or high-percentage recovery of the extraction solvent.

A flowsheet providing for utilization of noncombustible diluent (carbon tetrachloride) was presented by the USSR delegation, with provisions for raising the degree of dissolution of the fuel elements treated, destruction of organic plasticizers in the fuel, and distillation of ruthenium tetroxide with the aid of a mixture of ozone and oxygen blown through the process stream. Preliminary purification and separation of uranium from plutonium and neptunium are handled in the first cycle. A second extraction cycle with subsequent denitration and a single cycle for purification and separation of plutonium and neptunium are provided for as means of isolating standard grade uranium. A single extraction solvent is used, the final purification step for the plutonium and neptunium being carried out by a method involving sorption on highly basic anion exchange resin beds.

Reprocessing of waste process solutions after intensive concentration by evaporation is handled by control extraction for the purpose of preextraction of the valuable components in the stream and for producing concentrations of the transplutonium elements and fission products. Plutonium dioxide and neptunium

dioxide are obtained by precipitating the oxalates and calcining them. The extraction solvent is recovered in high percentages.

USSR specialists also presented a flowsheet utilizing synthine as diluent.

A surfactant is added to the filtered slurry in order to reduce the amount of formations at interphase contacts. Preliminary purification and separation of the uranium, plutonium, and neptunium are designed into the first step in the process. The organic phase containing uranium is scrubbed with a solution of sequestrant. Two more solvent extraction steps bring about complete purification of the uranium. The uranium back-extract is processed with hydrazine solution at temperatures of 80-90°C upstream of the second and third steps in the process. The extracting agent used for uranium extraction is a 25% solution of tributylphosphate in synthine. Two solvent extraction steps for plutonium and one step for neptunium, utilizing trialkylamine as diluent, are designed for the final purification and separation of the plutonium and neptunium. The plutonium dioxide is isolated by a denitration technique, while the neptunium dioxide is isolated by oxalate precipitation followed by calcining.

Processing of process effluents is handled by evaporation and control extraction for the purpose of making a complete extraction of the valuable elements, and also obtaining concentrates of the transplutonium elements and fission products. High-percentage recovery of the extracting solvent is not provided for.

The process flowsheets in question make it possible to reprocess spent fuel elements from VVÉR type reactors with end-products meeting exacting requirements, after appropriate improvements and finishing touches to the process.

Results of the discussion at the symposium demonstrated that solvent extraction methods for reprocessing spent reactor fuel are far from exhausted, and that there are still lots of opportunities for improving solvent-extraction methods. Some promising directions to take note of are:

compressing subsidiary operations through improved understanding of the chemical mechanisms underlying the process;

the use of reagents acting to contract the volume of wastes and effluents, e.g., the use of quadrivalent uranium in the recovery of plutonium. This calls for the study of the possibility of producing quadrivalent uranium directly in the extraction equipment by means of electrolytic reduction;

selection of new extraction solvents;

use of catalysts;

improvements in extraction process equipment, to the extent that batch production of equipment items becomes possible;

study of radiolysis of extracting solvents and of the effect exerted by radiolysis products on the reprocessing of spent fuel;

study of ways to lower the cost of solvent-extraction reprocessing of spent fuel, particularly as a result of the isolation of fission-fragment elements, an approach which has been finding many applications in chemical engineering (in the production of such fragments as neptunium, americium, technetium, etc.).

The development of extractors with short phase contacting times lends added interest to the study of the kinetics of the process with greater thoroughness, in addition to studies of the equilibrium state.

Problems pertaning primarily to fluoride volatility techniques in spent-fuel reprocessing are being studied, as the symposium showed, in the field of reprocessing of spent fuel by nonaqueous methods. Work along these lines is being pursued in the USSR and in Czechoslovakia.

Impressive success has been attained in the development of a technology utilizing that method, and in developing the requesite process equipment. Decladding of fuel elements by a meltdown technique followed by subsequent fluorination of the uranium dioxide in the declad meat is being studied in the USSR in a scaled-up laboratory unit. The burden of this research is directed toward studies of the properties of some of the fluorides of uranium, plutonium, and fission products, and also toward studies of the mechanism operative in decladding stainless steel fuel elements.

We learn from the materials presented at the symposium that certain technological operations, such as ridding uranium hexafluoride and plutonium hexafluoride of certain volatile fluorides (NpF_6, TcF_6, RuF_5), and concentrating of plutonium hexafluoride, have been given inadequate attention in the past period.

Discussion on the reports on spent fuel reprocessing costs revealed that systems analysis has to be developed and used in order to arrive at selection of the optinum variant, not only for recovery of spent fuel, but for the entire fuel cycle as a whole.

Analysis shows that the problem of transporting irradiated fuel has many ramifications, extending onto an international plane. In the opinion of the participants of this symposium, favorable conditions have now been brought about for beginning a study, within the COMECON framework, on the technical, economic, and production regulations and standards that will be necessary to future collaboration of the COMECON nations in this area.

The development of the nuclear power industry has posed a very intricate problem before the investigators, in terms of the reprocessing and disposal of radioactive wastes of different levels of activity. Generation of electric power to the extent of 1 MW per year, as a unit, means an average concomitant yield of 1 kg of fission products, and each kilogram of fission products will yield several hundred kilocuries of activity, even after five or six months of exposure before reprocessing. Considerable attention was given to this important topic at the sympoisum.

Soviet scientists consistently proceeded from the point of departure that dumping of effluents is permissible only after the content of radioactive isotopes has been brought down below the level of critical permissible concentrations, by appropriate separation techniques. The method of dilution to those concentration levels is inadmissible, since this would destroy the radioactive nuclides to be dumped, and the total quantity of radioactive nuclides would not be decreased thereby.

The need for selective isolation of radioactive nuclides (and especially long-lived ones) from high-level wastes, as well as the need to shorten the storage time of radioactive nuclides, while salvaging valuable emitters from these wastes, was emphasized. The use of inorganic sorbents for those purposes has made it possible to bring this method to the stage of pilot-facility testing.

The need to shorten the storage time of high-level liquid wastes led to an intensive study of the feasibility of immobilizing liquid high-level wastes in molten glasses, basalt, and bitumen. Trapping of radioactive wastes in bitumen, at specific activities upwards of 1 Ci/liter, was found to be quite feasible. It was shown that more work has to be done on immobilization and long-term storage of high-level wastes within the framework of studies of the fuel cycle as a whole.

In evaluating the overall preliminary results of the symposium, we may point out that interest and direct involvement in recovery of irradiation fuel on the part of COMECON member-nations has increased perceptibly in recent years. The share of technologically oriented work and study in this area has increased concomitantly.

At the present conjuncture, investigations aimed at improving the industrial technology of spent fuel reprocessing, and improving information exchange and contacts between scientific cadres of COMECON member-nations, have been acquiring added significance.

As the symposium materials demonstrate, efforts have to be concentrated on the development of equipment technology and cost studies, and maximum use will have to be made of the scientific research capabilities of the COMECON member-nations in this area, and on improving the coordination of work and projects between individual science organizations participating in this research.

COMECON NEWS BRIEFS

A coordination conference of specialists of COMECON member-nations was held in Moscow in July 1971. The purpose of the conference was to prepare a draft program of work on the topic "Development of nuclear equipment based on integrated circuitry and hybrid-film circuitry." Reports were heard on work being done in that field under the auspices of the permanent COMECON commission on the radio and electronics industry (KRÉP), on a series of integrated circuits being fabricated in the USSR, and on proposals put forth by the Soviet KRÉP delegation to expedite the use of radio and electronics equipment in COMECON member-nations' joint research projects, on the status of development and research work on nuclear physics equipment based on integrated circuits and thin-film circuits in COMECON member-nations. A draft program for collaboration of COMECON member-nations in this area was worked out at the conference, and appropriate proposals were advanced for discussion at the next regularly scheduled session of the work team on nuclear instrumentation.

A conference of specialists of COMECON member-nations on nuclear medicine was held in Budapest in September 1971. The conference discussed and prepared drafts of work plans for discussion at the sessions of the work team on nuclear instrumentation, on particular problems under the heading "Development of procedures and instruments for nuclear medicine." Proposals on applications of electronic computers to processing of the results of nuclear medical measurements were worked out, as well as a draft program on improved training of specialists in that area. The Hungarian delegation informed the participants of the conference on the progress of work toward arranging joint work by COMECON member-nations on the development of scintillation γ-ray chambers for radiation diagnostics.

The 22nd session of the work team on nuclear instrumentation, held in Mamaia (Rumania) in September 1971, discussed the compiling of a list of nuclear reactor monitoring and control instruments manufactured in COMECON member-nations, discussed the results of work done under the heading "Development of dosimetric and radiometric equipment for monitoring the radiation characteristics of nuclear reactors," heard reports on the varied assortment of detectors of ionizing radiations and photomultipliers used in nuclear instruments fabricated and used in the COMECON member-nations, and on the status of development and performance levels of those components, went on to discuss 15 plans of recommendations on standardization, approved a draft program for collaboration over the 1971-1973 period in the area of "Development of nuclear instrumentation based on integrated circuitry," a work plan drafted on the topic "Development of procedures and instruments for nuclear medicine," and the draft plan of work to be undertaken by the permanent commission in the field of nuclear instrumentation during 1972, including work on standardization of equipment and components. The work team prepared proposals on all of these topics for placement on the agenda of the XXI session of the permanent commission which is scheduled for November 1971.

A conference of specialists of COMECON member-nations on radiation shielding work was held in Prague in September 1971, and discussed topics concerning the design of custom-tailored and standard process equipment and accessories for use in glove boxes and hot caves in work with radioactive materials and irradiated materials, specialized production and coordinated cooperative production of equipment and accessories, coordination of scientific research work and design and planning work, and work on standardization of specialized lines of production. The conference discussed proposals put forth by the various delegations on collaboration in the field of radiation shielding practice, and approved the draft plan for collaborative efforts in this field.

Translated from Atomnaya Énergiya, Vol. 31, No. 5, p. 541, November, 1971.

THE OPENING OF THE KURCHATOV MEMORIAL

V. V. Anufrienk

A memorial to Igor Vasil'evich Kurchatov was opened in Moscow on September 20, 1971. It is situtated in Kurchatov square opposite the Institute of Atomic Energy (IAE).

The IAE was organized by I. V. Kurchatov in 1943 after his appointment as the scientific director of investigations on the subject of uranium. From this time until his death in 1960 Igor Vasil'evich was director of the IAE and scientific director of atomic energy research conducted in the Soviet Union. He lived on the premises of the IAE.

It was at the IAE that physical investigations of the problem of chain fission reactions were started as early as during the war. In 1946 the first nuclear reactor in the eastern hemisphere was built and put into operation. Under the direction of I. V. Kurchatov nuclear weapons were produced and the development of the first peaceful uses of nuclear power in the Soviet Union was started within a short time. In the last years of his life he greatly expanded the area of research on controlled thermonuclear reaction.

Addressing the assemblage Academician M. V. Keldysh the President of the Academy of Sciences of the USSR said: "Today we are unveiling a memorial to the greatest Soviet scientist, one of the most eminent physicists of our time, a government and social worker, and an organizer of science."

After the introductory speech from V. N. Yagodkin the secretary of the Interdepartmental Geophysical Committee of the Communist Party of the Soviet Union the meeting was addressed by the vicepresident of the council of Ministers of the USSR, Academician V. A. Kirillin, the Chairman of the State Committee of the Council of Ministers of the USSR for Science and Technology, E. V. Ostashev, the leading foreman of the Institute of Atomic Energy, and A. P. Aleksandrov, the director of the IAE.

During the unveiling ceremony, Kurchatov square and the balconies of the nearby houses were filled with people. Among them were many of his friends and students, staff members of the IAE and of other institutes, enterprises and institutions, carrying out work in the field of atomic energy. They well

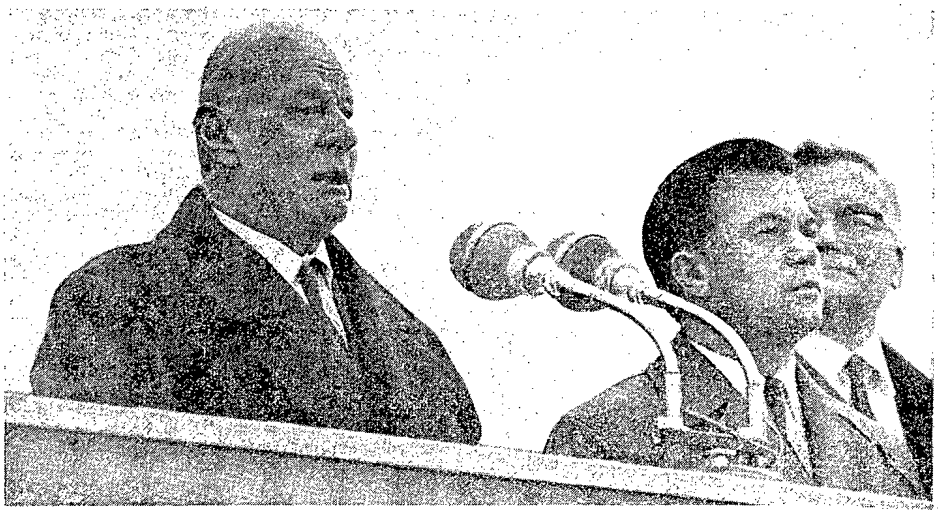

Academician A. P. Aleksandrov speaking at the meeting of the I. V. Kurchatov Institute of Atomic Energy.

Translated from Atomnaya Énergiya, Vol. 31, No. 5, pp. 542-543, November, 1971.

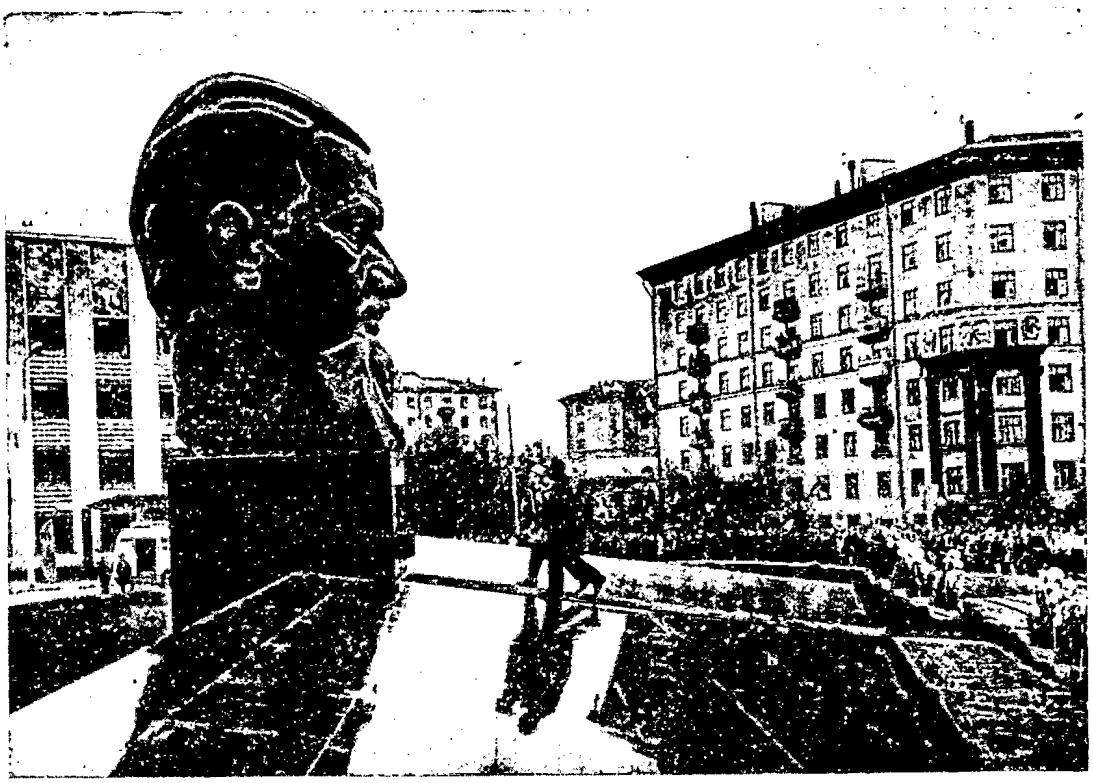

Laying wreaths at I. V. Kurchalov memorial. Photo A. I. Mel'gunov

remember restless, dynamic, and purposeful Igor Vasil'evich more as a jovial and humorous person and not stern as depicted in the memorial.

The editorial staff of the journal remembers Igor Vasil'evich with special pride as one of the main founders of the journal.

TWENTYFIVE YEARS OF THE PHYSICOPOWER INSTITUTE

V. V. Anufrienk

The Physicopower Institute was founded in Obinsk in 1946.

In 25 years the Physicopower Institute (PPI) has developed into a large scientific center ensuring, with the cooperation of adjoining organizations, the development of important projects in atomic science and technology in the USSR.

The PPI developed unique experimental complexes for investigations in the field of low-energy nuclear physics, reactor physics, thermal physics, materials science, and also test installations with thermal- and fast-neutron reactors. This enabled the PPI, together with other institutes and structural and design organizations, to work out projects for a whole series of atomic power stations.

In 1951, on the initiative of I. V. Kurchatov, it was decided to construct the first atomic power station in the world.

The PPI played a considerable part in the development of this station. This atomic power station with a capacity of 5000 kW was designed, built, and put into operation in 1954.

The operation of the first atomic power station in the Soviet Union and the world was an important event which was widely applauded by the entire world. The first atomic power station in the world went into the history of science and technology as the pioneer in the new field of power production, and atomic power engineering, which is of the utmost importance to humanity.

With the experience of the development of the first atomic power station the scientists of the PPI made a large contribution to the design of two blocks of the I. V. Kurchatov Beloyarsk atomic power station. Nuclear heating of steam on an industrial scale was accomplished for the first time in Beloyarsk atomic power station. The staff of the PPI also participated in the design of Bilibinsk atomic thermal power station intended for supplying electricity and heat to the mining enterprises and the housing blocks in Bilibino on the Chukotsk semipeninsula.

Work on the portable power station TES-3 was started in 1956 under the guidance of the PPI. The station was put into operation in 1961. In 1963 investigations were instigated on the development of an improved block-type atomic power station "Sever" for supplying electricity and heat to different regions of the country.

Another project, which has become the main project of the PPI during the last 15 years, covers work on fast reactors and liquid-metal heat-transfer agents. Investigations in these two related fields of atomic engineering were started in the late forties.

In 1954-1955 the results of the investigations on the first fast reactor BR-1 led to a complete confidence in the large coefficient of reproduction of nuclear fuel in fast-neutron reactors. An experimental fast-neutron reactor BR-5 was put into operation at the PPI in 1959. The data obtained on this reactor served as the basis for constructing and starting the experimental reactor BOR-60 at Melekess in 1970.

In the past years several fast-neutron reactors were designed for atomic power stations. At present, preparations are being made for launching the first industrial atomic power station with a fast-neutron reactor in the Shevechenko Gur'evskii region. The reactor is intended to be used for the generation of electric power and distillation of sea water. The third block of Beloyarsk atomic power station with an industrial fast-neutron reactor (having a capacity of 600 MW) has been designed and its construction is in progress. Fast-neutron reactors with a capacity of more than 1000 MW are being designed.

Translated from Atomnaya Énergiya, Vol. 31, No. 5, pp. 543-544, November, 1971.

The PPI marks its twentyfifth anniversary after the XXIV Congress of the Communist Party of the USSR. The resolutions of the congress not only restressed the significance of the development of science and scientific-technical progress but also designated an accelerated development of science and technology and a full utilization of their results in the USSR economy as one of the central problems of our society. The congress set forth specific tasks for scientists, putting emphasis on nuclear power engineering and, especially, the industrial utilization of fast-neutron reactors. Having participated in the preparation of the nuclear power engineering program, adopted by the congress, the PPI is now participating in its realization.

In parallel with the solution of practical present-day problems of atomic power engineering, the PPI carries out long-term research work, investigates fundamental problems of nuclear physics, reactor physics, thermal physics, materials science, chemistry, radiochemistry and so forth. The results of numerous investigations carried out at the PPI go beyond the realm of nuclear power engineering and are widely applied in other branches of science and technology.

V INTERNATIONAL CONFERENCE ON MAGNETOHYDRODYNAMIC POWER GENERATION

Yu. M. Volkov

The V International Conference on the Magnetohydrodynamic (MHD) method of generation of electric power was held in Munich in April 1971. Delegates from 25 countries and two international organizations were present at the conference. The conference was divided into three-sections: closed-cycle plasma MHD systems, open-cycle plasma MHD systems, and liquid–metal MHD systems.

The papers on closed-cycle plasma MHD generators, which represent MHD converters of thermal energy into electrical energy operating with nonequilibrium plasma of inert gases with easily ionizable impurities of alkali metals, dealt mainly with the problems of nonequilibrium plasma physics, gas-dynamics of the flow of such a plasma in MHD channels, plasma diagnostics, and the operation of experimental equipment. Designs of MHD power stations with a nuclear reactor as the energy source were also discussed and the corresponding economic estimates were given.

It should be mentioned that there is a noticeable increase in activity in this field compared to the previous conferences (Salzburg, 1966; Warsaw, 1968). This is apparently due to a better understanding of nonequilibrium plasma, especially of phenomena such as the different nature of instabilities and their effect on the electrophysical properties of a low-temperature plasma. Thus, in the paper entitled "Nonlinear phenomena in plasma related to ionization instability" by A. M. Dykhne (USSR) the development of ionization instability was investigated in detail and the state of the plasma with regular, finite amplitude, density waves as well as with well-developed turbulence was discussed at length; methods of determining the electrical characteristics of such a plasma are also suggested.

In the paper entitled "Faraday type MHD channel with essentially nonequilibrium plasma" by V. S. Golubev, M. M. Malikov, and A. V. Nedospasov (USSR) it was shown experimentally that despite the presence of strongly developed instability in a supersonic stream of nonequilibrium plasma in a magnetic field, it is possible to obtain specific generated power of the order of 100 W/cm^3, which corresponds to ~10% efficiency of conversion of thermal energy of the plasma stream into electrical energy.

In the paper entitled "Investigation of nonequilibrium MHD plasma under the condition of complete ionization of the impurity" by T. Nakamura and V. Redmuller (FRG) it was shown that in accord with the predictions of theory, the nonequilibrium plasma remains stable for complete ionization of the small alkali metal impurity (10^{-3}%); the effective Hall parameter can attain a large value (~5). Their estimates show that a MHD generator with turbulent plasma completely ionized small impurity can have parameters close to those of an MHD generator with turbulent plasma.

Thus, the more detailed study of the nature of nonequilibrium plasma carried out in the past few years, has shown that the presence of essentially unstable states of the plasma in the range of parameters, that are most suitable for efficient MHD generation, is not an insurmountable obstacle as was earlier believed.

In the review papers of M. A. Hoffman (USA) and T. Bon (FRG) and also in the joint papers of E. Bertolini and M. A. Hoffman (USA), E. Salpetro and R. Toski (Italy) designs of MHD stations with nonequilibrium MHD generators were discussed. The results of these papers show that for an exit temperature of 2000°K from the nuclear reactor and the pressure of the inert gas in the reactor equal to 10-30 atm an installation with turbulent plasma could be made which would ensure (in combination with a low-temperature steam station) a total cycle efficiency not less than 50%. However, it should be mentioned that these and other similar estimates are of a provisional nature, since they do not include a detailed study of the individual units of the equipment (including also the high-temperature nuclear reactor).

Translated from Atomnaya Energiya, Vol. 31, No. 5, pp. 544-545, November, 1971.

The progress in the development of high-temperature gas-cooled reactors in the USA (Prof. S. Vey of Westinghouse) and in the FRG (Dr. R. Foster, Nuclear Center at Ulich) was reported in the form of brief communications at the "round table" meeting. According to the assertions of the authors the corresponding programs of the USA and the FRG may serve as prototypes for developing nuclear sources of fuel for MHD stations.

In the section on "open-cycle plasma MHD systems" problems related to the development of MHD power stations operating on combustion products of hydrocarbon fuel (equilibrium plasma) were discussed. Considerable attention was devoted to experimental investigations of MHD equipment with high specific parameters (papers by V. A. Kirillin et al. (USSR), O. Sonju and J. Tino (USA), J. Dicks et al. (USA), R. Bunde et al. (FRG), D. G. Zhimernin et al. (USSR)), long-range development of peak stations (papers by A. E. Sheindlin et al. (USSR), A. Kantrovich and R. Rosa (USA)), and commercial stations (papers by U. Mori (Japan), S. Vei (USA), T. Bon (FRG), F. Chelsa and V. Jackson (USA) et al.).

The use of strong magnetic fields, plasma with large conductivity, and MHD channels with optimum profiles permits obtention in the investigated systems specific power up to 0.5-0.7 MJ/kg from unit mass flow of the combustion products and ~100 W/cm^3 from unit volume of the channel (O. Sonju and J. Tino).

The relative simplicity of the open-cycle MHD generator and small capital expenditure needed for constructing an MHD station makes the use of such MHD systems highly promising as peak stations covering short-period overloading in industrial consumption of the electrical power.

Further analysis of the designs of industrial MHD stations substantiate the strong dependence of the total efficiency of such stations operating on natural fuels, on the temperature of preheated air which acts as the oxidant in the fuel combustion chambers . The efficiency, which is dependent on this temperature, may vary within the range 45-60%.

In the section which dealt with liquid-metal MHD systems much attention was given to the discussion of the processes of dispersal of the operating substance, the schemes of the MHD equipment, and prospective economic estimates of different MHD systems.

The conference demonstrated that in recent years important results have been obtained in the field of MHD conversion of thermal energy into electrical energy; these results are of great interest for further development of this field of science and technology.

III INTERNATIONAL SYMPOSIUM ON RADIATION CHEMISTRY

A. K. Pikaev

The III International Symposium on Radiation Chemistry was held at Balatonfured (Hungary) in May 1971. About 200 specialists from 19 countries, including 50 from the Soviet Union, participated in the symposium. The topics discussed included: radiation chemistry of polymers, organic substances, and aqueous systems. One hundred and forty five papers were presented and discussed. The proceedings of the symposium will be published in the form of a book.

Radiation Chemistry of Polymers. The papers on this topic dealt mainly with radiation polymerization and modification of polymer products with the use of radiation induced copolymerization.

K. Shneider et al. (FRG) presented the results of investigations on the effect of the α-olefin structure on the course of reaction of copolymerization with vinylidene fluoride. Their results on the formation of 4 : 1 polysulfones in copolymerization of vinylidene fluoride with sulfur dioxide are interesting. The paper by T. O'Neil (Switzerland) was devoted to radiation emulsion polymerization of vinylacetate in equipment operating in a semicontinuous regime. It was found that in this case the radiation does not introduce any specific feature in the polymerization process and in respect of its properties the polymer thus formed is similar to polymers synthesized in ordinary systems. L. Kish and S. Polgar (Hungary) presented results on copolymerization of acrolein and acrylonitrile in urea channel complexes, obtained for the first time. L. Khodkevich and I. Mladenov (Bulgaria) presented a paper on the radiation–chemical method of preparing copolymers from latex, and discussed the results of investigations into the modification of polyvinylchloride (PVC) by natural rubber on irradiating a mixture of the latexes of these polymers. It was shown that addition of rubber to 10% in PVC appreciably increases its specific strength. Several papers (D. Hardy et al., Hungary, J. Metz, USA, A. Shapiro et al., France) were devoted to the characteristics of solid-phase polymerization of monomers. The papers presented by the staff members of the Institutes of the Academy of Sciences of the USSR and the L. Ya. Karpov Institute generated great interest and lively discussions.

Despite the large practical significance of investigations of radiation cross-linking of polymers, the papers in this field were relatively few and tended to deal with specific problems. On the other hand, in other fields of the use of ionizing radiation for modifying materials several interesting papers were presented. The papers on the synthesis and properties of wood–plastic and concrete–plastic materials merit attention.

In the paper by K. Singer and P. Dalager (Denmark) the production of wood–plastic materials with the use of electron radiation was discussed. Thin veneers (thick ~4 mm) were impregnated with monomers or monomer–polymer mixtures, and treated (these veneer sheets were intended for making parquet flow covering and for use in finishing work). It was shown that electron accelerators permit the organization of continuous production and in this case the manufacturing process is safer and more economical than with the use of γ-irradiation of ^{60}Co. The authors achieved an intensification of the process by impregnating the wood with monomer–polymer mixtures at high pressure (up to 10 atm). The second paper by K. Singer et al., was devoted to concrete–plastic materials. It presented the results of investigations of the tensile and compressive strengths of concrete compounds impregnated with various vinyl monomers and their mixtures. Polymerization was effected by an irradiation method. It was found that the largest increase in the strength (about 2-2.5 times) is achieved in the case of a styrol–acrylonitrile mixture (composition 6 : 4).

M. Hotoda (Japan) presented a paper on hardening of diallyl phthalate monomer–polymer mixtures on asbestos slabs by electron irradiation. The asbestos sheets prepared in this way are distinguished by high

Translated from Atomnaya Énergiya, Vol. 31, No. 5, pp. 545-547, November, 1971.

impact strength and resistance to solvents and alkalies. They have a pretty surface and are weather-resistant, which makes them suitable for use as lining material in construction.

Radiation Chemistry of Organic Systems. The papers in this branch of radiation chemistry were devoted to general theoretical problems, the nature and characteristics of intermediate products of radiolysis, radiolysis of certain specific systems, and radiation–chemical synthesis. Different physicochemical methods were used for elucidating the mechanism of radiolysis transformation: pulsed radiolysis, electron paramagnetic resonance, methods of luminescence and electrical conductivity, and so forth.

L. Christofer (USA) gave a review of the experimental results on the capture of low-energy electrons by molecules of various kinds. Christofer formulated a general mechanism of the process including the formation of primary negative ions in the excited state, whose life-time depends on the properties of the molecule. Three ranges of the life-time of these ions were investigated: 10^{-15} to 10^{-12} sec, 10^{-12} to 10^{-6} sec, and more than 10^{-6} sec. The last case is typical for polyatomic molecules having fairly high electron affinity. In the first case the molecule may have a very small electron affinity or, may even exhibit a repulsive effect. The paper by R. Shindler (FRG) on the rates of reaction of almost hot electrons with SF_6, CCl_4, and C_7F_{14} deals with this topic.

The problems of pulsed radiolysis of organic systems were discussed in three papers by Soviet scientists. N. A. Bakh et al., presented a paper on pulsed radiolysis of alkyl ketones, while A. V. Vannikov et al., presented a paper on the investigation of charged particles in organic liquids by pulse methods. In the paper by A. K. Pikaev et al., the properties of solvated electrons in irradiated liquid methyl alcohol were discussed.

The paper by I. Ito and I. Tabata (Japan) devoted to a study of the characteristics of interaction of positronium with organic substances, should also be noted. An interesting conclusion made in this paper is that with the aid of positronium it is possible to study the distribution of a solute in a stable matrix.

The problems of radiolysis of specific organic substances were discussed in many papers. In particular, seven papers on radiolysis of different hydrocarbons and their mixtures were presented by Hungarian scientists. Radiation–chemical synthesis was discussed mainly in papers by Soviet scientists (principally by the staff members of the L. Ya. Karpov Physicochemical Institute). The one paper on this subject presented by a foreign scientist dealt with radiation–chemical oxidation of ethylbenzene (E. Krė et al., Hungary). The results of an analysis of dosimetric systems were presented in several papers. For example, P. Heringer et al. (Austria) proposed using the process of the formation of CF_4 in the radiolysis of perfluorocyclohexane for the dosimetry of compound radiation of a nuclear reactor.

Radiation Chemistry of Water and Aqueous Solutions. The papers touched on the general problems of the mechanism of aqueous solutions in stationary conditions, pulsed radiolysis, radiolysis transformation in aqueous solutions of biologically important substances, and radiolysis of frozen aqueous solutions. Numerous problems were discussed: the mechanism of formation of molecular hydrogen (L. T. Bugaenko et al., USSR), isotope effects in the radiolysis of water (I. Draganich et al., Yugoslavia), effect of linear energy transfer (G. Pusho, K. Ferradini et al., France, K. Kendal et al., Great Britain), the mechanism of radiolytic transformations in aqueous solutions of formaldehyde and glyoxylic acid (V. Markovich, Yugoslovia and K. Segested, Denmark), iodide ions (L. Boter and E. Krė, Hungary), azide ions (I. Kralich, France), silver ions (M. Khaisinskii, France), ethylene glycol in the presence of iron ions (L. I. Kartasheva and A. K. Pikaev, USSR), etc. In some papers the pulsed technique was used for elucidating the nature and properties of short-lived intermediate products in the radiolysis of aqueous solutions. For example, R. Koster and K. Asmus (West Berlin) investigated the radiolysis of aqueous solutions of halide-derived unsaturated hydrocarbons by this technique and found that the attachment reaction of the OH radical in double bond is controlled by diffusion and is accompanied by the detachment of a hydrogen chloride molecule. Of the papers on radiolysis of aqueous solutions of biologically important substances the paper by G. Adams, K. Kendal, et al., (Great Britain), devoted to electron transport in enzyme solutions, is of special interest. Radiolytic transformations in frozen aqueous systems were discussed in the papers of V. I. Gol'danskii et al., USSR (on loss of electrons entrapped in alkaline ice at low temperatures by the tunnel mechanism), I. Kro and Ch. Stradovskii, Poland (on stabilization and kinetics of the loss of electrons in alkaline solutions), S. A. Kabakchi et al., from USSR (on temperature dependence of the optical characteristics, and the kinetics of loss of mobility of charged particles in ice).

As is seen from the symposium results, in radiation chemistry the interest in the fundamental problems of chemical action of ionizing radiation (role of electrons, ions, and excited states in radiolysis, nature and properties of intermediate products of radiolytic transformations including their reaction properties and so forth) has not diminished. Moreover, the symposium demonstrated the growing interest in applied problems of radiation chemistry; one of the most important directions in this respect continues to be radiational modification of materials (primarily polymers) and also radiation polymerization.

II INTERNATIONAL COMPARISON OF ACCIDENT DOSIMETERS

V. A. Knyazev

The second international comparison of accident dosimeters used in different countries for estimating the exposure to radiation of personnel in accidents, was carried out in May 1971. According to the recommendations of the meeting of experts, organized by the IAEA in February 1969 [1], photographic films, thermal and photoluminescent dosimeters are used for measuring γ-radiation dose; for estimating neutron dose, as well as activated materials whose dose sensitivity depends strongly on the form of neutron spectrum [2], track detectors with a gang of fission materials are used, which enable one to determine the dose and spectrum of neutrons both in air and on the surface of the phantom. It should be mentioned that the experts recommended that doses of γ-radiation and neutrons be expressed in rads.

The first international comparison of accident dosimeters was carried out at Valduc (France) in June 1970 using the homogeneous reactor CRAC [3]. The analysis of the data on the distribution of flux

TABLE 1. Results of Seventh Comparison of Accident Dosimeters (July 1970, Oak Ridge, mean of all measured values)

Pulse number	Energy release fission/pulse	Thickness and material of shield	Neutron dose D_N, rad	γ-radiation dose D_γ, rad	$D_N/D^*\gamma$
1	$7{,}64\cdot10^{16}$	without protection	310±5%	44,8±9%	6,8±9%
2	$5{,}15\cdot10^{16}$	12 cm. organic glass	42,6±17%	33,7±16%	1,42±37%
3	$7{,}16\cdot10^{16}$	12 cm, iron	106±14%	11,5±21%	9,8±18%

*Root mean square deviation from the mean value is shown as the error.

TABLE 2. Results of Second International Comparison of Dosimeters (May 1971, Cak Ridge, preliminary results)

Pulse number	Energy release fission/pulse	Thickness and material of shield	Neutron dose D_N, rad*		γ-radiation dose D_γ, rad*		$D_N/D^\dagger_\gamma$
			mean (of the results of foreign participants)	from the results of Institute of Biophysics and Physicopower Institute	mean (of the results of foreign participants)	from readings of IKS-A detector	
2	$9{,}1\cdot10^{16}$	13 cm, iron	137,8	130 ‡ 129/105 **	19,6	16,9	7
3	$6{,}3\cdot10^{16}$	12 cm, plastic	47,8	31 ‡ 46/33	48,0	43,8	1
4	$10{,}1\cdot10^{16}$	Without protection	390	360 ‡ 352/242 **	56,3	60	7

* Dosimeters were arranged in air at a distance of 3 m from the center of the reactor.
† The ratio is computed from the mean value of the doses.
‡ This value is reduced 1.6 times compared to the preliminary value due to an error in the determination.
** In the numerator – from the readings of track detectors, in the denomiantor – from the readings of activation detectors.

Translated from Atomnaya Énergiya, Vol. 31, No. 5, pp. 547-548, November, 1971. Original article submitted June 10, 1971.

of neutrons and dose of γ radiation shows that the majority of the dose values do not deviate from the mean by more than ±25%.

With the object of further improving the agreement among the readings of accident dosimeters IAEA organized the second international comparison of accident dosimeters at Oak Ridge (USA), in which Soviet specialists participated for the first time.

The comparison of accident dosimeters on the pulsed dosimeter reactor HPRR [4] at Oak Ridge was traditional in nature. Thus, for example, on July 20-31, 1970 the seventh comparison of dosimeters was carried out with the participation of specialists from other countries [5]. A definite practice was laid down, according to which three pulsed triggerings of the reactor were provided. The dosimeters were arranged in a circle at a distance of 3 m from the center of the reactor. The doses of γ radiation and neutrons in each pulse were measured in air and on the phantoms (one phantom has its front surface facing the assembly and the other has its lateral surface facing the assembly). For the second and third pulses an iron or plastic shield was placed between the reactor and the dosimeters. The average values of doses obtained in air are presented in Table 1.

The participants of the second international comparison communicated preliminary data on the dosimeter readings which are presented in Table 2. It should be noted that the neutron dose indicated was estimated from the results of analysis of 1/10 of all irradiated track detectors. The γ-radiation dose was measured from the readings of IKS-A detectors. A few participants did not present the preliminary data, or participated in measurements only partially. In the second international comparison a fourth pulsed triggering of the reactor, identical with the first pulse, was done. The final and complete results with the readings of neutron flux density must be communicated to the IAEA by all the participants after two months for compiling of the final report.

LITERATURE CITED

1. Nuclear Accident Dosimetry Systems, IAEA, Vienna (1970).
2. G. M. Obaturov et al., At. Energ., 27, 234 (1969).
3. First IAEA Measurement Intercomparison, Valduc (France). Final Report, IAEA, Vienna (1970).
4. I. A. Auxier, Health Phys., 11, 89 (1965).
5. F. F. Haywood, Intercomparison of Nuclear Accident Dosimetry Systems. Oak Ridge, ORNL (1970).

INTERNATIONAL CONGRESS ON PROTECTION FROM ACCELERATOR AND COSMIC RADIATION

V. N. Lebedev

The congress was organized by the European Council for Nuclear Research and was held on its premises from April 26 to 30, 1971. This was the third congress devoted to protection from very high energy radiation.

Two hundred and fifty specialists from 21 countries and three international organizations participated in the congress and 64 papers were presented.

According to the subject matter the papers were divided into the following groups: biological effects of protons, neutrons, ions, and scattered radiation, dosimetry of particle beams, track detectors and spectrometry, dose equivalent and quality factor of radiation, methods of determining dose equivalent, cosmic radiation, radiation safety in ultra-high-altitude flights, protection from electrons and muons, passage of radiation through slits and labyrinths, problems of radiation protection as applied to targets and absorbers of particle beams, radiation safety in particle accelerators, and problems of radiation protection in new accelerators.

For individual dosimetry of high energy particles, causing disintegration reactions solid-body dosimeters are now being used besides nuclear emulsions. J. Dutrannois (CERN) used polycarbonate (density 1.2 g/cm^3) of commercial type in the form of foil of 200 μm thickness (Macrofoil E). After treating the polycarbonate in alkali, traces of α-particles and particles from disintegration reactions in carbon and oxygen were recorded. The method, which is not sensitive to γ-radiation and electrons, and not directly to protons, has a fairly high sensitivity (10 tracks/cm^2 at 50 mrad) for use in individual dosimetry of hadron with a replacement period of the order of a year.

Considerable interest was shown in the results of checking the adequacy of the readings of individual neutron photodosimeters giving dose equivalent of neutrons beyond the synchrocyclotron shield, which were presented in the paper by V. Aleinikov (Joint Inst. Nucl. Res.). The overestimate of the dose equivalent by a factor of ten, measured by these dosimeters in the presence of high-energy particles, indicates the need for introducing a correction into the readings of photodosimeters which are dependent on the fraction of high-energy particles in the total dose equivalent.

The majority of papers (11) were presented in the section "Dose equivalent and quality factor of compound radiation of accelerators," in which both procedural and computational–experimental studies were discussed. The paper by D. Shrdoe (Yugoslavia) on a proportional counter generated great interest; in developing this counter a new approach to rem measurement has appeared, which is based on the concepts of microdosimetry. The counter is a simplified analog of the well-known Rossi–Rosentsweig counter operating independently without pumping through the operating gas. The scheme, which consists of several amplifiers with linear and logarithmic characteristics, precludes the need for the traditional multichannel analyzer and the measurement of the linear energy loss spectrum, and at the same time facilitates the obtentions, in final form, of the absorbed dose and the quality factor of radiation for any length of exposure. These advantages make this detector very promising for use in daily dosimetric measurements, and is not restricted to accelerators only.

M. Zel'chinskii and S. Pshona (Poland) reported a new individual compound radiation dosimeter, developed by them and based on the recombination principle. The dosimeter consists of three ionization chambers filled with a tissue-equivalent gas at a pressure of 10 atm. It is ready for commercial production.

Translated from Atomnaya Energiya, Vol. 31, No. 5, pp. 548-549, November, 1971.

In the section on protection from accelerator radiation several papers were presented. A. Van-Ginken compared the results of computation by the Monte Carlo method of internucleus cascade with measured spatial distribution of radiation flux in a steel absorber of proton beams with an energy of 29.4 GeV. A disagreement between the experimental and computational results was noticed for large distances from the beam axis. This led to an important conclusion that for large angles (>30°) the semiempirical Ranpht–Trilling formula is not applicable for double-differential cross sections of formation of secondary particles in inelastic interactions of hadrons with nuclei. The authors of a joint paper from Great Britain, GDR, and CERN also arrived at the same conclusion from the study of the angular distribution of fluxes and doses of radiations from targets bombarded with an extracted proton beam.

We should also mention the papers by R. Alsmiller (USA), in which an analytical method of computing traps of muon beams with energy less than 500 GeV was proposed, and by D. Teriot (USA) devoted to the computation of heterogeneous traps of muon beams with cavities located in the magnetic field.

Among the papers presented in the section "Radiation safety in high-energy accelerators" the paper by Hefert (ECRN) deserves special mention. It describes systems of control and monitoring of radiation, and presents, for the first time, the results of a study of radiation situations in starting storage rings, which was necessary in view of the potential possibility of large losses of proton beams in the entrance region and in the storage rings themselves.

The proceedings of the congress will be published in the second half of 1971.

During the duration of the congress the delegates visited the main buildings and the installations of the (CERN).

RADIATION SAFETY IN BELGIUM AND HOLLAND

E. A. Cramer-Ageev and G. I. Pavlov

A Soviet–Belgian–Dutch symposium on radiation safety was held in April 1971 at Brussels. The main task of the symposium was to discuss general principles of radiation safety involving problems of admissible levels, individual dosimetry including cases of radiation accidents, and safety in conducting experiments on reactors.

As in the USSR, in Belgium and Holland the national norms of radiation safety are based on the recommendations of the International Commision on Radiation Protection and "Basic norms of protection of personnel and population from ionizing radiation" published by IAEA. The high population density in Belgium and Holland, together with the absence of free territories, impose severe demands on the organization of radiation control in the environment and taking measures for protecting the population. Therefore, the system of government decrees and laws existing in these countries, for regulating the problems of radiation safety, impose, in a number of cases, especially rigid requirements on the protection of the environment from radioactive contamination. Thus, for example, according to Dutch legislation, the allowable content of α- and β-active substances is 10^{-15} and 10^{-12} Ci/liter in air and 10^{-14} and $3 \cdot 10^{-12}$ Ci/liter in water.

The ejection into, and concentration of aerosols in the surface layer of the atmosphere is monitored with the use of special air-intake devices placed around nuclear centers in Mole (Belgium) and in Petten (Holland). In Belgium the monitoring instruments are located in police stations. The level of γ-radiation is monitored with radiometers, whose readings are automically transmitted on radio communication channels.

The development of programs to deal with the occurrence of serious accidents in reactors or critical installations is given much attention, especially in Belgium. In Mole a technically well-equipped tower has been constructed for use in the direction of operations during accident situations. In the event of an accident, the director of the center takes charge of the operations. Communication with accident, fire, and other services is maintained by his assistants by telephone and radio. In accordance with government agreements, assistance can be obtained from the nuclear center at Saclay (France). Well-equipped automobiles and helicopters, ready for fast departure, are at the disposal of those in charge of operations. In the case of a serious accident alarm signals are given and illuminating lamps are lit to indicate the routes for evacuation of any buildings. In the case when the accident occurs in the reactor hall with ejection of a considerable amount of radioactive gases and aerosols, there is a provision for: immediate stopping of the reactor, prevention of ejection of radioactivity into the atmosphere through the tube and closure of the sluice chamber (the buildings are kept at low pressure). In Belgium, variants of the programs of action are worked out beforehand taking account of the nature of the radiation accident and meteorological and other conditions. In the case of contamination of air by aerosols or iodine vapors which exceed the maximum permissible concentration by one tenth, potassium iodide tablets are distributed. If the contamination of the air exceeds the maximum permissible concentration by forty times, the authorities start evacuating the population from the danger zone.

In Holland also, there exist programs of action in the event of an accident, but informing people of accident routines and maintaining reserve cars, equipment etc., are considered superfluous. Inside reactor buildings, storehouses of used-up fuels and other places of radiation hazard, ionization r-meters are installed with automatic cut-off scales. The instruments have two signalling thresholds, warning (0.7 μR /sec) and accident (70 μR/sec). Accident-zone dosimeters containing sulfur, indium, and gold in cadmium and without cadmium for recording neutrons, and TLD for determining α-radiation are placed in the

Translated from Atomnaya Énergiya, Vol. 31, No. 5, pp. 549-550, November, 1971.

reactor halls. In some cases individual belt-type accident dosimeters, developed at Harwell, are used. All the personnel are subjected to multipole photodosimetry. The results of the densitometry are processed centrally on a computer. The TLD find restricted use due to high cost.

The radioactive content of air at various locations is monitored mainly by the method of pumping through a stationary filter. The activity of the sedimented dispersed phase is estimated after a determined lag, by semiconductor spectrometers, or by using pseudocoincidence counters for eliminating the background caused by the decay products of radon. The sensitivity of the systems for a filtration rate of 2 m^3 /h and a sampling duration of the specimen of 1 h is $3 \cdot 10^{-15}$ Ci/liter.

In Belgium the present allowable surface contamination by α- and β-emitters is 5 and 50 dis/cm^2 · sec respectively. For tritium the allowable level is extremely high (25,000 dis/cm^2 · sec), which accounts for the appreciable ejection of tritium from the reactors.

The amount of incorporated γ-radiation is monitored by human-body radiation spectrometers (HRS). At present all workers are subjected to such monitoring on suspicion of contamination and also those starting to work or discharged from work. A measureable amount of radioactive substance was detected in 30-40% of the persons examined. For the monitoring of plutonium content, a multifilament proportional counter with argon–methane filling and with a fine NaI(Tl) crystal 2-3 mm in thickness is used.

In conducting investigations on reactors each new type of investigation undergoes several stages of evaluation and examination before permission is given to conduct it. First expert authorities evaluate the theoretical possibility of conducting the experiments; then the project is examined in detail, analyzing the degree of risk for the personnel and the population. After the improvement of the projects and their reexamination, permission is granted for conducting preliminary tests. A special group evaluates the safety in real conditions and, if necessary, new improvements are made. Experiments on the study of fission materials, irradiated in a high-beam reactor, went through this cycle. The complete coordination lasted 20 months.

I INTERNATIONAL SYMPOSIUM OF HIGH-ENERGY PHYSICS

A. A. Kuznetsov

An international symposium on high-energy physics was held in Dresden in April 1971. It was organized by the Joint Institute of Nuclear Research (JINR) in conjunction with the Institute of High-Energy Physics (IHP) of the German Academy of Sciences in Berlin.

About sixty original communications and review papers were presented at the symposium.

The main results of the most significant papers are briefly given below.

Strong Interactions. In the research papers and review articles devoted to the study of nucleon–nucleon collisions, the problem of a complete experiment for a unique determination of the amplitude of elastic scattering of nucleons by nucleons with energies up to 1 GeV was discussed. Another topic examined was the results of experiments conducted in recent years on the accelerators of the JINR and IHP in the range of high-energies.

In the review article by Yu. M. Kazarinov (JINR) the problem of elastic scattering of nucleons by nucleons in the range of synchrocyclotron energies was discussed. In particular, it was stressed that for energies up to 1 GeV, from the results of the studies carried out in several laboratories according to the complete experiment program, the amplitude of elastic scattering of nucleons by nucleons is determined unambiguously in the energy range 50-400 MeV. An unambiguous determination of the amplitude of scattering at 630 MeV, obtained recently of Dubna on the completion of experiments on Wolfenstein parameters, is possible only for certain assumptions about the nature of the meson formation processes.

In the energy range above 1 GeV interesting results were presented in the paper by P. K. Markov (Bulgaria). These results were obtained in an experiment on the determination of the real part of the scattering amplitude in elastic p–p interactions by the photoemulsion method at energies of 30, 50, and 70 GeV The data from this experiment confirm the dispersion relations and are in good agreement with the results obtained earlier at Dubna with the use of electronic devices.

The review paper by Yu. A. Troyan (JINR) on the investigation of inelastic neutron–proton interactions at energies higher than 1 GeV generated large interest. The experimental information, obtained in this field so far, is extremely limited and in some cases (for example information on isobar N(1470)) the results are contradictory. The acceleration of deuterons, realized recently on the synchrophostron of the high-energy laboratory of the JINR, offers the only possibility of obtaining intense, and sufficiently monoenergetic beams of neutrons with energies of several billions eV. The paper also mentioned forthcoming experiments with these neutron beams.

Several papers contained data from the investigations of the inelastic interaction of π^+- and π^--mesons with nucleons. In the analysis of the experimental data on this topic an approach was used that is characteristic for the investigation of the interaction of cosmic-ray particles with matter. We must mention the results of V. Chadra (Mongolia) on the mean multiplicity of charged particles in inelastic interactions of pions at a momentum of 50 GeV/sec, which obey the $E^{0.35}$ law rather than the logarithmic law.

The Polish group from Krakov (papers of T. Koren and E. Bartk) has for sometime been solely studying inelastic interactions with large multiplicity (8- and 10-ray events). They followed a somewhat unusual method of processing the experimental data assuming a dependence of the assymetry of the emission over plane and solid angles on the sum of the charges on the particles. It was shown that this dependence does

Translated from Atomnaya Énergiya, Vol. 31, No. 5, pp. 550-551, November, 1971.

exist and has a minimum at angles equal to zero. Unfortunately, no physical interpretation of the results was given.

The papers by U. Kaltvassen (GDR) entitled "$\pi\pi$-Phase analysis of the reaction $\pi^+p \to p\pi^+\pi^+\pi^-$ at 8 GeV/sec" and "Chu–Low analysis in the reaction $K^-p \to pK^-\pi^+\pi^-$ at 10 GeV/sec" were interesting. Two solutions for the phase of $\pi\pi$-scattering from 400-500 to 1000-1100 MeV, i.e., in the widely studied range of S^0- or ρ^0-mesons were studied from a large amount of statistical data. One of the solutions indicates the existence of S^0-mesons in the range of 700 MeV; the other solution shows that the phase slowly reaches 90° in the region near 1100 MeV and then decreases. The last fact is not interpreted by the authors as being due to resonance.

The paper by G. A. Leksin (IETP) entitled "Investigation of interaction of strongly unstable particles," which generated large interest in those present at the symposium, an essentially new problem is the development of the investigations of the resonance interactions with nucleons was posed, which can be carried out only in the study of the interaction of high-energy particles with nuclei. The same paper contained experimental results on the detection of the effect of rescattering of isobar N(1236) in carbon nuclei.

Investigations of Electromagnetic Interactions. Several papers were devoted to this problem, of which, we mention the following that were the most interesting: a) the paper by A. G. Dolgolenko (IETP) entitled "Measurement of the ratio of the decay probabilities $(k_L^0 \to 2\gamma)/(k_L^0 - 3\pi^0)$." It was found that this quantity is equal to $(2.13 \pm 0.43) \cdot 10^{-3}$, and is in good agreement with theoretical predictions, removing the contradiction among the results of previous experimental data; b) the review paper by I. A. Ivanovskaya (JINR) entitled "Neutral decay modes of η^0-mesons," which contains all the experimental results on this problem presently available; c) the review paper by L. I. Lapidus (JINR) entitled "Investigation of electromagnetic interactions with high-energy particles." This paper discusses recently started and completely new experiments on scattering of π^--mesons at electrons, on the accelerator of the IHP$_Z$ the results of which make it possible to obtain an idea of the pion structure. Furthermore, it discusses other problems; for example, analysis of all available experimental results on ep-scattering is presented with the purpose of extracting the most reliable information on the structure of protons: the suggestion of Akhaizer and Rekalo on the possibility of setting up polarization ep-experiments at large transmitted momentum is considered; the prospects of the investigation of electromagnetic interactions for small transmitted momentums (started on the accelerator ARUS in Erevan), when the most direct determination of the proton radius is possible, is mentioned.

Theoretical Papers. The papers in this section were devoted to the current problems of strong and electromagnetic interactions of hadrons at high energies. First of all we should mention the detailed reviews by G. Ranpht and I. Ranpht (GDR), in which theoretical models of hadron–hadron collisions with one fixed particle in the final state were analyzed. The investigation of this type of reaction (dominant at high energies) is important both for planning experiments on the yield of particles in new accelerators and for studying the dynamics of strong interactions at small distances.

A paper by V. Markovskii (JINR) and a communication by K. Bibl (GDR) were devoted to the application of the theoretical models based on duality, to inelastic processes.

In the field of elastic hadron–hadron collisions the method of dispersion rules of sums, proposed by Soviet theoreticians, continues to be applied effectively. Using this method the rotation of polarization in pion–nucleon scattering was predicted, which has been confirmed by recent experiments (paper by L. D. Solov'ev, IHP). In the papers by V. Brant and F. Kashlun (GDR) the same method is used for the study of partial waves in pion–nucleon interactions in the region of the first resonance. The paper by V. M. Barbashov (JINR), giving a review of the studies made at Dubna toward obtaining this representation in the so-called approximation of linear trajectories, using functional integration and the Bethe–Salpeter equation, was devoted to the investigation of eikonal representation at high energies.

Of the theoretical papers on electromagnetic interactions the paper by R. M. Muradyan (JINR) generated large interest. It gave a review of the work done at Dubna on the scale invariance of deep inelastic lenton–hadron interactions and the rules of sums facilitating the investigation of the structure of the electromagnetic current at small distances. Mention should also be made of the paper by Nguen Van H'eu (DRV), in which by use of the theory of analytic functions an estimate of the electromagnetic radius of a pion is given, on the basis of data obtained on oppositely directed beams. This result is of particular interest in connection with the experiment on electron–pion scattering carried out by the physicists of the JINR and the IHP (Serpukhov).

TWELFTH MEETING ON NUCLEAR SPECTROSCOPY AND THE THEORY OF THE NUCLEUS

K. Ya. Gromov and V. V. Kuznetsov

The twelfth meeting on nuclear spectroscopy and the theory of the nucleus was held in June 1971 at the Joint Institute of Nuclear Research (JINR) in Dubna. Such meetings have been held at this institute regularly at one to two year intervals since 1958. One of the important tasks of these meetings is to discuss the results of joint theoretical and experimental investigations of the structure of atomic nuclei, carried out in the JINR institutes of the countries participating in JINR. The discussion of the results of common studies is important for planning this collaboration.

More than 150 scientists of the JINR and the collaborating countries, i.e., Bulgaria, Hungary, GDR, Mongolia, Poland, Rumania, Soviet Union, and Czechoslovakia participated in the meeting: 115 papers were presented. The abstracts of the presented papers will be published in the form of a book.* Six plenary sessions and two seminars on the theory of the nucleus and the methods of experimental investigations were held: 39 papers were presented in the plenary sessions.

At present the main directions of experimental investigations into the structure of atomic nuclei may be considered the investigations of nuclei far from the β-stability band and investigations of the level structures of nuclei excited in different nuclear reactions. Precision investigations of β- and α-decay of nuclei close to the β-stability band continue to retain their significance. All these subjects were presented at the meeting.

The paper by V. I. Raiko (Laboratory for Nuclear Problems (LNP), JINR), gave a report of the work on developing equipment for investigating neutron-deficient isotopes far removed from the stability band, which are obtained on irradiating different targets by protons with energies of 660 MeV on the synchrocyclotron of the JINR (Program YaSNAPP – nuclear spectroscopy in proton beams). In 1970 the construction of an apparatus complex was completed which includes devices for irradiating targets, pneumatic rabbit, mass-separator, γ- and β-spectrometers, apparatus for storage and analysis of spectra with the use of a computer. There exists the possibility of studying isotopes of a number of elements with half-life periods up to 1-3 min. The great achievement of this group is the development of a new high-efficiency (up to 80%) fast-response (2-4 min) ion source for the separation of isotopes of rare-earth elements. Interesting papers by T. Fenesha (LNP, JINR), R. Arl't (LNP, JINR) and other papers on the results of studies of the schemes of decay of short-life isotopes in the YaSNAPP program were heard.

M. Finger (LNP, JINR) presented a summary of the systematic investigations of the level structure of even–even nuclei of platinum carried out in ISOLDE at CERN.

The paper by V. A. Karnaukhov (LNP, JINR) gave summaries of the study of decay of nuclei with ejection of protons (slow protons, proton radioactivity) and mentioned the perspectives of these investigations on heavy ion accelerators at the JINR. N. I. Tarantin (LNP, JINR) talked on the progress of the investigations of neutron-excess isotopes of light elements far away from the β-stability band. These studies were carried out with the aid of an electromagnetic mass-separator placed in the beam of the heavy ions.

Several papers were devoted to the investigations of the levels of atomic nuclei using nuclear reactions. Here we must mention the detailed and systematic investigations of deformed nuclei of rare-earth elements, about which K. Kaun from IYaI in Rossenderf (GDR) gave a talk. Gamma-quantas appearing in reactions of the type (α, 2n), (d, 2n), (p, n), etc., were studied. Much new interesting

*Nuclear spectroscopy and the theory of the nucleus. Preprint JINR, D6-5783, Dubna, 1971.

Translated from Atomnaya Énergiya, Vol. 31, No. 5, p. 552, November, 1971. 71.

information was obtained about the rotational levels of these nuclei. These studies are closely connected with the YaSNAPP program and part of the work is done jointly. E. Lyudzeevskii (Poland) reported interesting results of the study of excited states in nuclei of neutron-deficient isotopes of cerium and niobium, observed in (α, xn) reactions. Interesting studies were presented by R. P. Slabospitskii and Yu. N. Rakivnenko (Physicotechnical Institute, Academy of Sciences of the Ukrainian SSR, Khar'kov).

Review articles, systematizing the results of experimental investigations, were given by V. S. Jelepov and E. P. Grigor'ev.

Many interesting papers of a theoretical nature were presented. In the paper by V. G. Solov'ev (Laboratory of Theoretical Physics (LTP), JINR), were discussed the results of a study of structure of highly excited states of nuclei based on a simple spectroscopic model. N. I. Pyatov (LTP, JINR) talked on the results of a study of the rotational states of deformed nuclei. Ya. Blotski (Poland) presented the paper entitled "Closed shells for extra-heavy nuclei."

The collaboration of the laboratories of the JINR and the institutes of the collaborating countries in the field of experimental and theoretical investigations of the structure of atomic nuclei, continues to be developed actively. The laboratories of the JINR make available unique equipment which facilitates original experimental investigations into the structure of atomic nuclei: instrumentation complex of the YaSNAPP program, heavy-ion accelerators, pulsed reactors, etc. These possibilities create good prospects for further qualitative development of studies on the structure of atomic nuclei at the JINR.

INTERNATIONAL SEMINAR ON BINARY REACTIONS OF HADRONS AT HIGH ENERGIES

A. M. Baldin, A. L. Lyubimov,
and V. A. Meshcheryakov

An international seminar on binary reactions of hadrons at high energies was held at Dubna from June 3 to June 8, 1971. It was organized jointly by the JINR and the Academy of Sciences of the USSR. About 200 scientists from 12 countries and two international organizations participated in the seminar. The objective of the seminar was a detailed and thorough discussion of both the aggregate of main experimental data and the theories and models related to binary reactions of hadrons at energies of several billions electron volts, and to define the directions of further work based on this discussion.

The seminar was held at a time when important results were obtained on the accelerators at Serpukhov, which were thoroughly discussed at the seminar. Furthermore, an accelerator with counter proton beams had recently begun operation at CERN and the preliminary results of the first experiments on this accelerator were reported at the seminar. An accelerator at 500 GeV is about to be started at Batavia (USA). A combination of these circumstances enhanced the interest in the discussion of the available data and the paths of further research and also contributed to the high activity of the participants of the seminar, among which were a large number of leading scientists of the socialistic countries working in directions close to the topic of the seminar.

The system of review papers was the basis of the seminar; these papers taken together would give an up-to-date, general picture of experiment and theory related to the theme of the seminar. The review papers were supplemented by a small number of original papers. When the proceedings of the seminar are published (end of 1971), physicists will have a unique reference book on binary reactions of hadrons at high energies, which will summarize all the information on these processes available up to June 1971.

An important point in the seminar was the close interweaving of experimental information and theoretical problems and a combined discussion of both by theoreticians and experimentalists.

The seminar began with the discussion of problems related to the energy dependence of total cross sections of interactions (paper by V. I. Savrin and N. E. Tyurina (IHP)). The investigation of these interactions (the measurements on the accelerator of the IHP in Serpukhov play a special role) serves for a critical check on the basis of the theory of strong interactions, in particular, of the Pomeranchuk theorem. At present, experimental results are in agreement with the other possibilities. From this point of view the increase in the total cross section of K^+p-interactions, detected in recent experiments at Serpukhov, and the results of the experiment on $K_L^0 \rightarrow K_S^0$-regeneration in hydrogen are highly significant.

In the review paper by L. N. Strunov (JINR) it was shown that the results of measurements of πN-scattering and the regions of interference between Coulomb and nucleus amplitudes (obtained on the synchrophasotrons at Dubna and Brookhaven) facilitating the determination of the real part of the amplitude of elastic πN-scattering, are in agreement with the computations of the theory of dispersion relations. On the basis of the available experimental data theoretical model estimates make it possible to set the upper limit of the "elementary length" at about 10^{-15} cm, i.e., two orders of magnitude smaller than the radius of strong interactions. For a further lowering of this limit experiments to measure the real part of the amplitude of πN-scattering at higher energies are needed.

Van Rossum (Saclay, France) presented an impressive summary of data on the study of polarization in different processes of elastic scattering, indicating a rapid increase in the number of experiments on polarization measurement and an equally rapid increase in their accuracy. The latter became possible, due to

Translated from Atomnaya Énergiya, Vol. 31, No. 5, pp. 553-554, November, 1971.

the development of polarized hydrogenous targets. The best results are obtained with butanol targets cooled by ^{3}He (70% polarization at a high hydrogen content).

The review paper by L. Zolin, V. A. Nikitin, and V. A. Sviridov (JINR) was devoted to elastic proton–proton, proton–deuteron, and proton–neutron scattering at high energies. The following main facts were established: in accord with the theoretical predictions the behavior of the cross sections of elastic p–n scattering is similar to that of the p–p scattering cross sections; the diffraction cone of nucleon–nucleon scattering becomes narrow in accord with the predictions of the theory in the entire energy range up to 70 GeV, which means an increase of the region of interaction with an increase in energy. The real part of the amplitude of forward scattering in nucleon–nucleon scattering decreases with an increase in energy, which is in agreement with the predictions of the dispersion theory. The interest in continuing this type of investigation is now very great and a similar experiment using the same procedure will be carried out in the near future on the 500 GeV proton accelerator at Batavia (USA).

The participants of the seminar showed great interest in the comparison of the data on the slope of the diffraction cone of elastic proton–proton scattering at energies available with the Serpukhov accelerator, obtained by a group of workers at the JINR, with the preliminary results of measurements of this quantity in a close interval of transmitted pulses in the experiment with counter proton beams at CERN, reported by A. Diddens. This comparison indicates that the diffraction cone of elastic proton–proton scattering continues to narrow, up to energies of the order of 1500 GeV, although it is possible that in the transition from the energies of the Serpukhov accelerator to those of the CERN accelerator in counter beams the narrowing is slowed down.

The paper by Prof. Shopper (CERN) gave a review of the processes of np-charge exchange and the charge exchange in antiproton–proton and antineutron–neutron systems. The single nature of the dependence of the cross sections of np-charge exchange on the transmitted pulse in a very wide range of energies is noteworthy. In the review paper by Prof. D. Orir (Cornell, USA) the complex structure of the angular dependence for elastic scattering of those particles which form resonances with protons on protons, was pointed out.

The paper by I. M. Gramentskii (JINR) contained a review of quasi-two-particle processes, i.e., processes occurring through the formation of two particles in the intermediate state, of which one or both are resonance particles. An analysis of the energy dependence of the cross sections of quasi-two-particle reactions shows that there exist two classes of such reactions. In the reactions of the first type the cross sections decrease sharply with the increase in energy, whereas for the reactions of the second type the cross section remains practically constant. The second class of reactions apparently refers to processes of diffraction generation, which will give the main contribution to the quasi-two-particle reactions at high energies.

Unofficial reports about the research plans for the largest foreign accelerators caused considerable interest in the participants of the seminar. Prof. D. Orir talked about the experiments which will at first be set up at Batavia (USA). A very intensive preparation for physical experiments on this accelerator should be noted. Of 120 experimental projects submitted, more than 30 have been accepted, and according to the plans of the laboratory, some will start in January 1972. The construction of channels for particle beams, including one for an extracted proton beam, is being completed and experimental apparatus is being set up. Prof. H. Shopper talked about the most interesting experiments, which are being prepared at CERN, and also on the prospects of the development of the accelerator base at this center. Of the many experiments to be undertaken, mention should be made of the production of a beam of sigma-minus-hyperons with energy of 15 GeV/sec and with an expected intensity of several hundred particles per accelerator pulse. In the magnetic channel of this beam superconducting magnets are used and the extraction of the hyperons in the beam is accomplished by two Chernovskii counters.

It was assumed that the theoretical review papers would present to the participants of the siminar a clear picture of the achievements and difficulties of the theory in explaining the vast experimental information. Unfortunately we are still far from a clear understanding of even the binary hadron reactions and therefore a large number of hypotheses are used for explaining these phenomena. The method of dispersion relations, whose rigorous bases were put forth by Academician N. N. Bogolyubov as early as 1955, occupies an important place amongst these. Within the framework of this approach, different directions have been sucessfully developed. The asymptotic behavior of binary reactions (paper by O. A. Khrustalev,

IHP), the Pomeranchuk theorem and its generalization (paper by Nguen Van H'eu) are of considerable interest.

An analysis of a large number of binary hadron reactions with the use of dispersion relations was presented in the papers by L. D. Solov'ev (IHP) and G. Heller (FRG). Theoreticians noted a special pressing need for increasing the accuracy of the experimental data on exchange processes and on the polarization behavior at large energies.

Closely connected with the method of dispersion relations is the theory of complex momentum angles, to which a large contribution was made by I. Ya. Pomeranchuk and other Soviet theoreticians. This theory enables one to understand many regularities of the interactions at high energies and to make a number of predictions (paper by K. A. Ter-Martirosyan, ITEP).

Another approach to this range of phenomena was presented by V. A. Matveev and A. N. Tavkhelidze. It has its origin in the work of A. A. Logunov and A. H. Tavkhelidze proposing the so-called quasipotential approach, in the framework of which, for example, a qualitative description of the form of differential cross sections at high energies is obtained.

Summing up, it can be said that the picture of the behavior of binary reactions at high energies, emerging from numerous experiments, is essentially in accord with the expectations of the theoreticians. At the same time the existing attempts toward constructing a theory cannot pretend to give reliable quantitative predictions. Furthermore interesting qualitative regularities (for example, in scattering with large momentum transfer and in polarization phenomena) are detected, which do not have satisfactory theoretical interpretations. In view of this the investigation of binary reactions at high energies undoubtedly plays a role in the development of the theory of strong interactions, without which it is difficult to visualize the solution of the central problem of physics, i.e., the problem of developing the quantum field theory.

NUCLEONS AND WEAK INTERACTIONS

N. I. Pyatov

An international symposium on "Nucleons and weak interactions" was held at Zagreb (Yugoslovia) in June 1971. It was organized by the R. Boshkovich Institute with the support of the European Physical Society. The problems, lying at the boundary of elementary particle physics and the physics of the atomic nuclei, i.e., weak interactions between nucleons and their effect in atomic nuclei, were discussed at this symposium. More than 40 scientists from the largest scientific centers of Europe and the USA took part in it.

About 20 reviews from invited authors and original reports were heard and discussed at the meetings of the symposium. A brief account of the most important papers is given below. The theoretical aspects of weak interactions were discussed in the papers by G. Furnal (Italy), G. Pitsman (Austria), and G. Marks (Hungary). Different implications of models, constructed on the basis of the algebra of currents and the hypothesis of partial conservation of the axial current, were analyzed. In particular, the problem of disturbance of SR-symmetry in weak interactions and the possibility of checking SRT-invariance were discussed in detail. The possibility of developing a single theory of weak interactions based on the hypothesis of the existence of intermediate boson was also discussed.

A considerable number of the papers were devoted to the problem of nonconservation of evenness in nucleon–nucleon interactions. The theoretical aspects of this problem (models of nonleptonic Hamiltonians, obtaining partially nonconserved symmetry of potential and their application in nonrelativistic nuclear physics, the effect of short-range nucleon–nucleon correlations) was discussed in detail in the paper by E. Feshbach (USA) and D. Tadich (Yugoslovia). Some theoretical computations of the effects of nonconservation of the symmetry in atomic nuclei were presented in the papers of G. Cummel (FRG) and N. Vin-May (France). Usually the blending of the nuclear states with different evenness, caused by the disturbing weak interactions of nucleons, is computed. Both short-range nucleon–nucleon correlations and long-range interactions are considered in the framework of the present microscopic approaches. It was found that the computed circular polarization of γ-quantas in nuclear transitions are much smaller than the experimental values.

The existing experimental data, indicating the disturbance of evenness in atomic nuclei, were also discussed in detail at the symposium. In the paper by P. Bok (FRG) the sources of errors in the measurement of the effects of nonconservation of evenness were discussed. Similar problems were discussed also in the paper by E. Kupal (FRG). It was noted, that at the present level of experimental technique the systematic error is comparable with the magnitude of the effect. Thus, for example, in the paper by E. Kupal the following result was presented for the polarization in the ^{181}Ta nucleus: $P = +(2 \pm 4) \cdot 10^{-6}$. The strong effect of nonconservation of evenness detected in the nucleus ^{180}Hf is of interest. The following result for the circular polarization of γ-radiation with energy of 501 keV was given in the paper by B. Enchke (FRG): $P = -(28 \pm 2) \cdot 10^{-4}$. A theoretical explanation of this result is as yet very difficult. Finally, we mention the detection of nonconservation of evenness in the α-decay of the ^{16}O nucleus, which was reported by G. Wafler (FRG). The α-decay of the excited state with $I^{\pi} = 2^-$ and energy of 8.87 MeV was observed in this experiment. The measured α-width of this level was equal to $\Gamma_{\alpha} = (0.98 \pm 0.30) \cdot 10^{-10}$ eV.

Several papers were devoted to the problems of nuclear β-decay. E. Fiorini (Italy) gave a review of the experimental results on the research of double noninertial β-decay of atomic nuclei. The investigation of this decay permits the establishment of the degree of conservation of lepton number in nuclear physics. The absence of double noninertial β-decay means the conservation of the number of leptons in β-decay. The search for this process was conducted in many laboratories (in particular in the USSR).

Translated from Atomnaya Énergiya, Vol. 31, No. 5, pp. 554-555, November, 1971.

E. Fiorini reported new results on the research of β-decay $^{76}Ge \rightarrow {}^{76}Se$. The experiment conducted in the Monblansk tunnel gave a negative result. The life-time of ^{76}Ge was found to be more than $3 \cdot 10^{21}$ years.

The paper by P. Khornsha (CERN) discussed the results of experimental measurements of force functions of β-decay and the spectra of slow protons in light isotopes of xenon and mercury, far from the region of stability. These experiments give certain information on the nuclear matrix elements of β-decay, their energy dependence (force functions), the density of the nuclear levels at high energies of excitations and so forth, i.e., they give important information on the structure of highly excited nuclear stages. The theoretical problems related to nuclear matrix elements of β-decay were discussed in the paper by S. I. Gabrakov and N. I. Pyatov (JINR).

Short original papers were also presented.

The small number of participants gave the symposium the character of a working group and its good organization contributed significantly toward the success and fruitfulness of the discussions.

LIGHTWEIGHT MOBILE LABORATORY FOR COMPLEX FAULT DETECTION CONTROL

V. G. Firstov and N. S. Orlov

As a result of the joint work of the Central Scientific Research Institute of Heavy Machine Construction (National Republic of Bulgaria) and the All-Union Scientific Research Institute of Radiation Technology (USSR) an experimental model of a mobile complex fault-detection laboratory was made for the control of welding joints in field and assembly conditions.

The laboratory is mounted in the minibus "Latviya" (Fig. 1). The plan of the arrangement of the equipment is shown in Fig. 2. The inside of the minibus is divided into four compartments:

1. The cabin with chairs of the driver 1 and the head operator 18.

2. A saloon which contains the working bench 2, the chair of the second operator 3, the airheater 4, and the car battery 17. In the saloon there is an entrance door 16 to the laboratory.

3. The compartment for processing photographic material and film, in which are mounted a desk-cabinet 5 with tubs, drying cabinet 6, working bench of the operator 15 with negatoscope and control panel 14. The compartment is separated from the saloon by a light-proof screen.

4. The compartment for the equipment which houses the benzene heating equipment 7, benzene tank 8, fire extinguisher 9, store for fault-detection equipment 10, spare battery 13, battery charger 12, and the spare wheel 11. The access to the equipment compartment is through the rear door of the minibus.

The set of the basic fault detection equipment of the laboratory consists of a universal hose-type γ-defectoscope RID-11 and a portable pulsed x-ray instrument of type IRA. The γ-defectoscope RID-11 is a portable instrument and is intended for radiographic inspection of different welding joints and conduits of 15-250 mm diameter and total thickness of the wall up to 30 mm. The pulsed x-ray apparatus IRA-1D is intended for roentgenographic

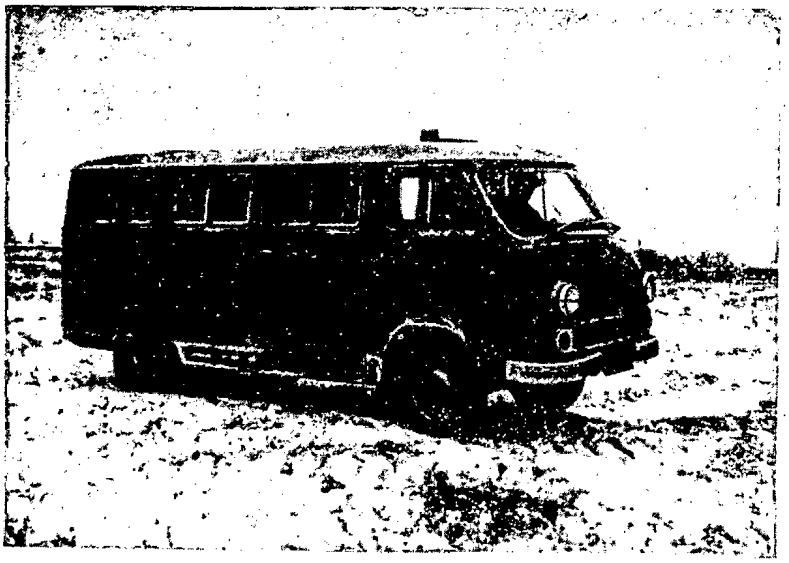

Fig. 1. Light-weight mobile laboratory.

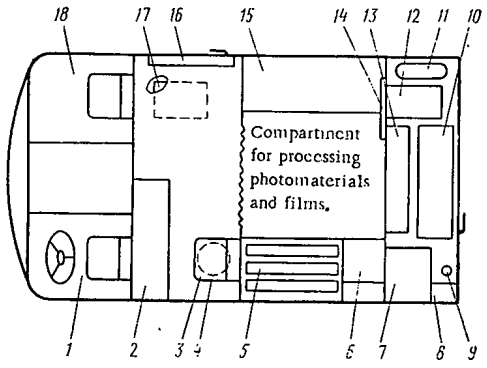

Fig. 2. Plan of light-weight laboratory.

Translated from Atomnaya Énergiya, Vol. 31, No. 5, pp. 555-556, November, 1971.

inspection of steel products of thickness up to 15 mm at a distance of 25 cm from the focus of the tube, using a film with sensitivity not less than 250 inverse roentgen and two magnifying screens of type UFD. The power supply to the apparatus in field conditions is obtained from a 12 V battery.

When necessary additional magnetic and ultrasonic fault-detection equipment can be incorporated into the existing equipment.

The technological accessories for conducting radiographic inspection include sets of flexible cassets, metallic screens, marking signs, sensitivity standards, standards for blackening density, defectometers and magnetic holders.

The set of the auxiliary equipment for processing and interpretation of γ-pictures consists of a desk-cabinet with tubs for photographic processing, frames for holding pictures, a drying cabinet, a negatoscope, and place for storing the processing solutions. The process of photographic work and the interpretation of γ-pictures is completely automatic; the power supply is obtained from the spare 12 V battery located in the equipment compartment. The battery has a capacity of 144 A/h and ensures a normal operation of the laboratory for 3-5 days.

The cabinet for drying the pictures operates in two modes: drying by hot air from the benzene heating equipment and by ventilation without air heating. The negatoscope ensures interpretation of the pictures with blackening density up to 2 for a maximum size of the light field 100 × 400 mm.

The laboratory also has a radiometer for the monitoring of radiation and also a set of individual dosimetric instruments of type KID-2 for the laboratory personnel. A remote signalling device with supply from 6 V battery ensures light and sound signals in the area of radiographic inspection.

Industrial tests of the experimental model of the light-weight mobile laboratory showed prospects for the use of such laboratories under the conditions of carrying out constructional-erection works. Since they ensure complex inspection a quick decision can be made as to the quality of the products under examination.

γ-DEFECTOSCOPE RID-32 OF NORMAL CLASSIFICATION SERIES SÉV

A. N. Mairov and N. S. Orlov

The development work on the γ-defectoscope RID-32, intended for radiographic inspection of the quality of weldings and large-size cast industrial parts with steel wall thickness up to 200 mm, was completed at the All-Union Scientific Research Institute of Radiation Technology.

The assembly of the γ-defectoscope (Fig. 1) contains a radiation head 1 with stand 2, transportable rechargable container 3, remote control panel 4, a trolley 5 with lifting mechanism, a set of spare instruments and devices 6, and control cable 7.

The radiation head of the γ-defectoscope is designed for use as a source of radiation from ^{60}Co with intensity of exposure dose up to $3.5 \cdot 10^{-2}$ R/sec at a distance of 1 m with the external dimensions of the ampoule not more than 11.5 × 12 mm. The intensity of the exposure dose of the γ-radiation at a distance of 100 mm from the surface of the radiation head does not exceed 100 mR/h and 2.8 mR/h at a distance of 1 m. Other radiation sources can be used in the equipment, for which the external dimensions of the ampoule do not exceed the dimensions indicated above.

The removal and the formation of the beam of γ-radiation is obtained with the use of a valve and a collimator; the dimensions of the field of irradiation at a distance of 1 m from the source can be regulated both in the horizontal and the vertical planes in the range of 200 to 600 mm.

Control of the apparatus is carried out from the console, the face panel of which has a scale for a time-counting mechanism with a range of exposures from 1 to 60 min, command buttons, lamps for electric and radiometric signalling on the position of the source and the valve and on the limiting values of the irradiation dose of the operator at the location of the console.

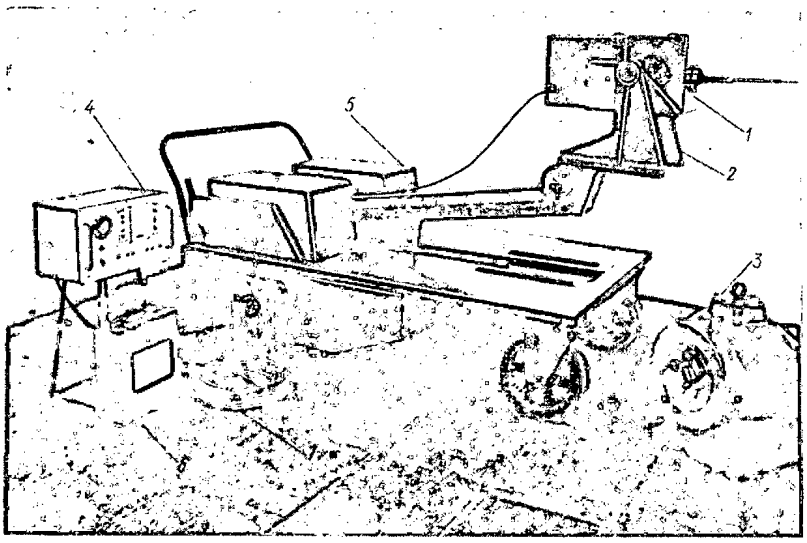

Fig. 1. Gamma-defectoscope RID-32.

Translated from Atomnaya Énergiya, Vol. 31, No. 5, pp. 557-558, November, 1971.

TABLE 1. Regimes of Isotope Radiography

Monitored product	Thickness of the basic metal, mm	Focal distance, m	Exposure time, min	Density of blackening of the picture	Sensitivity, %
Welded joint of steel with the intensification of the seam to a height of 20 mm on both sides. Film ORVO type RF-3	100	1	40	1,5	1,5
Cast steel. Film Ilford type A	140	1	12	1,5	1

In order to avoid an uncontrolled emission of radiation, a lock is placed at the upper lid of the radiation head which locks the valve in the closed position with simultaneous breaking of the power supply circuit for the radiation head drive.

The radiation head is mounted on a stand and can be rotated in the vertical plane by 45° above and 90° below the horizontal. A telescope-type sighting visor mounted on the radiation head ensures accurate orientation of the axis of the beam in relation to the object being monitored.

For enlarging the technological possibilities and shortening the idle time in radiographic inspection of the quality of large-size products, the γ-defectoscope is provided with a trolley with a lift mechanism. The trolley is a platform mounted on four wheels, of which, the rear ones can rotate and the front ones are fitted with a braking device. In transporting and storage the radiation head and the control console can be placed in the side pockets of the trolley and covered with lids.

The lifting mechanism ensures plane parallel displacements of the radiation head in the vertical plane up to a height of 1.5 m above the platform of the trolley and the rotation of the stand with the radiation head by 360° in the horizontal plane. The control of the lifting mechanism is accomplished by the use of an electromechanical drive connected to a three-phase grid of alternating current with a voltage of 300 V at 50 Hz.

The control console of the radiation head is connected to the control panel placed on the trolley; in operation without the trolley the control console is connected directly to an alternating current grid with 220 V.

For loading and reloading of the radiation head in operational conditions the assembly of the γ-defectoscope has a three-channel container designed to store two holders with ^{60}Co sources, of total intensity of exposure dose of γ-radiation up to $7 \cdot 10^{-2}$ R/sec at a distance of 1 m. When both the channels are loaded 0.4 mR/h at a distance of 1 m from the source.

Industrial tests of the experimental models of γ-defectoscope RID-32, conducted in workshop conditions made it possible to estimate the radiation environment in the monitored regions. In particular, for the illumination of the products by a wide beam, directed onto the object and having irradiation field dimensions 600 × 600 mm, the radius of the danger zone for the attending personnel (category A) is 10 m and for the workers of adjacent specialities (category B) is 25 m.

The radiographic inspection of the quality of different products confirmed the computed possibilities of the γ-defectoscope both with regard to the sensitivity and output (Table 1).

The results of the introduction of the first models of γ-defectoscope RID-32 showed that their use in large machine-building enterprises increases the output of the radiographic inspection by a factor of 2-3, and the economic effect of the introduction of one apparatus comprises 24 thousand rubles per year with a compensating period one year. The equipment is made on individual orders through the All-Union society "Isotope."

RADIOLOGICAL THERAPY CENTER IN NORTHERN IRAQ

A. N. Kozlov

In July 1969 an agreement was signed in Baghdad for the construction of a radiology center in Mosul with the aid of the Soviet Union. At the beginning of 1971 the equipment for the radiology center was delivered to Iraq; it consisted of γ-therapy equipment of type "Luch-1" with the initial activity of the source ^{60}Co at 4000 Ci; an apparatus for close-focus x-ray therapy of type RUM-7 at 60 V and 20 mA, and x-ray diagnosis apparatus of type RUM-10 at 145 kV and 250 mV, and also three sets of dosimetric apparatus.

The installation and adjustment of the equipment, and loading of the γ-apparatus "Luch-1" was carried out.

The solemn opening ceremony of the center was held on March 30, 1971. The rector of the university Dr. Mashat, addressing the meeting in the name of the President of Iraq, emphasized the significance of the creation of the Mosul radiological therapy center for the development of health protection in the northern regions of the country. He addressed warm words of gratitude to the Soviet People and to the Soviet specialists who participated in the construction of the medical center. In his reply, the Soviet ambassador in Iraq F. N. Fedotov, mentioned further development and strengthening of friendly Soviet–Iraq relations and collaboration in various fields including science and technology.

Arriving before the opening of the center in Mosul, a group of Soviet doctors together with Iraqi doctors, specialists, and trained local personnel, began the operation of the instruments and equipment of the installation. Simultaneously several tens of patients having serious oncological diseases were admitted for treatment. Soviet and Iraqi doctors conducted joint examination of these patients, established diagnosis, and gave appropriate treatment on the radiological equipment. Iraqi doctors obtained from their Soviet colleagues detailed consultation on all problems related to the organization and practice of the treatment of oncological diseases. Systematic x-ray investigations of patients, analysis of clinical conclusions and investigations were also carried out. A system of dosimetric service and individual dosimetric investigation was organized and inspection graphs and the ordinary maintenance of the equipment were worked out.

Translated from Atomnaya Énergiya, Vol. 31, No. 5, p. 558, November, 1971.

BRIEF COMMUNICATIONS

A delegation of Italian scientists visited the Soviet Union from June 27 to July 4, 1971 in conformity with an agreement of collaboration in the field of the peaceful use of atomic energy between the State Committee on the use of atomic energy and the National Committee of Atomic Energy of the Italian Republic effective from October 7, 1970. The delegation familiarized itself with the work on the physics of thermal- and fast-reactors.

The Italian scientists visited the scientific research institutes, State Committee for the Use of Atomic Energy of the USSR (GKAÉ SSSR), Physical Energy Institute (FEI), Scientific Testing Institute of Aviation Instruments (NIIAR), I. V. Kurchatov Institute of Atomic Energy (IAE), and also I. V. Kurchatov Belyarsk Atomic Power Station. In the institutes the Italian scientists were acquainted with the methods of designing thermal- and fast-reactors, critical assemblies, and the reactors BR-5 and BOR-60. In the Belyarsk Automatic Signal Transmitter (AST) they were acquainted with the operation of the first and the second blocks and also with the progress in the construction of the third block containing the fast-reactor BN-600.

* * *

From May 10 to 27, 1971 the State Committee on the use of atomic energy in the USSR organized a scientific-familiarization trip of the Soviet Union for the specialists of the member countries of the IAEA on standardization of radiation dosimetry. This was done through a voluntary contribution of the USSR to the technical assistance fund of the IAEA. The group consisted of scientists from 22 countries.

During the trip single-day seminars were arranged for the participants, in which lectures were given on the standardization and metrology of ionizing radiations, metrology in the field of measurement of the characteristics of radioactive aerosols, metrological safety and standardization of the measurements of the activity of nuclides, doses of ionizing radiations, and also on the measurements of the characteristics of neutron fields in power nuclear installations.

Included in the program were the Union Scientific Research Institute of Instrument Manufacture, D. I. Mendeleev All-Union Scientific Research Institute of Metrology, Institute of High-Energy, Physics, Medical radiology faculties of the Central Institute of Advancement of Doctors, Novo Voronezhsk" Automatic Signal Transmitter (AST), and the demonstration hall of the All-Union society "Isotope."

Within the State Committee of Standards of the Soviet of Ministers of the USSR discussions were held on the organization of scientific-research work in the field of standardization of radiation dosimetry.

* * *

The XXI session of the Scientific Committee of the United Nations on the effect of atomic radiation was held in June 1971 in New York. A Soviet delegation participated.

The committee discussed the following sections of the report that will be submitted to the XXVII session of the General Assembly of the UN in 1972: radioactivity of the environment, doses received by populations from medicine and professional radiations, genetic effects of radiation, radiation cancergenesis, and the effect of radiation on immunity.

The Committee forwarded a special report to the secretariat of the UN Conference on the contamination of the environment, stressing that the principles and the methods of estimating radioactive contamination, worked out by the committee, can be very useful for the work of the conference.

* * *

Translated from Atomnaya Énergiya, Vol. 31, No. 5, p. 559, November, 1971.

In May 1971 IAEA held (in Vienna) a meeting of experts to discuss the application of the Massbauer effect in scientific research and industry. Twenty-two specialists from 13 countries took part in the meeting. The use of γ-resonance spectroscopy in chemistry, biology, and in certain branches of solid state physics, methods of investigation, and also problems concerning experimental equipment were discussed.

Attention was also given to the use of Massbauer effect in industry and in scientific research in developing countries. Particular attention was given to the financing of exchange of experts between developing and developed countries and to the setting up of equipment and standard sources in developing countries.

* * *

The first meeting of the working group of the IAEA on the security of nuclear materials in use, storage, and transportation was held in Vienna in June 1971. Twenty-three experts from the member-countries of the IAEA participated in the meeting. This working group was created by the Agency in conformity with the resolution of a meeting of experts on methods and techniques of guarantees (Tokyo, December, 1969) with a view to work out recommendations for applying security measures.

In the draft of recommendations, worked out by the secretariat of the agency and discussed by the working group, several levels of security of fission materials are envisaged depending on their "attractiveness" and accessibility for passing into unlawful use; requirements on the system of counting, storage, and distribution and security of nuclear materials are defined.

Remarks on the draft of the secretariat were made in the meeting of the working group and it was decided to hold the next meeting in 1972.

* * *

A school on "Radioisotope thickness gage of polymer films in the chemical industry" was held in May 1971 in the "Atomic Energy" pavilion at the Exhibition of Achievements of the National Economy of the USSR (VDNKh USSR) in Moscow. The problems involved in the use of the principle of reflection of electrons from gaseous media for the measurement of thickness were also discussed. The recording of back-scattered β-radiation after its reflection from the gaseous medium and passage through controlled material facilitated the development of an essentially new construction of radioisotope devices. These devices are used in the control of thin polymer films and for one-sided measurement of sleeve films, prepared by the method of extrusion of melted polymer through an annular slit with its subsequent bulging. There appeared a possibility of control of thickness in closed volumes (spheres, probes, and other objects); model samples of such devices are at present undergoing tests under industrial conditions.

The radioisotope thickness gage (RTV) of sheet and film materials, developed by a group of the Riga Scientific-Research Institute of radioisotope devices and intended for operation in explosion-hazard conditions, was of considerable interest for chemical and cinephotography industrial enterprises. Such thickness gages were developed in the Soviet Union for the first time.

Much attention was devoted to the problems of metrology (calibration and checking of radioisotope thickness gages, computation of certain errors, development of sample and operating measures).

The problems of the effectiveness of the use of radioisotope technique in the chemical industry and the effectiveness of the use of radioisotope devices for measuring the thickness of polymer films were also touched upon. Thus, for example, the economic effect of the introduction of a single radioisotope thickness gage for the control and regulation of the thickness of polymer films is 15.0 to 25.0 thousand rubles per year. Equiping technical installations of different branches of the industry with radioisotope devices gives an economic effect of about 3.0 million rubles per year to the national economy.

* * *

A meeting on the "Use of radioisotope devices in technical projects" was held on May 31, 1971 in Kiev. This meeting was organized with a view to exchange experience in the use of radioisotope devices, the methods of control and regulation of production processes in technical projects, and orientation of the project organizations toward the prospects of production and delivery of radioisotopes devices in 1972-1973.

Specialists from project organizations, basic isotope laboratories, and scientific-research institutes took part in the meeting.

* * *

A meeting for the exchange of experience of the operation of isotope laboratories and sections on assembly and adjustment of radioisotope technique, located in the territory served by Leningrad division of the All-Union society "Isotope" was held in June 1971 in Riga.

The papers and communications elucidated the problems of use of radioisotope devices and the methods in automatization of the technological processes and the most important directions of further development of radioisotope devices were discussed.

"The usefulness of the current volume makes one look forward to the release of others in this series. . . . Should be required reading for engineers and astronomers concerned with the construction and planning of large radio telescopes."
— PHYSICS TODAY

WIDEBAND CRUCIFORM RADIO TELESCOPE RESEARCH

*Trudy #38 of the P.N. Lebedev Physics Institute**

Edited by **D. V. Skobel'tsyn**

Director, P.N. Lebedev Physics Institute
Academy of Sciences of USSR, Moscow

Translated from Russian

Concentrating on both construction and operation of radio telescopes, this volume deals with such specific problems as the weight of the structure, loads imparted by the wind, and the means for taking them into account. The tracking system and other components are also described, and the versatility of the instrument is demonstrated in observations of the solar supercorona and measurement of radio wave frequencies. This volume is an invaluable reference source for radio astronomers and engineers called upon to design their radio telescopes. Contributions are based on work done at the Lebedev Physics Institute, recently lauded by *Physics Today* for "the quality and imaginativeness" of its work.

CONTENTS: Control system for the east-west array of the DKRT-1000 cruciform radio telescope, **Yu. I. Alekseev** • Directional diagram frequency control in a wide band antenna array with cophasal signal summation at an intermediate frequency, **I. A. Alekseev** and **S. N. Ivanov** • Electrical beam control in a wideband antenna array with zoned phase inverters with frequency change, **Yu. P. Ilyasov** and **S. N. Ivanov** • Use of remote preamplifiers in meter-range antenna arrays, **R. D. Dagkesamanskii, S. N. Ivanov,** and **Yu. P. Plyasov** • Resolution of correlation arrays, **Yu. P. Ilyasov** and **Yu. P. Shitov** • Response of multielement correlation arrays to several sources, **Yu. P. Shitov** • Rigidity of a parabolic reflector loaded by its own weight (vertical position), **P. D. Kalachev** • Evaluation of the rigidity of a parabolic reflector loaded by its own weight (symmetrical loading), **P. D. Kalachev** • Investigation of the solar wind and brightness distribution of radio emission sources during observation of their scintillations, **V. V. Vitkevich** • Observations of scintillation of radio sources on inhomogeneities in interplanetary plasma, **T. D. Antonova, V. V. Vitkevich,** and **V. I. Vlasov** • Observations of the solar supercorona in 1964-1965 and the C character of scattering inhomogeneities in the supercorona, **V. F. Bedevkin and V. V. Vitkevich** • Measurement of the polarization of the total radio emission flux of the crab nebula at 3.3 and 1.6 cm, **V. A. Udal'tsov** • Increasing radiometer reliability. An automatic volume control system for transistorized radioastronomical detectors, **V. N. Brezgunov and V. A. Udal'tsov** • A modification of the interference method for polarization measurements of plane-polarized radiation, **V. A. Udal'tsov** • Selection of optimum parameters of radio telescope servosystems with allowance for wind disturbance, **G. G. Basistov** • Plasma escape from the sun, **M. V. Konyukov** • Amplitude fluctuations during propagation of electromagnetic waves in media with random characteristics, **V. I. Shishov** • A possible mechanism of nonequilibrium solar radio emission by β-decay electrons, **N. G. Basov and V. V. Vitkevich** • Radio wave frequency and propagation time in a spherically symmetrical gravity field, **B. M. Chikhachev** • A method for measuring the gravitational shift of radio wave frequency in an artificial earth satellite experiment, **B. M. Chikhachev.**

CB Special Research Report

Approx. 190 pages 1969 $22.50

*Place your continuation order today for books in this series. It will ensure the delivery of new volumes **immediately** upon publication; you will be billed later. This arrangement is solely for your convenience and may be cancelled by you at any time.

PLENUM PUBLISHING CORPORATION
Plenum Press • Consultants Bureau • IFI/Plenum Data Corporation
227 WEST 17th STREET, NEW YORK, N. Y. 10011

In United Kingdom: Plenum Publishing Co. Ltd., Donington House, 30 Norfolk Street, London, W.C. 2.

HANDBOOK OF NEUROCHEMISTRY*

Volume 4: Control Mechanisms in the Nervous System

Edited by **Abel Lajtha**

New York State Research Institute for Neurochemistry and Drug Addiction
Ward's Island, New York

The fourth volume of an important new seven-volume encyclopedic treatise presenting a comprehensive evaluation of the current chemical and biological literature on the nervous system and the function of the brain. Devoted to problems in the control of biological activities, this volume investigates transmitters and their metabolism, enzymes presumably involved in transmission and other neural activities, hormones related to control, and biological phenomena which are necessarily related to control. Contributions are prepared by an illustrious group of experts brought together under the editorial direction of Abel Lajtha and are skillfully arranged in a thorough manner. Thus it is possible for the reader to obtain, rapidly and economically, coordinated information on the numerous basic and vital problems relating to biological control of nervous tissue. This volume is unsurpassed as a reference, research, and instructional manual for anatomists, biochemists, biologists, biophysicists, neurochemists, neurophysiologists, molecular biologists, medical and brain research workers and clinicians working on the nervous system.

Approx. 505 pages PP March 1970 **$35.00** (354/04)

(Subscription price on orders for the 7-volume set: $30.00 per volume)

LCC No. 68-28097

SBN 306-37704-7

***CONTINUATION ORDER PLAN**
In order to facilitate the rapid delivery of important research information, a continuation order plan is available for volumes purchased in a series. The plan is of particular benefit to those readers who wish to remain thoroughly informed about the latest developments in their fields of research. Utilization of such a plan will ensure the delivery of each new volume in a series **immediately** upon publication and will eliminate a great deal of paper work on your part. Members of the plan are billed upon shipment of the book. This arrangement is solely for your convenience and may be cancelled by you at any time.

PLENUM PUBLISHING CORPORATION
Plenum Press • Consultants Bureau • IFI/Plenum Data Corporation
227 WEST 17th STREET, NEW YORK, N. Y. 10011

In United Kingdom: Plenum Publishing Co. Ltd., Donington House, 30 Norfolk Street, London, W.C. 2.